GUIDEBOOK 93-1

STATE OF ARKANSAS

ARKANSAS GEOLOGICAL COMMISSION

Norman F. Williams, State Geologist

Scales of Geological Heterogeneity of Pennsylvanian Jackfork Group, Ouachita Mountains, Arkansas: Applications to Field Development and Exploration for Deep - Water Sandstones

Prepared by
Dallas Geological Society

FIELD TRIP LEADERS

Douglas W. Jordan
Donald R. Lowe
Roger M. Slatt
Charles G. Stone
Anthony D'Agostino
Mark H. Scheihing
Robert H. Gillespie

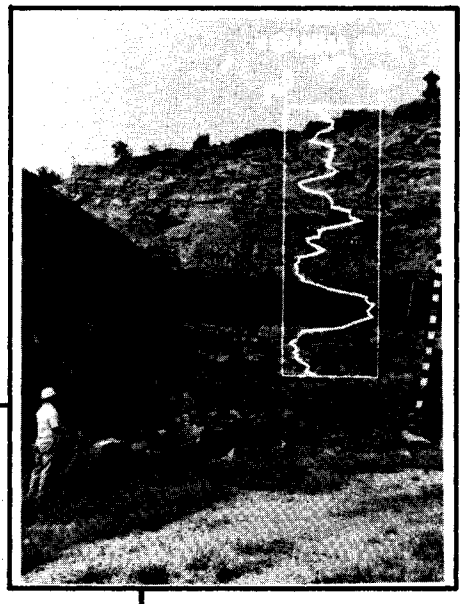

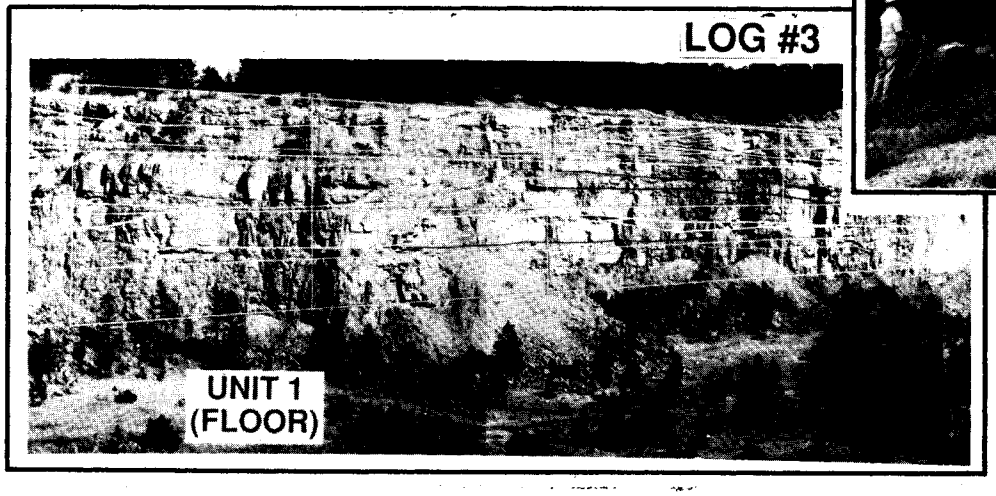

LITTLE ROCK, ARKANSAS

OCTOBER, 1993

Scales of Geological Heterogeneity of Pennsylvanian Jackfork Group, Ouachita Mountains, Arkansas: Applications to Field Development and Exploration for Deep-Water Sandstones

Guidebook
DGS Field Trip #3

April 4-7, 1991

American Association of Petroleum Geologists 1991 Annual Convention

Field Trip Leaders:

Douglas W. Jordan
ARCO International Oil and Gas Company
2300 West Plano Parkway
Plano, Texas 75075

Anthony D'Agostino
ARCO Oil and Gas Company
2300 West Plano Parkway
Plano, Texas 75075

Donald R. Lowe
Department of Geology
Stanford University
Stanford, California 94305

Robert H. Gillespie
ARCO Oil and Gas Company
2300 West Plano Parkway
Plano, Texas 75075

Roger M. Slatt
ARCO International Oil and Gas Company
2300 West Plano Parkway
Plano, Texas 75075

Mark H. Scheihing
ARCO Oil and Gas Company
2300 West Plano Parkway
Plano, Texas 75075

Charles G. Stone
Arkansas Geological Commission
Vardelle Parham Geology Center
3815 West Roosevelt Road
Little Rock, Arkansas 72204

1991 AAPG Annual Convention Field Trip Chairman:
Robert T. Clarke, Mobil Research and Development Corporation

This guidebook for the DGS Field Trip #3, "Scales of Geological Heterogeneity of Pennsylvanian Jackfork Group, Ouachita Mountains, Arkansas: Applications to Field Development and Exploration for Deep-Water Sandstones", was prepared for the American Association of Petroleum Geologists Annual Convention held in Dallas, Texas from April 7 - 10, 1991.

This Guidebook was originally published by the Dallas Geological Society, but is now out of print. In a letter dated March 27, 1992, Mr. Paul Buehrle, President, of the Dallas Geological Society and Mr. Robert T. Clarke, Field Trip Chairman, granted permission to the Arkansas Geological Commmission to reprint this volume. We wish to express our sincere appreciation to Messrs. Buehrle and Clarke and other members of the Dallas Geological Society for honoring this request. We of the Arkansas Geological Commission also thank Mr. Douglas W. Jordan and other representatives of the Arco Oil and Gas Company for their assistance in reissuing this guidebook.

Originally Published by the Dallas Geological Society, © 1991

ISBN 1-879325-15-2

Reprinted by the Arkansas Geological Commission,

1993

Contents

Scales of Geological Heterogeneity of Pennsylvanian Jackfork Group, Ouachita Mountains, Arkansas: Applications to Field Development and Exploration for Deep-Water Sandstones

Douglas W. Jordan
Donald R. Lowe
Roger M. Slatt
Charles G. Stone
Anthony D'Agostino
Mark H. Scheihing
Robert H. Gillespie

Introduction

On this field trip we will be visiting some of the finest outcrops of turbidites in North America. These outcrops have been visited and examined by hundreds of geoscientists over the past 30 years and have been the focus of numerous field trips, publications, and debates on deep-sea sedimentation and facies by both industry and university scientists. Our objective on this trip is not simply to repeat or summarize what is known about these sections or to review the sedimentology of the Ouachita flysch sequence, but to explore new aspects of Early Pennsylvanian Jackfork sedimentation. We do this by attempting to understand basic processes and facies of sedimentation and addressing problems facing petroleum geologists in discovering and developing deep-water reservoirs, many of which have been studied worldwide (see Appendix I).

At each of the outcrops to be visited (Fig. 1), we will address problems of basic processes of sedimentation and the implications of these processes for reservoir heterogeneity, lateral and vertical sandstone-bed continuity, and resulting reservoir quality. In order to make comparisons between outcrop and wireline data, we have developed techniques for generating outcrop gamma ray logs and will present and discuss the results at the major outcrop sections. Because well logs are one of the primary subsurface exploration tools in the petroleum industry, we feel that outcrop logs will provide a means of demonstrating what the explorationist can expect to be able to interpret, and not interpret, from logs in comparable subsurface depositional systems. Also, we will explore the outcrop implications of "thickening and coarsening" and "thinning and fining" upward log response trends.

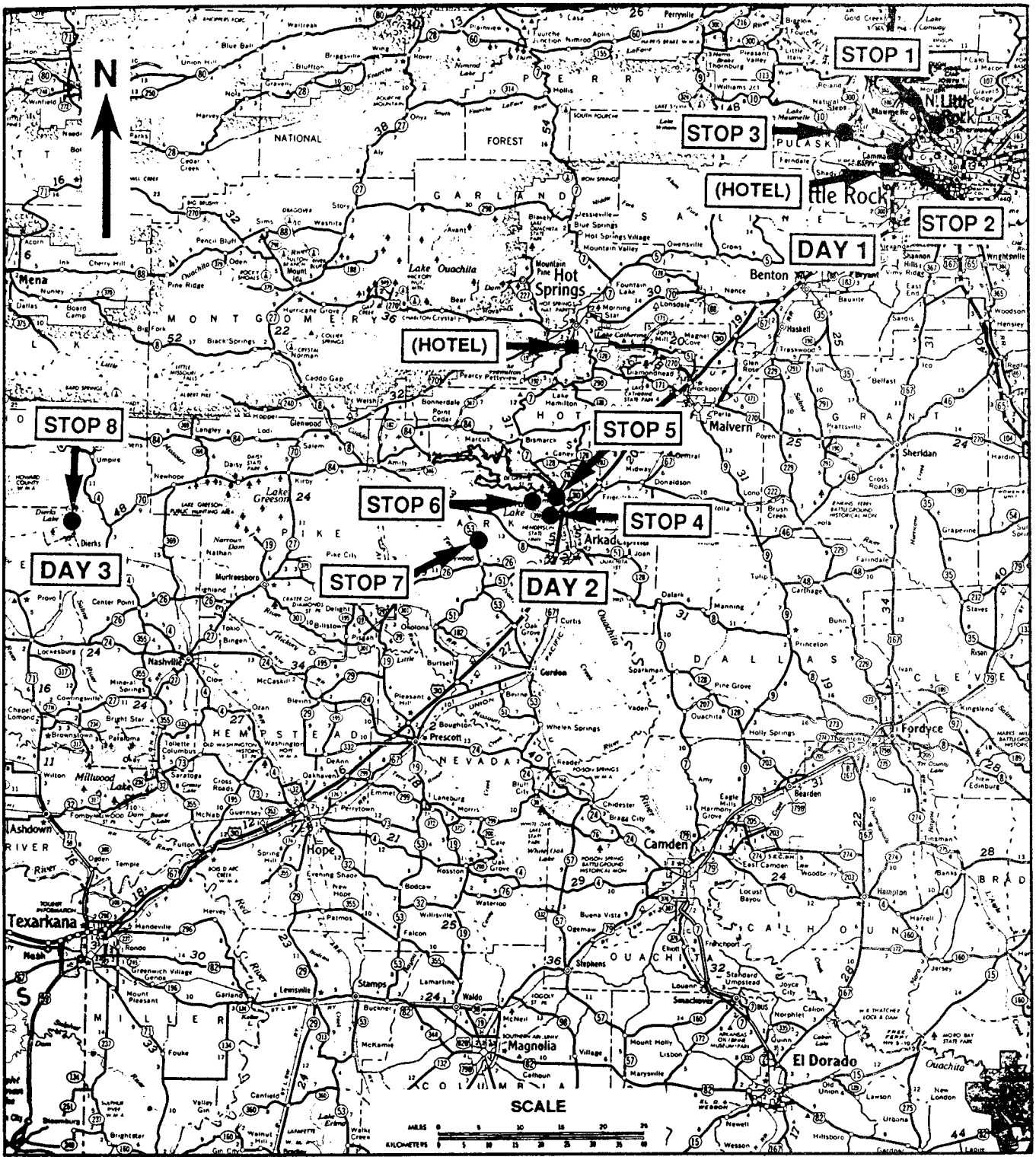

Figure 1. Route of field trip from Big Rock Quarry (STOP 1), I-430 cut (STOP 2), Pinnacle Mountain (STOP 3), southwest to Murray Quarry (STOP 4), to DeGray Lake Spillway (STOP 5) and Intake (STOP 6), Hollywood Quarry (STOP 7), and to Dierks Lake Spillway (STOP 8).

In addition to exploration applications, we have attempted to describe these turbidite sequences in term of vertical and lateral heterogeneity ranging from "single well" to "interwell" to "field wide" scales of particular concern to geoscientists involved in oil and gas field development. We do this through the use of gamma ray log interpretation exercises that illustrate log values versus reservoir quality, by making quantitative as well as qualitative estimates of the lateral continuity of individual sandstone units and beds, and by "scaling up" stratigraphic intervals into grid blocks and applying some numerical descriptors to these blocks as might be done in a reservoir simulation. We will focus in particular on two types of interwell- and field-wide-scale depositional units or geometries common to most turbidite sequences: lenses and sheets.

We hope that this trip will provide participants already familiar with the Ouachitas with some new views of these classic turbidite sequences and those unfamiliar with the Ouachitas, Jackfork, or turbidites in general, with an introduction to submarine depositional processes and the characteristics and heterogeneity of their deposits.

Geologic Setting and Location

General Stratigraphy

The Ouachita Mountains of Arkansas and Oklahoma (Fig. 2) represent part of a deeply eroded range of mountains that fringed the

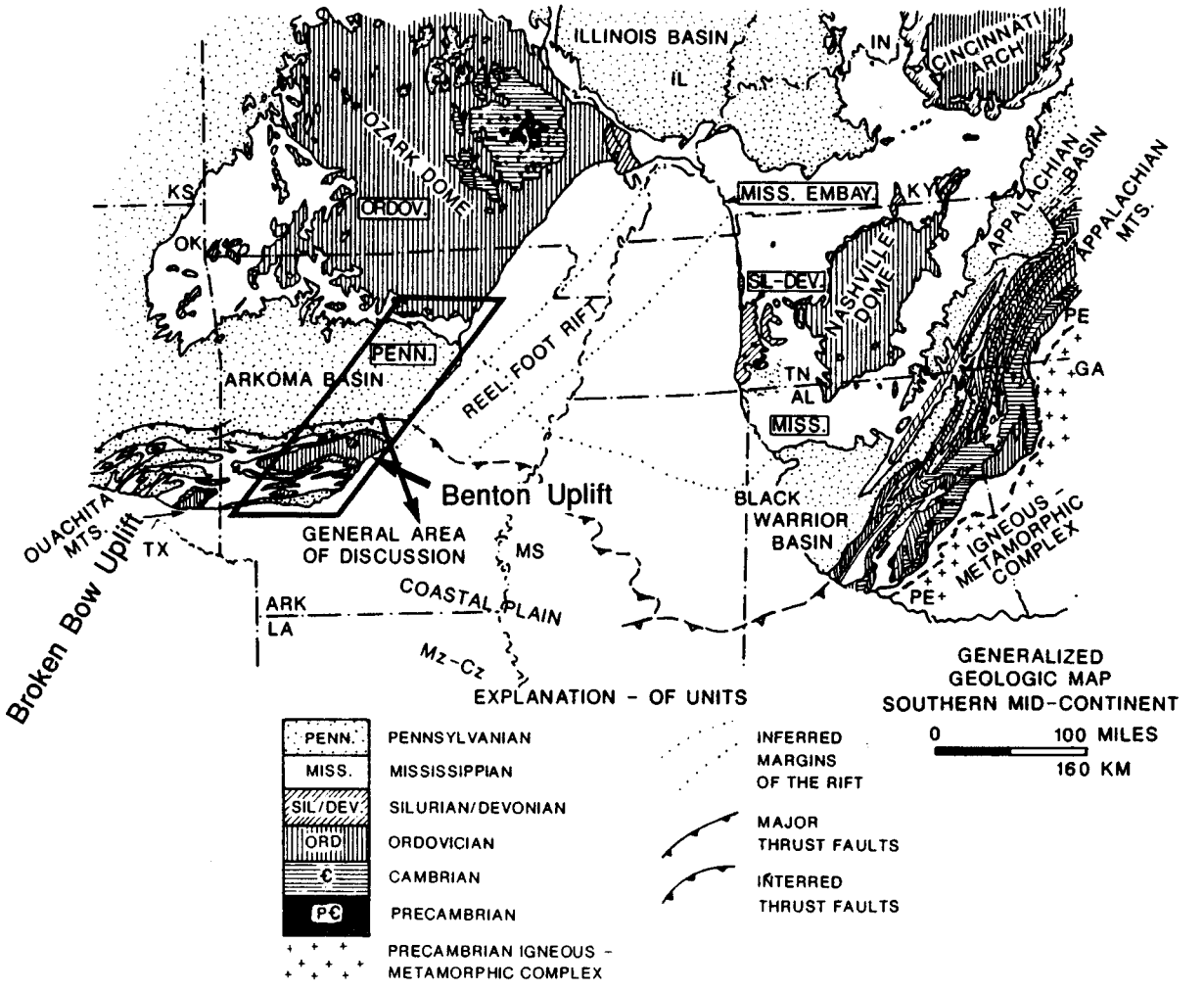

Figure 2. Geologic map of the south central and southeastern United States, with general area of field trip shown (from Link and Roberts, 1986).

eastern and southern margins of the North American craton throughout much of the late Paleozoic and early Mesozoic. Unlike the Appalachian Mountains, which form the eastern segment of this range, the southern part of the orogen, represented by the Ouachita Mountains of Arkansas and Oklahoma, the Marathon Mountains of west Texas, and small uplifts of Paleozoic rocks in Mexico, is now largely buried beneath younger sediments of the Gulf Coastal Plain. As a consequence, resolution of the geology of this large and complex orogenic belt must be based on studies of the small remaining outcrop areas, subsurface data, and geophysical surveys.

The Ouachita Mountains represent the largest outcrop segment of the Ouachita orogen. Exposed strata range from late Cambrian to middle Pennsylvanian in age (Fig. 3) and form part of a heavily deformed and locally metamorphosed fold and thrust belt that was thrust northward during the late Paleozoic over the southern margin of the North American craton (Fig. 4). They have been locally intruded by Cretaceous alkalic intrusive rocks, widely represented by deeply weathered basaltic dikes and locally along the eastern and southern margins of the belt by larger syenitic intrusive bodies, as in Magnet Cove and south of Little Rock.

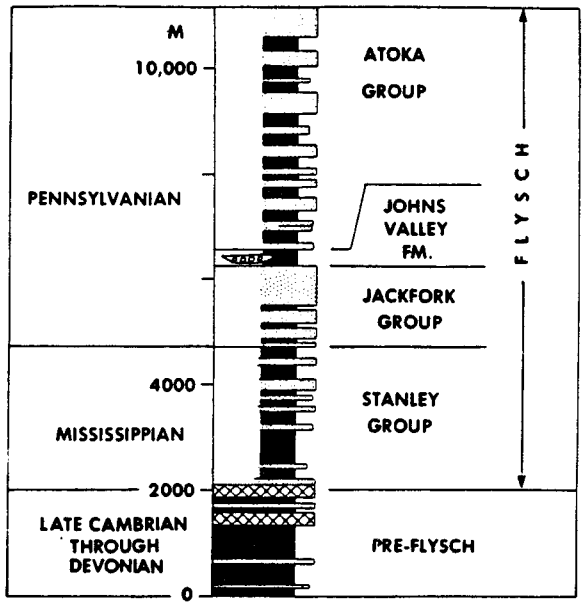

Figure 3. Stratigraphic column of Paleozoic rocks in the Ouachita Trough, Arkansas.

Paleozoic rocks in the Ouachita Mountains are generally divided into two principal facies. The 10,500 foot thick late Cambrian to early Mississippian sequence, including rocks from the Collier Shale through the Arkansas Novaculite, constitutes the pre-flysch or pre-orogenic facies. These are composed largely of shale, chert, and a minor amount of coarser clastic debris and represent a prolonged interval of mainly deep-water, sediment starved deposition.

The pre-orogenic succession is overlain by 30,000 to 45,000 feet of deep-water clastic strata of the flysch or orogenic facies. The flysch ranges in age from early Mississippian (Meramecian) to late Middle Pennsylvanian (mid-Atokan) and is divided regionally into four major sedimentary units (Fig. 3).

Flysch Sequence

Flysch strata in the Ouachita Trough crop out on the flanks of the Benton and Broken Bow geanticlinal uplifts, which exposes the older, pre-flysch portion of the Ouachita succession. The flysch marks orogeny and uplift of sedimentary and metasedimentary sequences, initially outside of the Ouachita Trough but later within the basin itself. Debris derived from these uplifts flooded into the Trough through fringing alluvial and deltaic systems and was dispersed from east to west across an immense predominantly fine-grained axial submarine complex.

Today, Carboniferous rocks in the Ouachita Mountains comprise a folded and faulted clastic succession estimated to be between 30,000 and 45,000 feet thick. Of this thickness, about 20,000 feet of strata were deposited from the Meramecian-Chesterian (Stanley Group) through Morrowan (Jackfork Group) Epochs, derived largely from extra-basinal sources. During the Atokan Epoch, another 25,000 to 30,000 feet of strata (Atoka Formation) accumulated, mainly along the northern part of the basin and derived in large part from uplifted older Ouachita rocks. Near the middle, the Atoka shallows from deep-water flysch through deltaic into alluvial sediments. The sequence thins drastically when traced northward to shelfal sections along the southern flank of the Ozark Dome (Fig. 4).

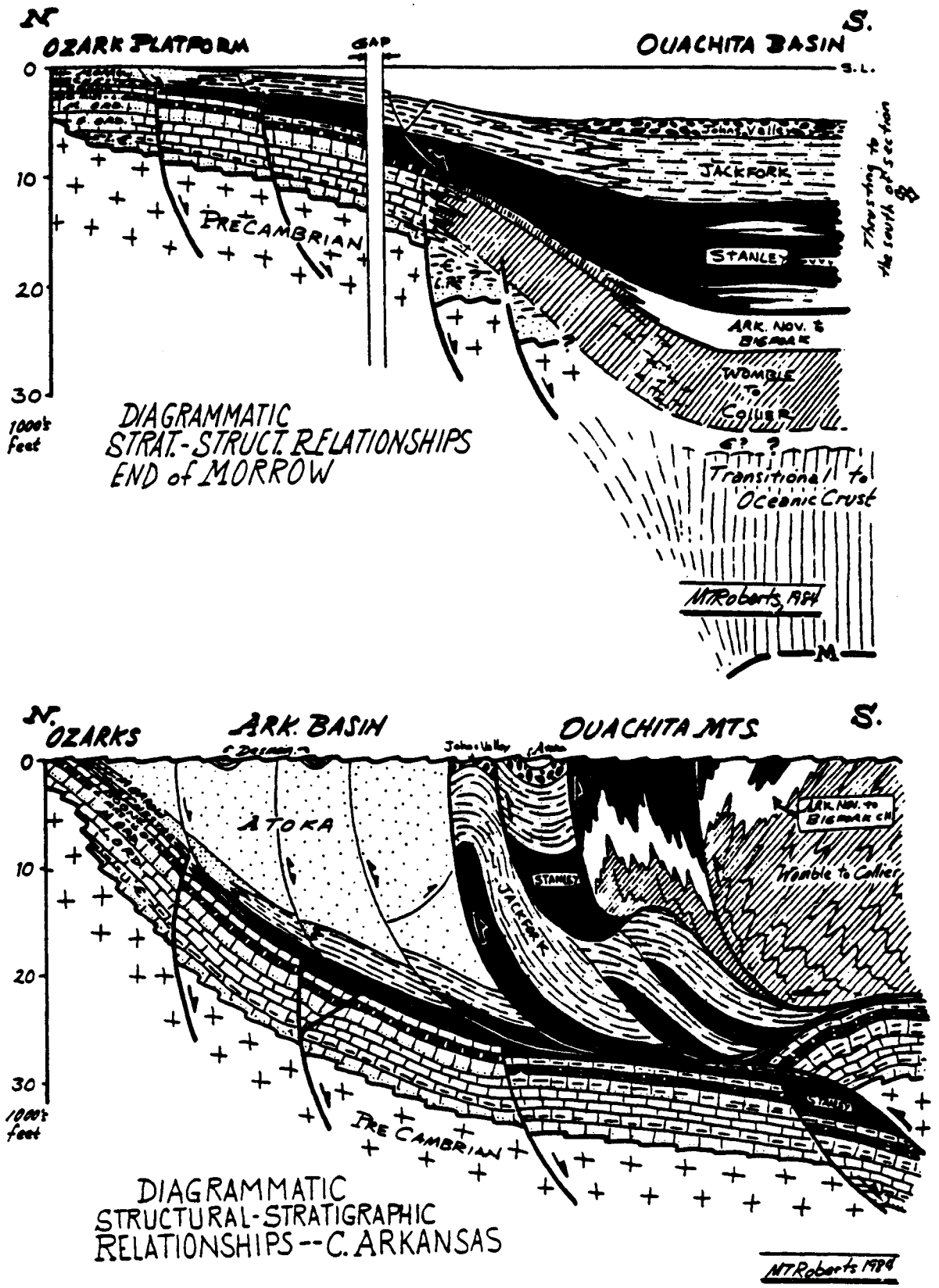

Figure 4. Structural and stratigraphic relationships of pre-Atokan units in central Arkansas (from Link and Roberts, 1986).

This enormously thick flysch section consists largely of interbedded units of sandstone and shale deposited by sediment gravity flows. Their dominant character is the rhythmic alternation of sandstone and dark gray to black shale layers. The overall monotony of the succession and difficulty in dating because of few fossils have resulted in the naming of relatively few stratigraphic units. The main formally defined units that can be traced throughout the Ouachitas include the Stanley Group (Mississippian) and the Pennsylvanian Jackfork Group, Johns Valley Shale, and Atoka Formation.

Stanley Group

The Stanley Group consists of from 1,000 to over 10,000 feet of strata composed, in order of decreasing abundance, of shale, sandstone, debris flow deposits, tuff, and siliceous shale. The predominant lithology is shale, commonly black, fissile, carbonaceous, pyritic, and non-calcareous. Sandstone occurs throughout the Stanley Group, becoming more prominent toward the top. Dry gas shows, some approaching economic volumes, have been found in a number of exploration wells in Oklahoma.

The lowest part of the Stanley in the Broken Bow uplift and areas immediately to the north includes a number of silicic tuff beds and tuffaceous debris flow deposits clearly derived from a southern source, whereas near Hot Springs, Arkansas, the basal Stanley includes the Hot Springs Sandstone and associated massive non-volcanogenic debris flow deposits that flooded into the basin from the northeast (Niem, 1976; Dickerson, 1986). The intervening basin axis is defined by a series of bedded barite deposits formed by the flow of dense barium-rich brines from submarine springs down the basin slopes and ponding along the basinal axis (Hanor and Baria, 1977).

Turbiditic sandstones throughout the Stanley Group are predominantly fine-grained and matrix-rich (Morris, 1974). They are composed largely of quartz but include significant amounts of feldspar and meta-sedimentary lithic detritus. The source areas probably consisted of uplifted older sedimentary and metasedimentary rocks south and east of the Trough.

Jackfork Group

Stratigraphic Position and Age of the Jackfork

Overlying the shaley Stanley Group is the more sandy Jackfork Group. The Jackfork was first described by Taff (1902) and included as part of the Chesterian (Mississippian) Series of the Mid-continent. White (1937) examined a meager fossil flora of *Lepidodendron*, *Calamites*, and seeds. He interpreted a post-Mississippian age for the Jackfork and demonstrated a floral affinity to the Morrowan (Early Pennsylvanian) Hale and Bloyd Formations of northwestern Arkansas. These formations are now interpreted as part of the Arkoma Basin shelf. Cline (1960), Morris (1971), and Gordon (1973), among others, documented and established the correlation of the Jackfork to the Hale and lower part of the Bloyd Formations of Arkansas, and the Sausbee Formation of the Arkoma Basin shelf of Oklahoma.

The Jackfork Group is divided into five formations based, in part, on the presence of distinctive siliceous shale units in Oklahoma. These are, from oldest to youngest, the Wildhorse Mountain Formation, the Prairie Mountain Formation, the Markham Hill Formation, the Wesley Shale Formation, and the Game Refuge Formation. Morris (1971) showed that this five-fold subdivision is not practical in the central Ouachitas of Arkansas and established the Irons Fork Mountain Formation (lower Jackfork used in this guidebook) and the Brushy Knob Formation (upper Jackfork). Figure 5 shows the stratigraphic correlation of the Jackfork from the deep trough of Arkansas to the Arkoma Basin shelf of northwest Arkansas and central Oklahoma. Some workers recognize an informal middle portion where differentiation of the units is not always clear. The Jackfork attains a thickness of about 6700 feet along the trough axis and is thinner and shalier in western sections in Oklahoma.

Dating of the Jackfork has been, for the most part, predicated on the dating of the correlative units on the shelf. The paleobotanical study by

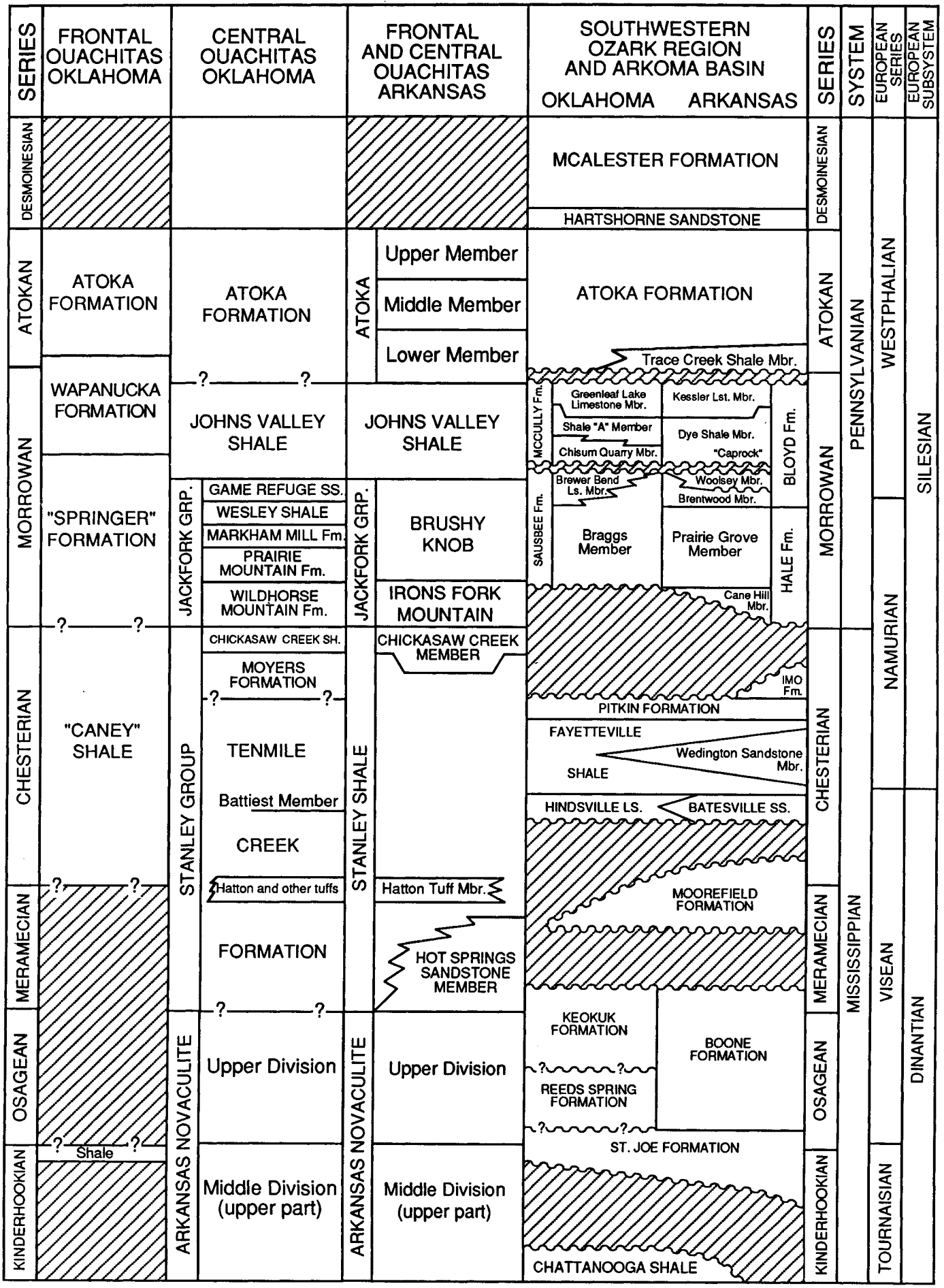

Figure 5. Correlation chart for Mississippian and Pennsylvanian formations between deep-water Ouachita Trough and shelfal areas to the north. Modified after Morris, 1971, and Sutherland and Manger, 1979.

White (1937) set the stage for a post-Mississippian determination. Studies, by various authors, of fusulinid foraminifera, brachiopods, algae, bryozoans, ostracods, and ammonites, were presented in Sutherland and Manger (1977). These studies clearly established the Morrowan age for the correlative shelfal units of the Arkoma Basin. Gordon and Stone (1969) documented Morrowan ammonites, brachiopods, and trilobites in the Jackfork of Oklahoma and Arkansas.

Paleontologic samples for this study were collected at a number of points from the DeGray Lake Spillway (STOP 5), Dierks Lake Spillway (STOP 8), and I-430 (STOP 3) localities. Samples were taken from shales associated with muddy turbidites, debris flows, and laminated zones. The samples were examined for conodonts, radiolarians, forams, and palynomorphs. No samples contained any conodonts or radiolarians. Two samples (Jack 27, 31) contained poorly preserved specimens of the palynomorph *Densosporites* sp. This form is restricted to the Morrowan of North America (Gerhard, pers. comm.). Three samples (Jack 30, 32, 33) contained rare to abundant specimens of the arenaceous foram genera *Bathysiphon*, *Ammodiscus*, and *Thuramminoides*. *Thuramminoides* is restricted to the Morrowan and Atokan of North America (Loeblich and Tappan, 1988). The recovery of specimens of *Thuramminoides* and *Densosporites* add to the very short list of age-diagnostic fossils recovered from the Jackfork of the central Ouachitas, and further solidifies the interpretation of a Morrowan age for the unit. The paleontologic sampling is summarized in Table 1.

Paleoenvironmental Interpretations of the Jackfork

Taff (1902) and other early investigators interpreted the Jackfork as a shallow-water deltaic deposit associated with the hypothetical southern landmass of Llanoria. Their chief evidence was the rare occurrence of plant impressions and the sand-rich nature of the formation. In his study of the paleobotany of the Jackfork, White (1937) discussed the recognition of the exotic or transported nature or those plant fossils. He also was a proponent of the idea that the deposition of the Jackfork was at least in part due to slides and slumps from shallow water into deep water.

Most investigators of the Jackfork interpreted a deep-water setting based on the dominance of turbidites, debris flows, associated sedimentary structures, and the absence of any in situ shallow-water fossils. Chamberlain (1978) interpreted trace fossil ichnofacies to reach a mid to lower bathyal (less than 2000 m) interpretation for the Jackfork of the central Ouachitas of Arkansas. He documented the presence of the *Nereites* ichnofacies association. This ichnofacies is typical of classic flysch sequences composed of interbedded dark shales and turbiditic sandstones. The traces in the *Nereites* association are typically complex horizontal deposit-feeding traces. They reflect the absence of nutrients in the water column and their concentration in the first few centimeters below the sediment-water interface. Chamberlain documented the ichnotaxa *Spirophycos*, *Helminthopsis*, *Lophoctenium*, *Scolicia*, *Phycosiphon*, *Scalarituba*, and *Chondrites*. Members of this association have been noted at the DeGray, Hollywood Quarry, and Dierks Lake localities.

Fossils recovered as part of this study do not provide any definitive paleobathymetric indications. The palynomorphs could be present in shallow or deep water. Their concentration depends more on relatively diminished rate of accumulation of clastic sediment. The arenaceous forams are associated with the muddy-bottom communities of a clastic-dominated shelf (McKerrow, 1978). Their presence, especially at Dierks Lake Spillway, serves to document the transport of sediment derived from shallow environments along the axis of the Ouachita trough.

Lithology and General Sedimentological Characteristics of the Jackfork

Fine-grained, quartz-rich sandstone makes up the bulk of the coarser part of the Jackfork Group. The beds range from a few inches to hundreds of feet thick and were deposited by west- and north-flowing turbidity currents. High-velocity flat lamination, ripple cross-lamination, water-escape structures (dish and

SAMPLE NO. (AND LOG DEPTH)	LOCATION	FOSSILS RECOVERED	COMMENTS
Jack 25 (32')	Dierks East	barren	
Jack 26 (48')	Dierks East	barren	
Jack 27 (105')	Dierks East	poorly preserved *Densosporites* sp.	lam. shale Morrowan
Jack 29 (52')	DeGray West	organic/woody flakes & rods	debris flow
Jack 30 (330')	DeGray West	organic/woody flakes & rods arenaceous forams	debris flow
Jack 31 (547')	Dierks West	silicified wood fragments *Densosporites* sp.	muddy turbidite Morrowan
Jack 32 (32')	DeGray East	one arenaceous foram	muddy turbidite
Jack 33 (14')	Dierks East	silicified wood fragments arenaceous forams	muddy turbidite
Jack 36 (378')	DeGray West	silicified wood fragments	condensed section?
A48	I-430	arenaceous forams	debris flow

Table 1. Summary of the paleontologic samples collected for this study (palynomorph analysis performed by J. Gerhard, consulting palynologist; foraminifera by T. D'Agostino).

pillar structures), and convolute lamination are the most common sedimentary structures. Grading is present locally, but is difficult to see because of the uniformly fine grain size of the beds.

We will examine "typical" Jackfork sandstone sequences at Stops 4 through 8 in the southern part of the Ouachita Mountains.

Jackfork sandstones are considerably cleaner and somewhat more quartzose than Stanley units. Jackfork sandstones were derived from fringing alluvial and deltaic systems that prograded to the edge of the Ouachita Trough via the Illinois Basin, uplifted sedimentary sequences in the Appalachian orogen, and probably from a fringing fold and thrust belt east and south of present exposure (Figs. 6A-B), emptying vast quantities of detritus into the basin. Paleocurrent analysis by Morris (1974) deduced an overall east-northeast to west-southwest trend for sandstones in Arkansas.

Illitic shales and mudstones are interbedded with the sandstone units and make up predominantly shale packages up to 75 feet

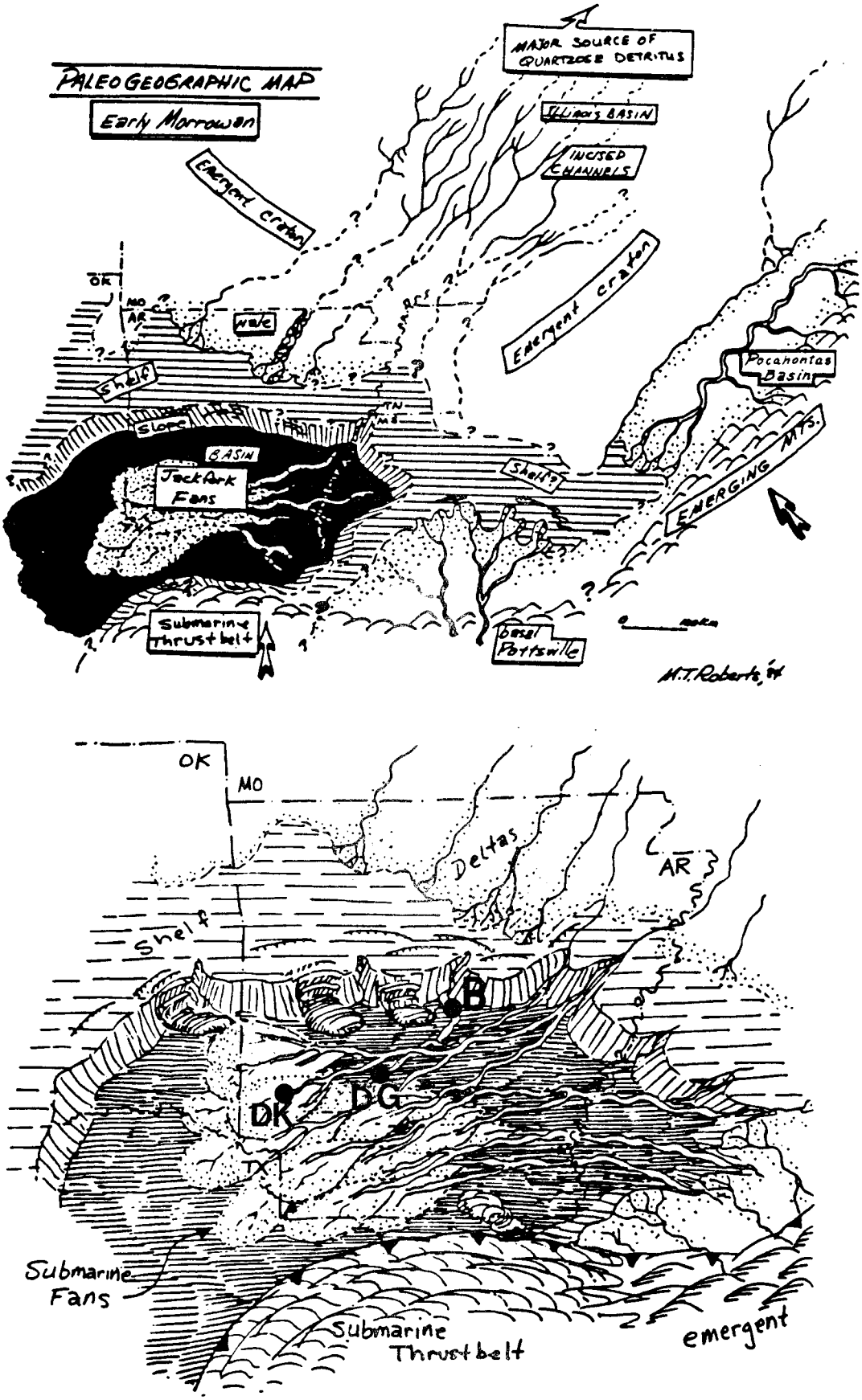

Figure 6. Caption on facing page.

thick. They are dark to medium gray in color and most represent deposition by dilute, low-energy turbidity currents. Many mudstones, when examined closely, contain floating shale and sandstone clasts, bits of woody material, and admixed sand grains. These represent debris flows up to 100 feet thick and the watery, slurried tails of muddy turbidity currents that left mudstone deposits a few inches thick capping underlying turbidites. We will examine these deposits at Stops 5 (DeGray Lake Spillway), 7 (Hollywood Quarry), and 8 (Dierks Lake Spillway).

Along the northern front of the Ouachitas, Morris (1971) has described a zone of chaotic bedding characterized by contorted bedding, large displaced sedimentary blocks, mud-matrix debris flow deposits, and unusual sand-matrix mudstone-clast breccias. Although deformation along this belt has been accentuated by later tectonism, there is little doubt that the zone marks a major slope leading into the Jackfork basin. The slope was the site of mud and sand deposition and repeated failure and downslope movement of accumulating sediments as massive slides, slumps, and incompletely mixed flows. We will see some of these units at Stops 1 (Big Rock Quarry), 2 (Interstate 430 roadcut), and 3 (Pinnacle Mountain State Park) on the field trip.

Johns Valley Shale

The Johns Valley Shale, 400 to 2500 feet thick, is recognized across the frontal Ouachita Mountains. It consists of shale and in the western parts, units containing exotic redeposited limestone and chert blocks, many of which can be correlated with carbonate units on the shelf to the north and west. The Johns Valley is differentiated from the Jackfork Group and Atoka Formation in the southern areas where it contains more sandstones and exotic boulder beds are absent.

Atoka Formation

The Atoka Formation likely marks uplift along the southern margin of the Ouachita Trough itself and migration of the depositional axis to a position along and just north of the present frontal Ouachitas. Sandstone and shale occur in roughly equal proportions. The sandstones are lithic rich and characterized by abundant plant matter and plant-produced tool marks on the bed bases. They were emplaced by turbidity currents receiving debris from south, north, and east and flowing east to west down the Trough axis.

Organic Geochemistry

Twenty seven shale samples from the Jackfork were collected from 10 localities (not all locales are included in this field trip) for analysis of weight % Total Organic Carbon (TOC) and % Vitrinite Reflectance (VR). Only 20 of the 27 samples were analyzed for VR. Results are tabulated in Table 2.

The data in the table are arranged vertically as they would trend from east to west, and are

Figure 6. (A) Paleogeographic map showing the probable source areas and distribution systems for early Morrowan Jackfork sediments in the Ouachita Trough. In the Morrowan, most clastic sediments bypassed the Illinois Basin, moving down through the Reelfoot Rift and passing over the shelf edge into the Ouachita Trough. The Trough was clearly confined to the south and additional major sediment sources probably included overflow from the Black Warrior Basin to the east and uplifted areas to the south (diagram from Link and Roberts, 1986). (B) Diagrammatic paleogeography during deposition of the Jackfork Group (from Link and Roberts, 1986). Location of Big Rock quarry (B), DeGray Lake (DG), and the Dierks Lake (DK) areas are shown. The section at Big Rock Quarry (North Little Rock) was presumably deposited on or near the slope that fed a submarine deep-water system, and the DeGray section was deposited in the middle part of a system, but not necessarily the same system that was present at Big Rock Quarry. The Dierks Lake section (DK), some 60 miles to the west of DeGray, was deposited in the outer portion (?) of the middle part of a deep-water system.

LOCATION	VITRINITE REFLECTANCE n	Range	Mean	TOTAL ORGANIC CARBON (WEIGHT %) n	Range	Mean	EST. LOSS OF KEROGEN (WEIGHT %)
North Little Rock Quarry, Ark.							
upper Jackfork	2	2.1-4.3	3.2	2	0.9-1.8	1.0	0.1
lower Jackfork	1		4.2	1		1.0	0.1
I-430 Roadcut							
upper Jackfork	2	5.1-5.5	5.3	2	0.8-1.3	1.1	
lower Jackfork	2	4.6-4.7	4.7	2	1.0-1.1	1.0	
Food-4-Less Grocery (upper Jackfork)	1		5.1	2	0.6-1.5	1.1	
Pinnacle Mountain State Park (lower Jackfork)	1		4.8	1		1.3	
Maumelle Section (lower Jackfork?)	1		4.4	1		1.0	
DeGray Dam Spillway (upper Jackfork)	4	1.7-2.6	2.1	8	0.8-6.0	1.8	0.1
Hollywood Quarry (upper Jackfork)	1		1.7	1		1.2	
Dierks Dam Spillway (lower Jackfork)	3	1.4-1.5	1.5	7	0.7-1.7	1.2	0.0
Rich Mountain, Okla. (lower Jackfork)	1		0.7	1		0.9	0.2
Kiamichi Mountain, Okla. (upper Jackfork)	1		1.2	1		0.7	
TOTAL	20	1.4-5.5	3.8	29	0.6-6.0	1.3	

(For calculating TOTAL averages, equal weight was given to each location).

Table 2. Organic geochemistry of Jackfork samples, Arkansas and Oklahoma.

separated into lower and upper Jackfork units: Big Rock Quarry in North Little Rock, Arkansas occurs farthest to the east, and Kiamichi Mountain occurs farthest to the west in eastern Oklahoma. There is a clear trend of decreasing VR from the east toward the west, possibly reflecting greater prior tectonic burial and thermal maturity in eastern Arkansas (Houseknecht and Matthews, 1985).

TOC's generally average about 1.0% in Jackfork shales throughout the area, with suggestions of slightly lower values in the more basinal facies at Kiamichi and Rich Mountains. The anomalously high range and higher average TOC values at DeGray Lake Spillway result from two samples of shale (2.2 and 6.0 % TOC) that are very coaly and contain pyrite and abundant plant fragments.

Original (pre-burial) TOC values were estimated from nine samples subjected to Rock-Eval analysis. The estimated carbon lost during burial is calculated as a function of both the original organic matter composition (kerogen type as defined by Rock-Eval hydrogen index) and the maturation level of the kerogen (as defined by the Rock-Eval transformation ratio). Since the shales are within a turbidite sequence, the assumption was made that the original type was Type III. Calculations were compared with analyses of other mature and partially mature source rocks. The results (Table 2) indicate that 0.0-0.2% TOC has been lost during maturation, which translates to a loss of 0-20% for these shales.

TOC values of about 0.5% in shales are generally considered the minimum for hydrocarbon source rock potential. Thus, the Jackfork shales may have been potential source rocks when buried through the oil-generative window, even though they are now "overcooked". By analogy, shales inter-bedded with turbidite reservoir sandstones should not be overlooked as potential hydrocarbon source rocks in other areas.

Petrography

Provenance of the Jackfork and Previous Studies

Some of the earliest studies of the Jackfork concerned stratigraphic position and age and are discussed elsewhere in this guidebook. Bookman (1953) and Goldstein (1959) produced some of the first basic petrographic and petrologic analyses of the Jackfork. Bookman interpreted the heavy mineral suite and inferred a southern tectonic source for the Jackfork, basically Miser's (1921) Llanoria. Goldstein's study resulted in the proposal of a source from the west or "Texas craton" which since then, has never been proposed or supported. Klein (1966) studied the petrology and dispersal patterns and proposed that the Jackfork derived most of its quartzose material from the Illinois Basin but much of the feldspathic and lithic constituents were derived from the south. Morris (1971) argued against a southern source but was the first to suggest a source from the Black Warrior Basin or Appalachia. Danielson et al. (1988) used petrographic analysis and mapping to reach the conclusions that the Jackfork contained contributions from northeastern (Illinois Basin), eastern (Black Warrior Basin) and southern (tectonic highland) sources. Owen (1984), Owen and Carozzi (1986), and Miller (1985) all used petrography and cathodoluminescence analysis of quartz to refine this tripartite interpretation and conclude that most of the Jackfork sandstones were derived from a southern source with a stage of residence in shallow-water facies of the Black Warrior Basin, namely the Parkwood Formation, before being cycled into the deep Ouachita Trough. The Illinois Basin and northern Ouachita shelf were minor source areas.

A summary of significant mineralogic components in the Jackfork samples analyzed

	Average		Minimum		Maximum	
	Dierks	DeGray	Dierks	DeGray	Dierks	DeGray
Quartz	90.8	86.3	86.5	82.5	94.2	96.6
Feldspar	1.8	1.9	0.6	0.0	3.7	6.0
Lithics	6.1	7.3	4.0	2.5	10.7	16.2
Matrix	9.9	7.1	0.5	0.5	29.8	20.6
Cement	33.7	32.0	17.7	20.1	45.7	42.3
P Porosity	0.1	0.8	0.0	0.0	1.5	15.0
S Porosity	1.6	2.4	0.0	0.0	7.0	8.5
Total Porosity	1.8	4.0	0.0	0.0	7.0	16.0
MGS (microns)	199.1	190.9	109.1	73.7	312.1	728.4

Table 3: Summary of major mineralogic components and textural data for 16 samples from the Dierks Lake Spillway west and 43 samples from the DeGray Lake Spillway east and west localities. P = primary, S = secondary, MGS = mean grain size.

for this study is shown in Table 3. The values are similar to the previous studies. The data show that the upper Jackfork Sandstone at DeGray Lake Spillway (STOP 5) is slightly richer in feldspar, lithic fragments, and is more porous than samples from the lower Jackfork Sandstone at the Dierks Lake Spillway locality (STOP 8). The samples at Dierks have slightly more quartz, matrix, cement, and are less porous. Additional data for these localities are presented in the Field Trip Itinerary and Description section for the individual stops as well as in Appendix II.

Deep-sea Sedimentation Processes and Facies

During this field trip, you will have the opportunity to examine the products of the spectrum of deep marine sedimentation processes, so a brief discussion of processes and resultant facies is presented here.

Most submarine sediment gravity flows originate as slope failures, such as slumps or slides, but mix, entrain fluid from the surrounding water mass, and evolve into turbulent flows downslope. As a consequence, most sediment flows begin as high-density mixtures (particle concentration greater than 40%) and gradually decrease in density as water is added to the flow and sediment is deposited. In contrast, fluid gravity flows originate as sediment-free water and gradually erode sediment from the bed over which they move. They tend to begin with and maintain a relatively low density (less than 10%) throughout their existence.

Submarine sediment gravity flows are named and classified on the basis of end-member processes that keep larger grains suspended within the flows. Based on their response to an applied shear stress, such as gravity, sediment and fluid mixtures exhibit either fluid or plastic behavior. Four end-members are: turbidity currents, fluidized and liquified flows, and cohesive or debris flows.

In natural deep-sea systems, two of these processes, turbidity currents and debris flows, are of quantitative importance. Liquefied flows may be important locally, especially in systems dominated by fine- to very fine-grained sandy sediments. Fluidized and grain flows occur, but are not relevant to the deposition of major submarine deposits. However, dispersive pressure, in concert with flow turbulence or flow cohesion, is important in influencing the textural development of some turbidity current and debris flow deposits.

Turbidity Currents

Turbidity currents are responsible for the transport and deposition of over 90% of sandy deep-sea deposits and probably for more than 50% of muddy sediments. Our basic knowledge of the structure and motion of turbidity currents derives from a series of flume experiments conducted by Middleton (1966, 1967). These and subsequent studies have demonstrated that turbidity currents, when fully developed, can be divided into a number of discrete zones. These include (a) an energetic head, (b) the body, and (c) a tail.

The head is a thickened region at the front of the flow. The geometry is related to shear and displacement of ambient sea water beneath which the flow is moving as well as to the properties of the flow itself. On steep slopes, the head is energetic and commonly erosive, and large sediment-charged vortices are shed from the rear. On lower slopes, turbulence within the head declines, and deposition begins toward the rear. The idealized turbidity current deposit (Fig. 7) was first outlined by Bouma (1962) and explained dynamically by Walker (1965). The Bouma Sequence includes five divisions, Ta through Te, representing successive stages in flow evolution and decline.

It is apparent, however, that many deep-sea sands show structures that do not fit within the Bouma Sequence, especially massive sandstone units that are common in deep-sea channels. The deposition of these thick-bedded, coarse-grained sandstones was, for many years, attributed to a variety of poorly understood processes such as "fluxoturbidity currents", grain flows, and sandy debris flows. Today, it is thought that they represent

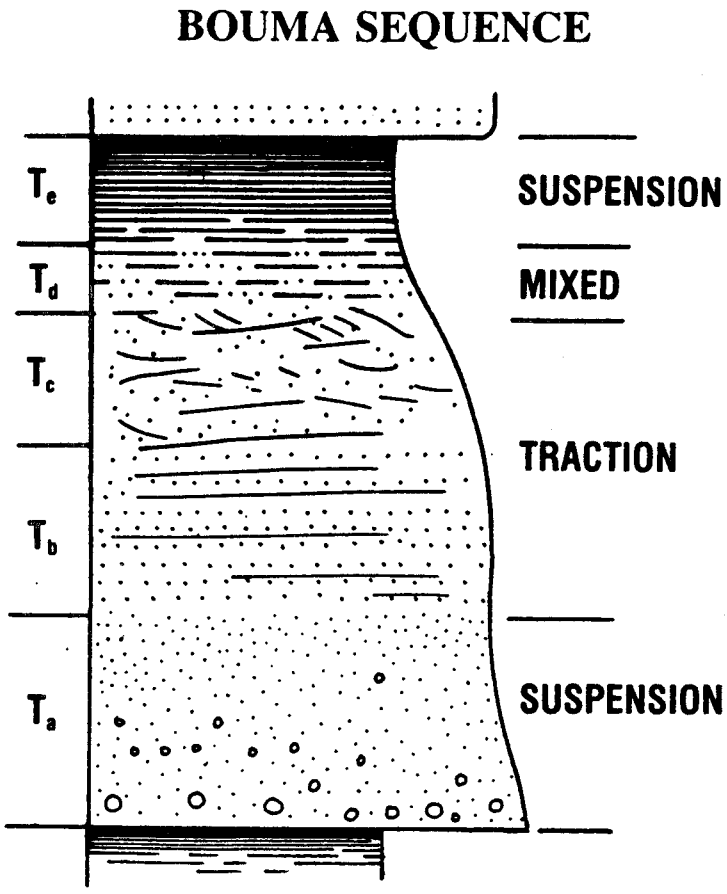

Figure 7. The Bouma sequence and style of sedimentation represented by each division. Ta represents the waning stages of high-density sedimentation whereas Tb-e represents deposition from low-density currents.

high-density turbidity currents or hyperconcentrated flows in which grain concentration plays a critical role in grain support.

Lowe (1982) has argued that submarine failures of sediment having a wide range of particle sizes, from cobbles and pebble down to fine silt and clay, will move as high-density turbidity currents in which the particles move together but as dynamically discrete grain populations that are maintained in motion or 'suspension' by three different combinations of processes: (1) The finest grains, less than about 0.5 mm in diameter, will be fully suspended, individually or collectively, by flow turbulence; (2) Larger grains, 0.5 to about 10 mm in diameter, cannot be fully suspended by fluid turbulence alone. They can be suspended in dense sediment clouds, however, where the buoyancy provided by finer grain sizes and the high concentration of the grains themselves effectively reduce their settling velocity to that of much finer grains; (3) Pebbles and cobbles cannot be fully suspended in most flows, but tend to move along the bed as dense bed-load layers called traction carpets in which grain collisions dominate transport.

Because each of these three grain populations is supported by different processes, they tend to be deposited independently as the flow declines. The ideal composite model of a high-

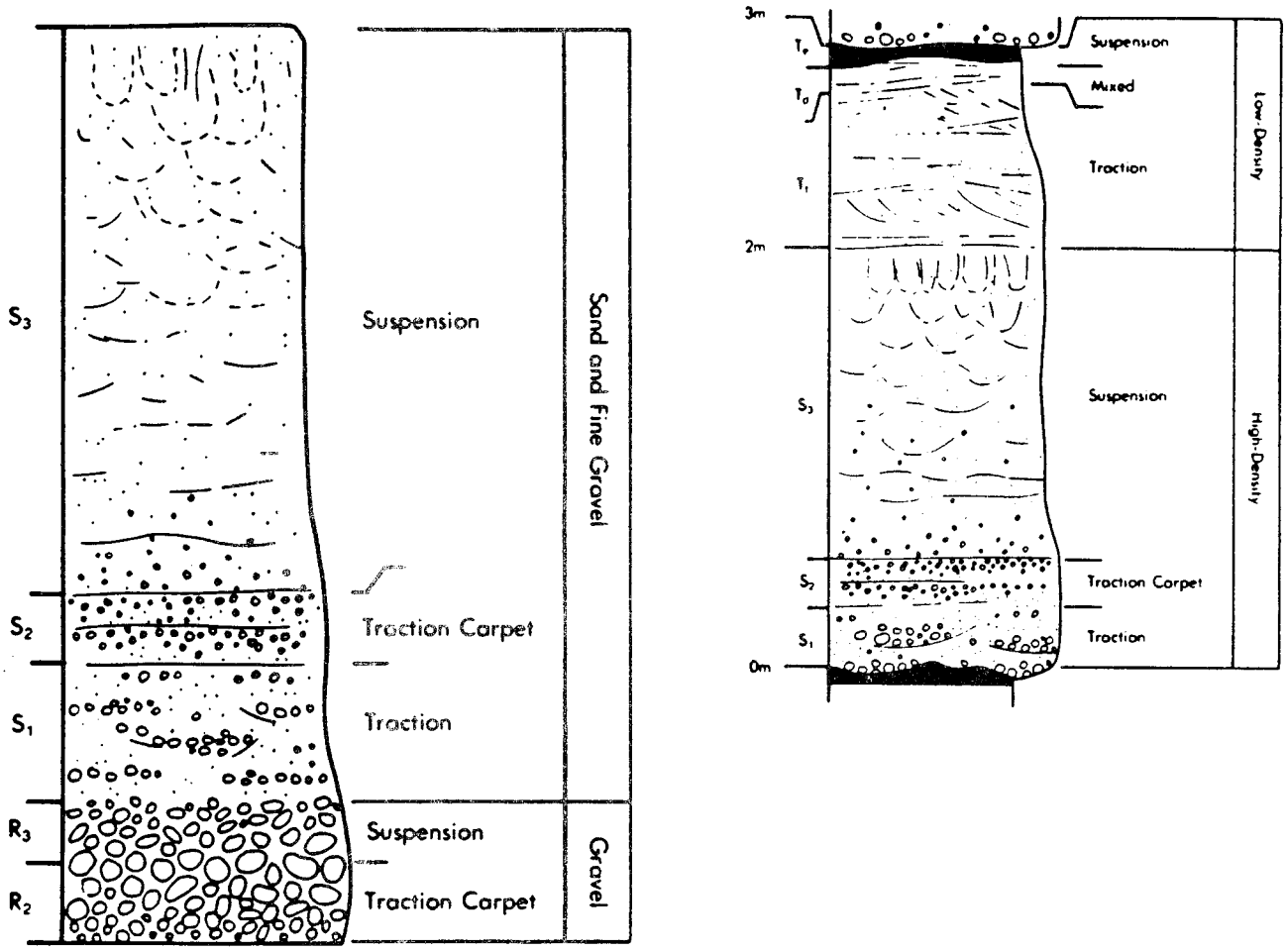

Figure 8. Deposits of high- and low-density turbidity currents. Left: Ideal sequence of subdivisions deposited by a single high-density turbidity current declining through discrete gravelly (R2 and R3) and sandy (S1, S2, and S3) sedimentation intervals. Right: Ideal deposit of a sandy high-density turbidity current showing both sandy high-density (S1, S2, and S3) and later low-density (T) turbidite divisions. Both from Lowe (1982).

density turbidity current deposit is shown in Figure 8. Generally, the coarsest material is deposited first to form gravelly inversely graded, traction carpet (R2) or normally graded, suspension deposited (R3) layers. The remaining high-density sandy flow may move as a relatively steady, non-depositing current, laying down thin units of current-structured sandstone (S1), develop traction carpets as fallout from the suspended load begins (S2), and eventually collapse with wholesale rainout of the entire coarse-grained suspended load, which accumulates by direct suspension sedimentation (S3). The remaining finer grains generally constitute a low-density flow that may move further downslope before deposition begins.

Because different particle populations within a flow are supported by somewhat different processes, they tend to be deposited at different times as the flow declines and to accumulate at different positions downslope. Generally, pebble- and cobble-sized material is deposited within submarine canyons and proximal deep-sea fan channels. The coarser sand and granule-sized sediment moves further downslope and is abruptly dropped out along upper and mid-fan channels, to form coarse-grained, thick-bedded channel sands, and on the upper portions of mid-fan depositional lobes. The finest grains move downslope as low-density flows and out onto mid-fan depositional lobes, the outer fan, and basin plain.

In the Ouachitas, we will see a variety of deposits representing both high- and low-density turbidity currents.

Debris Flows

Cohesive debris flows encompass a broad spectrum of rheological behavior and sediment-fluid mixtures. Within many flows, large cobbles and blocks of exotic rock and intrabasinal sedimentary clasts are fully supported and suspended within a cohesive mud matrix. As these flows slow, they tend to freeze abruptly, locking in the matrix-supported texture that existed during flowage (Fig. 9A).

In many debris flows, the largest clasts are not actually suspended within the mud-water matrix but remain more or less in contact with

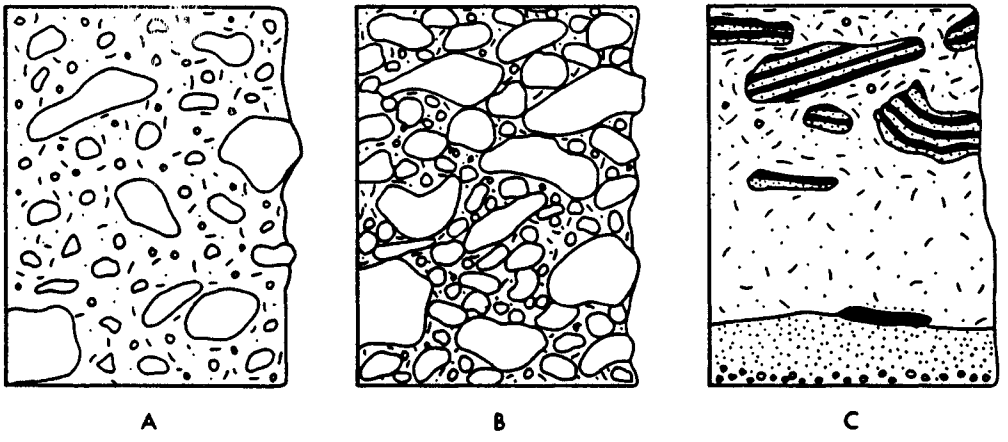

Figure 9. Cohesive debris flow deposits. (A) Massive, structureless, matrix-supported diamictite or pebbly mudstone deposited by a debris flow in which the clasts were fully supported by the muddy matrix. (B) Massive, structureless, clast-supported muddy conglomerate deposited by a debris flow in which the clasts were lubricated but not fully supported by the muddy matrix. (C) Stratified deposit formed by deposition from a watery debris flow. The coarsest, densest sediment has settled to the base of the flow as turbulence declined. Only in the uppermost part of the flow was coarse sediment locked in before settling by the presence of a cohesive matrix. The largest, but low density clasts floated at the top of the flow. From Lowe (1982).

one another while rolling, sliding, and intermittently bouncing downslope. The clay-water matrix lubricates their movement and aids in their support because of buoyant effects. The deposits of such flows are largely clast supported (Fig. 9B) and may include a relatively small proportion of clay. Some debris flows are turbulent at some stage in their evolution and support clasts larger than might otherwise be maintained by buoyancy and matrix cohesion alone. During deceleration, initial deposition may involve the fallout of the coarsest grains forming a relatively clean, basal layer (Fig. 9C). Later freezing of the remaining laminar flow produces a muddy matrix-supported cap to the initial deposit (Fig. 9C).

In the Ouachitas, we will see a variety of debris flow deposits. Small matrix-supported debris flow deposits fill channels at STOP 1 and large, massive units up to 30 feet thick occur at STOPS 5 and 6. STOP 8 shows deposits resulting from dilute, turbulent debris flows representing the tails of muddy turbidity currents.

Liquefied Flows

Liquefaction is the process whereby loosely packed, water saturated sediments are disturbed, the grain-supported framework temporarily broken down, the grains settle through their own upward-moving pore fluids, and a more tightly packed, more stable grain framework is re-established. Liquefied flows originate when masses of already deposited sediment liquefy and move downslope as thick, non-turbulent flows, resedimenting through the expulsion of excess pore water and the settling of grains to the base of the flow where they accumulate by direct suspension sedimentation without significant tractive movement along the bed. The resulting single flow deposits may be massive to crudely graded and commonly show water escape structures (Fig. 10).

Current structures produced by bed-load movement of grains are absent. Liquefied flows that become turbulent downslope and entrain additional water evolve into high-density turbidity currents.

Liquefaction and the development of liquified flows is favored by the deposition of fine-grained, non-cohesive sediments on slopes. Rapidly deposited fine-grained sands and silts have been shown to be particularly susceptible to liquefaction and to be capable of moving long distances as simple, laminar liquefied flows before resedimenting (Lowe, 1976).

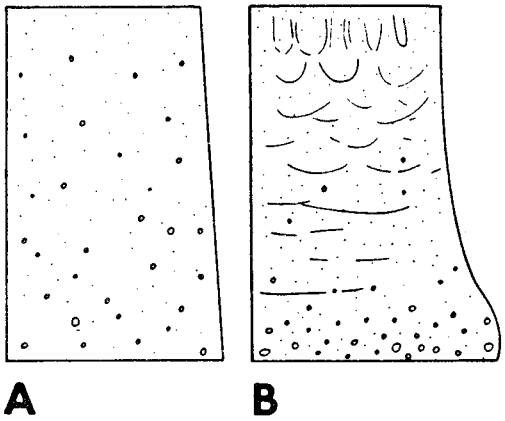

Figure 10. Liquefied flow deposits. (A) Sandy flow characterized by massive to crudely graded sand lacking current and water-escape structures. (B) Sandy to gravelly deposit showing dish and pillar structures formed by water escape.

Liquefaction may be triggered by pressure fluctuations within unstable sediments accompanying deposition, by earthquakes, or by waves. Most liquefaction occurs within the upper 50 m of the sediment pile. More deeply buried sediments bear a considerable load resulting from the accumulation of overlying layers and are less susceptible to framework breakdown and liquefaction. The setting of the Carboniferous Ouachita Trough, in which large volumes of predominantly fine-grained sediment was poured onto steep fringing slopes and delta fronts, would have been particularly conducive to the development of liquified flows.

Liquefied flows commonly originate by retrogressive failure in which an initial failure produces a scarp that migrates upslope through continued loss of support and failure of sediments along the scarp (Fig. 11). The resulting deposit consists of a sand package

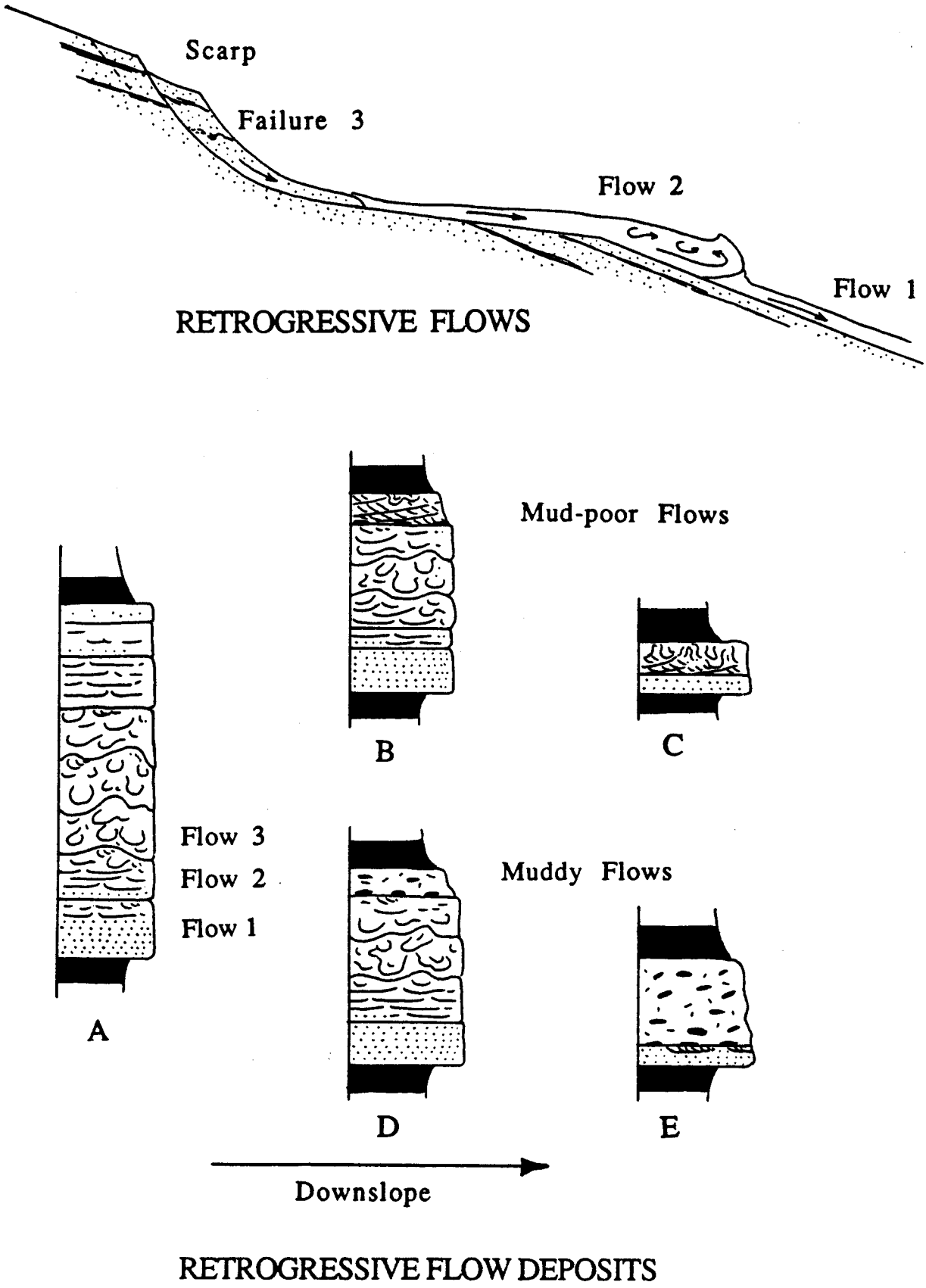

Figure 11. (Caption on following page).

made up of numerous individual flow layers or sedimentation units that were deposited in quick succession. In the Ouachitas, many sandstone packages 3 to over 15 feet thick are made up of many individual beds, commonly 5 to 15 inches thick, that are generally flat-laminated toward the base of the package and show extensive soft-sediment foundering and water-escape structures toward the middle and top of the package (Fig. 11). These packages may represent retrogressive flow sequences (Lowe, 1989).

Outcrop Gamma-ray Logging

Introduction

Interpretations of gamma-ray log shapes have been a principal tool in the analysis of subsurface depositional environments, from which variables that are important to reservoir description (such as lateral and vertical bed continuity), net pay definition, and reservoir quality can be interpreted. For example, an upward increase in API values or gamma-ray counts over a given stratigraphic interval on a gamma-ray log is often taken to indicate a vertically fining/"dirtying"-upward sandstone-shale sequence, probably laterally discontinuous and having a lenticular geometry (Selley, 1979; Shanmugam and Moiola, 1988). Conversely, an upward decrease in API values or counts over a given stratigraphic interval is often taken to indicate a vertically coarsening/"cleaning"-upward sandstone-shale sequence, probably laterally continuous and having a lobate or sheet-like geometry (Selley, 1979; Shanmugan and Moiola, 1988). Unfortunately, gamma-ray log shapes may be affected by a number of geological variables other than grain-size and clay content, so that interpretations given in the examples above may be erroneous (Rider, 1990).

Two techniques were utilized to generate gamma-ray logs of outcrops viewed on this field trip. These techniques allow the direct observation and measurement of characteristics of the strata responsible for a particular gamma-ray log response.

These techniques have been successfully utilized in order to demonstrate to geologists, engineers, and geophysicists the applications and potential pitfalls of gamma-ray log

Figure 11. Retrogressive flows (top) and retrogressive flow deposits (bottom).

Top. Retrogressive flows form when an initial failure forms a scarp. Successive failures along the scarp result in scarp retreat and the generation of a series af flows that move downslope, accelerate, become turbulent, and evolve into turbidity currents.

Bottom. As seen in the Jackfork Group, many sandstone units are composite layers made up of a number, commonly 3 to 12, of individual sandstone beds, each probably representing an individual flow. Individual flow units in the Ouachitas are between 5 and 15 inches thick; thicker flow packages range from about 3 to over 15 feet thick. "A" shows a generalized flow package in a proximal setting. It consists of several discrete flow units. In the Ouachitas, flow units toward the middle of thicker flow packages show undulating contacts representing zones of liquefaction and soft-sediment loading and foundering. Downslope, flow behavior depends on the amount of entrained mud. Purely mud flows would evolve as a series of debris flows (not shown). Mud-poor flows tend to leave packages that pass upward into cross-laminated units in intermediate (mid-fan ?) regions ("B") and into thin flat- (Tb) and cross-laminated (Tc) turbidites at their distal extents ("C"). Muddy flows develop tails that are watery, mobile debris flows. These deposit slurried muddy sand beds above the current deposits in intermediate ("D") and distal ("E") regions. Some distal deposits consist largely of sandy debris flows separated by fine, organic-rich, laminated, hemipelagic shales.

interpretation of vertical sequences, depositional environments, and reservoir quality from a single well, as well as lateral correlation and continuity of beds between wells. Also, by generating gamma-ray logs of outcrop strata that are analogous to subsurface oil and gas fields or exploration prospects, reservoir geologists/engineers and explorationists can obtain a much better understanding of their field or prospect from gamma-ray logs in surrounding outcrops and wells. Geologists in the past have sometimes measured gamma radiation of outcrops with a hand-held scintillometer in order to evaluate lithology and organic content of beds, as well as to correlate strata between outcrop sections and subsurface wells (Provo et al., 1977; Howe, 1989). The purpose of logging outcrops in the Jackfork Group is to expand upon these efforts.

The two different techniques utilized for outcrop gamma-ray logging are used under different conditions. The first technique employs a standard scintillometer tool (sonde) run from a typical logging truck. This technique is used to log cliff or quarry faces that are inaccessible by foot. The second technique uses a commercial, hand-held gamma-ray scintillometer to log readily-accessible outcrops.

These techniques measure the characteristics of the strata responsible for a particular gamma-ray log response and demonstrate applications and potential pitfalls of interpreting vertical sequences, depositional environments, lateral continuity, and reservoir quality from gamma-ray logs. Analysis of outcrop gamma-ray logs from a locality considered to be analogous to an oil field or exploration prospect can help reservoir geologists/engineers and explorationists obtain a much better understanding of their field or prospect.

Most subsurface logs represent data at a single line or point in space, but these data may change rapidly in a very short distance away from a borehole. It is therefore important to have a knowledge of the depositional system in order to reduce risk in interpreting log patterns for resource prediction and evaluation. Logging of strata exposed in outcrops where the geometry and stratification character of the deposit can be observed is the focus of this portion of the guidebook.

Truck-Mounted Gamma-Ray Sonde

The gamma-ray sonde that is used in this study is about 7 feet long and weighs approximately 100 pounds. This sonde is sufficiently sturdy so that the source crystal can withstand the impacts it receives as the tool is lowered and raised along the rock face.

A standard logging truck is driven to the top of the quarry or cliff to a pre-selected logging site, which is typically a smooth, vertical cliff with few obstructions. A small tripod with a sheave-wheel on top is positioned at the cliff edge to guide the logging cable over the edge. The sonde is lowered down the vertical face by cable to the base of the cliff (Fig. 12). The sonde is then raised at a constant rate (10 ft/min) and gamma-ray measurements are continuously recorded. The logging rate is slower than conventional (borehole) rates since, on a cliff face, the gamma-ray tool is exposed to less than half of the rock mass normally encountered in a borehole.

A rope is attached to the base of the sonde and is used to guide the sonde past protuberances as it is drawn upward (Fig. 12). This technique is also necessary to ensure that the tool is kept in close proximity to the cliff face.

Gamma-ray measurements in subsurface logs can be affected by minor borehole washouts (especially when used with a heavy mud); however, extraordinarily large cave-ins or solution caves can significantly decrease the count rate. Tests at the outcrop were performed to determine the maximum distance away from a cliff face that the gamma-ray tool could be positioned before the count rate is adversely effected. Repeated measurements of a single sample site show that the sonde may be up to 2 feet away from the face and have little effect on the count rate. However, the variance in count rate significantly increases beyond this distance.

Other steps useful to ensure quality outcrop logs include: (1) having photographs of the cliff available during logging, (2) hanging a scale marked at one-foot increments over the

cliff during photographing and logging (Fig. 12), (3) providing walkie-talkie communication between the logging truck and the ground observer, and (4) marking on the sonde the exact gamma-ray recording point (mid-way down the length of the sonde) so that the observer on the ground can mark on the photographs, and/or relay to the logging truck via walkie-talkie, the exact location on the cliff of any key measurement site.

Upon completion of logging, the data can be displayed in a standard depth format (Fig. 12).

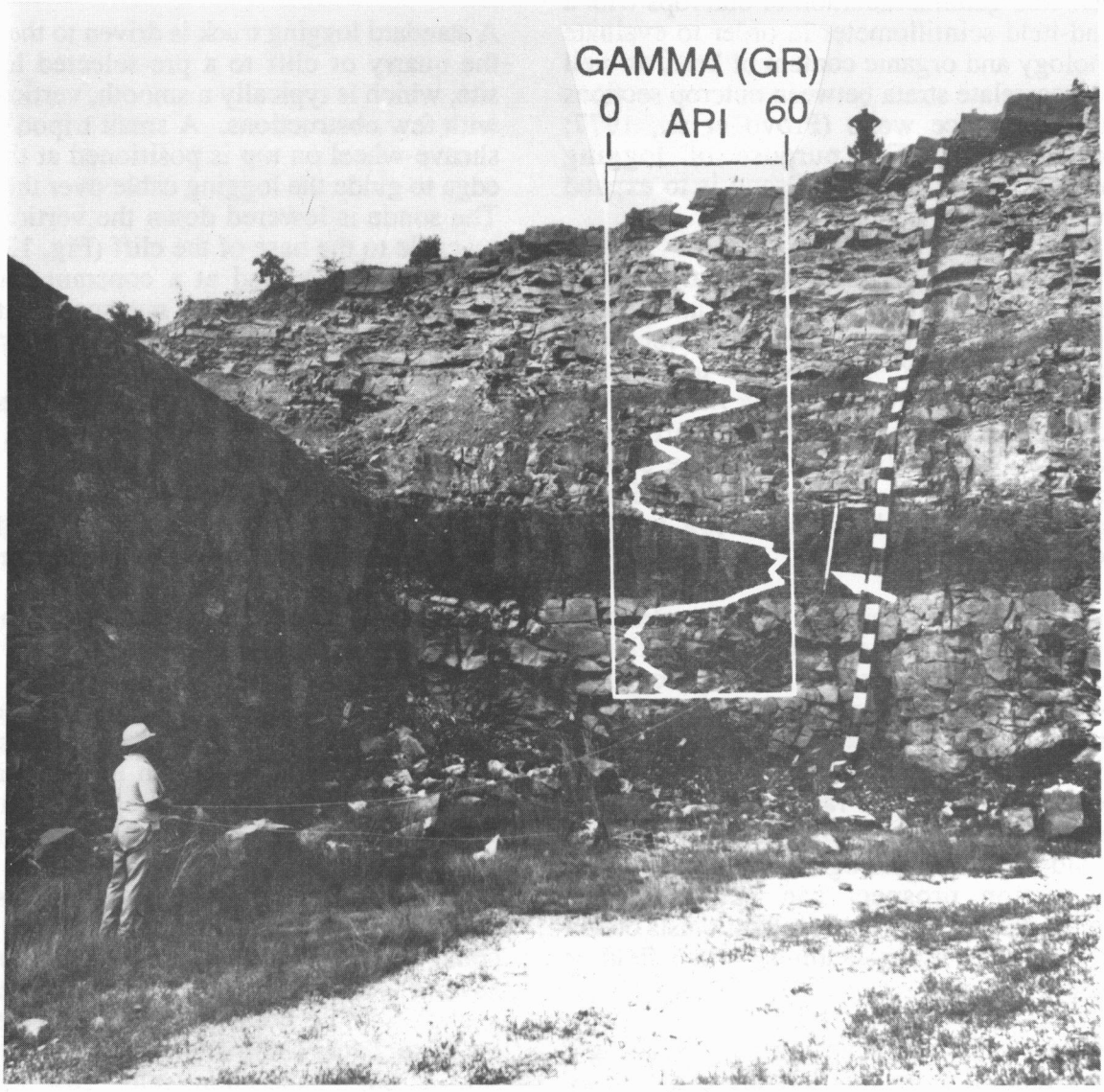

Figure 12. One method of gamma-ray outcrop logging used in this guidebook. Sonde (large arrow) is raised from the base of the west wall of Hollywood Quarry (STOP 7) by a cable (small arrow) attached to the logging truck (not in view). The person at the base of the quarry wall is using a rope attached to the sonde to guide it past rock protuberances as it is drawn upward. This logging run produced the gamma-ray log that is superimposed upon the quarry wall in the photograph. Note the scale marked in one foot increments.

Hand-Held Gamma-Ray Scintillometer

For this type of logging, a lightweight, portable Scintrex™ GIS-5 Integrating Gamma Spectrometer is used. This instrument has the capability of measuring elemental or total radiation. The instrument is allowed to warm up and, after calibration, the "Total Count" mode is selected. Background radiation is considered to be relatively constant. Further details on the mechanics and specifications of the instrument are found in the Scintrex™ manual.

The method of obtaining values at the outcrop is to simply lay the edge of the scintillometer that contains the sodium iodide detector on the rock surface (Fig. 13), select the appropriate count time (the method is described below), and push the reset button to begin gathering data. Typically, measurements are made at two-foot sample intervals. Caution is exercised to ensure that true vertical thickness is measured to define each sample increment. Selected stratigraphic sections are also logged at half-foot intervals, which provides more detail. This aspect is discussed in a later section of this guidebook.

Tests in the field were conducted to determine the optimal sampling rate and number. Three, 5, and 10 measurements with sampling rates of 1, 3, 10, and 100 seconds (the only rates available on the Scintrex™ model that was used) at each station were compared. For example, a gamma-ray reading at a 10 second sampling rate was found to be almost exactly the same as a 3 second reading multiplied by 3.33. It was concluded that the most efficient method of obtaining data is to take five total count readings for three seconds each. The highest and lowest values are discarded, and the other three readings are averaged to give the gamma-ray value at that station. The data can then be displayed in standard well log curves as a function of stratigraphic depth, utilizing a scale calibrated in "counts per second". But since the original data are collected at 3 second sampling rates, it is recognized that the scale is actually displaying "counts per 3 seconds".

A typical example of gamma-ray logs obtained with the hand-held scintillometer is shown in Figure 14, superimposed on an outcrop face.

Figure 13. Another method of sampling outcrop face with hand-held, gamma-ray spectrometer.

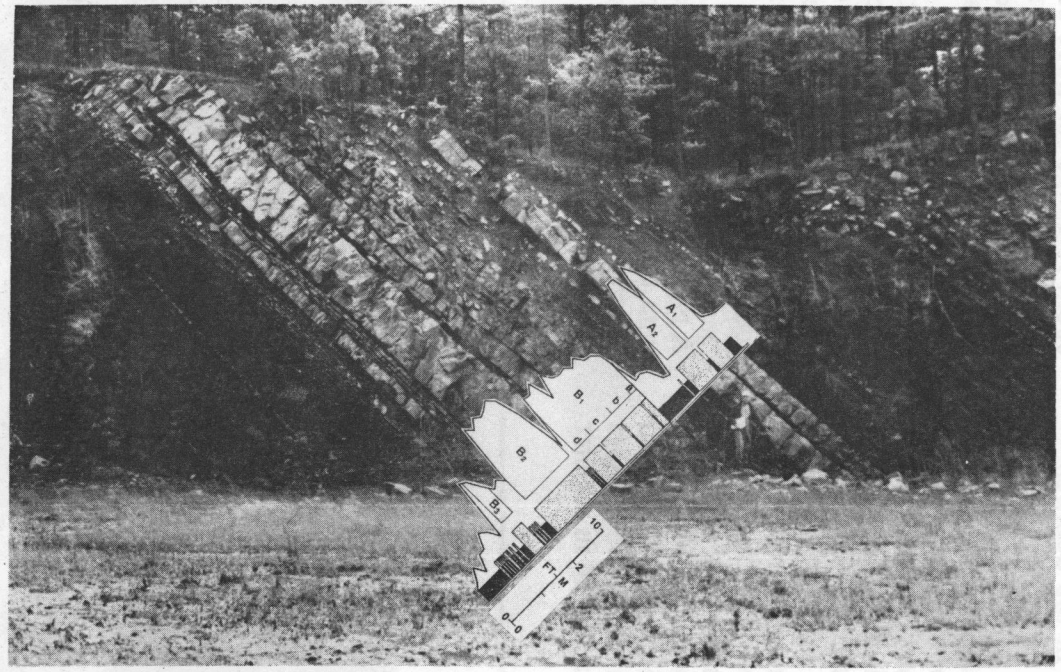

Figure 14. Gamma-ray log obtained with a hand-held scintillometer (0.5 foot sample spacing) and detailed measured section along the east wall of DeGray Lake Spillway (STOP 5).

Field Trip Itinerary and Description (Day 1)

Laterally Discontinuous, Lenticular Facies

Stop 1

Big Rock Quarry, North Little Rock, Arkansas

Purpose:

The purpose of this first stop of the field trip is to investigate sedimentary processes, reservoir and field-scale heterogeneities, and methods of modelling in a "proximal" deep-water depositional setting.

Description of Locality

Big Rock Quarry, located along the north bank of the Arkansas River in North Little Rock, Arkansas (Fig. 15), provides perhaps the largest continuous exposure of proximal deep-sea flysch deposits in North America. The quarry was a source of crushed stone in the 1950's but is used today mainly for storage of sand dredged from the Arkansas River.

The vertical faces of Big Rock Quarry expose a two-dimensional view of the lower part of the upper Jackfork Group that is up to 200 feet high and nearly 3000 feet long. Lower Jackfork shales are exposed in the floor of the northern part of the quarry. Regional paleocurrent analysis (Morris, 1977) and facies studies (Link and Roberts, 1986) suggest that this area lay close to the northeastern edge of the deep-water Ouachita Trough during Jackfork deposition. Sediments from sources in the Appalachian Mountains, more southern orogens, and possibly the Canadian Shield, moved across alluvial and deltaic plains, poured onto the fringing slopes leading into the deep-water trough, and flowed generally westward within the basin. Rocks exposed within the quarry are thought to represent some of the most proximal Jackfork units in the Ouachita Mountains.

Previous interpretations have suggested that this quarry contained fourteen upper submarine fan channel deposits (and the sequence pinches out about 2.5 miles away) (Stone and McFarland, 1981); at least fourteen coalescing and stacked channelized packages of an inner (upper) fan valley (Moiola and Shanmugam, 1984); and channel-fill and levee deposits in a submarine canyon or upper part of a submarine fan channel system (inner fan valley system) (Link and Stone, 1986a; Link and Roberts, 1986). The lateral dimensions of the major sandstone bodies are unknown but may have reached several miles (Fig. 16; see discussion under 'Interpretation' heading).

Figure 15. (figure shown on page 26). Topographic map (courtesy of the Arkansas Geological Commission) of the Big Rock Quarry and surrounding area. Very small arrows starting at southwest end of bridge spanning the Arkansas River over Murray Lake traces route of field trip from hotel to Big Rock Quarry (STOP 1). 'Gloops and glumps' are local terms referring to large sandstone olistoliths comprising parts of the Jackfork Group. Jackfork sections at Oak Grove Quarry and Jeffrey Quarry depict the lateral extent of the sandy deposits exposed at Big Rock Quarry. Levy Cut, located south of Interstate 40 on State Route 365, is briefly discussed in the text.

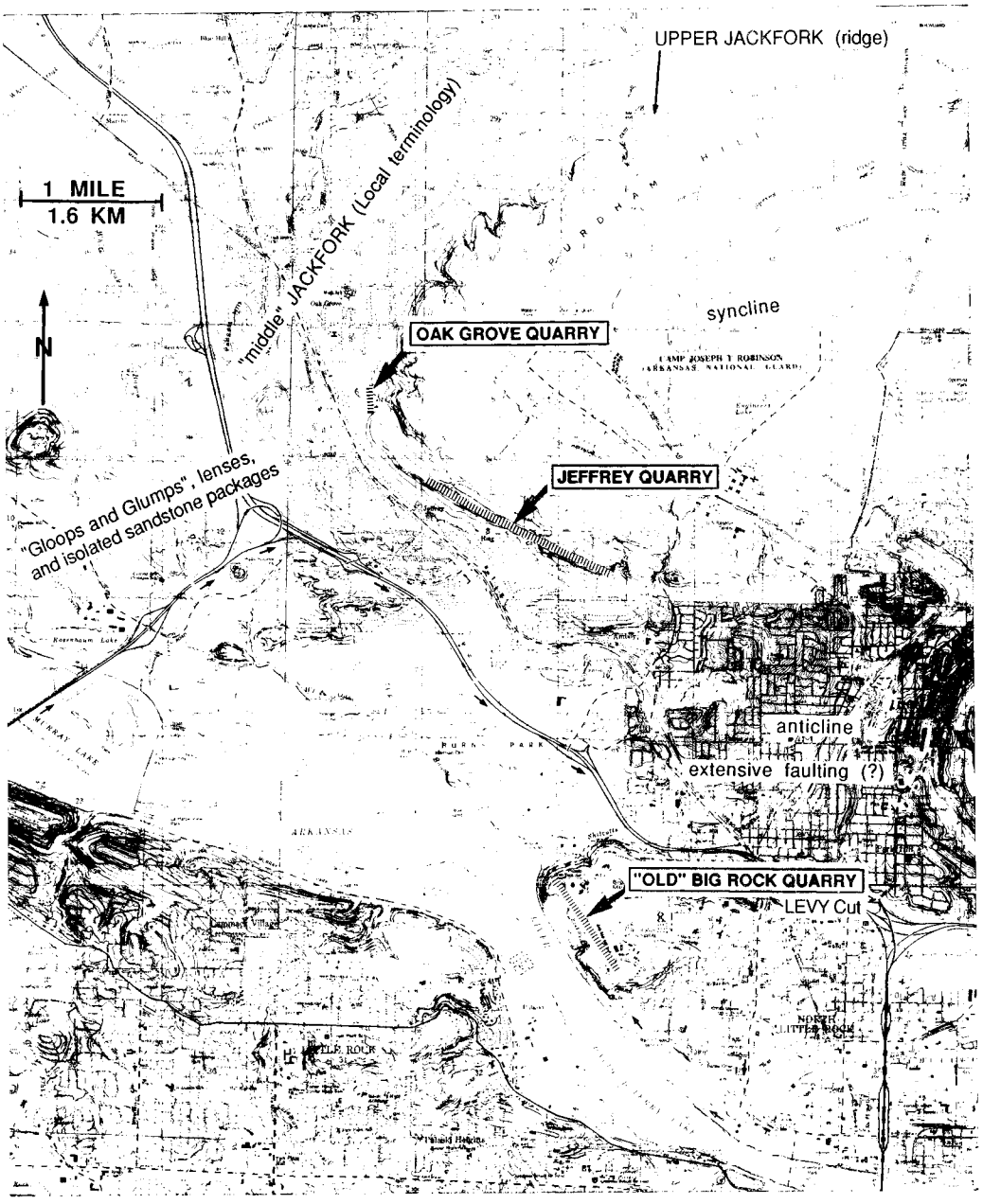

Stratigraphy and Sedimentation

The quarry section can be divided into three main lithologic units (Fig. 17) : (1) a basal unit, representing the upper portion of the lower Jackfork Group, (2) a section of sandstone and shale, 75 to 150 feet thick, at the base of the upper Jackfork Group, and (3) a capping unit of interbedded shale-clast breccia and sandstone.

The lower Jackfork mudstone underlies much of the quarry floor, but is well exposed only toward the northwestern end of the quarry. The erosive nature of the lower to upper Jackfork contact is well exposed at the Levy outcrop section (Fig. 18) and at the I-430 outcrop (STOP 2). At the Levy outcrop, about 3 miles northwest of Big Rock Quarry, upper Jackfork sandstones fill a large channel cut into underlying lower Jackfork mudstone. The mixing and deformation exhibited by the basal shale here and in adjacent outcrops suggest that it may constitute either a large

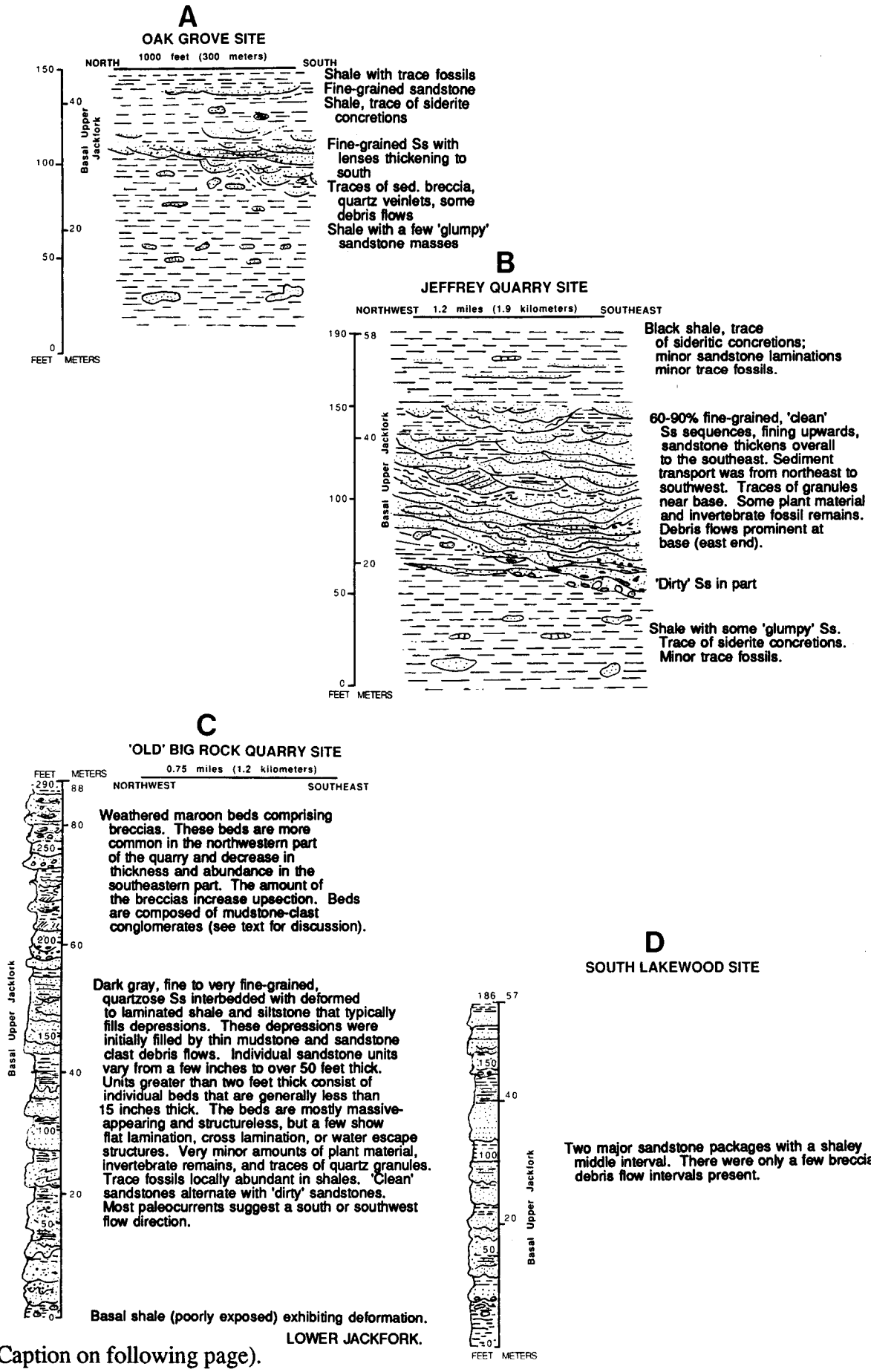

Figure 16. (Caption on following page).

slump sheet, emplaced before deposition of the upper Jackfork sandstone and shale, or that the upper Jackfork is a large soft-sediment glide or tectonic sheet emplaced by shearing along the contact.

Within the sandstone and shale section exposed in Big Rock Quarry, virtually every major and minor lithologic unit is discontinuous. Individual units vary from a few inches to over 50 feet thick. Units greater than two feet thick invariably consist of individual beds or layers that are generally less than 15 inches thick, and are composed of dark gray, fine- to very fine-grained quartzose sandstone. The beds are mostly massive-appearing and structureless but a few show flat lamination, cross lamination, or water escape structures. Wavy and undulatory bed contacts are common and were probably produced by liquefaction and sediment foundering. Most beds were emplaced by turbidity currents. The thinness of individual beds and the paucity of ripped up mudstone clasts and clearly scoured bases suggests, however, that the currents were not highly erosive.

Thicker sandstone units, from 5 to 50 feet thick, are lenticular and interrupted by inclined accretionary bedding, truncation surfaces, or internal scour surfaces when traced across the outcrop. When viewed from the northwest end of the quarry (Fig. 19), a number of the thick sandstone units can be seen to lens out from southeast to northwest against the overlying breccia. These units could represent sheets that moved downslope as large slides.

In the southeastern part of the quarry, near the base (Fig. 20), many small, scoured depressions are eroded into sandstone units. These depressions were filled initially by thin mudstone- and sandstone-clast debris flows or drapes of laminated mudstone. The common association of scours, mud drapes, and small debris flows suggests that after the scours were cut, they were draped by fine muddy sediments. These observations are supported by the core description of Link and Stone (1986a), discussed later. An excellent example of a larger scale, shale-draped scour filled by sandstone occurs approximately 7 miles north of Big Rock Quarry at Jeffrey Quarry (Fig. 21; see Fig. 15 for location).

These scours are unusual because they are not filled with coarser sediment or lag deposits left by energetic erosive currents that would be required to cut the depressions if they are channels. It seems unlikely that the small debris flows at the bases of the channel-fill were effective in eroding the depressions. Possibly these features are channels eroded by turbidity currents that bypassed the local area without leaving deposits. If so, it seems unusual that the channel-fill consists largely of fine- to very fine-grained sandstone that should also have bypassed the area. More likely, the channel-like truncation surfaces represent excavations or scars left by large slope failures and slides (Fig. 22). Such failures should have been abundant on slopes leading into the deep-water trough. The contained sandstone might then represent sediments trapped in the scar and locally left on the slope during large-scale floods of

---

Figure 16. (shown on page 27). Schematic field sketches depicting lithology and lateral extent of northern part of sandy submarine canyon fill near Little Rock. Refer to Figure 15 for locations of sections oriented in a generally north to south direction which may have been the orientation of the canyon opening. Sediments were fed generally from east to west. (A) Basal upper Jackfork sandstones near the axis of the March Syncline at the Oak Grove site. The strata strike north-south and dip some 10° to the east. (B) Laterally equivalent to sequence in A, but sequence contains more sandstone (it is presumably closer to the axis of the ancient submarine canyon); south flank of Marche Anticline. Strata dip 23° to the north. (C) 'Old' Big Rock Quarry within the axis of the Big Rock Syncline. Dips range from 0 to 10° across the entire exposure. The section averages 80% sandstone. (D) Column representing a series of partial exposures that were mostly destroyed during the construction of I-40 and U. S. Highways 67-167 along the southern border of Lakewood in North Little Rock, approximately 6.1 miles due east of 'Old' Big Rock Quarry. Located on the south flank of the Big Rock Syncline, the strata strike east-west and dip 30° to the north.

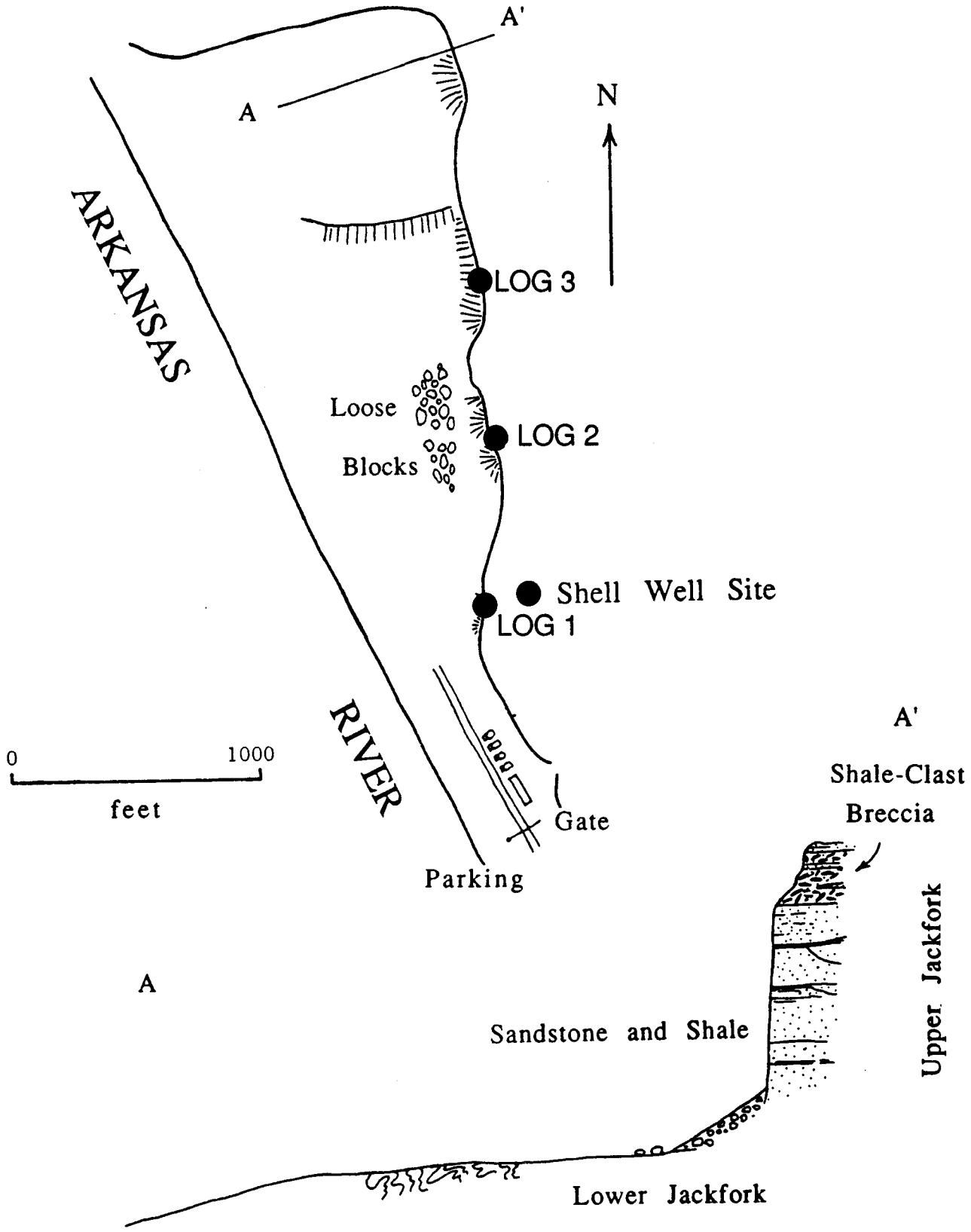

Figure 17. Generalized map and cross-section of Big Rock Quarry. Location of gamma-ray logging sites and Shell core hole are shown.

Figure 18. Upper Jackfork sandstones cut into lower Jackfork shales at the Levy cut. Note deformed nature of underlying shales and apparent lenticularity of channel sandstone.

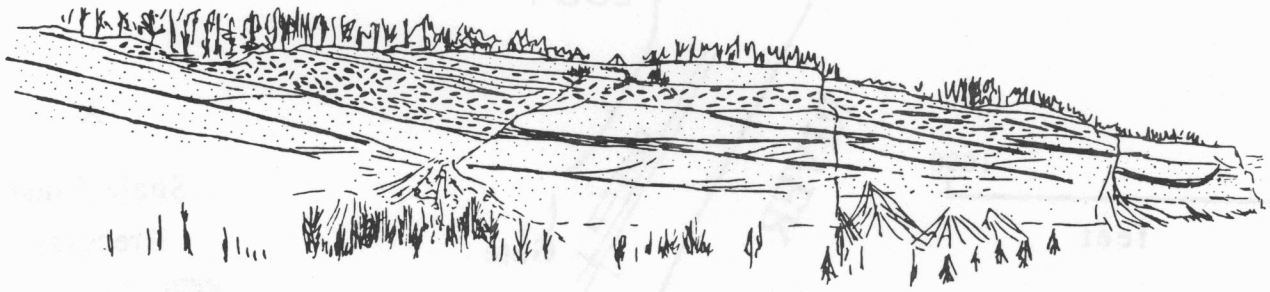

Figure 19. View from top of northern face of Big Rock Quarry showing pinching out of large sandstone packages beneath mudstone-clast breccia. Note abundance of surfaces inclined at angles to bedding and perhaps defining accretion surfaces or channel margins.

---

coarse sediment into the basin. However, the dominance of fine-grained sandstone in the quarry implies that this represents the coarsest sediment being transported across this portion of the slope. Coarser sediments may have moved through slope channels in other areas (see STOP 3), but it seems unlikely that Big Rock Quarry provides an example of proximal feeder systems. Downslope depositional sites (such as those we will see on Day 2) actually show substantially coarser-grained sediments.

The uppermost unit exposed along the quarry face consists of from 5 to 20 feet of mudstone-clast conglomerate and breccia. The matrix varies from clean fine-grained sandstone to muddy sandstone. The unit is unusual for several reasons: (1) it contains an extremely high percentage of mudstone clasts (over 50%) in a clean sandstone matrix, making it unlikely that it represents a cohesive debris flow; (2) it contains thin, undisturbed layers of sandstone from less than an inch to over 2 feet

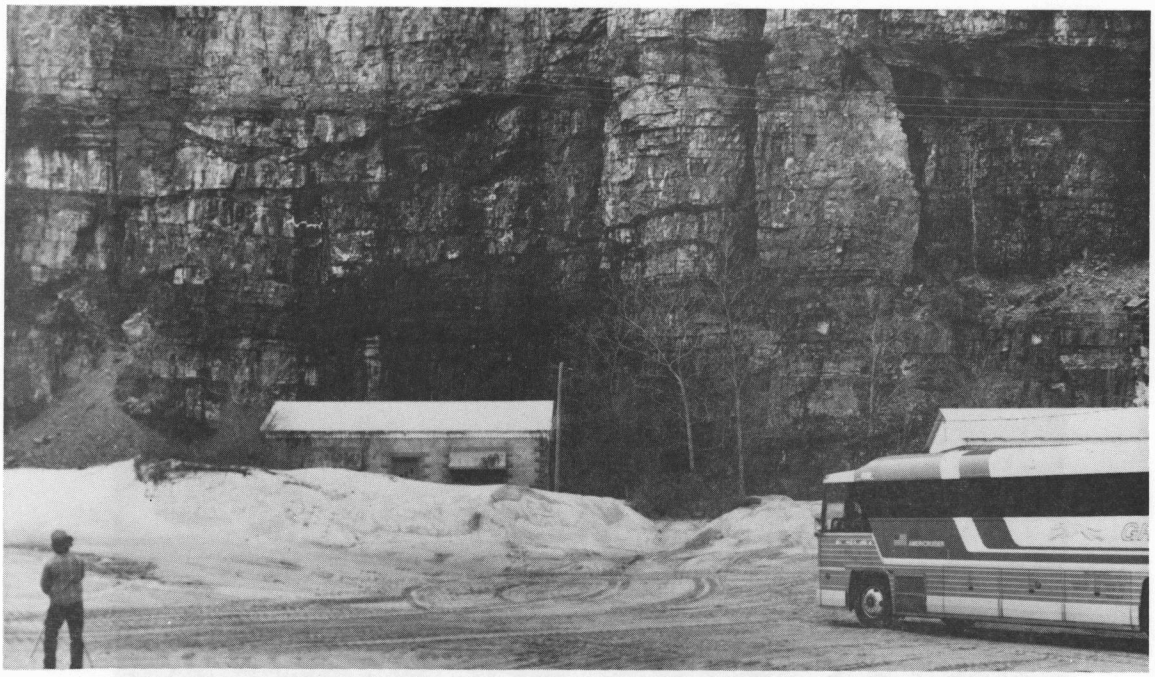

Figure 20. Southeastern part of Big Rock Quarry showing many small, scoured depressions eroded into sandstone units.

Figure 21. An excellent example of a large scale, shale-draped scour filled by sandstone. Jeffrey Quarry (see Figure 15 for location and Figure 16 for description). These scours are unusual because they are not filled with coarser sediment or log deposits left by energetic erosive currents that would be required to cut the depressions if they are channels. More likely, the channel-like truncation surfaces represent excavations or scars left by large slope failures and slides.

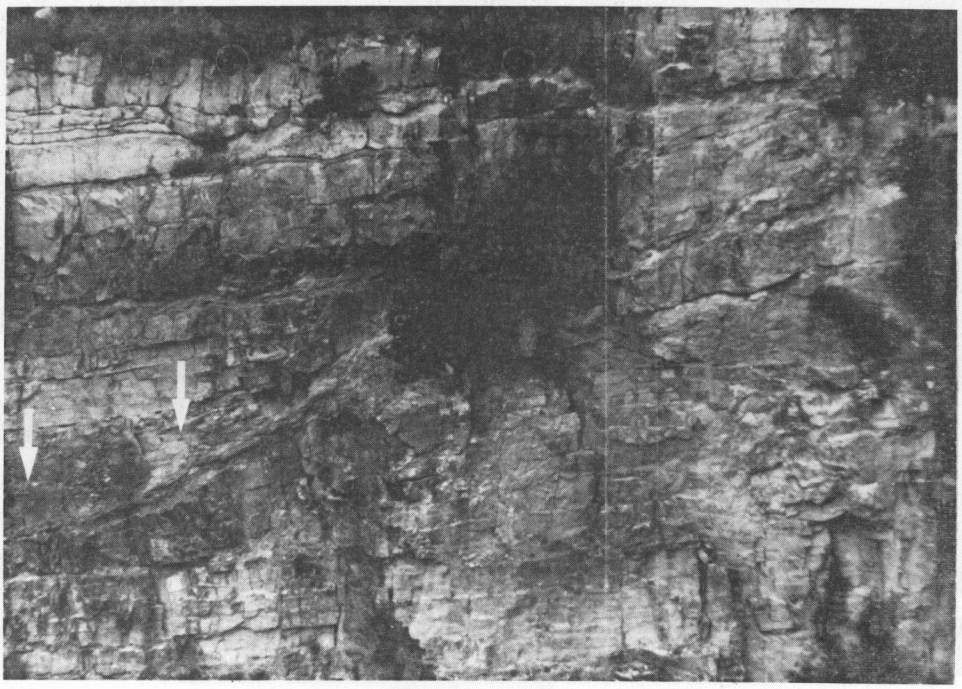

Figure 22. Northwest (approximately depositional dip-oriented) face of Big Rock Quarry showing high-angle truncation surface which may represent scar left by large slope failure and slide. Coarse conglomeratic breccia (arrows) lies above the truncation surface.

unlikely that it represents a cohesive debris flow; (2) it contains thin, undisturbed layers of sandstone from less than an inch to over 2 feet thick enclosed in breccia; (3) breccia blocks fallen to the quarry floor (Fig. 23 A-B) commonly show a crude alignment of mudstone clasts that outline original layers which have not been completely obliterated, and (4) the mudstone clasts are commonly blocky and some are oriented at nearly right angles to bedding, suggesting little shearing and squeezing during flowage. These units probably formed as dense sand slurries formed by local slope failures. Most have not travelled far. More turbulent flows moved downslope beyond the present area and may have deposited the interlensing, intact units of clean sandstone. Sandstone beds within the breccia define large low-angle cross stratification or dipping accretionary bedding (Fig. 24) that has been interpreted by some to have formed on natural levees. Mapping of these beds suggests they accreted laterally toward the north.

Interpretation

Overall, Big Rock Quarry exposes a slope or base-of-slope succession of the type that might be expected on the proximal parts of deep-sea fans within slope channels or canyons. The lateral variability of individual sedimentation units and thicker sediment packages reflects the activity of localized movements, such as slumps and slides, as well as the importance of depressions of all scales in localizing flows. Scour and successive slope failures have cut out many originally more continuous units. Sedimentation was dominated by turbidity currents, possibly liquefied flows, debris flows, and slides and slumps (Fig. 25).

The overall thickness of the sandy units exposed at Big Rock Quarry decreases in a northerly and easterly direction (see Fig. 16). and suggests that what is present within the upper Jackfork in this area represents the coarser clastic fill of a submarine (slope?) canyon. Field relationships suggest that the Big Rock Quarry and several exposures in the

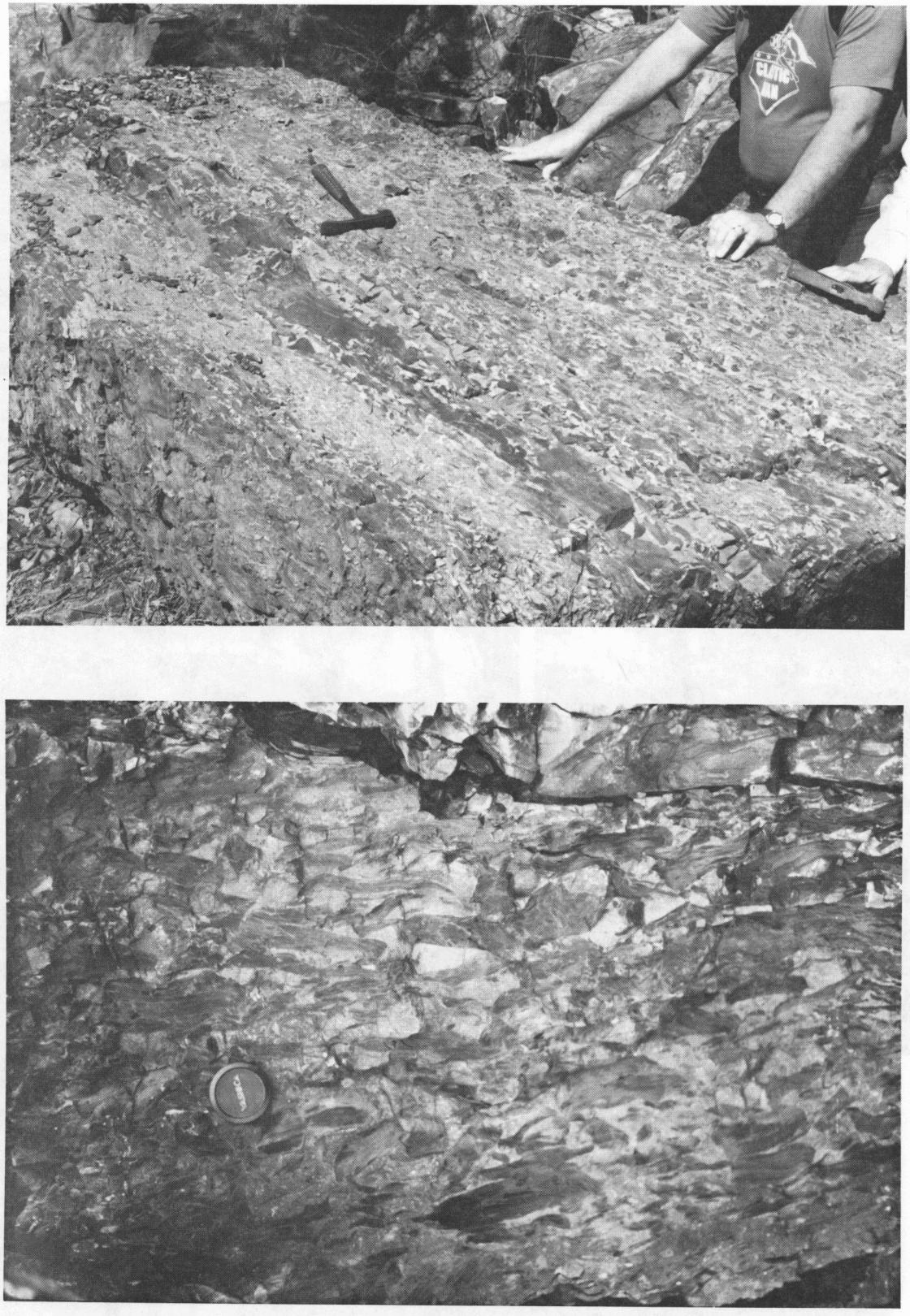

Figure 23. Fallen block on floor of quarry derived from upper part of quarry section. (A) Crude alignment of mudstone clasts that outline original layers which have not been completely obliterated. (B) Close-up of fallen block shown in A. Mudstone clasts are commonly blocky and oriented at nearly right angles to bedding, suggesting little shearing and squeezing during flowage. These units probably formed as dense sand slurries formed by local slope failures.

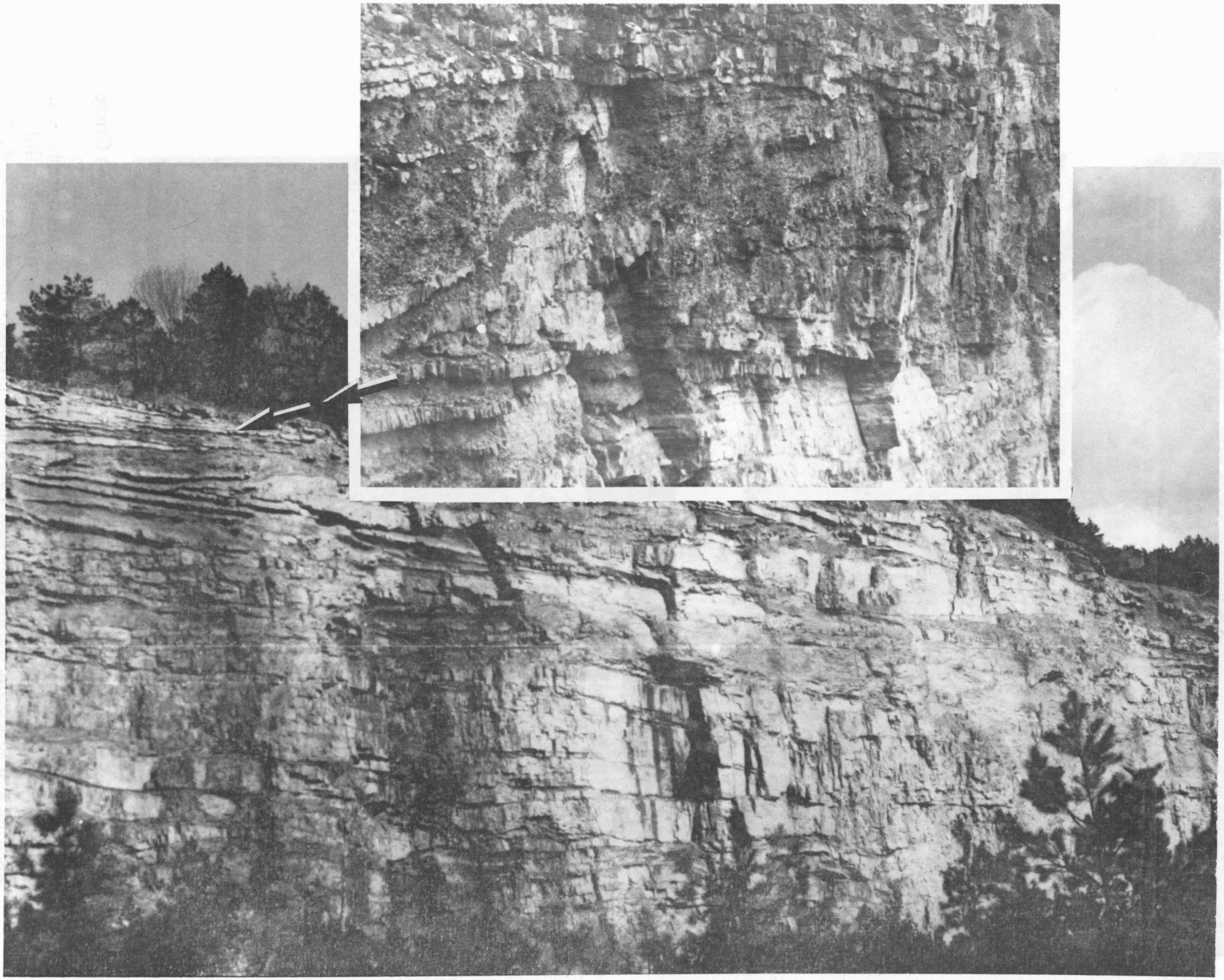

Figure 24. Quarry wall depicting sandstone beds within the breccia that define large low-angle cross stratification or dipping accretionary bedding that has been interpreted by some as having formed on natural levees. Inset details oblique view of northward-dipping strata.

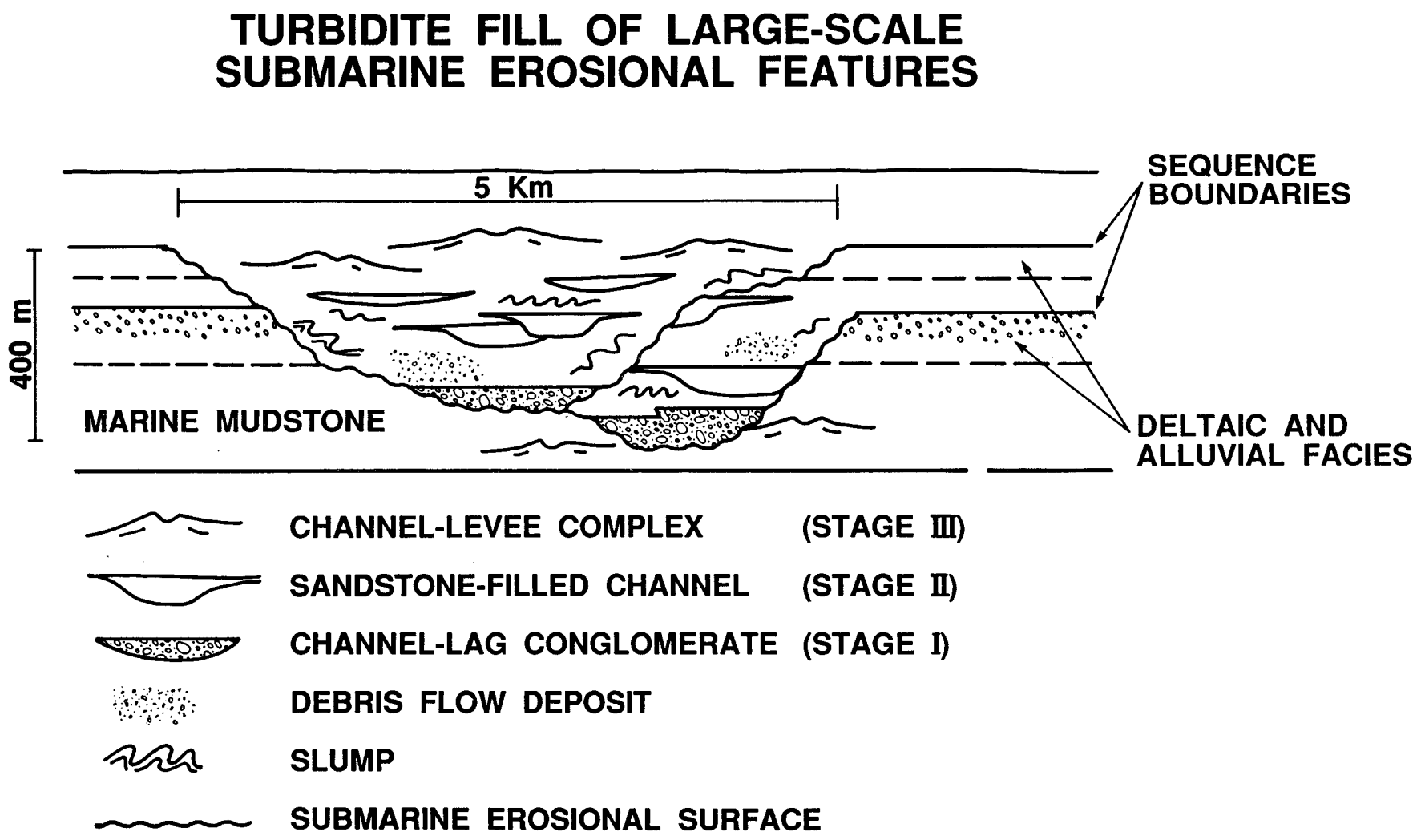

Figure 25. Fill of large-scale submarine erosional channels. Note different stages in filling of the channels (after Mutti, 1984). Sedimentary deposits comprising the sedimentary fill within the large submarine erosional feature at Big Rock Quarry include debris flow deposits, slumps, channel-lag conglomerates, sandstone-filled depressions, and possible channel-levee accretionary beds at the top of the quarry.

to the northeast of the Oak Grove site. The basal upper Jackfork Sandstone is thicker at the Big Rock Quarry site and to the west (at the I-430 roadcut) than in exposures in the northwest and southeast. This suggests proximity to the axis of the sandy submarine canyon fill.

Reservoir Implications: Log Correlation of Laterally Discontinuous Strata

Three gamma-ray logs, obtained with a logging truck and spaced 500 and 600 feet apart (Fig. 26), were measured along the northeast quarry wall. A close-up view of the stratification and correlative gamma-ray log at log station #1 is shown in Figure 27. Description of a detailed lithologic section was not possible because of the steepness of the quarry wall. However, Figure 28 compares log #1 with a subsurface core of the upper part of the same interval taken approximately 50 feet behind the quarry wall several years ago by Shell Oil Company and described by Link and Stone (1986). The correlation between the log response and gross lithology is good. The exception to this occurs in the thinly-bedded interval between 20 and 40 feet. The log response depicts this interval as a thicker sandstone sequence than is actually the case.

The three logs (Fig. 29) taken at this site illustrate potential problems in well log correlation of laterally discontinuous strata. On several field trips, participants have correlated these logs prior to examining the outcrop (Fig. 30A-C). Typically four or five distinct stratigraphic intervals are subdivided on the logs (Fig. 30A). However, when the quarry is examined, most beds are not laterally continuous at the 500 and 600 foot spacing of the logs. A better correlation, made after studying the quarry face, is shown in Figure 31. In comparing this correlation to that shown in Figures 29 and 30, it is particularly noteworthy that the thick sandstone from 88-168 feet on Log #2 is a discontinuous sandstone slump upon which younger sandstone beds onlap, and (2) the cleaning upward sandstone unit at 0-30 feet on Log #3 is a laterally discontinuous sandstone bed near the top of the quarry face. In the subsurface, these beds, though thick, would not extend between typically-spaced wells (40 acre spacing), so knowledge of the expected depositional geometries would help clarify the degree of uncertainty associated with well log correlations.

Sandstone/shale Ratios

Sandstone/shale ratios for the Jackfork exposed in Big Rock Quarry were calculated in an effort to quantify lateral and vertical variability of the deep-water facies. Ratios were determined by counting sandstones and shales within equally-sized rectangular cells superimposed on enlarged outcrop photographs (Fig. 32A). A cell contains an area that is 500 feet wide and 50 feet high. Each cell was overlain by a 0.1" x 0.1" grid which defined the actual point that was counted. Three outcrop sections were examined.

Section 1

Three equally-sized cells were outlined on the outcrop photograph of the southeastern end of Big Rock Quarry (Fig. 32B). Sandstone/shale ratios were calculated for each cell and results are presented at the bottom of the photograph.

Comparing these results with visual observations on photographs points out: (1) overall lithologic differences between units are not as large as would be estimated by simple visual observation, and (2) the presence of thin-bedded units drastically alters interpretation of sandstone/shale ratios. For instance, cell number 3 contains lenticular sandstone bodies overlain by a combination of thick-bedded sandstones and thinly-interbedded sandstones and shales. One might visually estimate a sandstone/shale ratio of 1.5 (60% sand); however, counting the sandstones and shales within the cells produces a much higher value of 4.65 (approximately 82% sand). Based upon these counted data, this unit actually proves to be the most sand-rich of the three cells.

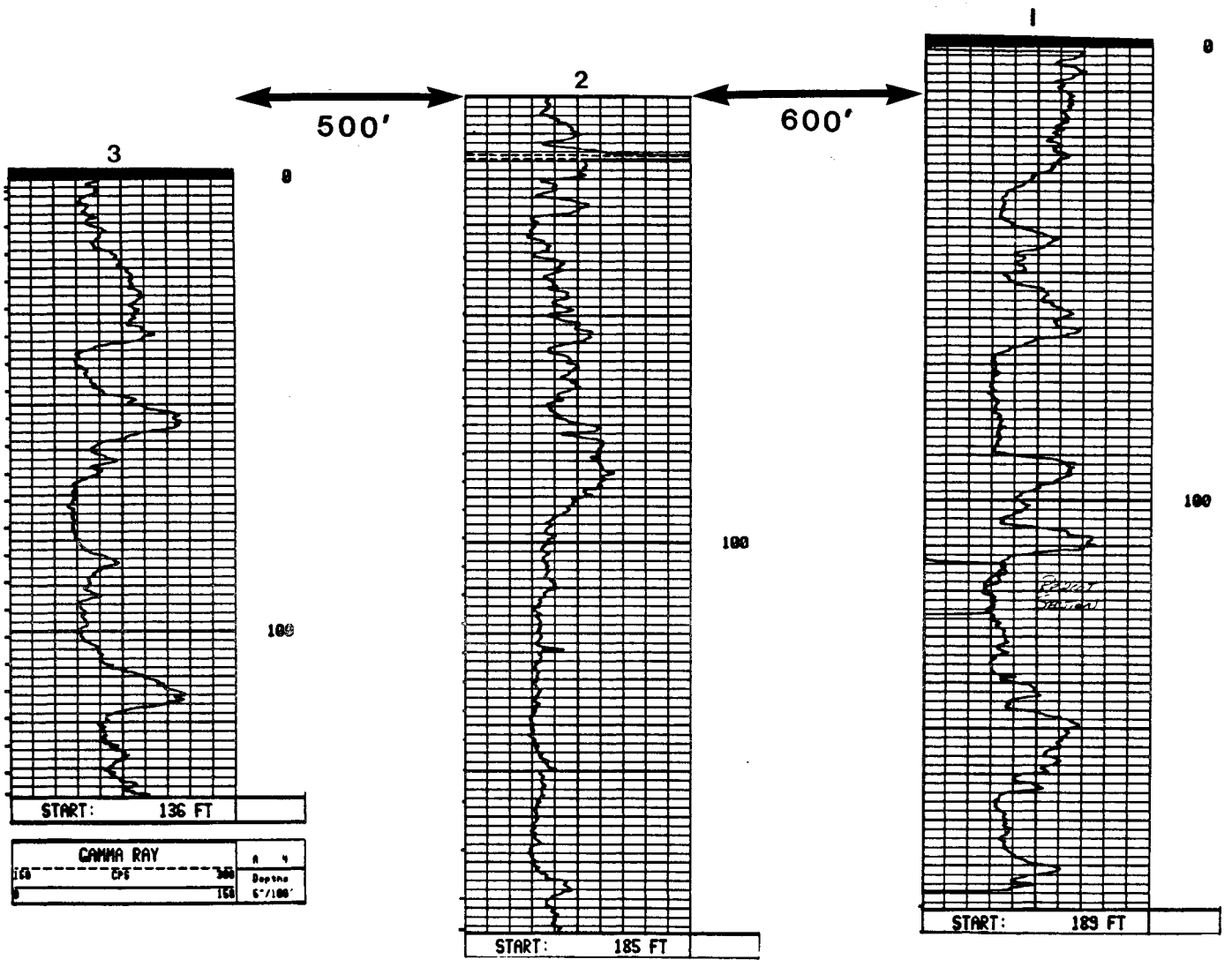

Figure 26. Gamma-ray logs obtained with a logging truck along the northeast wall of Big Rock Quarry. Datum is top of quarry.

Section 2

This outcrop section (Fig. 33A; shown in Figure 32A as the first row of cells on the far right portion of the photograph) is divided into 4 cells with each cell further subdivided into 2 sub-cells (a & b). Sandstone/shale ratios for the sub-cells and the entire cell are shown at the bottom of the photograph.

Results show that sandstone/shale ratios are vertically and laterally highly variable. The lower portion of the section contains large lenticular sandstone bodies which have high sandstone/shale ratios (3b = 5.30 and 4b = 4.64); whereas, the upper portion of the section contains thinner sandstone bodies which grade laterally into shaley deposits with lower sandstone/ shale ratios (1b = 2.76 and 2b = 2.55).

Results also indicate that sandstone/shale ratios are highly variable depending upon: (1) the lateral continuity of major units, and (2) the relationship of these units to the cell pattern established for point-counting. For example, units 3b and 3a display the most dramatic change as interbedded sandstones and shales of unit 3b (ratio = 5.3) grade into massive sandstones within unit 3a (ratio = 93.7). However, if considered as a single cell (cell 3a + 3b), the overall ratio is 9.67. This is of the same magnitude as the value for cell 3b; however, it is not of the same magnitude as

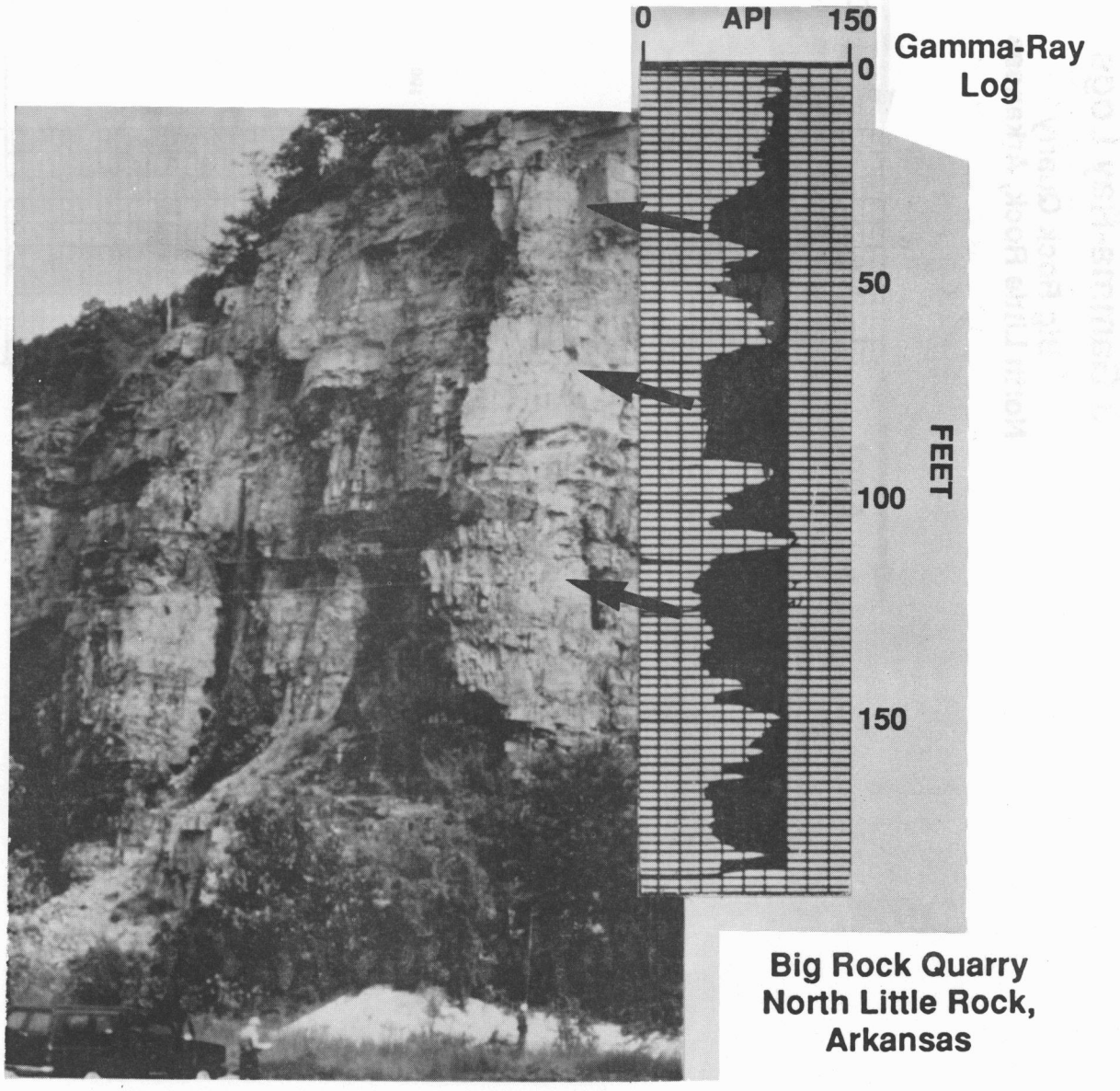

Figure 27. Comparison of gamma-ray log #1 at Big Rock Quarry with the quarry wall at the logging site. Arrows point to individual beds depicted on the log.

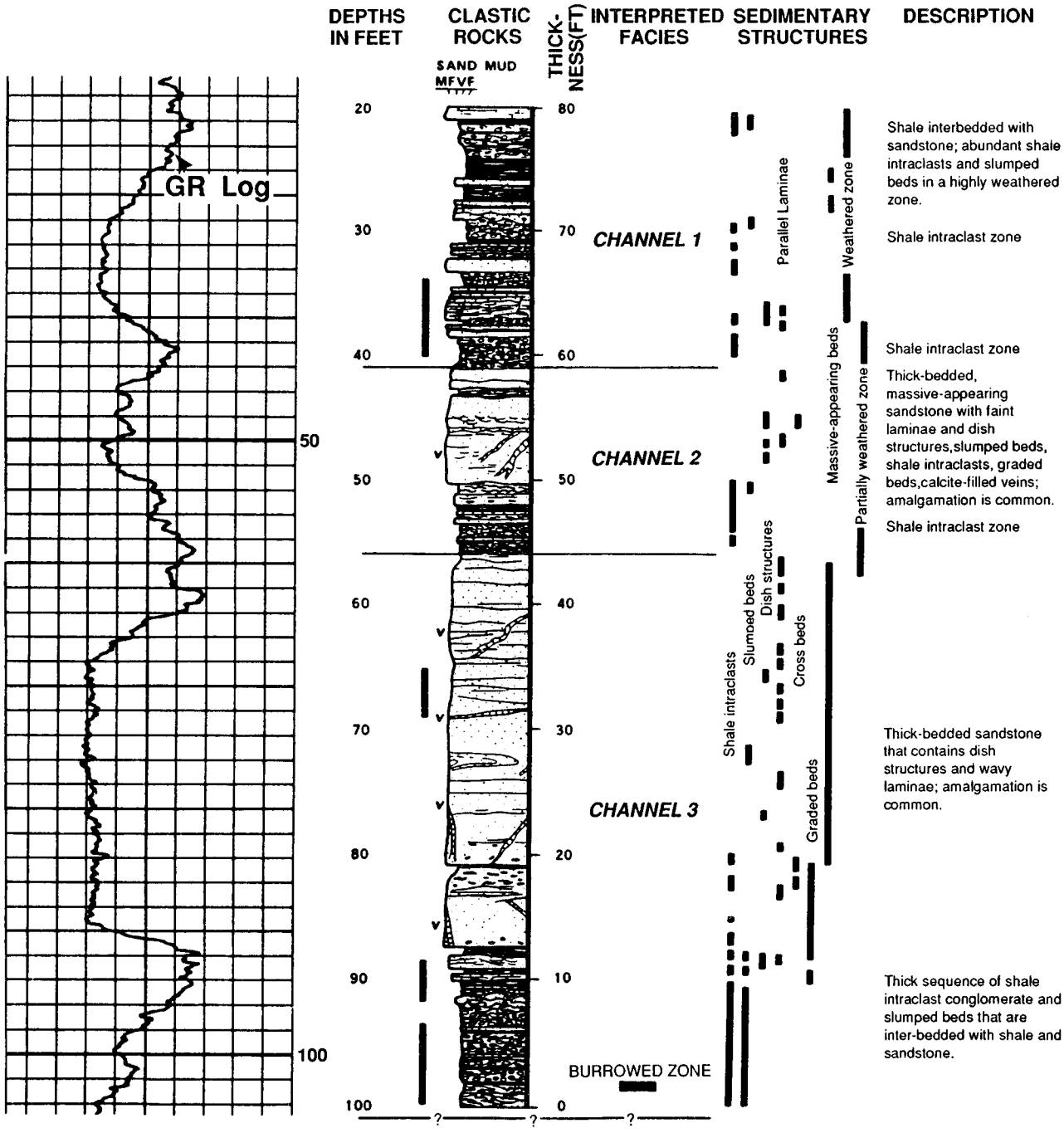

Figure 28. Comparison of gamma-ray log #1 at Big Rock Quarry with a Shell Oil Company core taken 50 feet behind the quarry face at the logging site. Core description is after Link and Stone (1986).

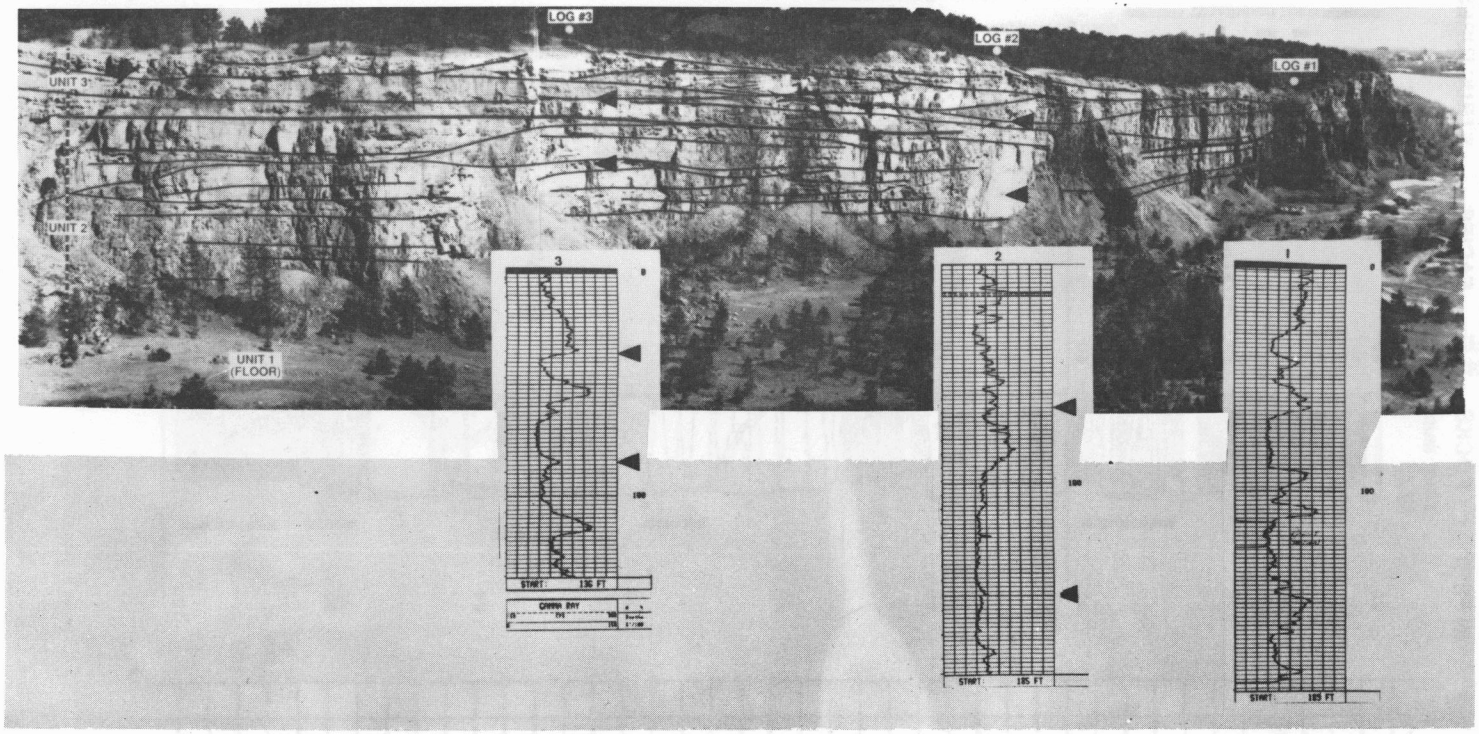

Figure 29. Three gamma-ray logs positioned at log sites on quarry face. Key bedding boundaries are outlined in black on outcrop wall. Correlation points between the log and the outcrop location of the log trace are shown at black triangles. Note extreme lenticularity. Compare with Figures 30 and 31.

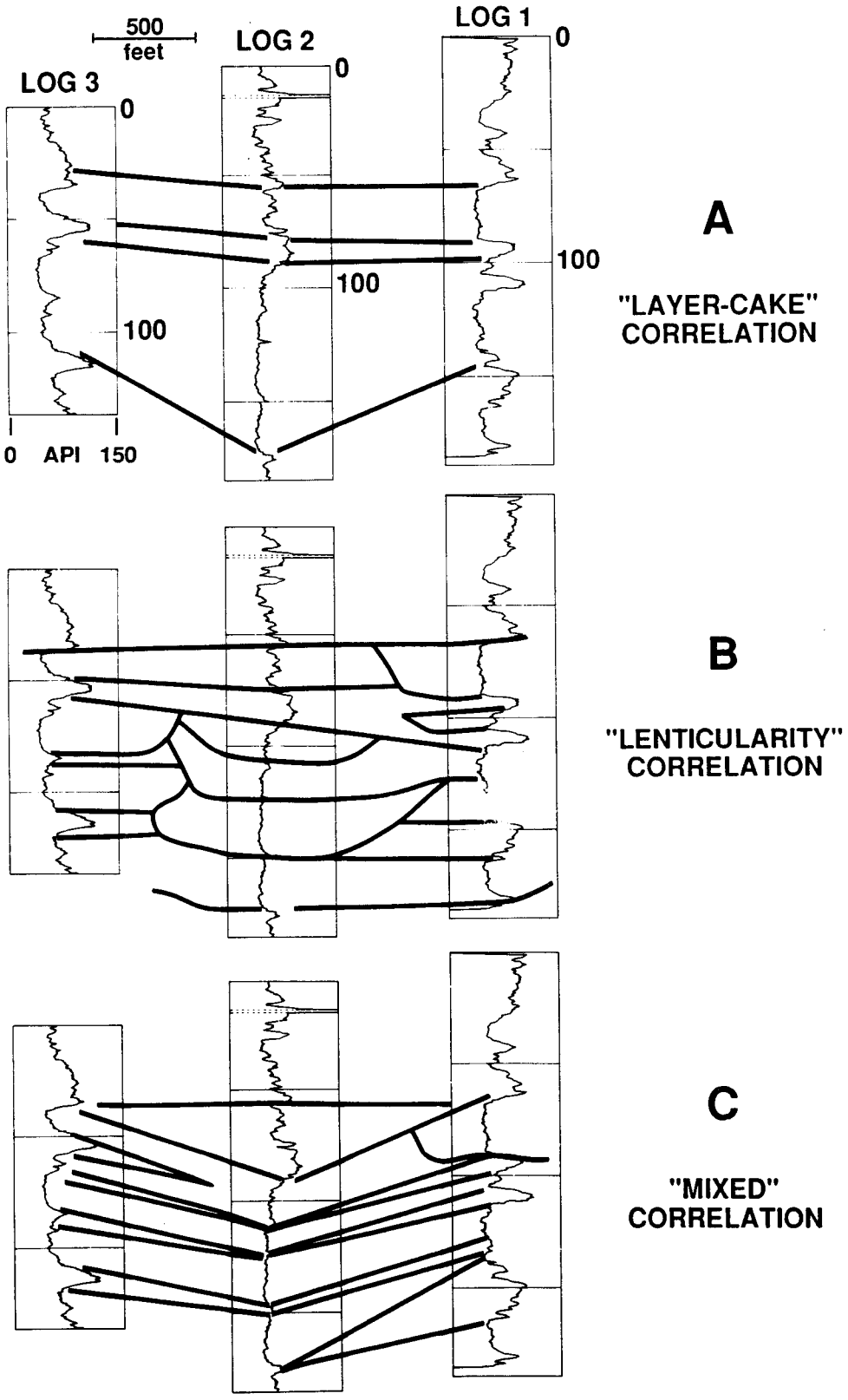

Figure 30. Three possible, but incorrect, correlations of gamma-ray logs from Big Rock Quarry, illustrating (A) layer-cake, (B) lenticular, and (C) mixed correlations. Correlation shown in A is probably the most common correlation made before studying the outcrops. Correlation in B invokes numerous channels and erosion of section. Correlation C document changes in thickness of interbedded shale.

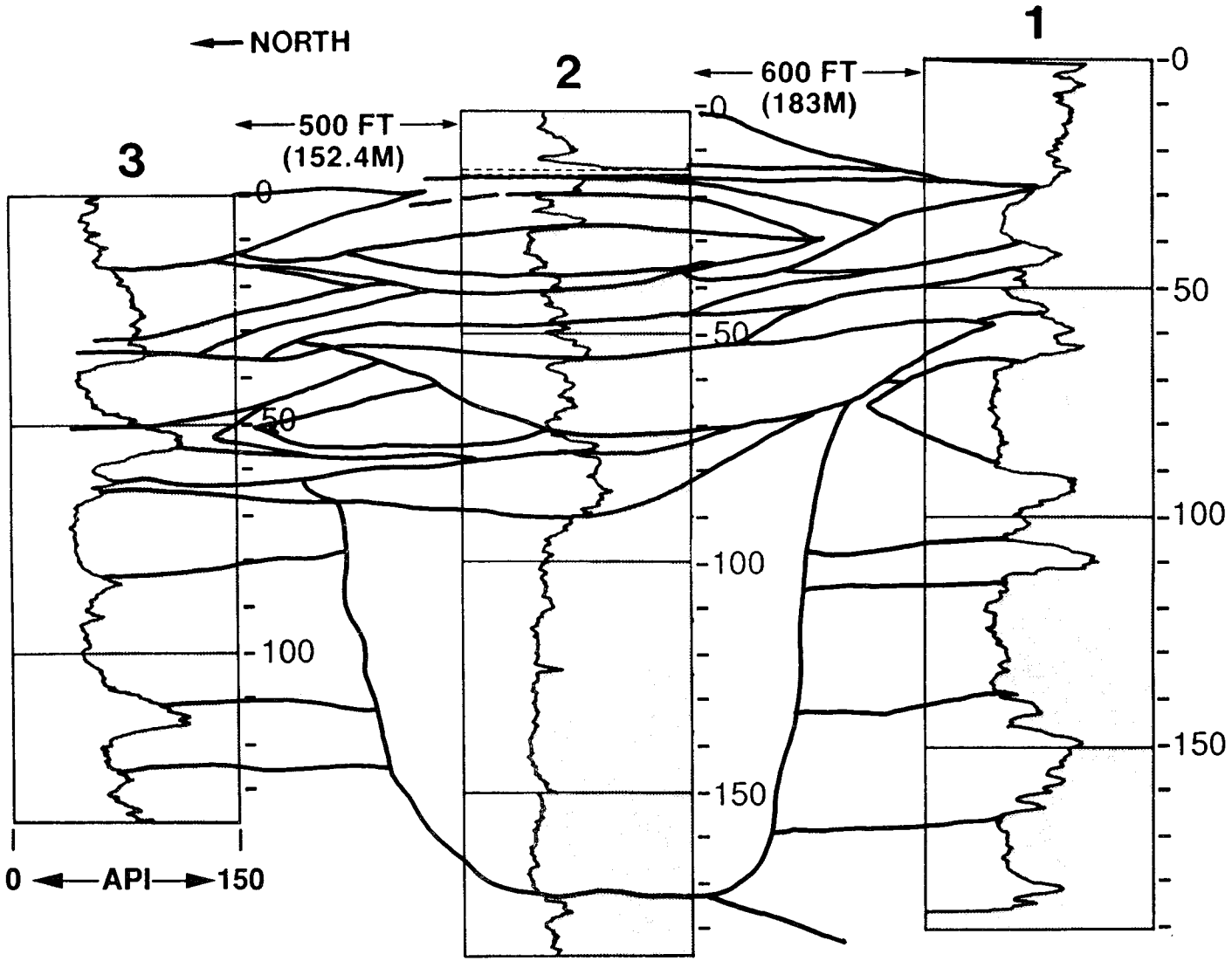

Figure 31. Stratigraphic correlations of gamma-ray logs #1, 2, and 3 at Big Rock Quarry, based on field sketches.

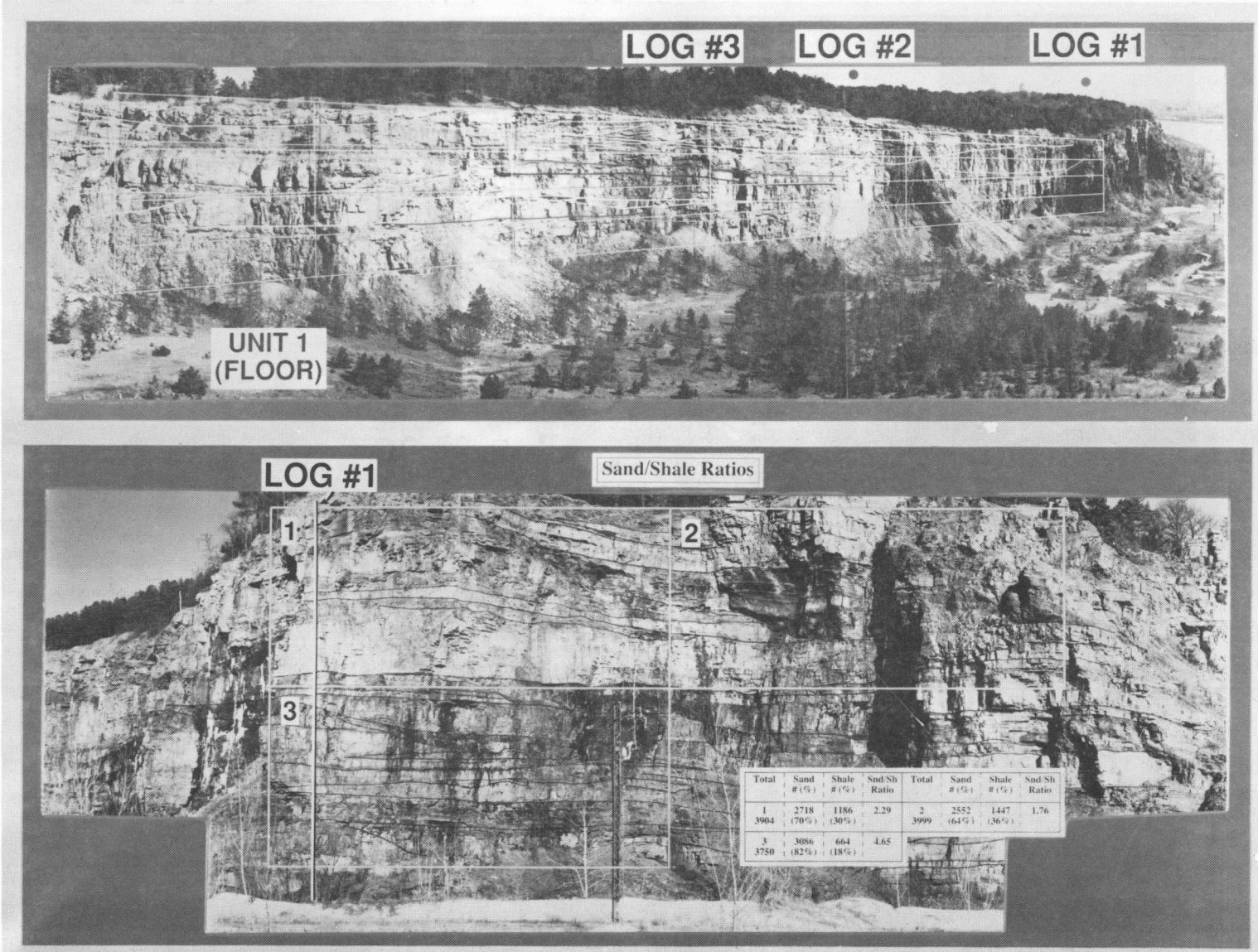

Figure 32. Grid cells and sandstone/shale ratios. (A) General view of rectangular cells (each cell is approximately 50 X 500 feet) along oblique view of Big Rock Quarry. (B) Section 1, southeastern part of quarry, with 3 rectangular cells. Location of Log #1 shown.

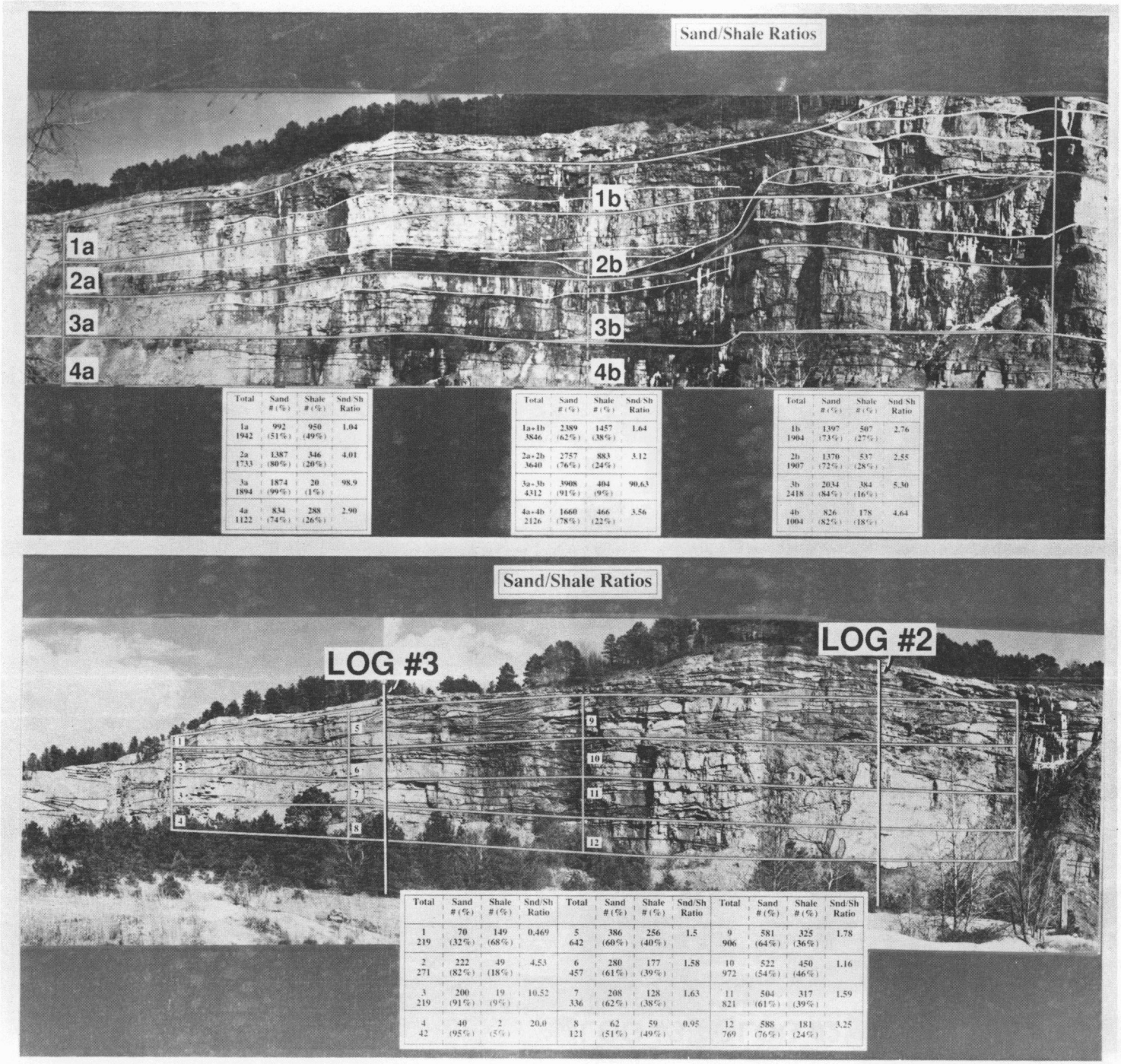

Total	Sand # (%)	Shale # (%)	Snd/Sh Ratio
1a 1942	992 (51%)	950 (49%)	1.04
2a 1733	1387 (80%)	346 (20%)	4.01
3a 1894	1874 (99%)	20 (1%)	98.9
4a 1122	834 (74%)	288 (26%)	2.90

Total	Sand # (%)	Shale # (%)	Snd/Sh Ratio
1a+1b 3846	2389 (62%)	1457 (38%)	1.64
2a+2b 3640	2757 (76%)	883 (24%)	3.12
3a+3b 4312	3908 (91%)	404 (9%)	90.63
4a+4b 2126	1660 (78%)	466 (22%)	3.56

Total	Sand # (%)	Shale # (%)	Snd Sh Ratio
1b 1904	1397 (73%)	507 (27%)	2.76
2b 1907	1370 (72%)	537 (28%)	2.55
3b 2418	2034 (84%)	384 (16%)	5.30
4b 1004	826 (82%)	178 (18%)	4.64

Total	Sand # (%)	Shale # (%)	Snd/Sh Ratio	Total	Sand # (%)	Shale # (%)	Snd/Sh Ratio	Total	Sand # (%)	Shale # (%)	Snd/Sh Ratio
1 219	70 (32%)	149 (68%)	0.469	5 642	386 (60%)	256 (40%)	1.5	9 906	581 (64%)	325 (36%)	1.78
2 271	222 (82%)	49 (18%)	4.53	6 457	280 (61%)	177 (39%)	1.58	10 972	522 (54%)	450 (46%)	1.16
3 219	200 (91%)	19 (9%)	10.52	7 336	208 (62%)	128 (38%)	1.63	11 821	504 (61%)	317 (39%)	1.59
4 42	40 (95%)	2 (5%)	20.0	8 121	62 (51%)	59 (49%)	0.95	12 769	588 (76%)	181 (24%)	3.25

Figure 33. Grid cells and sandstone/shale ratios. (A) Section 2, central part of quarry, with 8 sub-cells uaed for computational purposes. (B) Northern part of quarry with 12 rectangular cells.

cell 3a. Grid cells must be assigned with a consistent set of criteria (lithology, facies, etc.) and a constant sense of scale. For example, if a cell encompasses a uniform lithology, then the larger cell size may be just as accurate as the smaller (sub-cell) size. If a cell encompasses highly variable lithologies, then a smaller grid may be necessary to accurately reflect the true sandstone/shale ratio.

Section 3

The central and northwest portions of Big Rock Quarry were also gridded into 12 cells (Figure 33B). Sandstone/shale ratios are presented on the bottom of the photograph.

Sandstone/shale ratios cannot be used as isolated data. For instance, a large sandstone-rich slump feature occurs in the lower right corner of the outcrop photograph over which log #2 was run (Fig. 33B; cells 10, 11, and 12). This sandstone mass creates abnormally high sandstone/shale ratios within the cells. However, this slump is limited extent, and the sandstone /shale ratios are not representative of the entire cell.

Outcrop vs Log Data

Sandstone/shale ratios were also measured from the gamma-ray logs at location sites #1, #2, and #3 to compare and calibrate log responses to lithologic properties. The logs were subdivided into vertical units that corresponded to the cell boundaries drawn on the outcrop photographs. Sandstone/shale ratios were calculated by determining (1) the shale base line on the gamma-ray log (assumed to represent a clean, 100% shale), and (2) the line of maximum gamma-ray deflection (assumed to represent a clean, 100% sandstone). The interval between these two end points was divided into thirds. The portion of the curve remaining to the left of the 33% shale cut-off line (drawn one third left of the clean shale base line) was counted as sandstone, and the portion of the curve to the right of this line was counted as shale. Sandstone/shale ratios were calculated, and comparisons of log and outcrop derived ratios are presented in Table 4.

Sandstone/shale ratios calculated from gamma-ray logs at log site #1 closely match the corresponding values obtained from computations within the outcrop grid cells. Log and outcrop data are comparable (82% log versus 79% outcrop for cell 3 and 68% to 70% for cell 1) in this geologic setting where thinly-bedded units are minimal. The 33% shale cut-off used in the log-measuring technique appears appropriate in this case.

Log and outcrop ratios at log site #2 match poorly. The slump-feature (Fig. 33B) appears on the gamma-ray log as nearly 100% sandstone, but the surrounding beds observed on the outcrop face consists of interbedded sandstones and shales within the remaining portions of the cell. Also, thin-bedded sandstones and shales that can be observed on outcrop photographs are included in the computation, but most of these units are too thin to be resolved by the gamma-ray logging tool and are not represented on the log curves. A gamma-ray logging sonde with a shorter crystal would improve thin bed resolution; however, this shorter, lighter tool is less rugged and more likely to damage or failure during outcrop logging.

Results at logging site #3 are mixed due to problems of thin-bed resolution by the logging tool and poor photographic coverage of the lower section of the outcrop.

This exercise demonstrates that (1) Sandstone/shale ratios are sensitive to how grid cells are defined in relationship to major lithologic units and (2) Outcrop derived ratios and log derived ratios are similar in simple geologic situations where thinly bedded intervals are minimal.

Cell	Log Location #1		Log Location #2		Log Location #3	
	Outcrop	Log (33% Shale Cut-Off)	Outcrop	Log (33% Shale Cut-Off)	Outcrop	Log (33% Shale Cut-Off)
1	2.29 (70%)	2.11 (68%)	9 1.78 (64%)	7.71 (89%)	1 0.469 (32%)	23.8 (96%)
3	3.84 (79%)	4.65 (82%)	10 1.16 (54%)	0.71 (41%)	2 4.53 (82%)	4.0 (80%)
	–	–	11 1.59 (61%)	– (100%)	3 10.52 (91%)	– (100%)
	–	–	12 3.25 (76%)	– (100%)	4 20.0 (95%)	3.33 (77%)

Table 4. Big Rock Quarry sandstone/shale ratios. Comparisons of outcrop and log-derived values.

STOP 2

I- 430 Roadcut, Little Rock, Arkansas

Purpose:

The purpose of this stop is to view a downslope (?) section equivalent to that exposed at Big Rock Quarry (approximately 5 miles to the east) and to view sedimentary features that could not be studied at STOP 1 because of the steepness of the quarry face. The location of the roadcut is on the west side of Interstate 430 south in northwestern Little Rock, just north of the Arkansas Highway 10 exit ramp (Fig. 34A).

Description of Locality

This section is absolutely sliced to pieces by faults. Any inference regarding vertical trends, contacts, etc., at this outcrop may be regarded as suspect. The sequence lies along the flank of the Big Rock Syncline and beds generally dip steeply to the north. The lower Jackfork consists of a sequence of black carbonaceous shales with siltstone interbeds and laminae that are intensely sheared. The upper Jackfork consists of interbedded thin and thick-bedded sandstone and thinner shale and siltstone. The lower part of the sandy sequence consists of highly fractured and faulted quartzitic sandstones (Fig. 34B), many which may be exotic sandstone blocks.

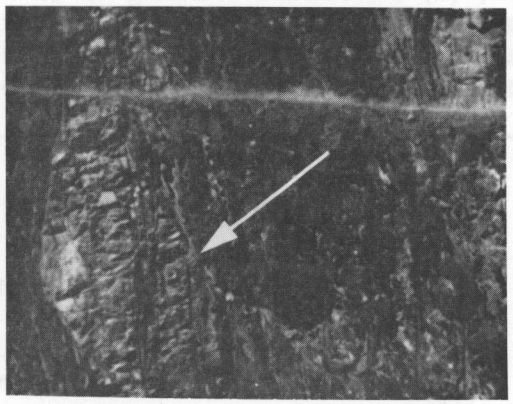

B

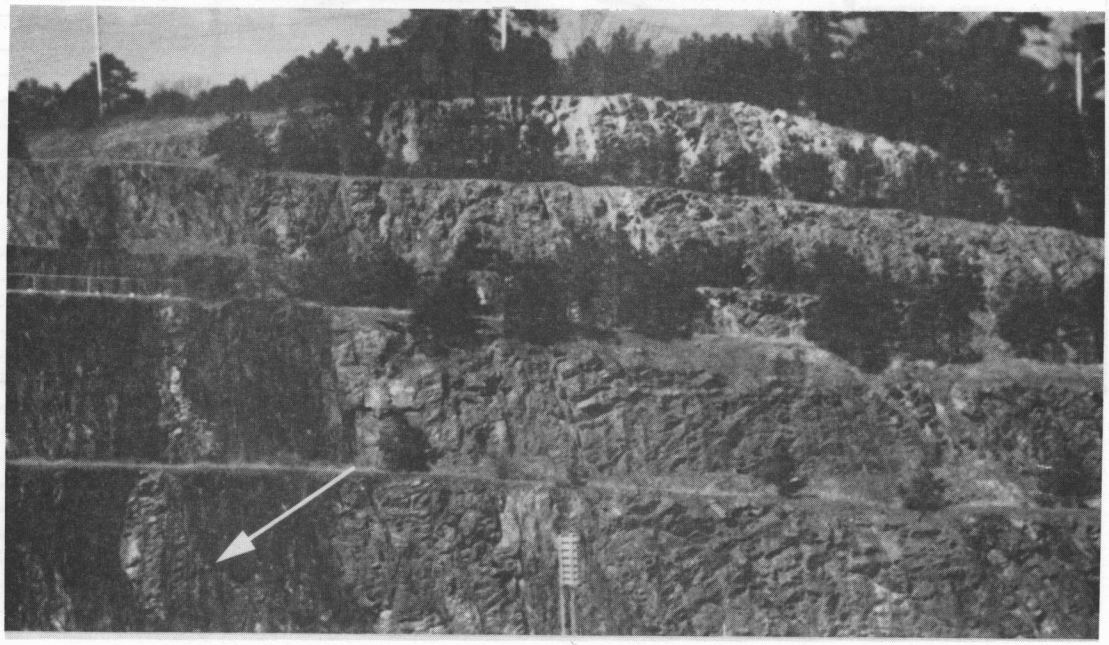

A

Figure 34. (A) West side of Interstate 40 roadcut at the State Route 10 exit ramp. Basal part of sandy section showing faulted (arrow) Jackfork sandstone and shale with possible sedimentary slide features. (B) Close-up of photograph shown in A displaying interbedded nature within pod of sandstone and shale, and northward-dipping fault plane (arrow). Photograph courtesy of Arkansas Geological Commission.

Interpretation

This section is interpreted as the same stratigraphic sequence as at Big Rock Quarry: lower Jackfork shales overlain by upper Jackfork sandstones (Fig. 35). The thinning- and fining-upward sequences of sandstone beds (Fig. 36) were interpreted to represent submarine fan-channel deposits that were deposited farther downslope than equivalent strata at Big Rock Quarry to the east (Stone and McFarland, 1981; Link and Stone, 1986b; McFarland, 1988). Link and Stone (1986b) suggest a succession of events led to the deformation observed at this locality: (1) Southward slumping down the continental slope, (2) Northward stacking of several thrust-fault slices, (3) Folding during several episodes, and (4) Backfolding and faulting caused, in part, by the piling up and crowding

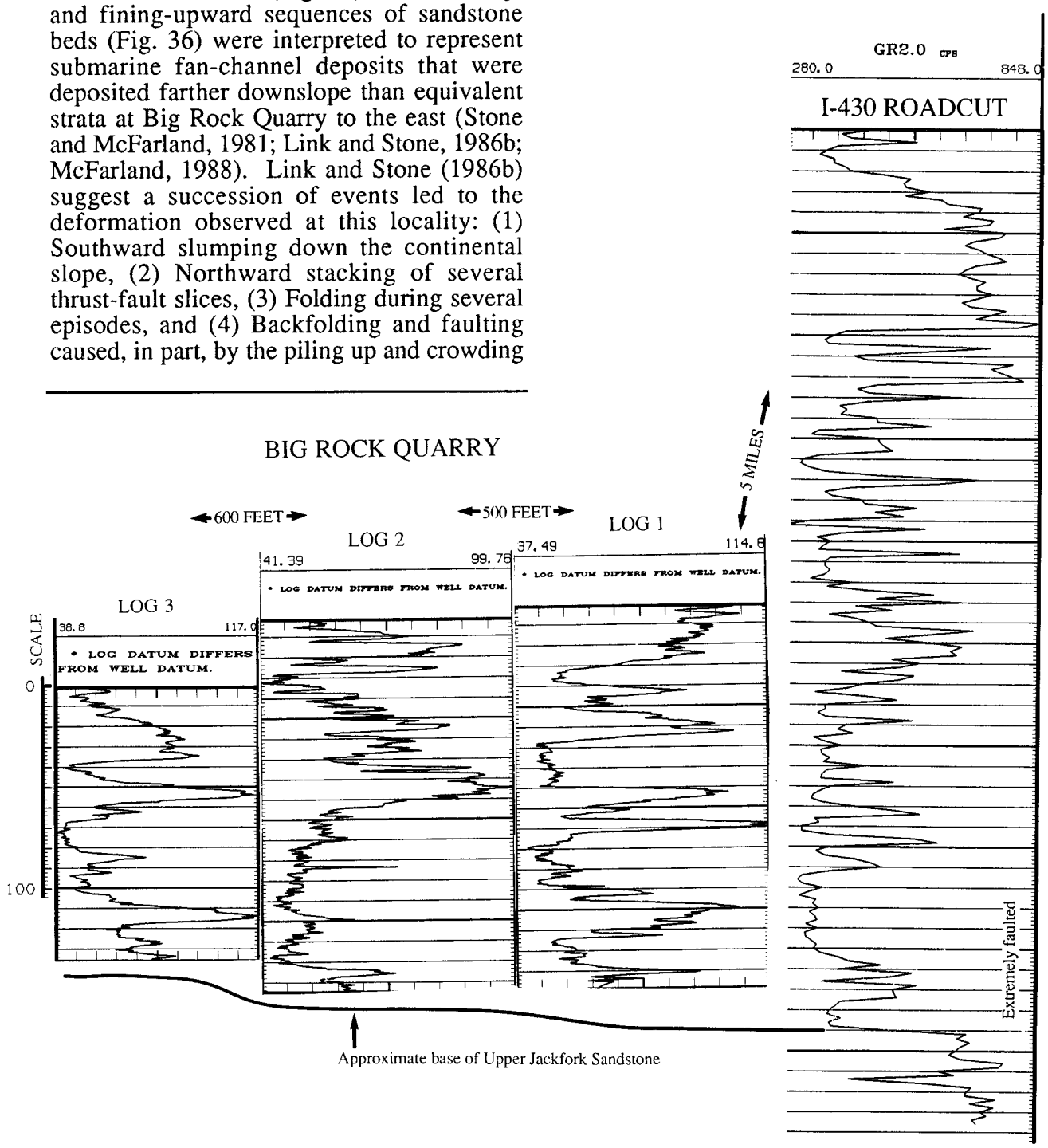

Figure 35. Gamma-ray logs hung on the approximate (erosional?) base of the upper Jackfork Sandstone. The section at the Interstate 430 roadcut is inferred to be stratigraphically equivalent to the section at Big Rock Quarry. Note changes in horizontal scale.

at the toe of the larger thrust sheets. The last 3 events took place in late Paleozoic time as the Ouachita Mountains were being formed. Hydrothermal quartz veins of late Paleozoic age also cut through the lower part of the section near the base (Stone and McFarland, 1981).

Several intervals in the highly-contorted lower Jackfork shale beds contain soft-sediment-deformation, but many of the beds have been offset and contorted by tectonic processes. Can you tell the difference? What is the evidence? What is the depositional setting of the shale? Look for trace fossils, especially *Chondrites* (thin, branching, siltstone-filled tubes). One or two types of trace fossils reflecting specialized activity may assist in offering clues to the nature of the depositional substrate and/or overlying water column. Within the sandstones, look for the mudstone-clast conglomerate and breccia similar to that found in the float block on the quarry floor. In addition, an interesting interval lying about 125 feet above the base of the upper Jackfork sandstone contains massive-appearing, 'clean' sandstone overlain by flat- to small scale cross- laminations, capped by an interval with climbing ripples within a whitish-gray sandstone and shale sequence. What are some of the possible scenarios for deposition of these beds? Which parts of the sequence suggest deposition from high-density and low-density flows? Could contour currents be involved?

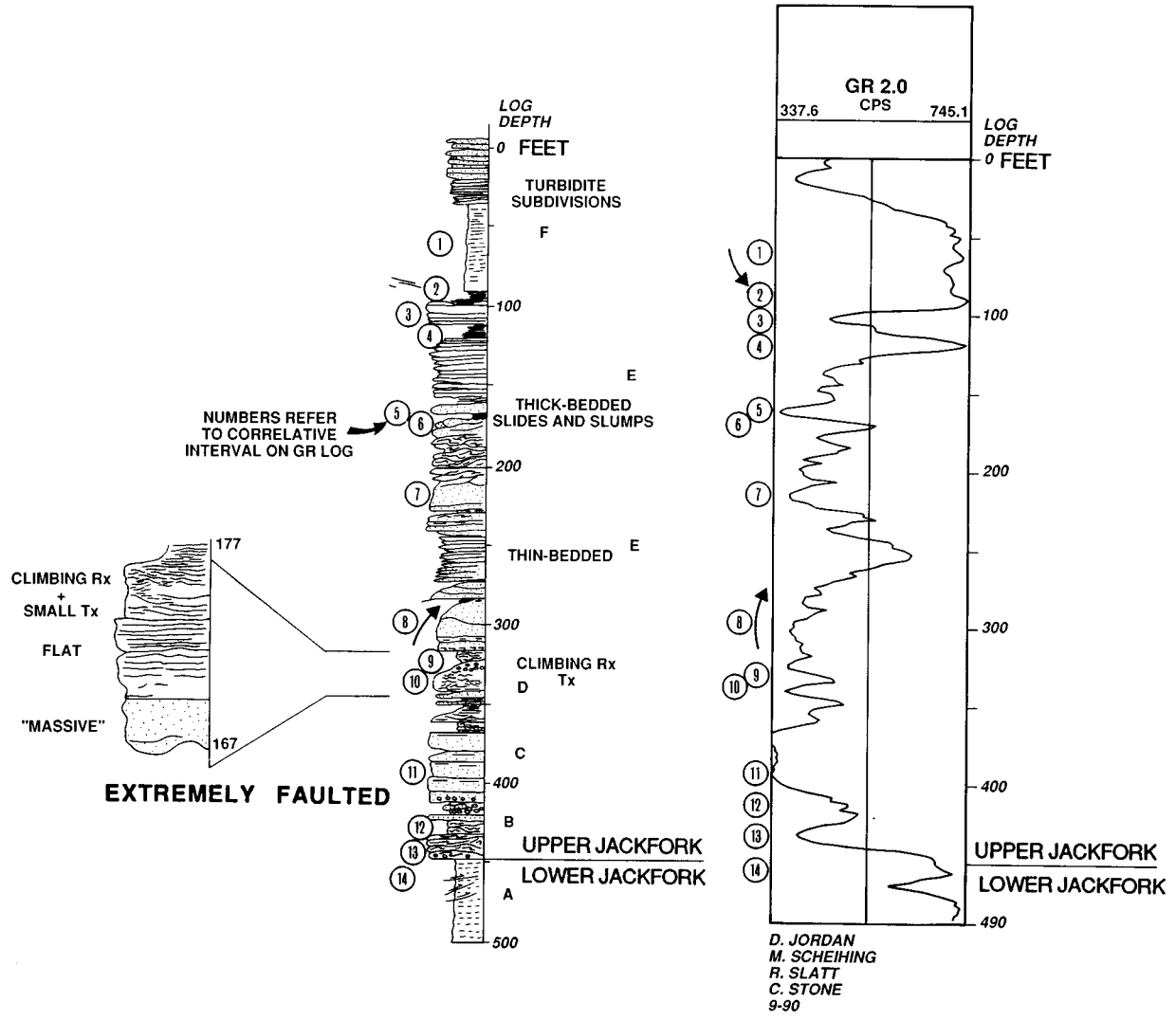

Figure 36. Stratigraphic column and gamma-ray log character of the lower and upper Jackfork exposure along Interstate 40.

Notes

STOP 3

Visitor Center, Pinnacle Mountain State Park, Arkansas

Purpose:

The purpose of this stop is to view a melange interval that is overlain by massive-appearing, matrix-free sandstones, and discuss possible origin of the sedimentary package.

Description of Locality

Extending west of STOPS 1 and 2 is an east-west trending chain of steep hills that locally reach 1,000 feet in elevation (Fig. 37). These hills are made up of thick, but apparently discontinuous units of moderately to steeply-dipping sandstone and shale of the upper part of the lower Jackfork ('middle' Jackfork according to local terminology) (Stone and McFarland, 1981). We will examine these rocks in an abandoned quarry near the Visitor Center of Pinnacle Mountain State Park (Figs. 37 and 38).

The Jackfork sequence in and around the Visitor Center consists of fine- to medium-grained quartzose sandstone and intervening shale units that probably total 200-400 feet thick. In general, the exposed sequence dips south at 15 to 45 degrees, but mapping (Fig. 38) suggests that much and perhaps all of the exposure is a melange of large blocks of stratified sandstone, some including as much as 200 feet of section, in a matrix of mudstone and diamictite.

From the parking area southward along the quarry pond, three general lithologic units can be recognized. A "basal" unit or units of stratified quartzose sandstone is exposed on both sides of the parking area. It totals about 50 to 60 feet thick and is underlain and overlain by stratified mudstone. A "middle" unit, exposed only on the west side of the pond, includes about 70 to 90 feet of diamictite composed of disarticulated and contorted blocks and beds of sandstone encased in unstratified mudstone (Fig. 39). Invertebrate fossils of shallow-water organisms have been reported from sandstone blocks in this and similar melanges just west of this area.

The uppermost unit exposed at the southern end of the quarry consists of over 100 feet of resistant, evenly-bedded, finely laminated, clean, quartzose, fine- to medium-grained sandstone (Fig. 40).

Interpretation

None of the sandstone units at this stop can be traced continuously for over a few hundred (up to 600) feet. Some adjoining lenses may exceed three-quarter of a mile in length. Most terminate abruptly against shales or sandstone units with different orientations, suggesting that all are blocks. Stone and McFarland (1981) suggest that these sandstone units could represent (1) resistant beds caught up and mixed with intervening mudstones between thrust faults, (2) remnants of individual submarine fans (favored interpretation), or (3) sandstone slabs that have slid downslope into deeper parts of the basin.

Where relatively complete sections of sandstone units can be identified, they show an internal succession of textures and structures suggesting that they formed as erosive, fining- and thinning-upward, channel-fill units (Fig. 41). In all probability, they represent the fill of large slope channels, eroded into underlying slope mudstone, that have been detached and incorporated into large downslope slides.

Reservoir Implications

Another hypothesis is that the lowest "unit" of mainly sandstone consisting of 55 feet of sandstone exposed on the eastern side of the

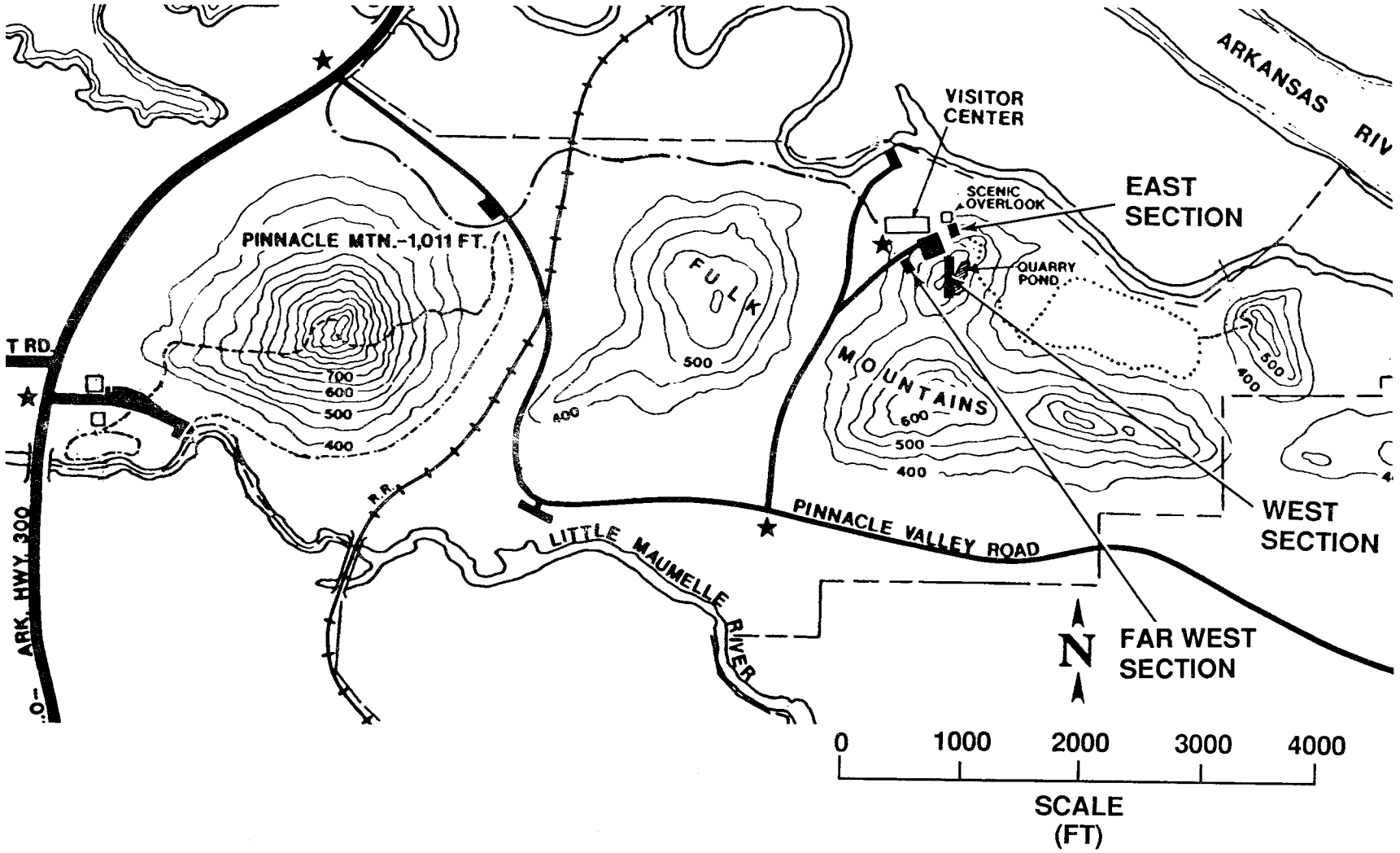

Figure 37. Location of Pinnacle Mountain State Park Visitor Center and outcrop sections near quarry pond.

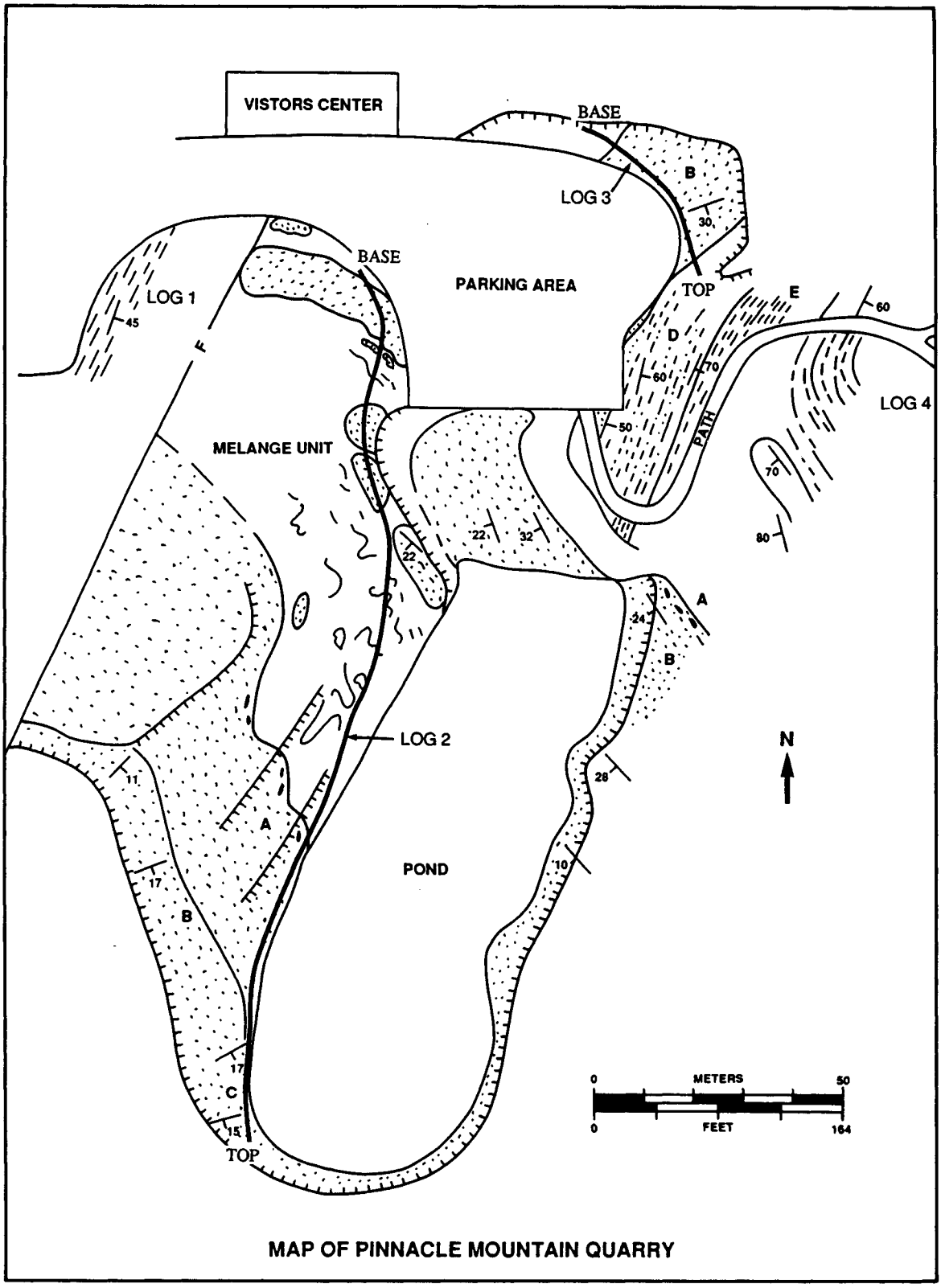

Figure 38. Geologic sketch map of the Visitor's Center area at Pinnacle Mountain State Park, Arkansas. Large blocks of medium- to fine-grained quartzose Jackfork sandstone (stippled) are interbedded and mixed with units of muddy diamictite and laminated mudstone and shale, respectively. The letters (A, B, C, D, and E) refer to localities where sub-facies shown in the stratigraphic column (Fig. 41) can be seen. Location of gamma-ray log paths are shown.

Figure 39. West side of the quarry pond, melange interval comprising over 100 feet of contorted blocks and beds of sandstone encased in unstratified mudstone.

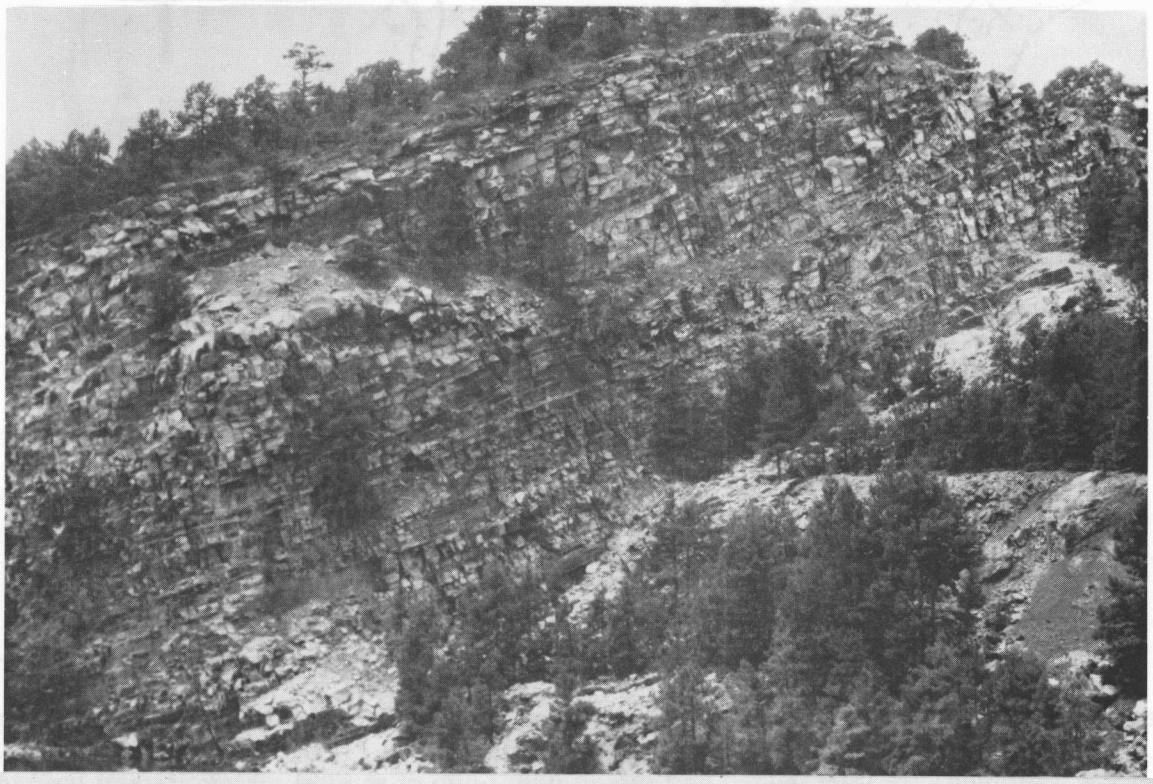

Figure 40. The uppermost interval exposed at the southern end of the quarry consisting of over 100 feet of resistant, evenly-bedded, finely laminated, clean, quartzose, fine-to medium-grained sandstone overlying a melange unit.

IDEALIZED CHANNEL-FILL SEQUENCE

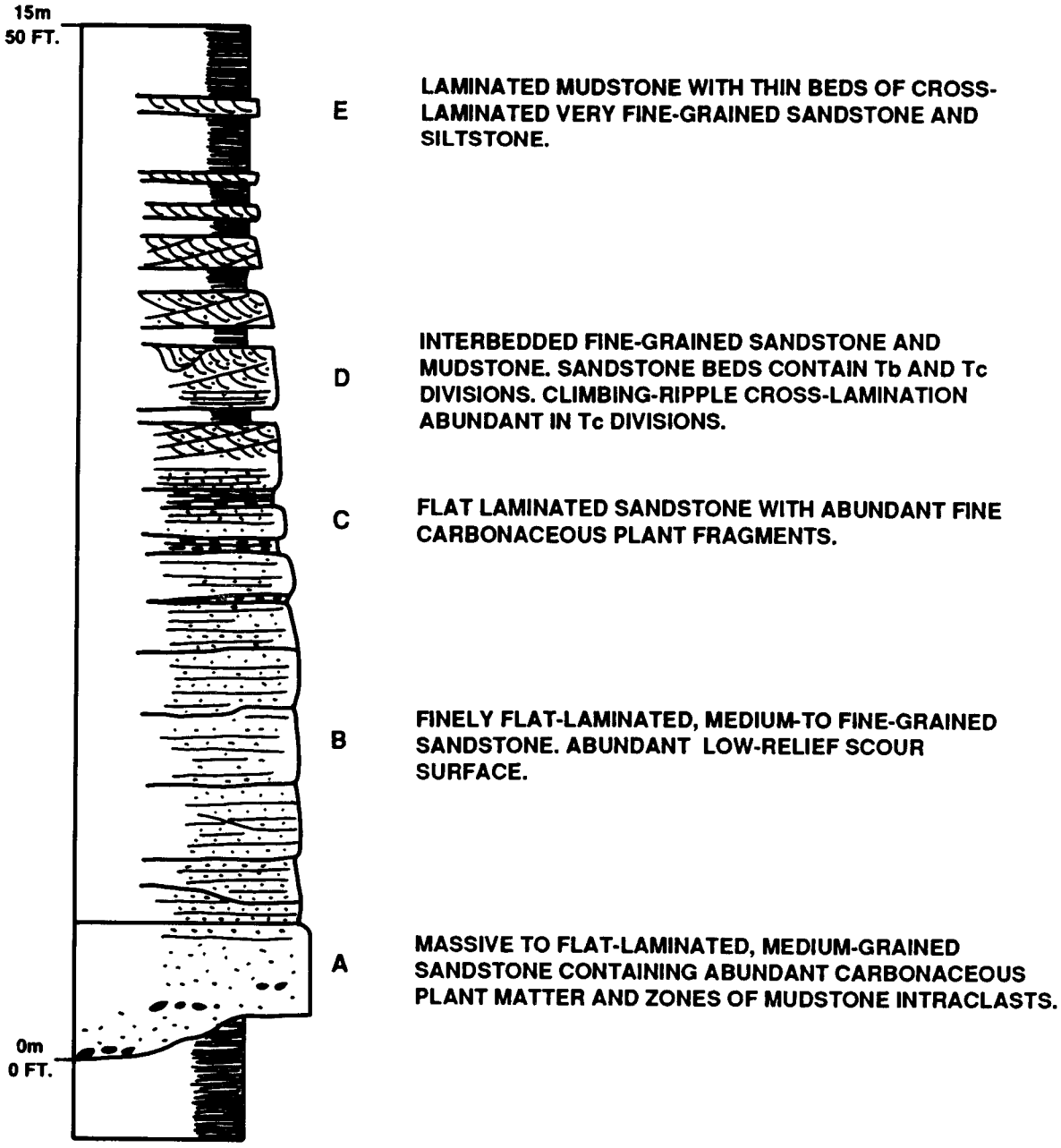

Figure 41. Schematic composite stratigraphic column of an idealized channel-fill sandstone and interbedded mudstone and shale sequence present at Pinnacle Mountain State Park. Letters denote main sub-facies located in Figure 38.

parking lot is the same sandstone interval that correlates to the lower sandstone unit (25 feet) exposed on the western side of the parking lot.

Correlations shown in Figure 42 might then be valid. It is not clear if this sandstone was deposited within a channel elsewhere, only to have been detached and incorporated into a large downslope slide, or if this sandstone is in fact a lenticular body deposited within an 'in situ' channel. It would be difficult to interpret this sandstone body as a detached channel sandstone within a hydrocarbon reservoir based on a correlation of similar logs.

Note on the log the presence of several sandstones in the diamictite interval. These sandstones are not bedded, as might be interpreted from the logs alone, but are actually detached and convoluted blocks of sandstone that are a few to greater than 10 feet in diameter ("glumps and gloops" by local terminology). Using only the character of the logs for correlation purposes and in the construction of cross-sections for modelling, a possible oil field reservoir may be doomed if these sandstone blocks were interpreted as laterally continuous sandstone beds!

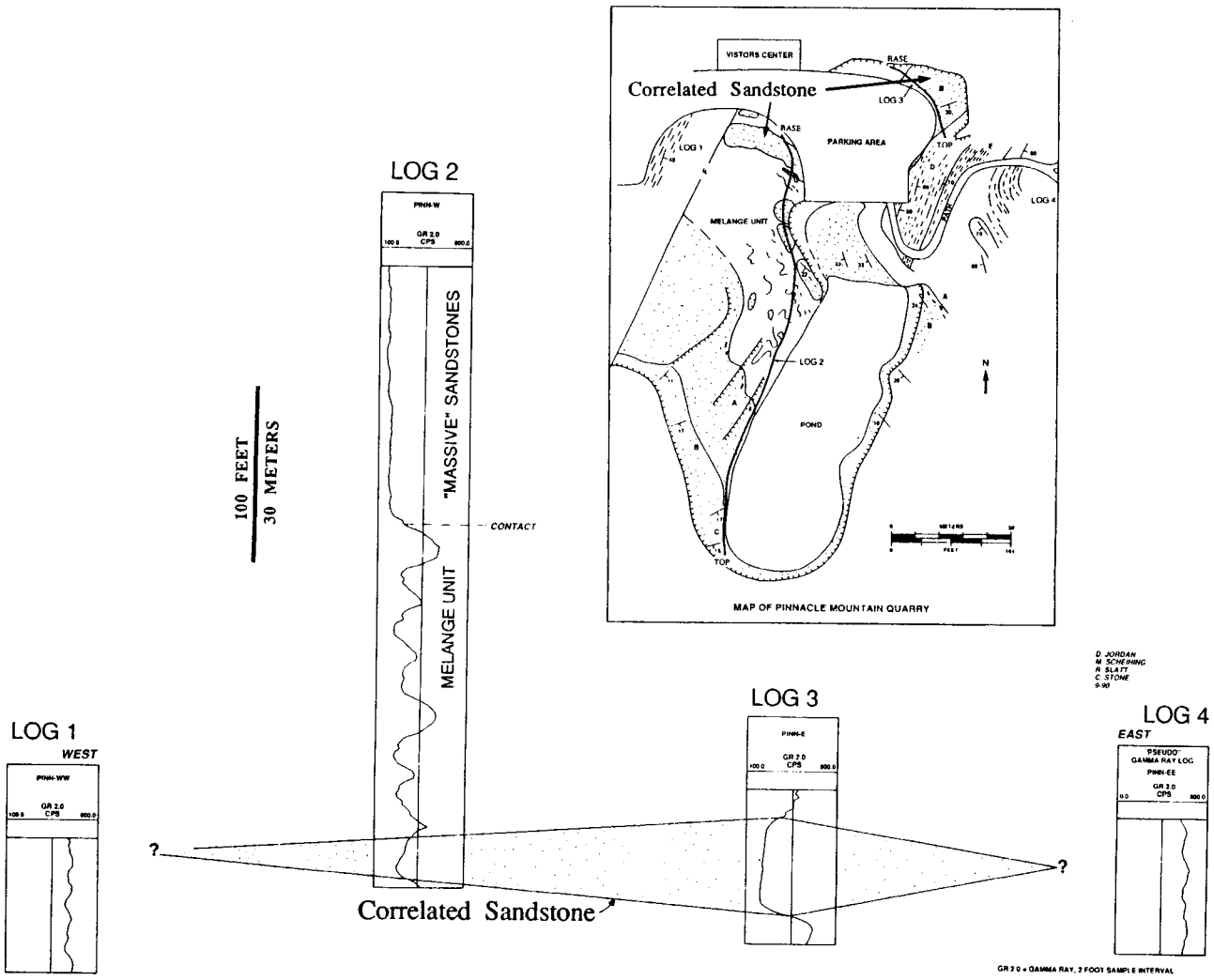

Figure 42. A possible correlation of lower sandstones across the parking lot at the Pinnacle Mountain Visitors Center. This correlation suggests that the sandstones are lenticular and they pinchout to the east and west due to faulting, because the sandstone body is a slide block (part of the overlying melange interval), or the sandstone body is an in situ channel-fill deposit.

Field Trip Itinerary and Description (Day 2)

Laterally Continuous, Sheet-like Facies

Stop 4

Murray Quarry, near Arkadelphia, Arkansas

Purpose:

The purpose of this first stop on the second day of the trip is to view and discuss the sedimentology, lateral geometry, and heterogeneity of the uppermost part of the upper Jackfork. The sandy deposits have much more continuity than the deposits seen on the previous day at the stops near Little Rock. This stop, having steeply dipping but strike-oriented beds, is a prelude to STOP 6 where upper Jackfork rocks are more accessible but viewed in dip-oriented sections.

Description of Locality

Approximately 150 feet of southward-dipping upper Jackfork Sandstone are exposed at the abandoned Murray Quarry near DeGray Lake (see Fig. 59 and 62 for location of Murray Quarry in relation to sections around DeGray Lake). Although not easily accessible, two stratigraphic sections have been measured by Breckon (1988), who interprets the succession to be a combination of levee overbank, channel-fill, and extrachannel deposits.

Interpretation

The upper part of the section is deeply incised and infilled with shale and thin bedded sandstones, and is interpreted by Breckon (1988) to be the stratigraphically younger Johns Valley Shale.

The base of one incisement is lined with clasts and boulders (Fig. 43) which were deposited as a deep-water channel lag or it is an accumulation of rubble which slid down the channel walls after incisement.

Reservoir Implications

Although we have not examined this section in detail, nor obtained gamma-ray logs, it is worth noting the greater number of thinner beds and greater lateral continuity of many individual beds than were present at STOPS 1, 2, and 3 of Day 1. These beds are more likely to have a three-dimensional sheet-like geometry.

Notes

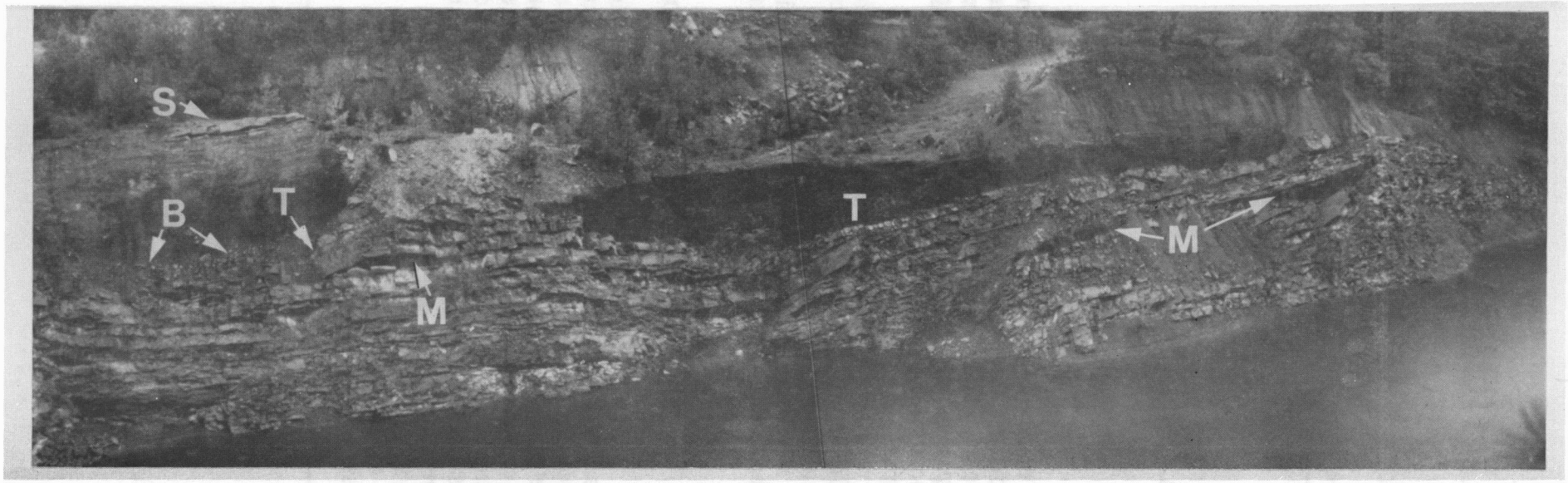

Figure 43. Murray Quarry, near Arkadelphia, Arkansas. This section exposes the uppermost part of the Jackfork. Note the presence of more laterally continuous sandstone beds than were apparent at the Stops of Day 1, the erosional truncation (T) of the uppermost part of the Jackfork that is overlain by sandstone boulders (B) within a mudstone matrix, and isolated lenticular mudstones (M). Some isolated sandstones occur within the shale (S).

Stop 5

DeGray Lake Spillway, Bismarck, Arkansas

Purpose:

The DeGray Lake Spillway, north of Arkadelphia, Arkansas near Bismarck exposes a 1,000 feet vertical succession of steeply-dipping turbidite strata. These strata record repeated cycles of turbidite sedimentation in a deep marine basin. Our studies have focused on depositional processes represented at this section; generation of gamma-ray logs along both sides of the spillway; understanding relationships of gamma-ray logs to predicting reservoir quality; petrographic and biostratigraphic characteristics of the units; and measuring and correlating stratigraphic packages and individual beds across the spillway and elsewhere in the immediate area.

Description of Locality

The succession is superbly exposed and easily accessible along two spillway walls (referred to in this guidebook as DeGray Lake Spillway east and west sections) that are spaced approximately 300 feet apart.The entire vertical section of the east wall has been measured in detail by Morris (1977) (Fig. 44) and Breckon (1988); individual measured segments have been published by Moiola and Shanmugam (1984). The overall vertical sequence grades upwards from thin-bedded sandstones and shales at the base, through thicker-bedded sandstones, into massive pebbly sandstones and conglomerates at the top. Major cycles of sandstone deposition are separated by shales, 10 to 30 feet thick, of hemipelagic or debris flow origin. The section is several hundred feet lower in the Jackfork section than the exposures at Murray Quarry (STOP 4).

Interpretation

Stratigraphy and Sedimentation

There have been a number of published interpretations of the depositional processes and setting represented by upper Jackfork rocks exposed in this section (Table 5). Two basic types of sediment gravity flows are represented by deposits within this section: (1) turbidity currents and (2) debris flows. Turbidity currents were responsible for deposition of virtually all of the sandstone beds within the DeGray Lake Spillway section. Many probably began as retrogressive failures of submarine slopes as suggested by the common compound character of sandstone units (see Fig. 11). Thicker sandstone units are composites of many thin, 2 to 20 inch-thick sedimentation units representing individual flows. The lowest beds are typically blocky and show flat lamination. Higher beds show undulating contacts produced by soft-sediment deformation and foundering of one bed into underlying, liquefied beds (Fig. 45A). The uppermost beds in a package are usually thinner and show flat bases and tops.

At DeGray Lake Spillway there is a continuous spectrum from 3 to 10 foot-thick sandstone packages representing more proximal flow sequences to thin sandstone beds, 1 to 3 feet thick, representing intermediate flow stages; to beds less than 1 inch thick, representing distal flow (Fig. 45B). These units provide a downslope spectrum representing the various stages in the evolution of mud-poor, fine-grained turbidity currents produced by retrogressive failures. Figures 52-56 show detailed descriptions, by Don Lowe, of some representative packages and sedimentation units present at DeGray Lake Spillway.

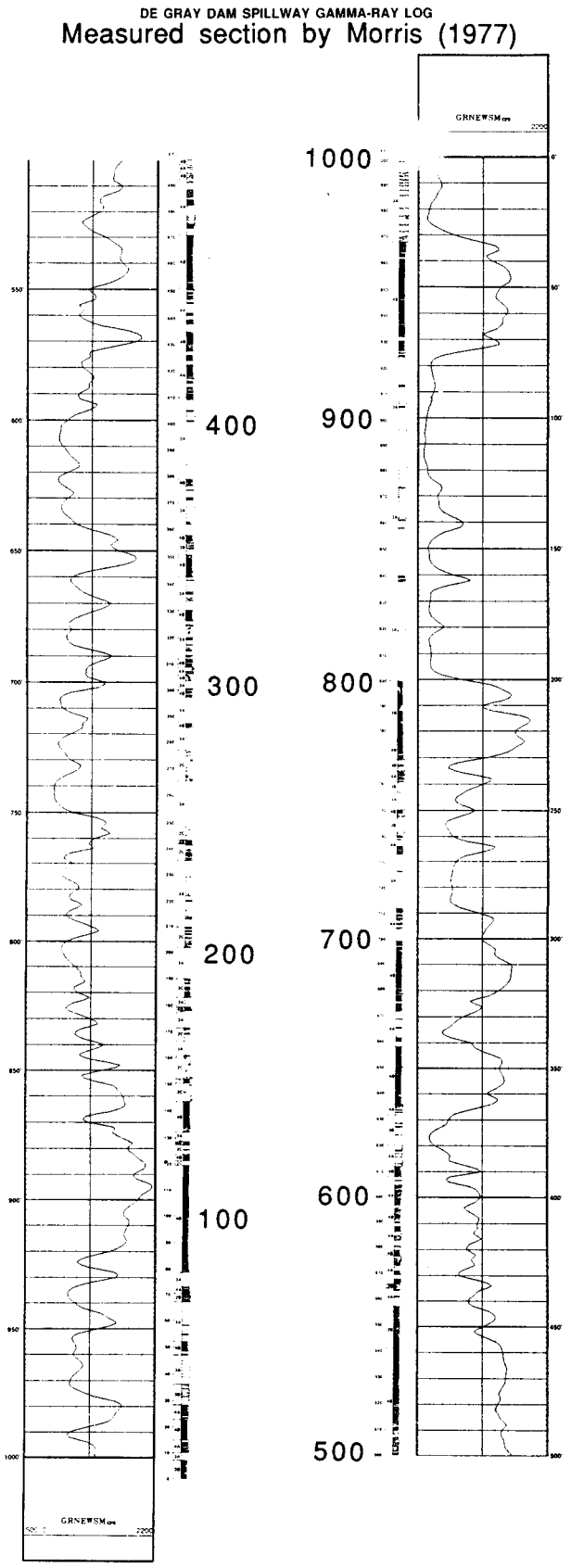

Figure 44. Measured section by Morris (1977) of the east wall of DeGray Lake Spillway and associated gamma-ray log measured at two-foot intervals with the hand-held scintillometer.

Interbedded distal and proximal turbidites deposited on an abyssal plain (Morris, 1973)
Lower slope- outer fan lobe, lobe fringe and interlobe deposits; massive sandstone/pebbly sandstone interval at the top of the section comprises a major distributary channel (possible middle fan) (Lock and Fisco, 1979).
Prograding sequence of middle fan, submarine fan channel, and outer fan lobe deposits; coarse deposits at the top are middle fan channel fills (Stone and McFarland, 1981; McFarland, 1988).
Middle fan channel and interchannel crevasse splay deposits. Overall prograding system. The uppermost coarser-grained intervals may represent an inner fan transition zone. (Moiola and Shanmugan, 1984; Link and Roberts, 1986).
Submarine channel-fill (Shanmugan et. al., 1988).
Middle-fan or suprafan, channel-fill and lobe complex overlain by chaotic and sandy deposits of a major inner-fan channel-fill complex (Breckon, 1988).

Table 5. Published interpretations of the DeGray Lake Spillway section.

The Jackfork Group at the DeGray Lake Spillway section is close to the southeastern limit of Jackfork outcrops in the Ouachita Mountains. If the bulk of the sediments were derived from the northeast as some have inferred, this section should be located further downfan than that at the Big Rock Quarry. We might expect this to be reflected in a number of ways:

(1) The overall sand/shale ratio might decrease down fan, although submarine slopes and proximal fan areas outside of channels are also characteristically sites of mud deposition. Much of the coarser sand and most of the fine sand bypasses the upper fan and upper mid-fan areas, moving further downslope in turbidity currents and accumulating in lobes or more distal outer fan regions. Perhaps this criterion is less useful than might be expected, especially within predominantly fine-grained systems like the Jackfork.

(2) The coarsest grain sizes should decrease down fan. It is noteworthy that perhaps the coarsest sediment in the Jackfork anywhere in the Ouachitas occurs **near the top** of the DeGray Lake Spillway section (Fig. 46A) and at the adjacent DeGray Intake section (STOP 6).

(3) The frequency and scale of channeling should decrease down fan. It is difficult to assess the abundance of channels in the DeGray Lake Spillway section compared to that in Big Rock Quarry because lithologic units in the Spillway crop out for only a short distance along strike (Fig. 46B). Overall, there appears to be less channeling and bed lenticularity and more lateral bed continuity than in the Big Rock Quarry (discussed in detail below). This is verified at the Intake section (STOP 6).

(4) Large scale, slope-related slides and debris flows might decrease down fan, away from the bounding basinal slopes. Two of the largest debris flows that we will see on this trip are located in the upper part of the DeGray Lake Spillway section. One is nearly 30 feet thick. There are, however, fewer small debris flow deposits and nothing like the sand-matrix mudstone-clast breccias seen in the Big Rock Quarry. Evidence for repeated local slides and debris flows is also missing in the spillway section.

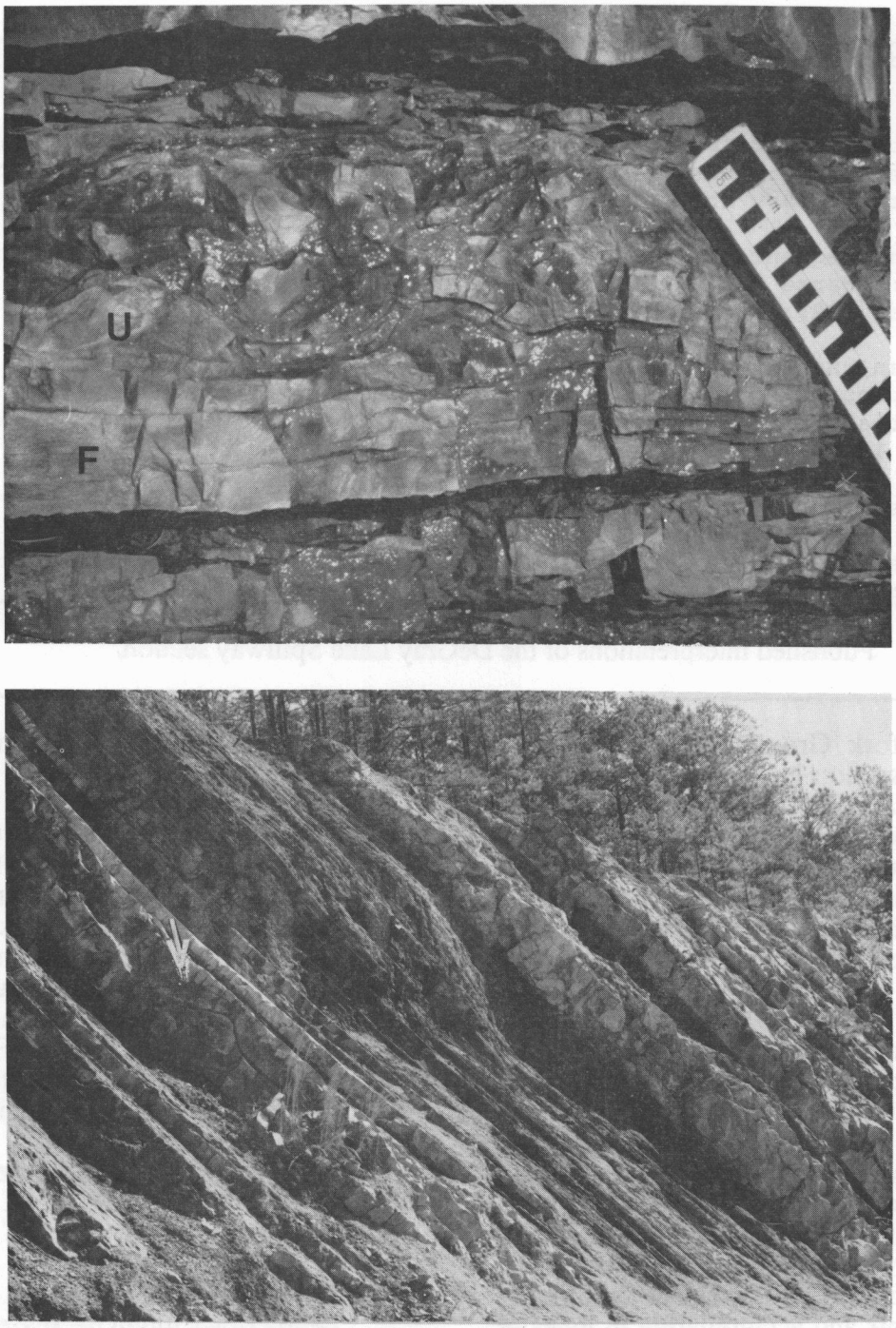

Figure 45. Typical sandstone units within the DeGray Spillway east section are composites of many thin, 2 to 20 inch-thick sedimentation units representing individual flows. (A) The lowest beds are typically blocky and show flat (F) or slightly undulatory lamination. Higher beds show undulating contacts (U) produced by soft-sediment deformation and foundering of one bed into underlying, liquefied beds. Photograph from 145 feet on the section by Morris (1977), 855 feet on gamma-ray log. (B) Various packages of individual flows are represented in this vertical sequence, the difference in sedimentation units and lithology being the result of changes in the volume and velocity of the individual flows. Sandstone packages representing more proximal flow sequences are overlain by thinner sandstone beds (arrow) representing intermediate flow stages to beds representing distal flow. Compare with Figure 11. Photograph from 130-190 feet on the section by Morris (1977), 874-814 feet on gamma-ray log.

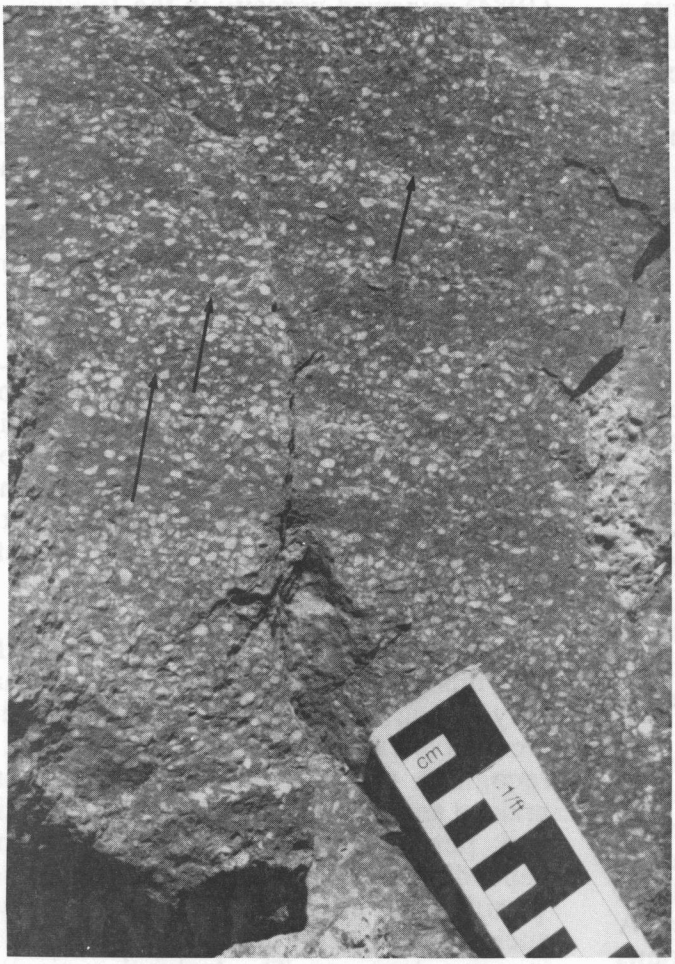

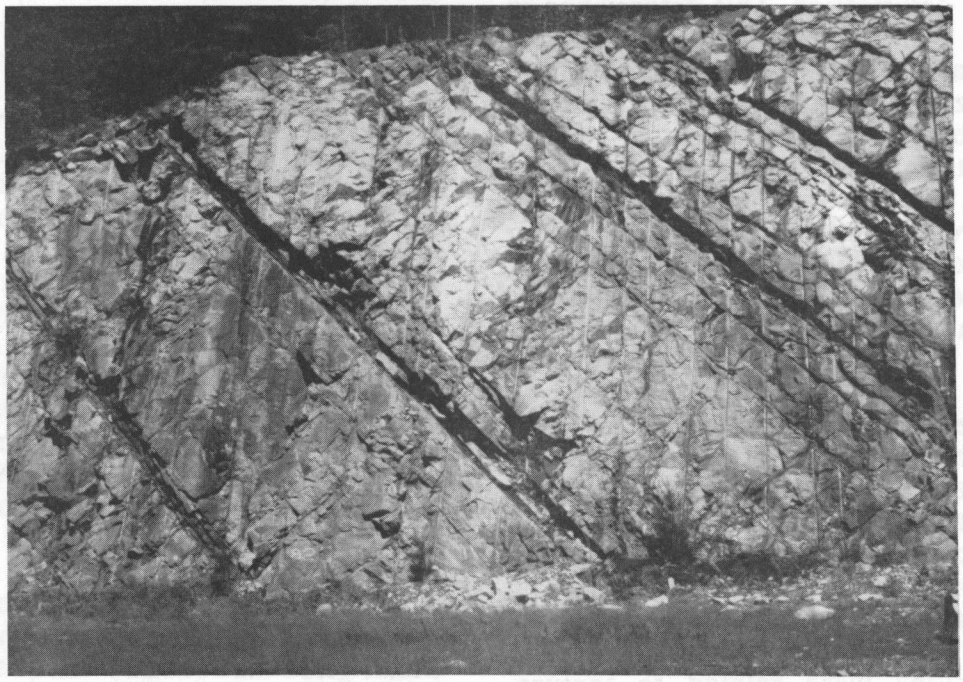

Figure 46. Features of the upper portion of the DeGray Lake Spillway section. (A) Pebbly sandstone at the top of the east section (980 feet on the section of Morris, 1977; 20 feet on the gamma-ray log). This part of the section contains some of the coarsest sediment in the Jackfork anywhere in the Ouachitas. Note inversely graded beds (arrows) possibly representing gravelly, inversely graded, traction carpet (R2) layers deposited from a high-density sandy flow. (B) Thick, massive-appearing to amalgamated sandstones separated by thin mudstones representing possible channels near the top of the DeGray Lake Spillway east section. These units crop out for only a short distance along strike and it is difficult to ascertain the lateral geometry. Section is at 820-925 feet on the measured section of Morris (1977) and 75-180 feet on the gamma-ray log.

It seems that the DeGray Lake Spillway section of the Jackfork probably represents a more basinal setting less directly associated with slopes and slope processes as inferred in Big Rock Quarry (STOP 1) or Pinnacle Mountains (STOP 3), although the sediments were probably derived primarily from the south or southeast (see discussion below).

Petrography and Textural Characteristics

The basic petrographic analysis presented in this study (see Appendix II for data), although limited in geographic and stratigraphic extent, shows some of the same trends mapped by Danielson et al. (1988). Particularly, their maps show the southern outcrop belt of the Jackfork, which includes the DeGray Lake Spillway and Dierks Lake Spillway (STOP 8) localities, to be in the region of highest lithic content with a slight decrease towards Dierks. The present study supports this idea. The small but consistent occurrence of vitric tuffs and dacitic VRF's at DeGray (see Appendix II, Figure II-I) also fits with the common proposal of a southern "tectonic highland", possibly resulting from volcanism related to a southward dipping subduction zone. A number of samples also contain quartz grains which display a feature associated with cataclastic deformation. This deformation is associated with grinding action under great pressures along fault planes in shear zones. The quartz grains display Boehm lamellae, which are bands oriented parallel to the crystal C-axis that typically contain streaks of dirty inclusions. The presence of grains displaying this feature is another factor pointing to a southern 'tectonic highland' source terrain for at least a portion of the Jackfork. Examples of the Boehm lamellae are shown in Figure 47A and B.

All of the studies mentioned earlier used petrographic analysis to some degree to support the interpretations of provenance. At the same time, the authors were building a detailed picture of the mineralogic composition and variability of the Jackfork. The study by Morris et al. (1979) resulted in a benchmark paper on the Jackfork because data and interpretations were related to texture, framework and clay mineralogy, porosity, and depositional facies. Stone and Lumsden (1984) reviewed porosity in the Jackfork and concluded that the bulk of the porosity in the Jackfork is secondary in origin and results from deep burial diagenesis, as opposed to surficial weathering. They also speculated on the possibility of quartz dissolution and a relationship between interbedded shaliness and secondary porosity but show no data to support their speculation. The work presented here would also indicate that the bulk of the porosity in the Jackfork is secondary in origin (Fig. 47C-D). Ten samples from DeGray Lake Spillway contain small percentages of a organic/hydrocarbon residue, possibly bitumen, which is added to the total porosity values for those samples. The material is not a cement or a pore-filling alteration product but resides in intergranular pores. It is therefore counted in the total porosity values.

All workers generally agree that the Jackfork is a moderately to well sorted, dominantly very fine to fine grained quartz arenite/lithic arenite typically well cemented by quartz. All recognize the presence of some coarser grained and conglomeratic units. Calculations and percentages vary between authors depending on the method used for mineral 'partitioning', an example being quartz types such as monocrystalline, polycrystalline, mosaic, chert, etc. The Jackfork typically is shown to contain 80-95% quartz, 1-5% feldspar (plagioclase + K-spar), 2-10% lithics (MRF, VRF, PRF, SRF), and 10-25% matrix (detrital + authigenic clays + grains too small to identify petrographically). Kaolinite, illite, chlorite, and halloysite have been documented. Quartz is uniformly reported as the dominant cement with minor amounts of limonite, siderite, hematite, and dolomite. Muscovite, biotite, zircon, rutile, apatite, and fossil fragments are the commonly reported accessories and heavy minerals. A complete compilation of mineralogical data, textural data, and normalized percentages (for classification) that was prepared for the present work are presented in Appendix II, and representative photomicrographs are shown in Figures 48-50.

A number of data cross-plots (See Appendix II) are presented in this study. These include: Mean grain size (MGS) vs. quartz cement, MGS vs. total porosity, MGS vs. normalized lithic %, normalized lithic % vs. total porosity

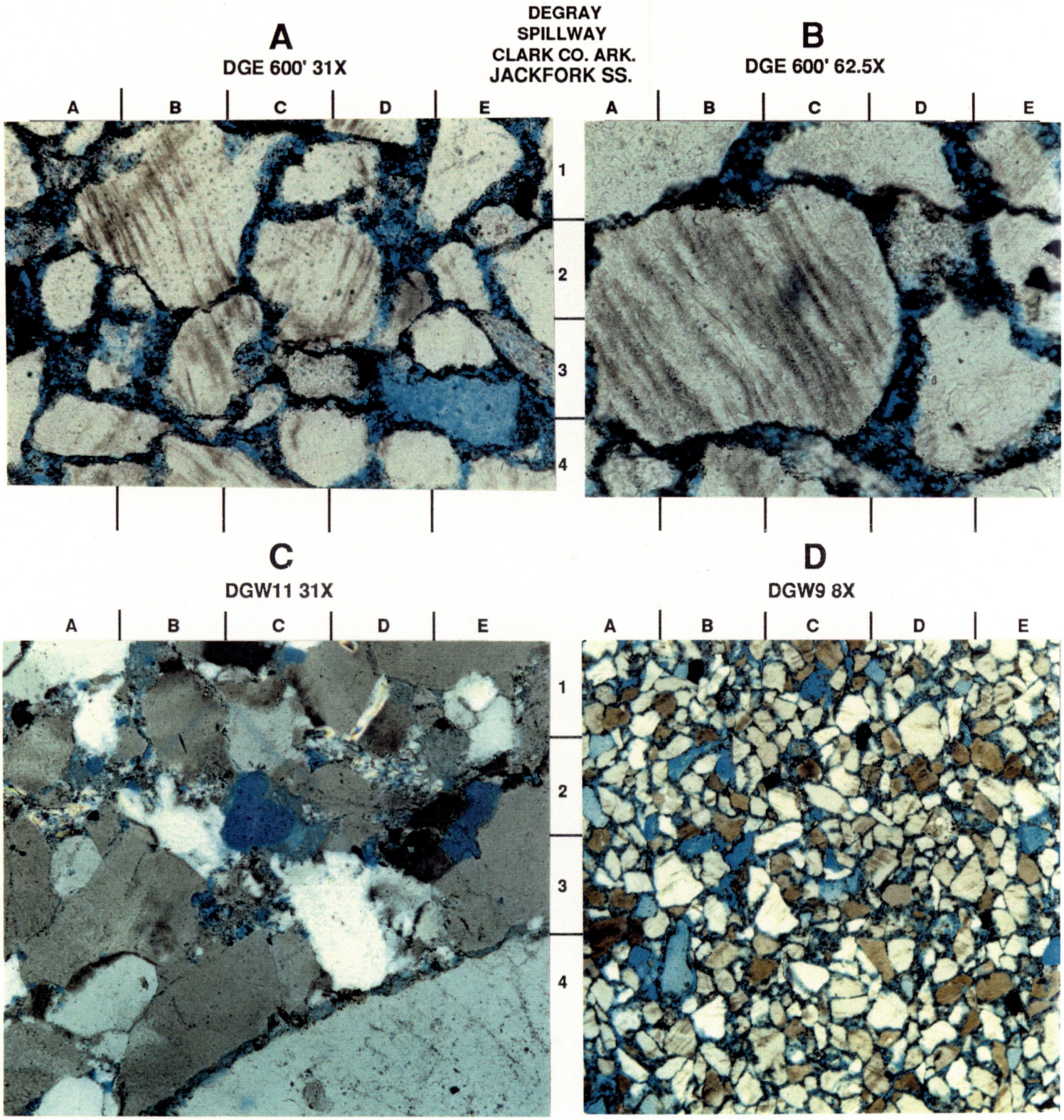

Figure 47. (A) Sample at DeGray East 600' log depth (400' measured section), quartz grains showing prominent Boehm lamellae (31X). (B) Same sample as in A above. Close-up of prominent wavy Boehm lamellae (62.5X). (C) Sample at DeGray West 34' log depth (sample DGW11), illustrating the habit of scattered secondary pores in the Jackfork observed in the DeGray and Dierks localities (31X). (D) Sample at DeGray West 340' log depth (sample DGW9) illustrating the most porous sample (16%) analyzed in this study. Note the preserved primary (intergranular) and secondary (intragranular) porosity.

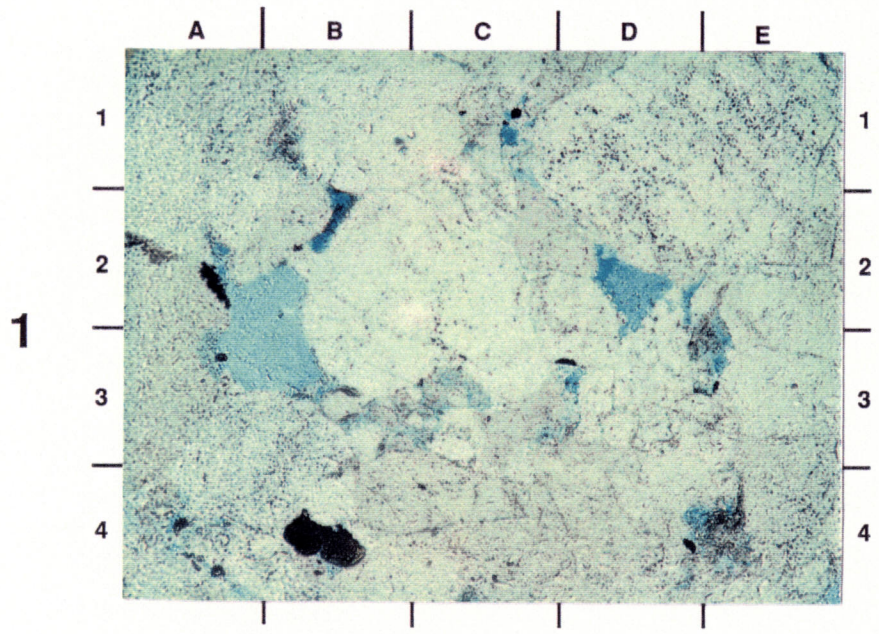

1

SAMPLE 190' 40X
Quartz - 39.5%
Quartz Cmt. - 39.5%
Feldspar - 3.0%
MRF - 7.0%
PRF - 1.0%
Chert - 2.0%
Mica - 0.5%
Hvy. Mnrl. - 0.5%
Matrix - 2.0%
Porosity - 5.0%
F. - Upper Med. Grnd.
Very Quartzose
Well Sorted

100u

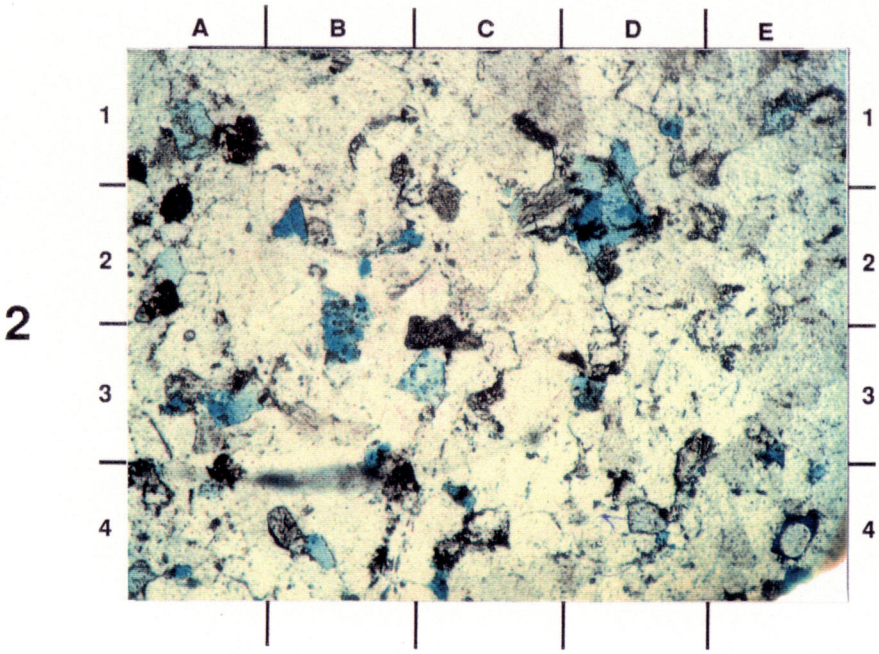

2

SAMPLE 254' 40X
Quartz - 43.5%
Quartz Cmt. - 35.5%
Feldspar - 2.0%
MRF - 9.0%
Chert - 3.0%
Mica - 0.5%
Hvy. Mnrl. - 0.5%
Matrix - 3.0%
Porosity - 3.0%
F. - Med. Grnd.
Somewhat Lithic
Well Sorted

100u

Figure 48. Petrographic comparison of sandstones from DeGray Lake Spillway. Sample 1 at 190' (log depth) on the east side has slightly less matrix and lithic fragments than sample 2 from 254'. Compare samples with log character of the sample site shown in Figure 58.

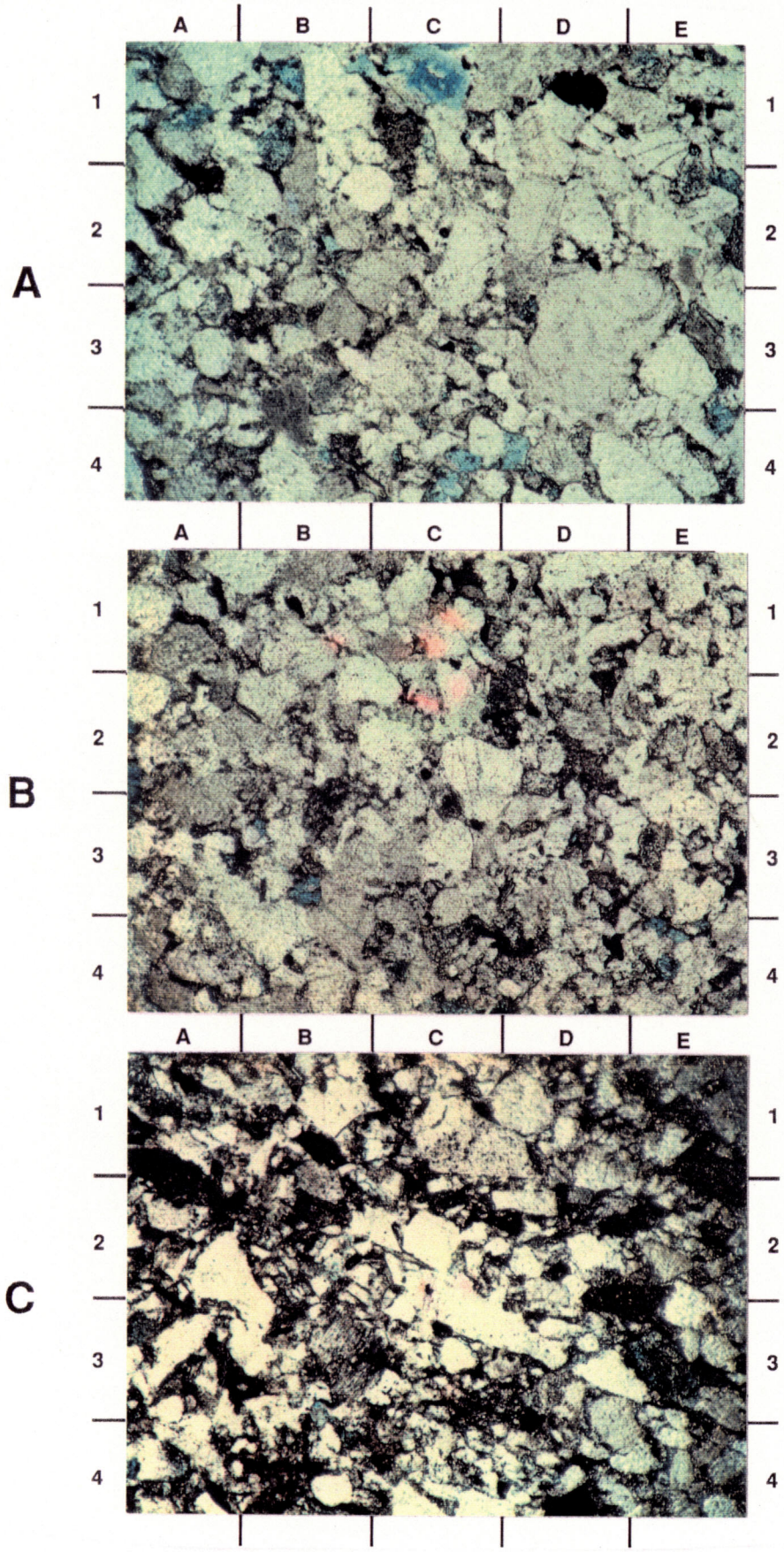

Figure 49. Petrographic comparison of sandstones from Dierks Lake Spillway on the west side. Note increasing 'dirtiness' from sample A to sample C. Sample A at 430' (log depth) on the west side has less matrix and lithic fragments than the sample B from 506' and the sample C from 590'. Compare sample intervals with log characters shown in Figure 58.

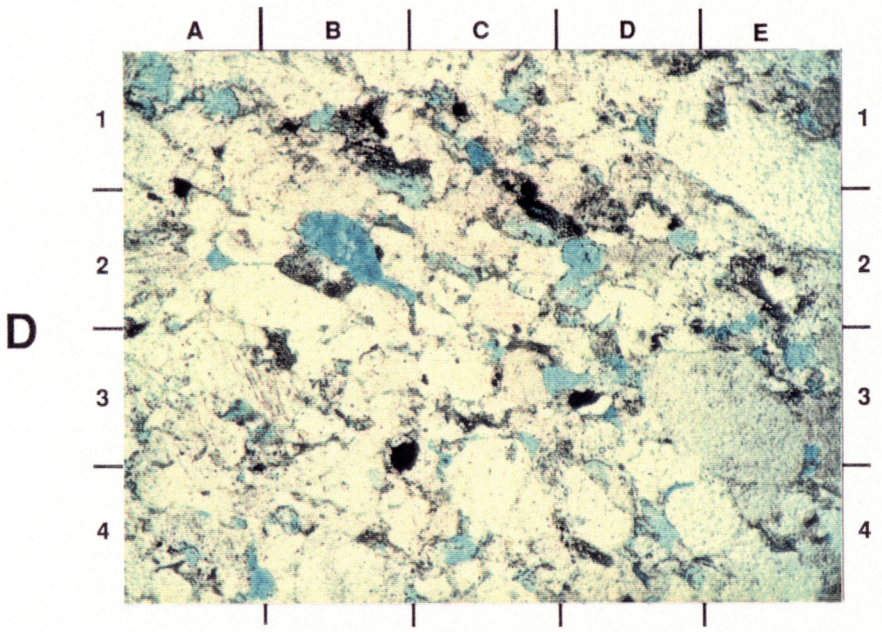

SAMPLE 34' 40X
Quartz - 41.5%
Quartz Cmt. - 40.0%
Feldspar - 4.5%
MRF - 6.0%
Chert - 1.0%
Mica - 0.5%
Hvy. Mnrl. - 1.5%
Matrix - 1.0%
Porosity - 4.0%
F. - Med. Grnd.
Very Quartzose
Well Sorted

100u

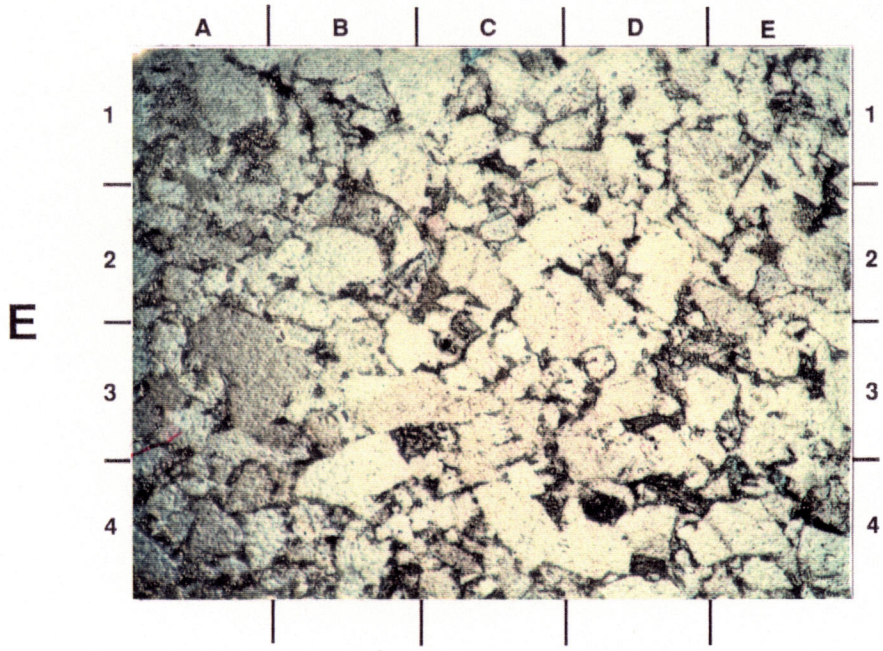

SAMPLE 230' 40X
Quartz - 36.0%
Quartz Cmt. - 33.0%
Feldspar - 2.5%
MRF - 7.5%
PRF - 0.5%
Chert - 10.0%
Mica - 1.0%
Matrix - 8.5%
Porosity - 1.0%
V.F. - Med. Grnd.
Mod. Sorted
Matrix - rich
Cherty

100u

Figure 50. Petrographic comparison of sandstones from Dierks Lake Spillway on the west side. Sample D at 34' (log depth) on the east side has slightly less matrix and lithic fragments than sample B from 230'. Compare sample intervals with log characters shown in Figure 58

%, and normalized matrix % vs. total porosity %. These cross-plots are used to illustrate a few points about the relationships of grain size, cementation, matrix content, and porosity. Although the plots display some scatter, there are trends that fall out. The plots show that coarser grained rocks tend to be more heavily cemented and less porous. Finer-grained rocks have higher lithic and matrix percentages and are more porous. The bulk of the most porous sands have a lithic content between approximately 6% and 16% and matrix content between approximately 5% and 15%. These relationships were first noted in the Jackfork by Morris et al. (1979). The obvious hypothesis then, is that the coarser, cleaner, more quartzose rocks, although probably having possessed higher original porosity, were more effective conduits for diagenetic fluids and as a result are now simply tightly cemented. The finer rocks were less permeable by virtue of higher detrital matrix but were more prone to secondary porosity development due to the higher lithic content, and now display the greatest porosity. It must be cautioned, however, that porosity can be a relative term and that the porous rocks of the Jackfork range between approximately 4% and 10%.

Petrography, Gamma-ray Response, Sedimentology, and Depositional Models

Figure 51 shows gamma-ray logs obtained with the hand-held scintillometer at 2-foot sample spacings for the east and west walls of the spillway. Figures 52-56 display plots of petrographic data, gamma-ray log curves, and lithologic sections with descriptions of the depositional units. These figures are of select sections from DeGray Lake Spillway east and west sections, are numbered 1-5, and the following discussion is intended to provide examples of the relationship between log response and detrital matrix content and the lack of relationship between log response and textural parameters. In reference to matrix content, our gamma logs can be used to interpret reservoir quality, but they do not reflect changes in grain size, sorting of framework grains, or porosity.

Section Number 1 (Fig. 52), from the west side of the DeGray locality, extends from 0 to 42 feet on the log interval (approximately 958 to 1000 feet on the east section description by Morris, 1977) with an additional 7.5 feet of outcrop described above the zero point on the gamma-ray log. Although only two short intervals were sampled, the trends in mean grain size reflect the trends visible in the outcrop. Samples DGW11 and DGW12 reflect the mixture of medium to coarse sand with granules and pebbles (up to 8 mm). This coarse material is prevalent near the base of the sequence at approximately 34 feet (log depth). Near the top of the sequence, at approximately 0-2 feet, characterized by samples DGW14 and DGW15, the mean grain size of the sand has diminished to fine or medium, pebbles are absent, and granules are rare. The two sampled intervals also show the generally very low (<5%) matrix content of these beds. This low matrix content results in the low gamma-ray counts logged. Sample DGW12 spans the contact between a sand and a conglomerate. The plot of polycrystalline quartz, which jumps from 8% to 46.5% across that contact, reflects the nature of the quartz pebbles and their probable derivation from a metamorphosed quartz terrain.

Section Number 2 (Fig. 53) extends from 805'-852' (log depth) or about 152'-202' on the section by Morris (1977) on the east side of the DeGray Lake Spillway locality. The outcrop reveals a complex vertical sequence of fairly thick massive or flat laminated sands, labeled A-E, interbedded with shales, contorted and cross-laminated sands, with local dish structures and vertical dewatering channels. Units A and B, characterized by samples DGE4-DGE9, show internal variability in grain size with no distinctive trends. Unit C, characterized by samples DGE11 and DGE12, appears to coarsen upwards as seen in the plot of MGS. Unit D, characterized by samples DGE15-17, fines upwards. Through all these sand units, and the intervening beds, the percent of matrix shows a gradual decrease upwards from approximately 10% at the base to approximately 5% at the top. There are fluctuations within the trend but there is a distinct decrease upwards which results in the cleaning-up or apparent "coarsening-up" appearance of the log curve. This section illustrates the strong control matrix has on the log response and the independence of log response from grain size. The apparent coarsening-upward trend, which would

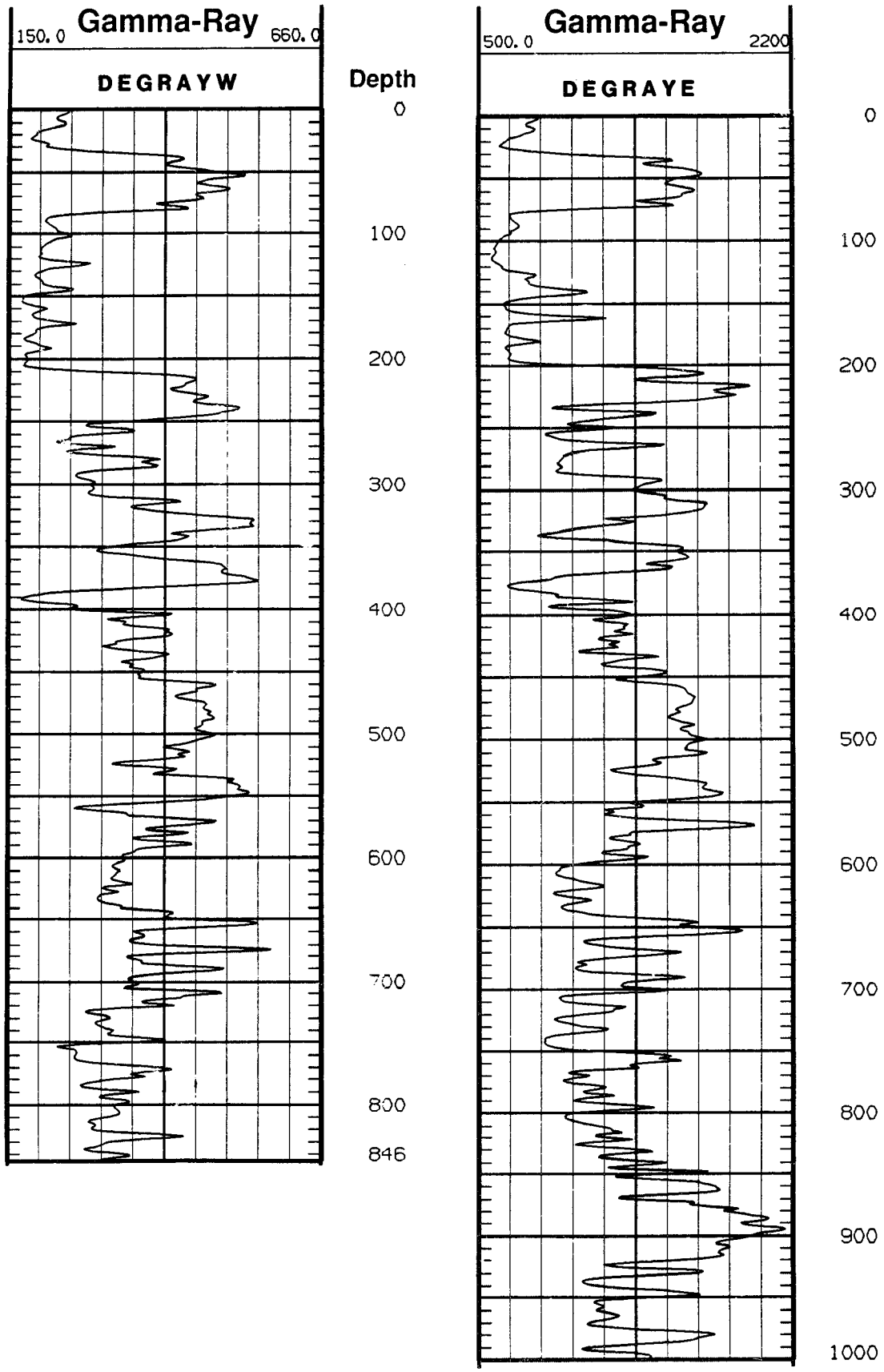

Figure 51. Gamma-ray logs obtained with a hand-held scintillometer (two foot sample spacing) along the east and west walls of DeGray Lake Spillway. The two walls are spaced about 300 feet apart.

commonly be interpreted as representing a prograding lobe sequence, is really a complex of massive-appearing turbidites, slurried beds, flat-laminated sands, and shales. The sequence displays no definitive evidence of progradation of facies.

Section Number 3 (Fig. 54) extends from 815'-846' (log) on the west side of the DeGray Spillway locality and correlates in part with Section Number 2 on the east side. The massive, flat-topped, structureless sandstone at the base of the section correlates with Unit C on the east side. The overlying interbedded sandstone/shale unit with contorted sandstones correlates with the shale between Units C and D on the east side. Sandstone Unit D, from the east side, correlates with the massive sandstone in the middle of Section 3.We can interpret no systematic "cleaning" or "coarsening-up" in these sandstones based on log character, but rather a higher degree of variability. The log response for Unit C and the correlative west side unit seem to show a sharp drop in gamma-ray counts and a "dirty" zone near the top which results in the "shoulder" in the log curve at approximately 833'. The shale between Units D and E on the east side, produces a major shale deflection on the log of Section 2, but only a minor deflection in the log of Section 3 on the west side. This gives the D/E correlative units on the west side the appearance of a bi-lobed sand at approximately 812-'820'.

Section Number 4 (Fig. 55) extends from 336'-362' (log) on the west side of the DeGray Lake Spillway locality. It correlates with Section Number 5 on the east side and comprises what would probably be interpreted, from log character, as two sands. One "clean" sand at approximately 353' (log) and a "dirtier" sand at approximately 340' (log) separated by a shale. The lithologic column and outcrop show us a much more complex picture. The "clean" sand is composed of at least nine depositional units labeled A-I, including two laminated shales. There is little change in grain size through Units A-D. In Unit E/F the plot shows a gradual fining upward trend, a decrease in sorting, and an increase in matrix. This trend extends from the massive, dish-structured Unit E to the flat laminated and cross-laminated Unit F. The log is deflecting back to the right in response to the increasing matrix content of Unit F and the interbedded shales above 348'. The sands at 342' and 342.5', represented by samples DGW9 and DGW8, appear to be one sand on the log, even though they are just somewhat thicker interbeds in a thick interval of interbedded sands and shales.

Section Number 5 (Fig. 56) extends from approximately 320'-350' (log) on the east side of the DeGray Spillway locality. It correlates with section Number 4 on the west side. The outcrop section is composed of units that appear to correlate well across the spillway and the two sections have similar log response. Section 5 also appears to be one thick "clean" sand and a thinner "dirtier" sand separated by a shale. Depositional units A-I are easily recognized with some subtle differences. Unit A is slightly thinner and displays the same coarsening-up trend from the interbedded sand and shale below. Unit B, a cross-laminated sand interbedded with fissile shale, correlates across the spillway with very little change. Unit C, the massive sand with faint dish structures, is thicker on the east then it is on the west. Unit D, a cross- and flat-laminated sand, is two feet thick on the east side, but only one foot thick on the west side. The combined Unit E/F is slightly thinner on the east side but the same stacking sequence of sedimentary structures is preserved despite the thinning. The grain size trend on the east side in Section 5 is similar to the trend on the west. It remains consistent from Unit A through the base of Unit E, then fines upwards to the top of Unit F. The trends in matrix content and porosity are the same as seen in Section 4. Matrix is high in sample DGE21, in the lower interbedded sand/shale interval, then remains fairly constant through sample DGE26 at the top of Unit F, which has a value of 15.5%. The upper interbedded sequence is shaley with sand characterized by sample DGE28 resulting in the low gamma-ray deflection in the log at approximately 324'.

A significant point we wish to make about these correlations of depositional units/ mineralogy/log response is one that may dramatically impact interpretations of depositional units based on log curve shape. You will see a number of examples that show apparent "coarsening-upward cycles" which are commonly associated with "prograding lobes". This topic is discussed in the section on lateral continuity of beds. At Dierks West,

SECTION NO. 1 DEGRAY WEST

DESCRIPTION

THIN, FINE CONGLOMERATE AND GRANULES SCOURED SURFACE WITH DOWNCUTTING UP TO 30-40 CM INTO UNDERLYING BED.

PROBABLE SCOUR SURFACE, FINE TO MEDIUM GRAINS

FINE TO MEDIUM GRAINED LAMINATED SAND OVERLYING CONGLOMERATE UP TO 6 CM RESTING ON AN EVEN, CONTINUOUS SURFACE.

FINE GRAINED, SILTY, SLIGHTLY MICACEOUS.

MEDIUM TO COARSE GRAINED, UNDULATORY BEDDING

ROLLED MASSES OF FINE TO MEDIUM SS.

1000' (MORRIS, 1977)

GENERALLY FLAT, CONTINUOUS SILTY ZONE.

FINE GRAINED, SLIGHTLY MICACEOUS.

PEBBLES, MAX. OF 6-7MM, AVERAGE 3-4MM.

CUT-OUT OCCURS OVER LATERAL DISTANCE OF 1.2M.

LOADING OR SCOUR LATERAL AT THIS CONTACT.

NORMALLY GRADED CONG.-SS UNIT.

PEBBLE CONGLOMERATE, MAX. 11MM, AVG. 5-6MM.

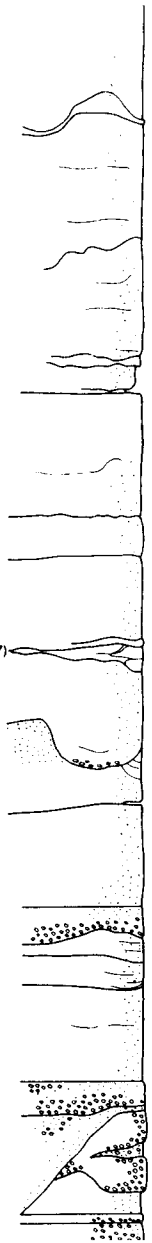

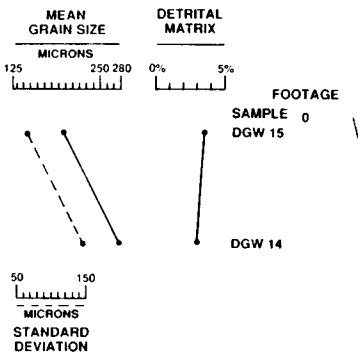

10'

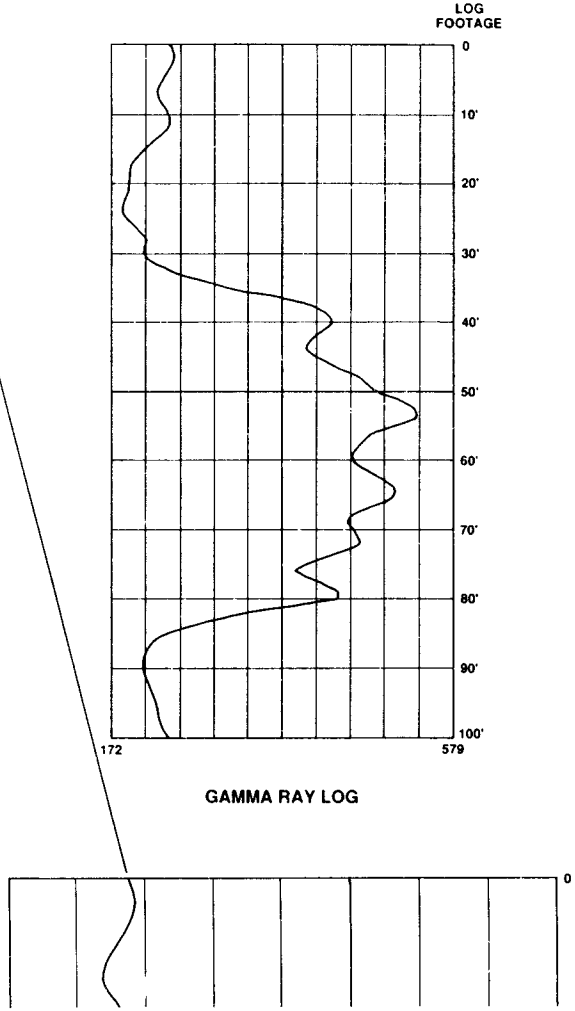

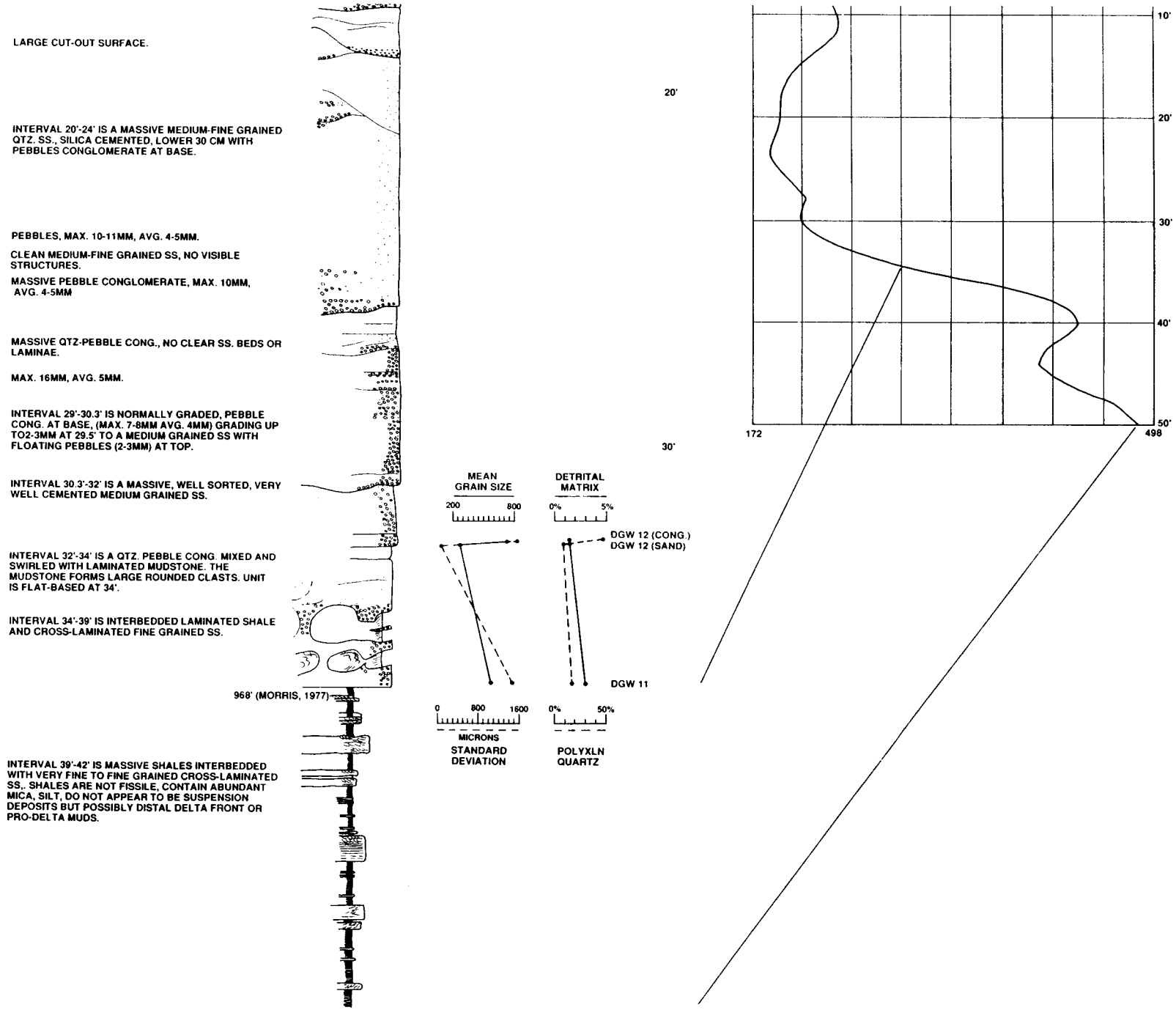

Figure 52. Detailed lithologic log plot for Section Number 1, DeGray West, 0'- 42' (log depth).

SECTION NO. 2 DEGRAY EAST

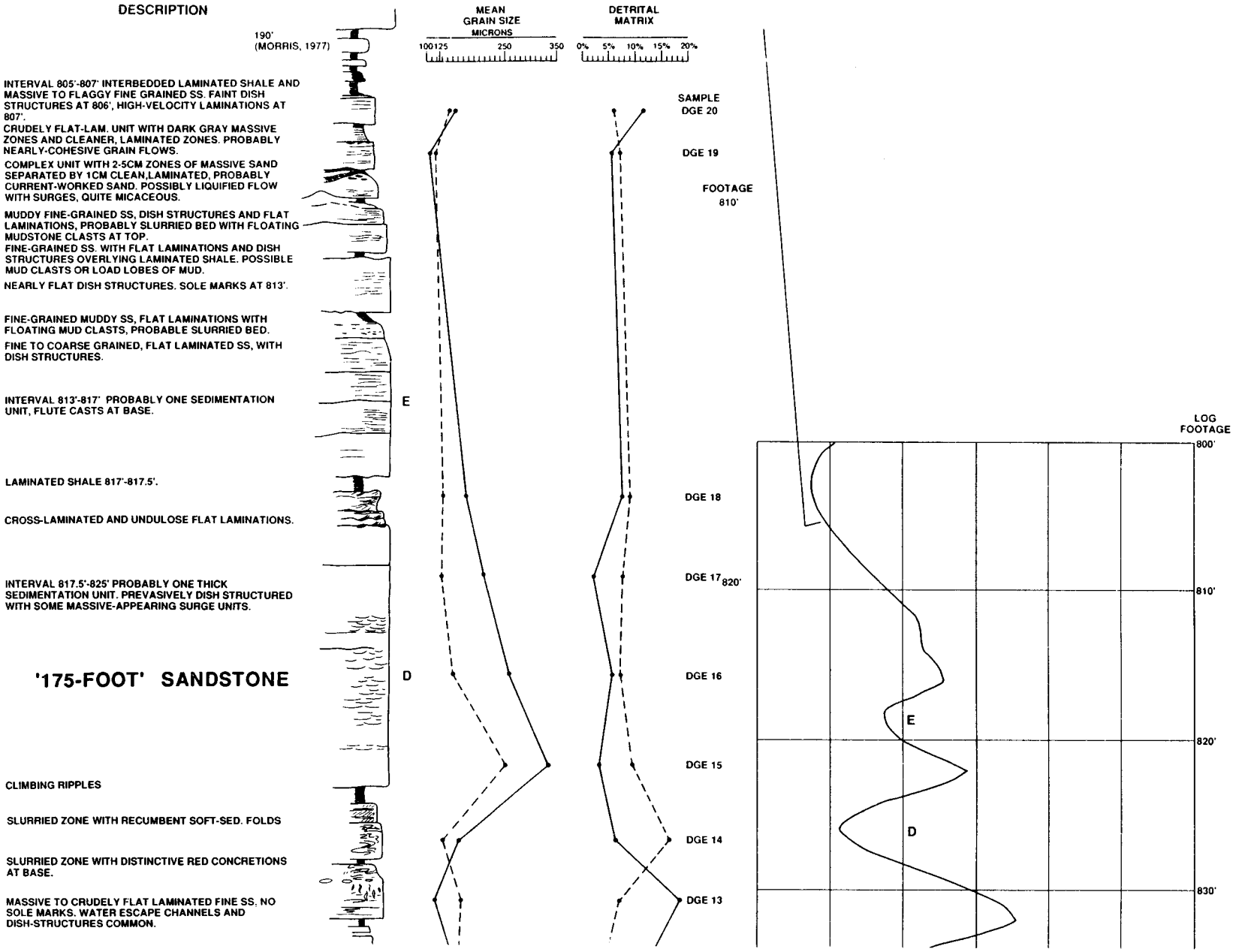

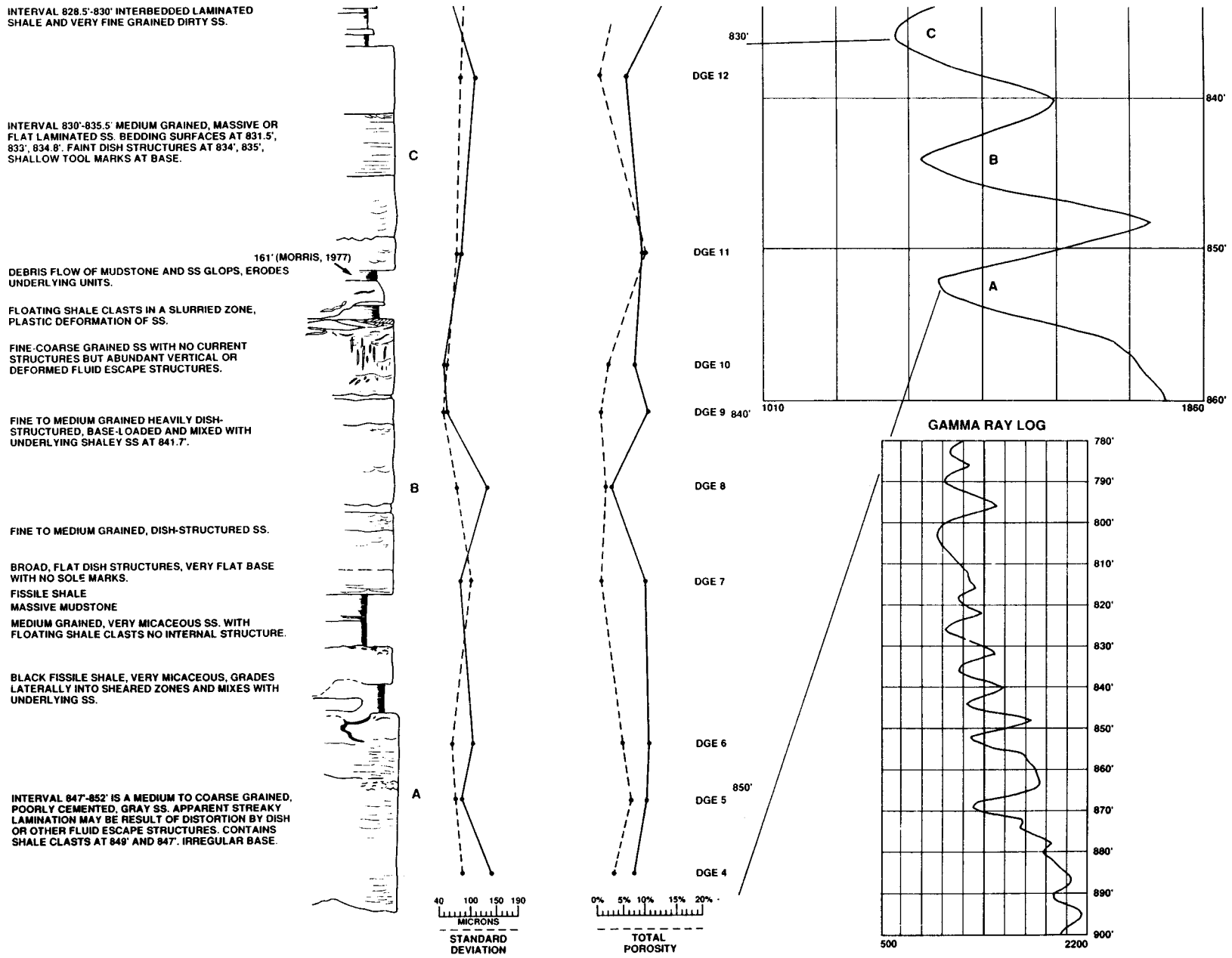

Figure 53. Detailed lithologic log plot for Section Number 2, DeGray East 805'-852' (log depth).

SECTION NO. 3 DEGRAY WEST

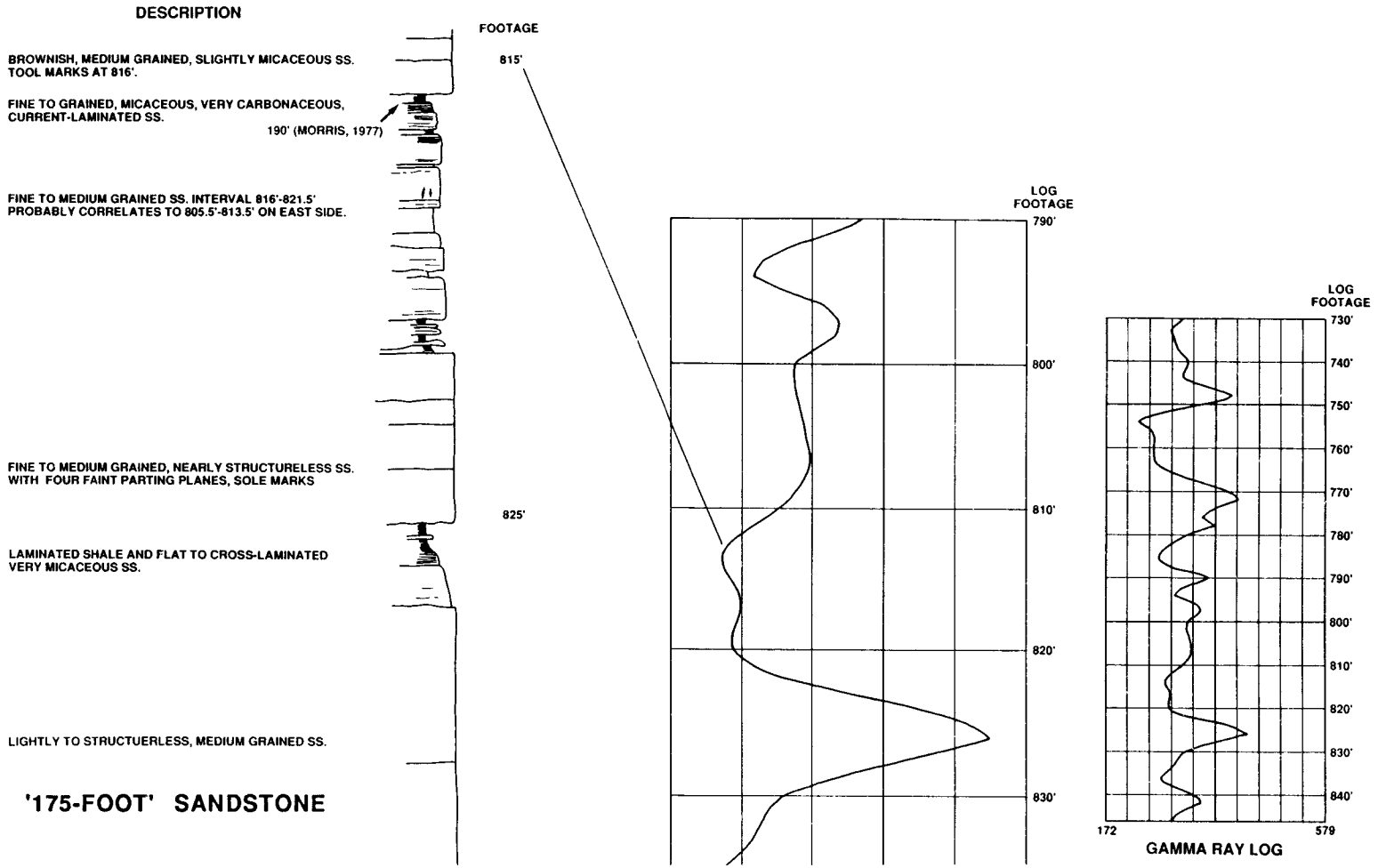

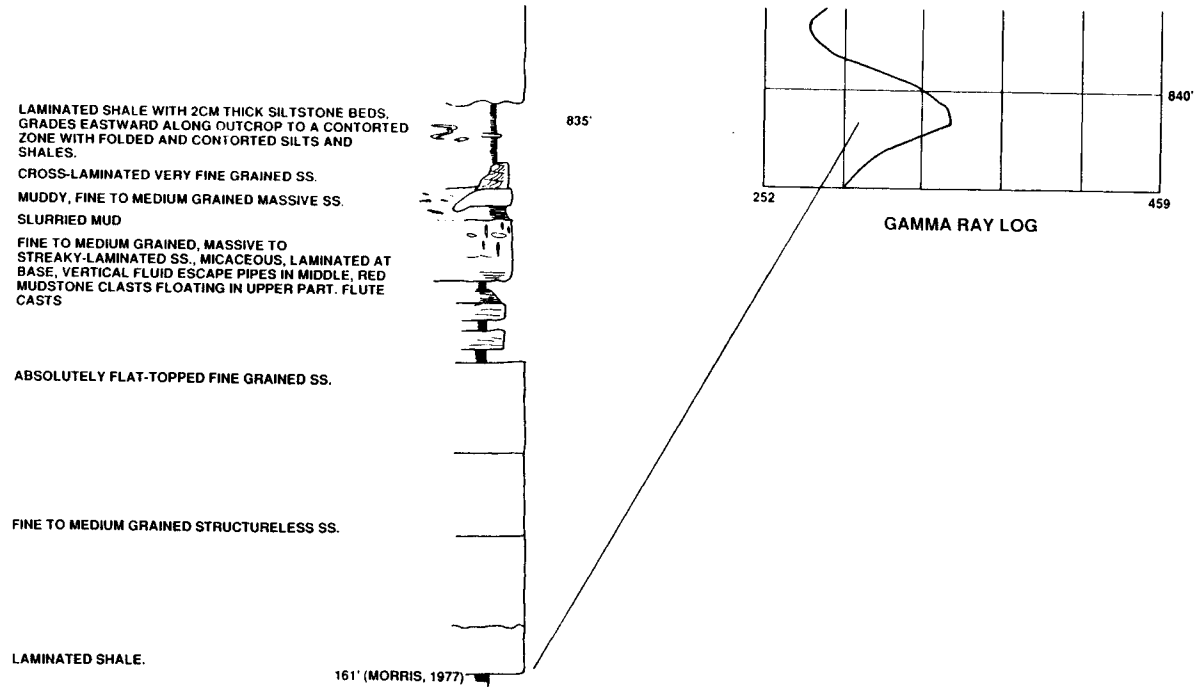

Figure 54. Detailed lithologic log plot for Section 3, DeGray West, 815'-846' (log depth).

SECTION NO. 4 DEGRAY WEST

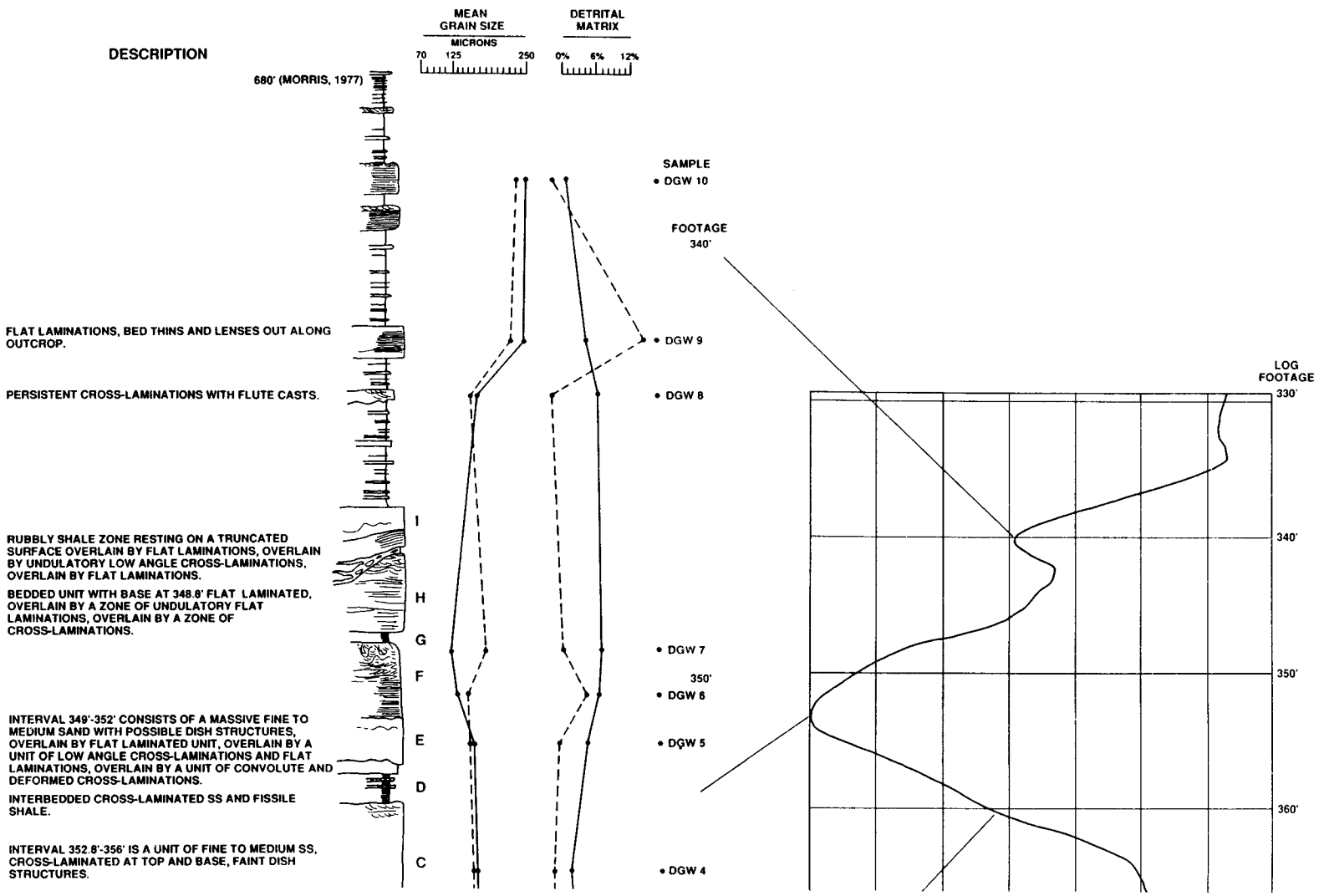

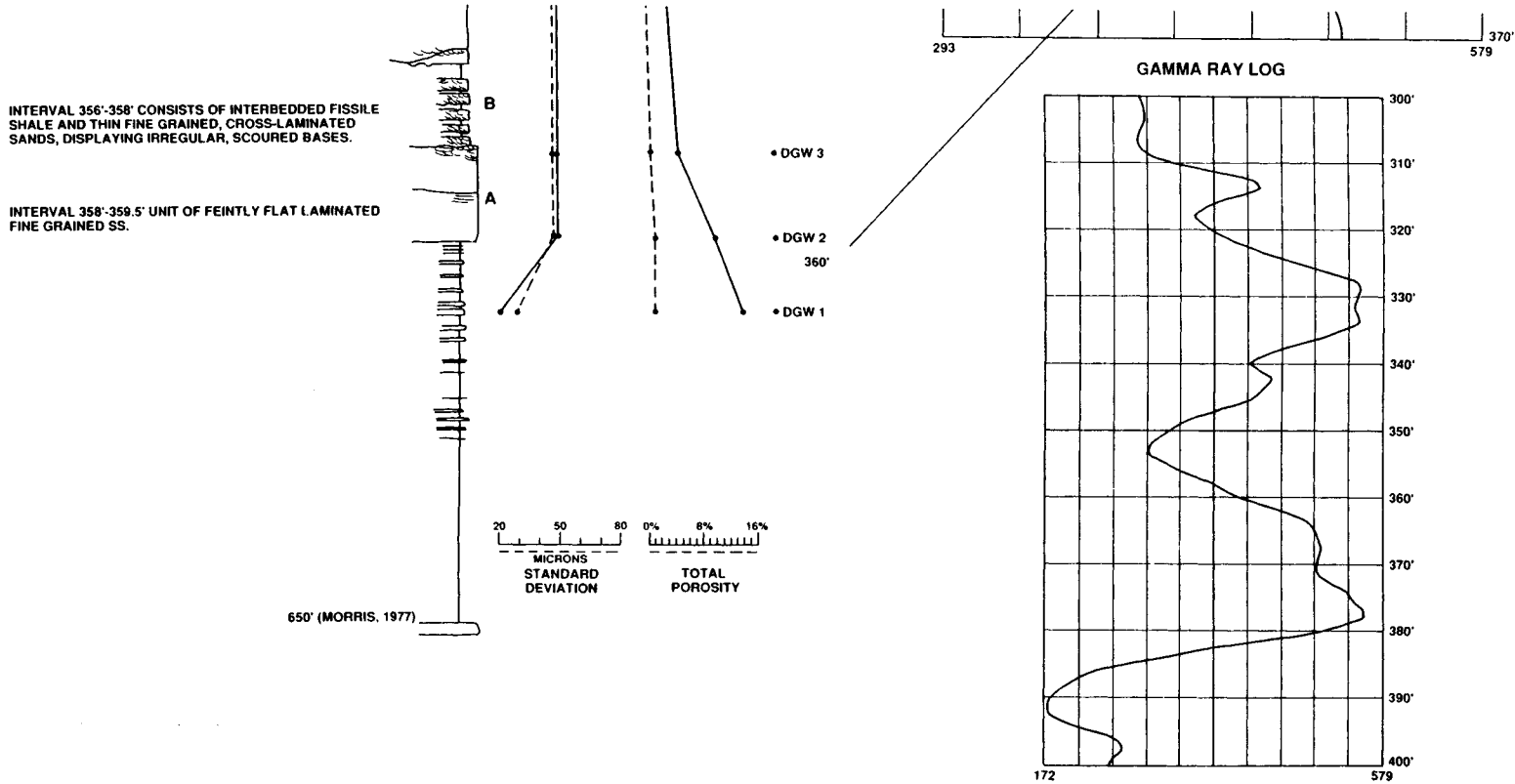

Figure 55. Detailed lithologic log plot for Section Number 4, DeGray West, 336'-362' (log depth).

SECTION NO. 5 DEGRAY EAST

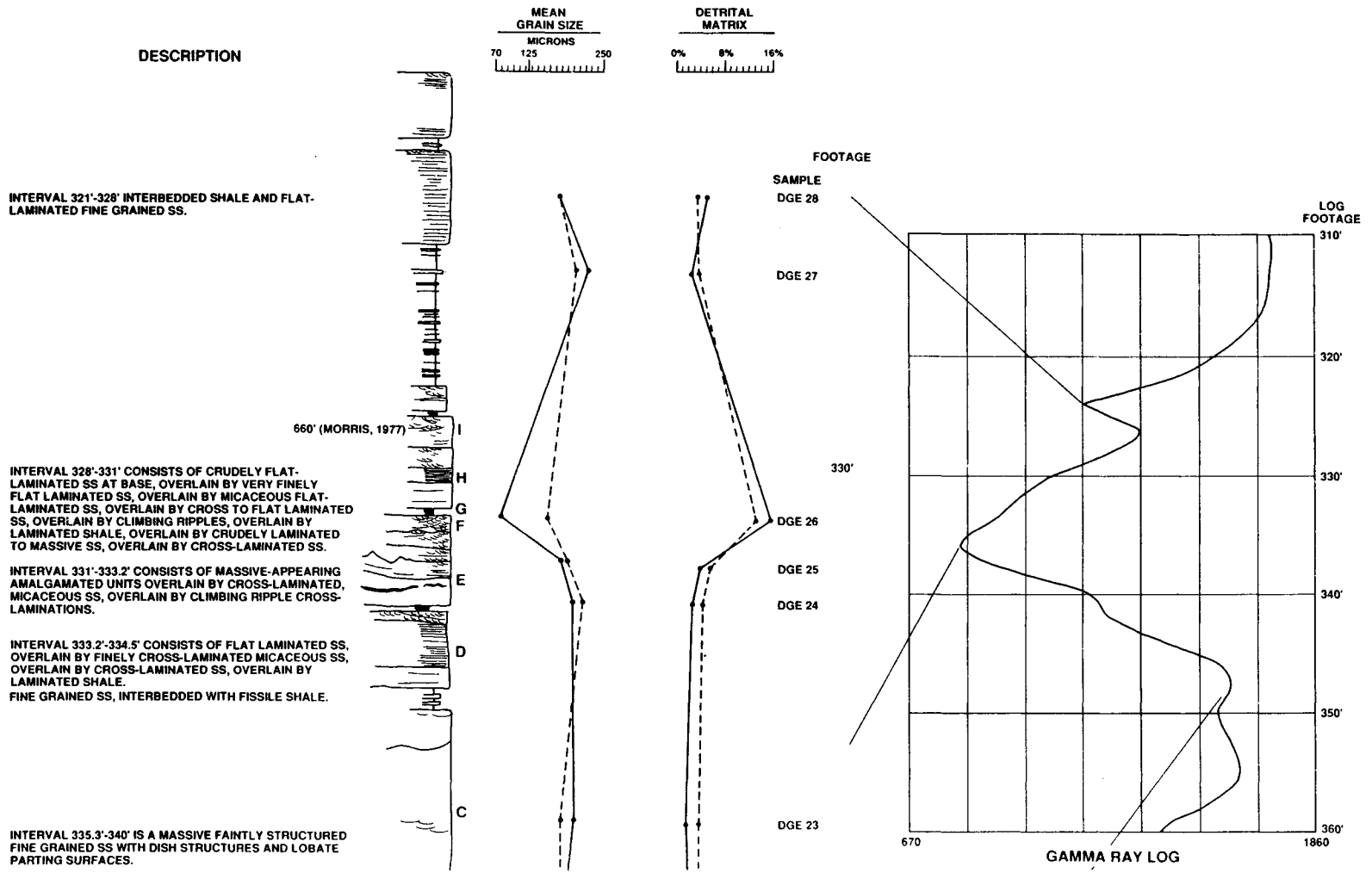

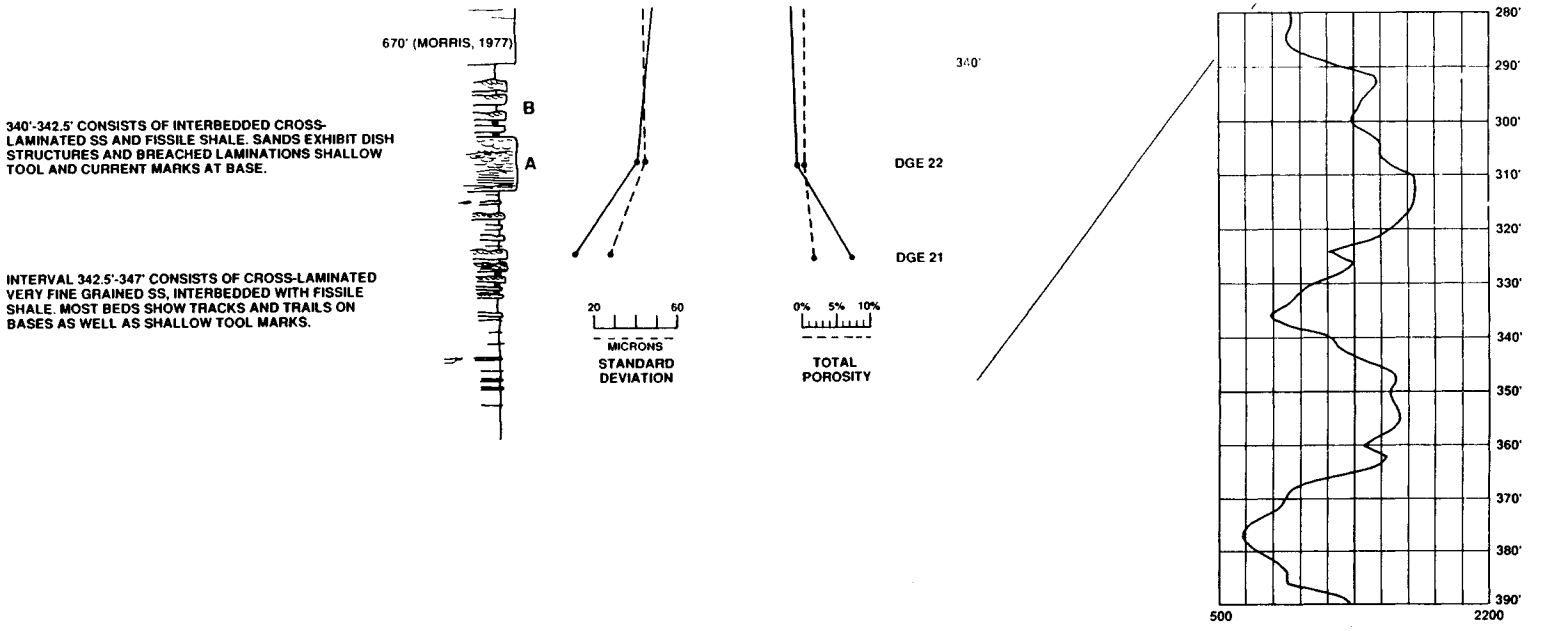

Figure 56. Detailed lithologic log plot for Section Number 5, DeGray East, 320'-350' (log depth).

you will see a two dramatic examples of "fining upward cycles" on the log, that would commonly be associated with channel facies. These example intervals show no sedimentologic indications of being parts of prograding lobes or channels, and more often are not coarsening upwards or fining upwards in concert with the log character. They are typically "cleaning" or "dirtying" upwards in terms of detrital matrix.

The packages of sandstones interpreted on the logs are invariably composed of numerous depositional units which are much thinner than the "sandstones" discernable on the logs (also discussed later). These depositional units can be characterized as traction deposits, suspension deposits, slurried flows, graded units, or expressions of a continuum of deposits common in a gravity-driven depositional system. Individual depositional units frequently display unchanging, coarsening, or fining upward trends internally. The vertical stacking of depositional units results in a near-random stacking of individual grain size trends that are not reflected in the log response. The mineralogy, hence gamma-ray log response, of a particular turbidite may depend more on the mineralogy of the deposit(s) that "sourced" the turbidite. Depositional processes or influences on provenance which influence the distribution of certain mineralogical components in the source area may have a greater impact on the mineralogy of the turbidites than the gravity-driven processes that produce the units we attempt to decipher through logs.

Reservoir Quality Characterization

Gamma-ray logs may provide a measure of clay content which may affect reservoir quality (porosity and permeability). Higher gamma-ray counts are usually interpreted as indicating relatively finer grain-size and/or relatively higher clay content of strata. However, not all clay minerals contain measurable radioactive elements and some sand-size minerals do contain radioactive elements, so that gamma-ray measurements are not a universally reliable indicator of reservoir quality (Rider, 1990). The Jackfork Group is very quartzose, lacks significant feldspar which might contain radioactive potassium, and contains non-radioactive illite clay. Therefore, these strata provide an opportunity to visually investigate the relationship between gamma-ray counts and detrital clay content (i. e., the higher the gamma count, the poorer the reservoir quality).

To demonstrate this relationship, the gamma-ray logs at DeGray Lake Spillway were first calibrated to relative reservoir quality on the basis of visual estimates of matrix (including clay) content (i. e., the lighter-colored the sandstone, the less the matrix content). Petrographic and gamma-ray analysis of a limited number (seven) of Jackfork sandstone samples from the spillways at DeGray Lake and Dierks Lake (Table 6, see also Figures 48-50) demonstrate that the lower count rates of gamma rays are associated (in 6 out of 7 samples) with a lower amount of matrix (including clay) material and higher visual porosity.

Gamma-ray log data collected at DeGray Lake Spillway also suggest that thinner sandstones contain more matrix (are of finer average grain-size) than thicker sandstones, and thus have poorer reservoir quality. The relationship between bed thickness and grain-size of turbidites previously has been demonstrated by Potter and Scheidegger (1966), Sadler (1982), Middleton and Neal (1989), and Slatt et al. (in press). A decrease in grain-size associated with a decrease in bed thickness is a result of both more and coarser-grained sediment being carried in suspension in a flow of greater turbulence than in a less turbulent flow. Lower energy flows produce thinner and finer-grained beds. A plot of bed thickness vs. gamma-ray counts for beds at the spillway shows that, in very general terms, the thicker the bed, the lower the count and the cleaner the sandstone (Fig. 57). The high degree of scatter of data points (R squared equals 0.34) is due to the fact that the area of investigation of the gamma-ray scintillometer (1 foot in diameter; data from Scintrex manual) is greater than the thickness of some of the beds measured. Consequently, radiation from adjacent shale beds is detected.

The scale of relative reservoir quality for the DeGray Lake Spillway is illustrated in Figure 58. The term relative reservoir quality is stressed because, in fact, absolute reservoir quality of these rocks is poor based upon porosity and permeability measurements

SAMPLE NO. (AND LOG DEPTH)	CPS	Q	QCM	FEL	MRF	CHT	MAT	OTH	POR	GS	SRT
DIERKSW 1 (590')	440	33	13	6	22	2	16	7	1	VF	P
DIERKSW 2 (506')	370	45	26	5	11	1	7	4	1	VF-F	M
DIERKSW 3 (430')	295	45	22	2	12	1	2	11	5	F-M	M-W
DIERKSW 4 (230')	270	36	33	3	7	10	8	2	1	F	M
DIERKSW 5 (34')	230	42	40	4	6	1	1	2	4	F-M	W
DEGRAYE 1 (254')	261 (860)**	44	35	2	9	3	3	1	3	F-M	M-W
DEGRAYE 2 (190')	203 (670)**	40	40	3	7	2	2	1	5	F-M	W

KEY: CPS: COUNTS PER 3 SECONDS
Q: QUARTZ
QCM: QUARTZ CEMENT
FEL: FELDSPAR
MRF: METAMORPHIC ROCK FRAGMENT
CHT: CHERT
MAT: MATRIX
OTH: OTHER
POR: POROSITY
GS: GRAIN SIZE
SRT: SORTING

**: TEN-SECOND READING; ADJUSTED TO THREE-SECOND READING (RECORDED ABOVE)

Table 6. Gamma-ray readings and petrographic characteristics of seven samples from the Jackfork in Arkansas.

(Table 7) and visual observations; porosities are normally less than 5% and permeabilities are less than 0.01 md. Most porosity is occluded by cement (primarily siliceous) and matrix.

Reservoir Implications

Lateral Continuity and Correlation of Stratigraphic Intervals

Stratigraphic intervals and even thick sandstone beds can be correlated across the spillway from east to west. Figure 51 shows gamma-ray logs obtained with the hand-held scintillometer at 2-foot sample spacings for the east and west walls of the spillway, and it is obvious that thick stratigraphic intervals and 'hot shales' can also be correlated on the logs across the 300 feet separating the east and west walls. In addition, the pebbly sandstone and conglomerate beds at the top of the sequence form resistant ridges which can be traced continuously along strike over a distance of several miles in the field and on air photographs (Breckon, 1988), indicating the sequence is laterally continuous for long distances (Fig. 59). Gamma-ray logs superimposed on the east and west sections are shown in Figures 60A-C and 61A-C.

A subsurface well, spudded in Cretaceous sandstones and penetrated the Johns Valley Shale and Jackfork Sandstone, is shown in Figures 62 and 63. The Shell Rex Timber Co. 1-9 well is over 5 miles southwest of the DeGray Lake Spillway. A comparison with the interval from 2690'-3525' on the subsurface gamma-ray log with the interval on the outcrop gamma-ray log from 0'-890' on the DeGray east section suggests that correlations of stratigraphic intervals, and many individual packages, are possible.

We will first deal with the issue of lateral continuity of individual beds, and then discuss

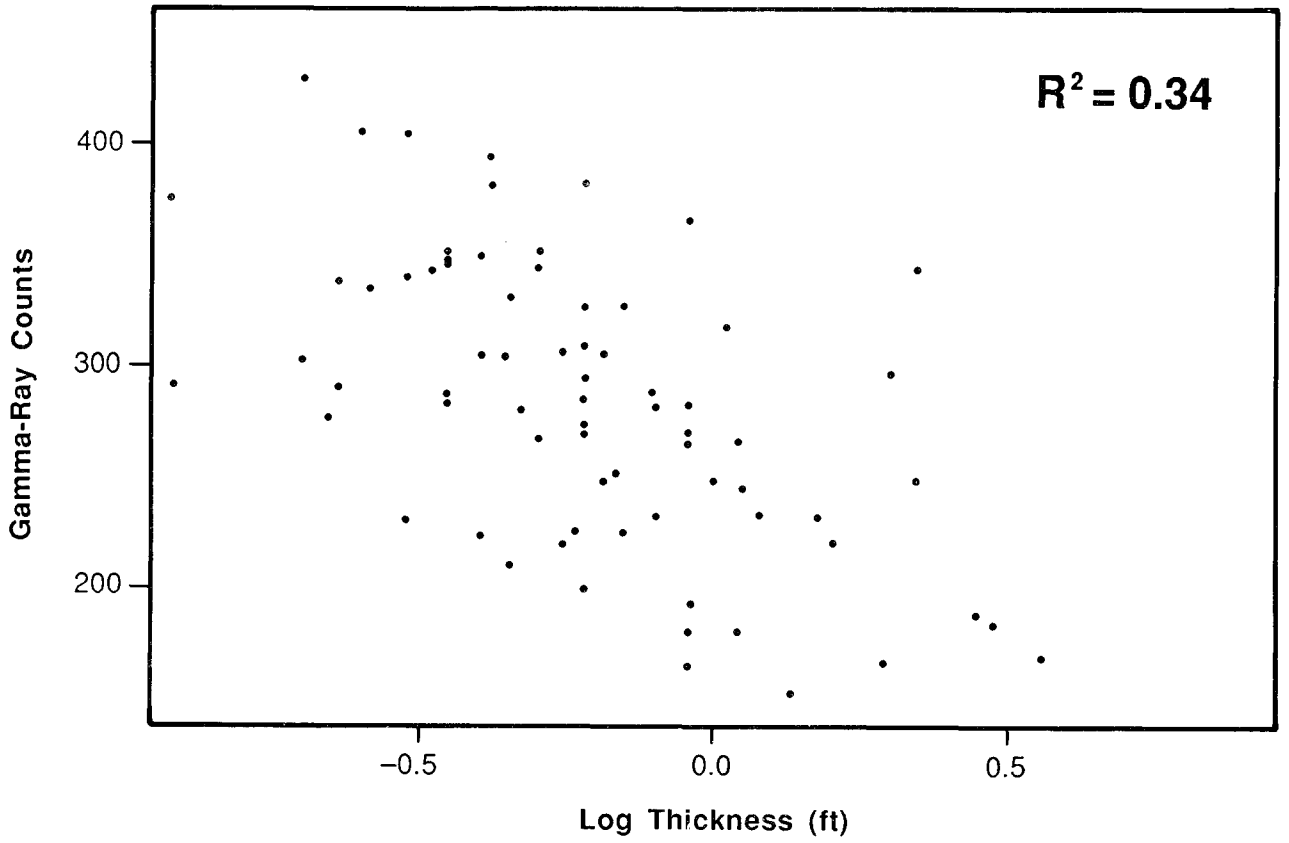

Figure 57. Plot of gamma-ray counts vs. log of sandstone bed thickness for 110 sandstone beds measured along the east and west walls of the DeGray Lake Spillway at 365-460 and 375-470 feet (log depth). The thickness distribution of the sandstone beds was determined to be log normal, so the logarithm of the bed thickness was used to convert to a normal distribution.

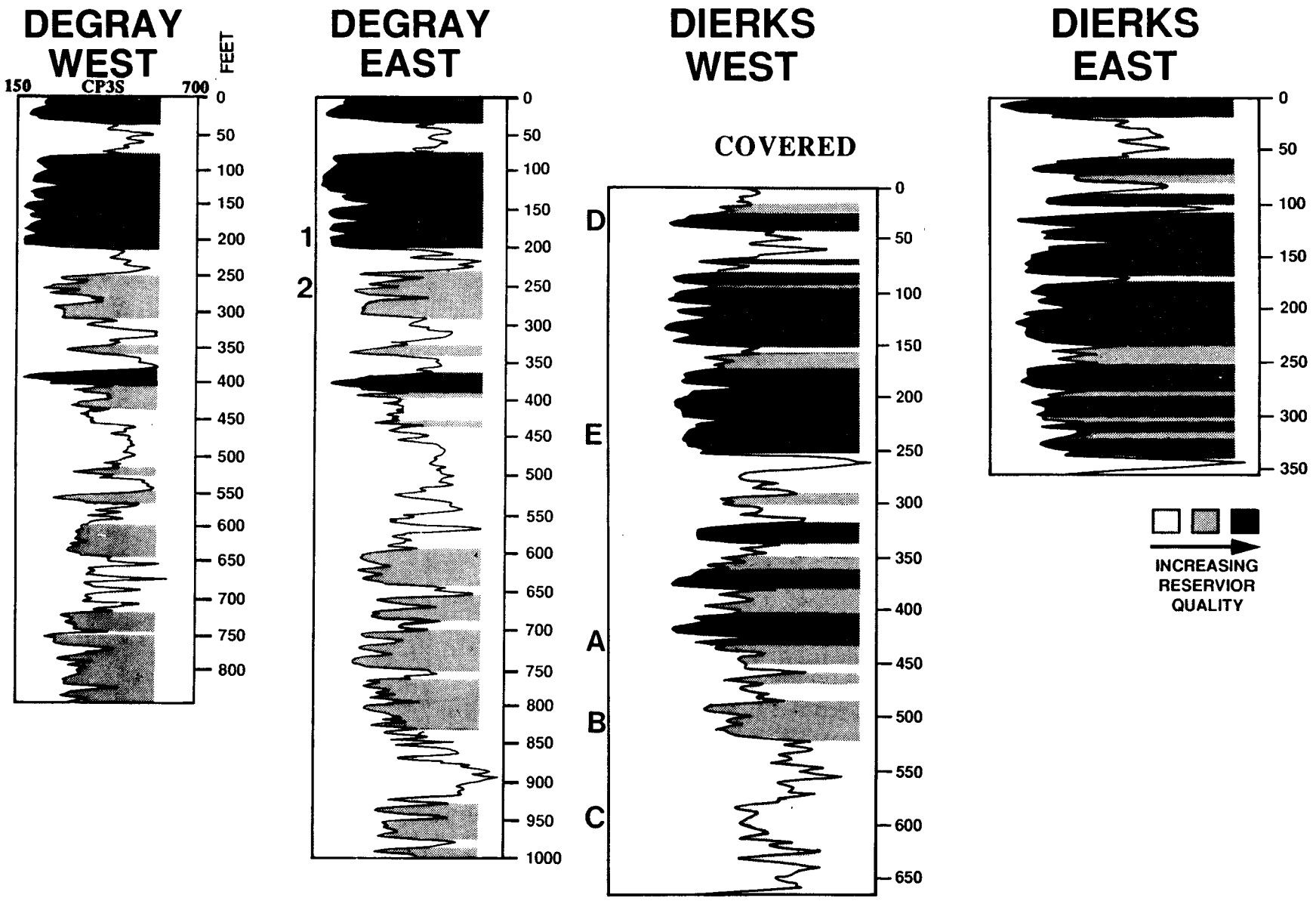

Figure 58. Characterization of reservoir quality on gamma-ray logs form DeGray and Dierks Lake spillways. Darker shades denote increasing reservoir quality. Refer to Figures 48, 49, and 50 for petrographic comparison of samples 1 and 2 at DeGray Lake Spillway and A-E at Dierks Lake Spillway.

SAMPLE NO. (LOG DEPTH)	PERMEABILITY TO GAS (MD)	POROSITY	GRAIN DENSITY GM/CC
DEGRAYE			
369 ft.	0.003	1.9	2.65
381 ft.	0.001	2.5	2.65
528 ft.	0.12	5.4	2.66
DEGRAYW			
383 ft.	0.001	2.3	2.65
394 ft.	0.001	2.1	2.65
531 ft.	0.098	5.5	2.66
BIGROCKQ			
Tan Sandstone	0.004	3.1	2.67
Gray Sandstone	0.001	1.8	2.70

Note: The low porosity and permeability of the rocks indicates the variability in gamma ray readings is a result of variable clay content in the sandstones.

Table 7. Routine petrophysical analyses of outcrop samples from the Jackfork Sandstones. Note extremely low porosity and permeability of these "tight" sandstones.

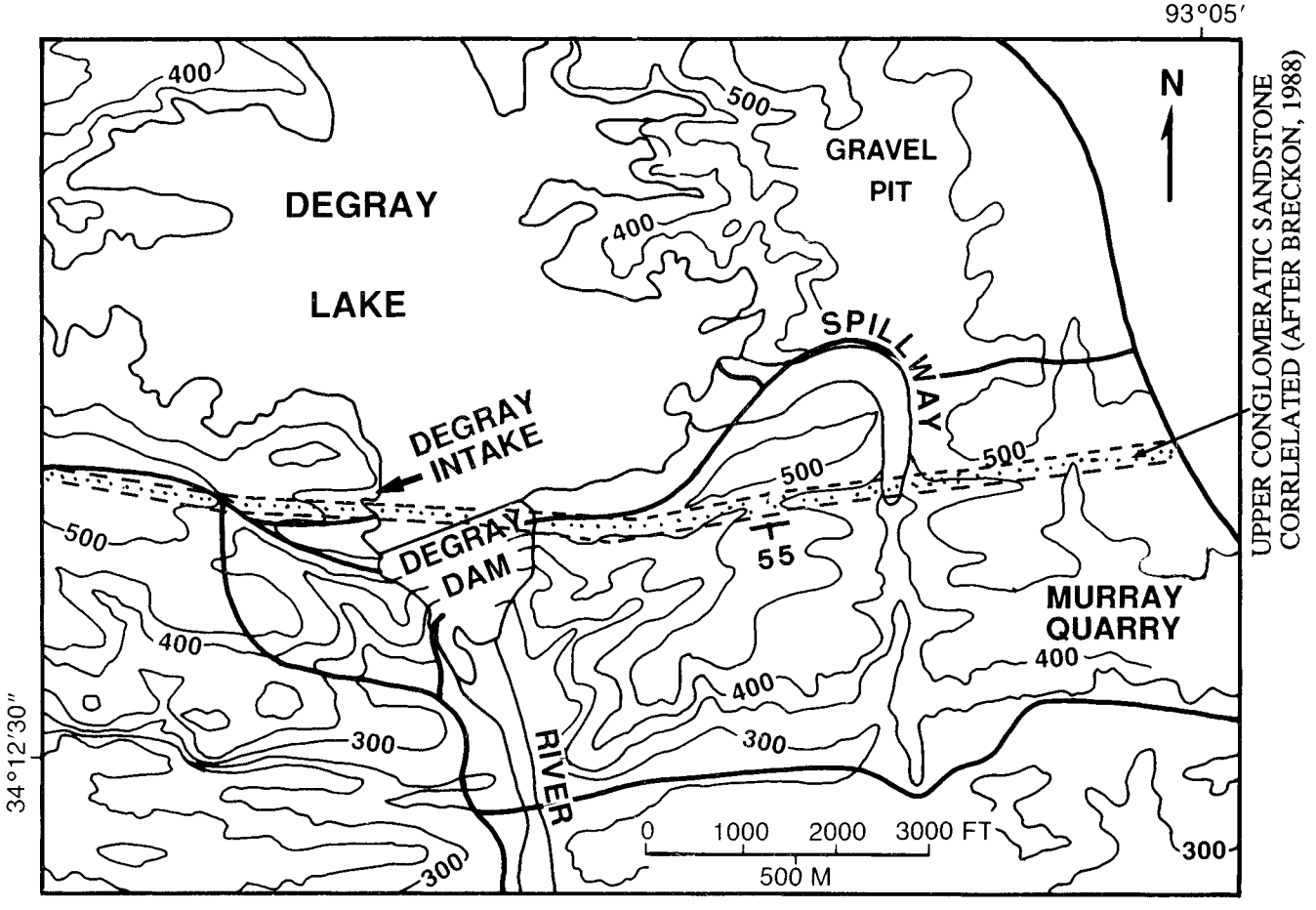

Figure 59. Correlation of conglomeratic (pebbly) sandstone present at the top of the DeGray Lake Spillway section and pebbly sandstone at the top of the DeGray Intake section (STOP 6). After Breckon, 1988. Location of Murray Quarry (STOP 4) shown. Other sections in the Jackfork that had gamma-ray logs measured are near DeGray Dam.

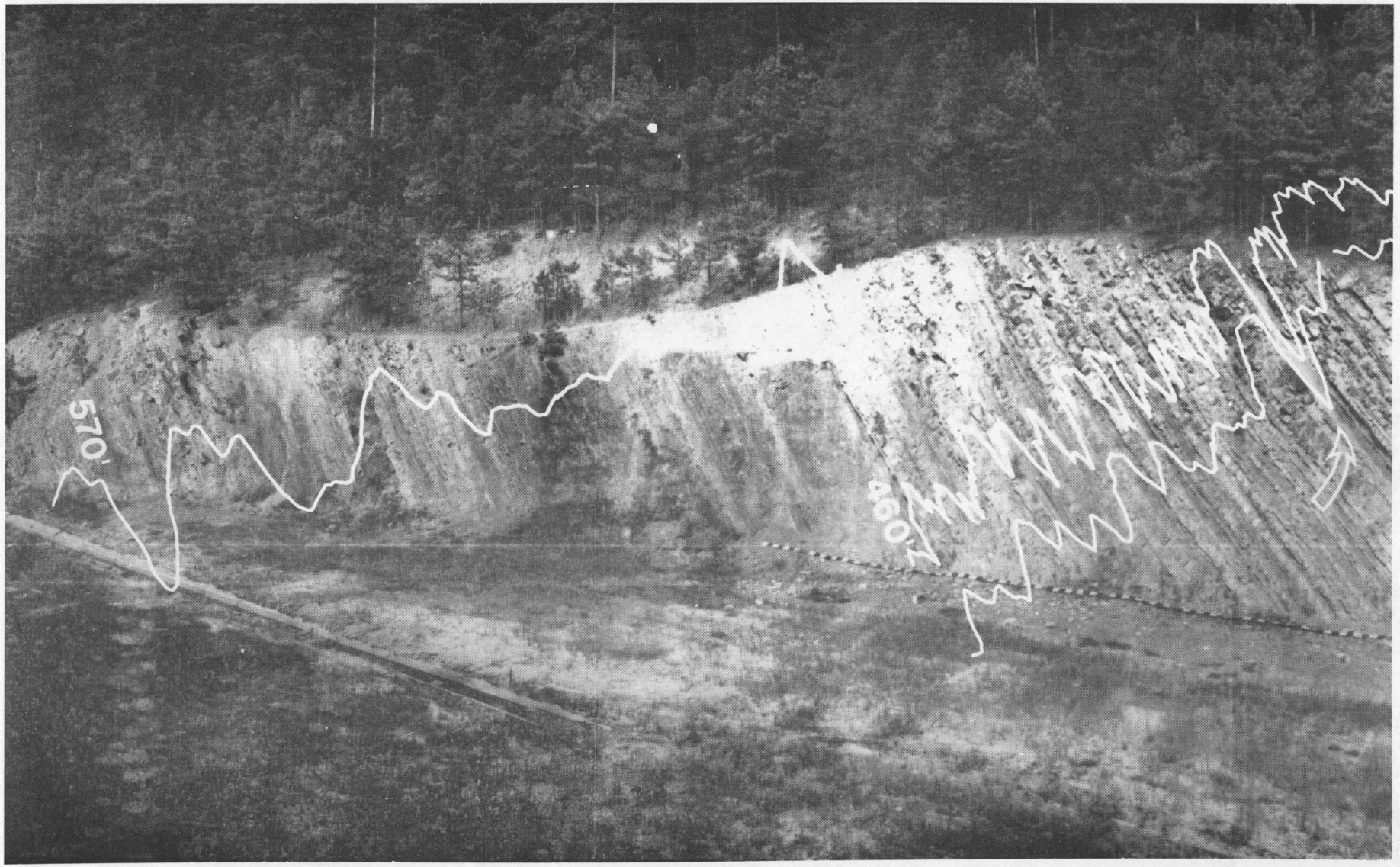

Figure 60. (A, B, C) Gamma-ray logs superimposed on DeGray Lake Spillway east section. Point of overlap for the three photographs is shown at arrows and double arrows. Pertinent log footages are shown. Scale at base of outcrop is in one-foot increments. The logs that were sampled at 0.5-foot spacings are depicted on the logs by the more 'ratty' or detailed nature of the trace when compared to the logs sampled at the 2.0-foot spacing.


288'
320'
365'
B

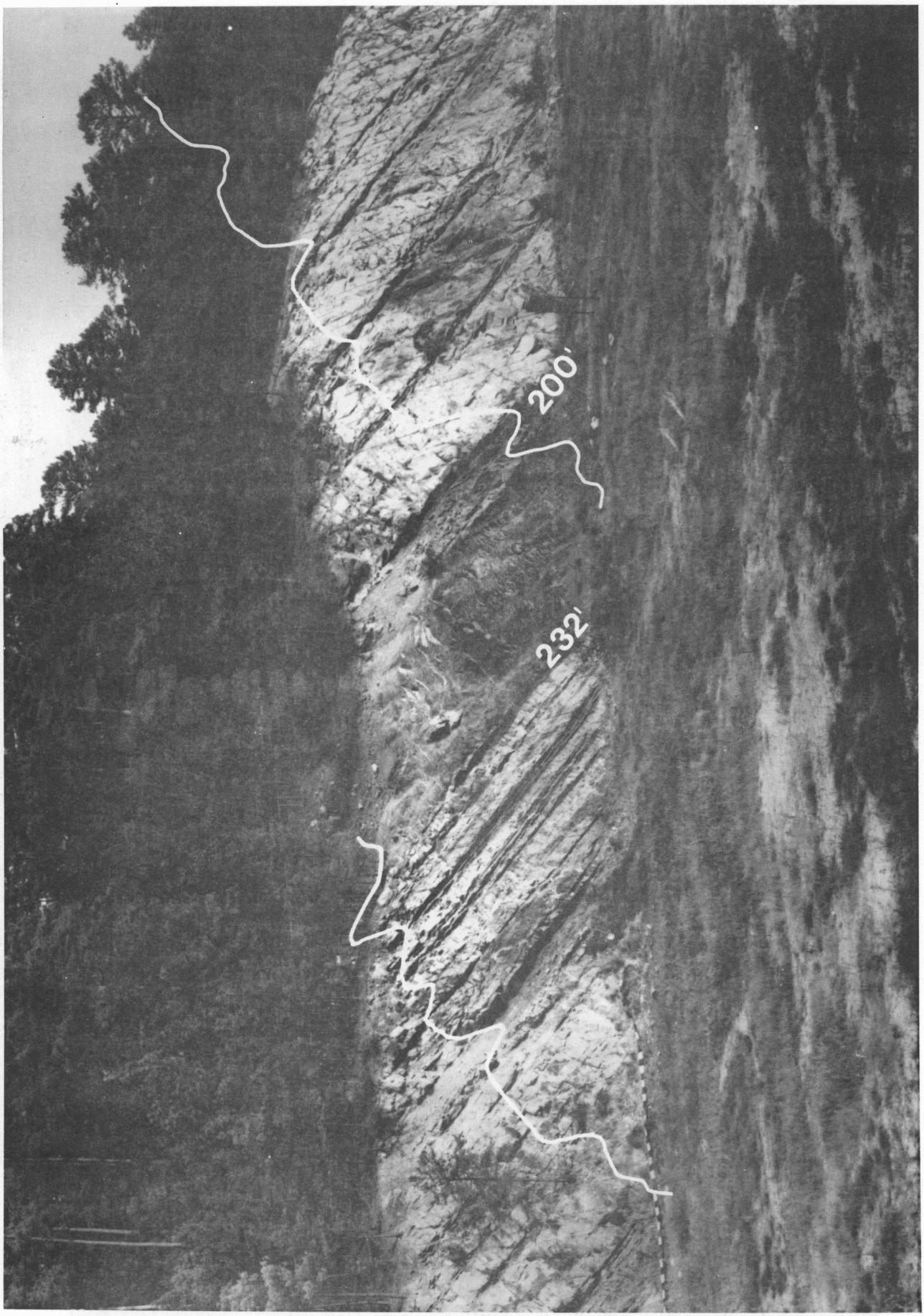
200'
232'

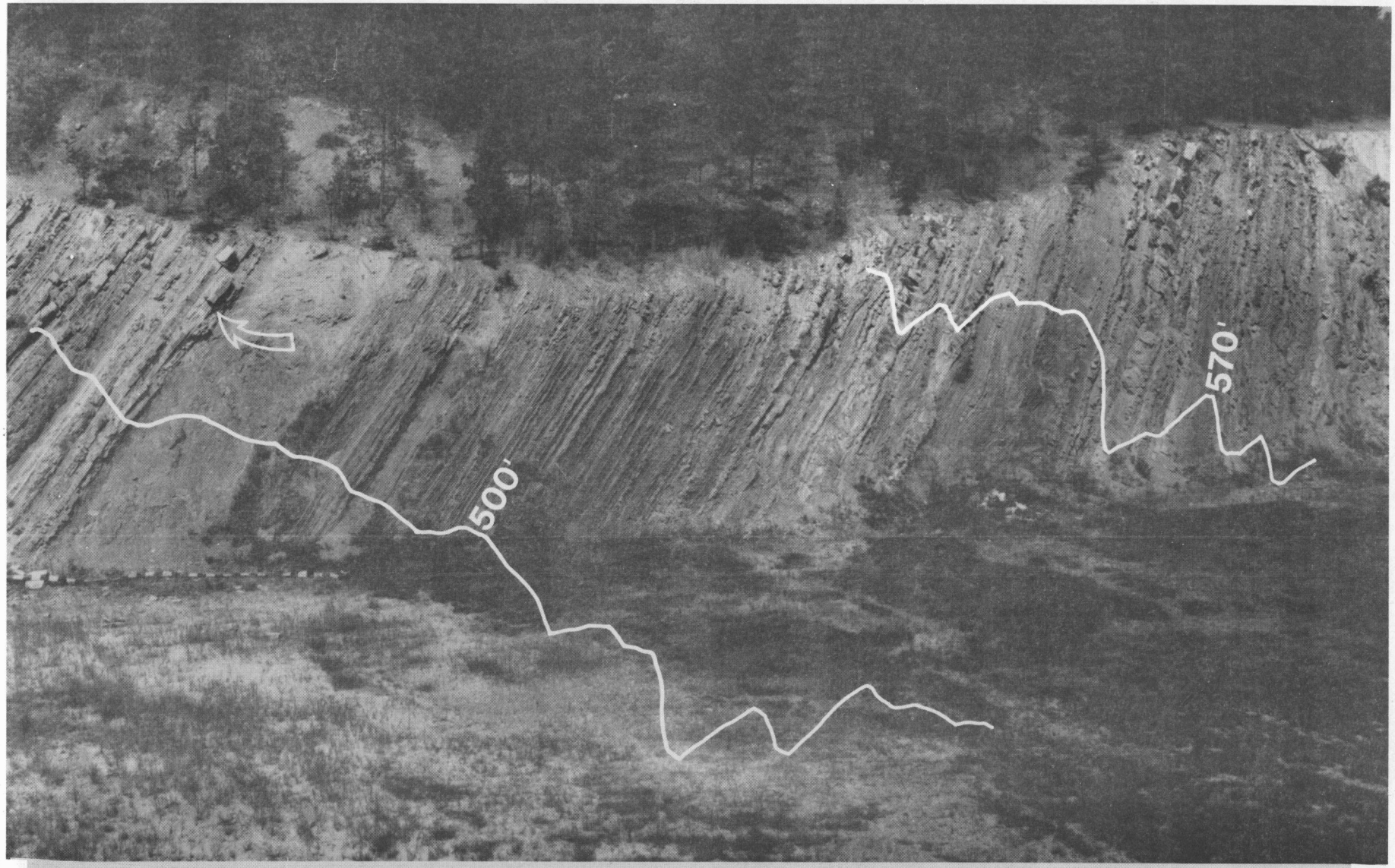

Figure 61. (A, B, C) Gamma-ray logs superimposed on DeGray Lake Spillway west section. Point of overlap for the three photographs is shown at arrows and double arrows. Pertinent log footages are shown. Scale at base of outcrop is in one-foot increments. The logs that were sampled at 0.5-foot spacings are depicted on the logs by the more 'ratty' or detailed nature of the trace when compared to the logs sampled at the 2.0-foot spacing.

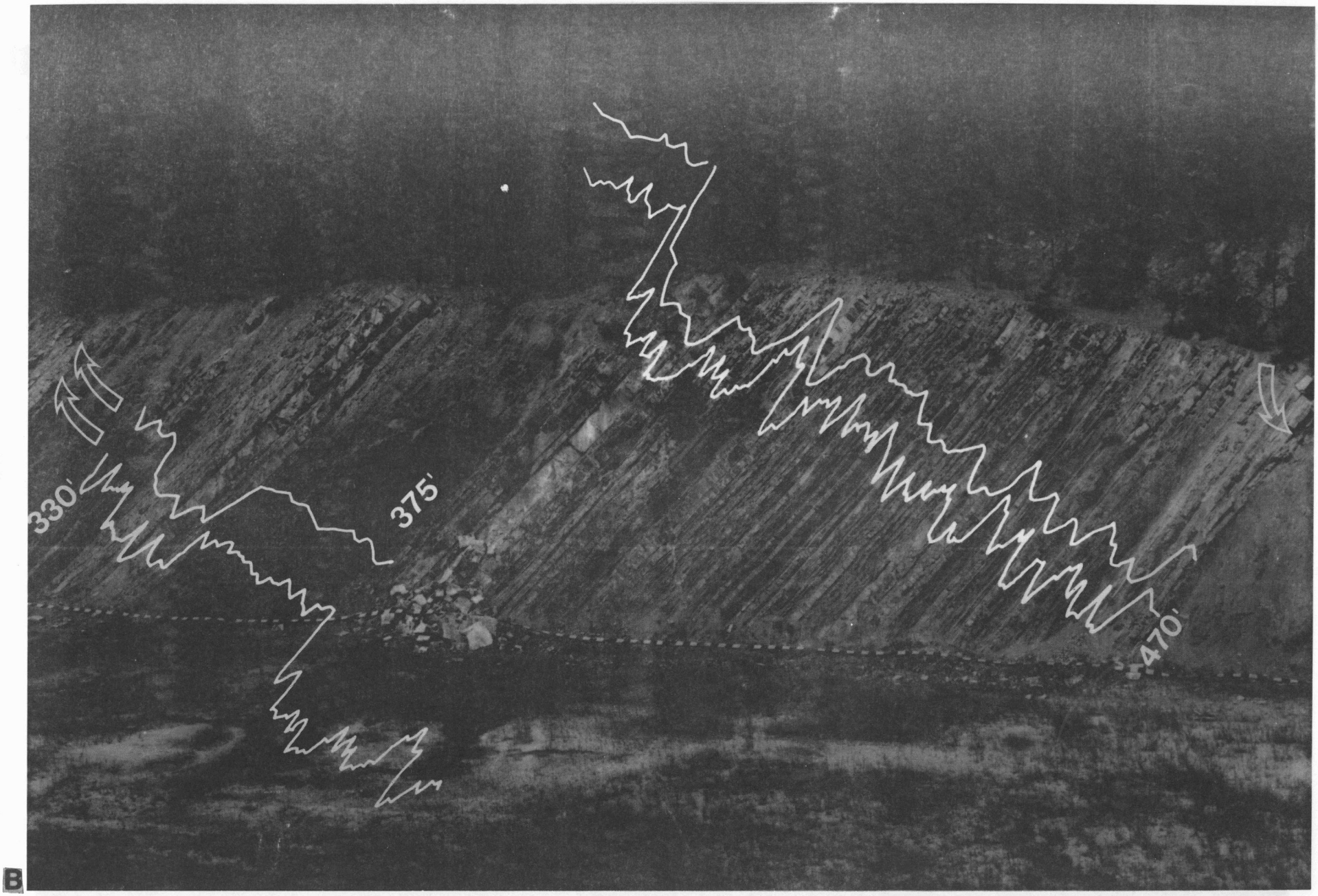
330'
375'
470'
B

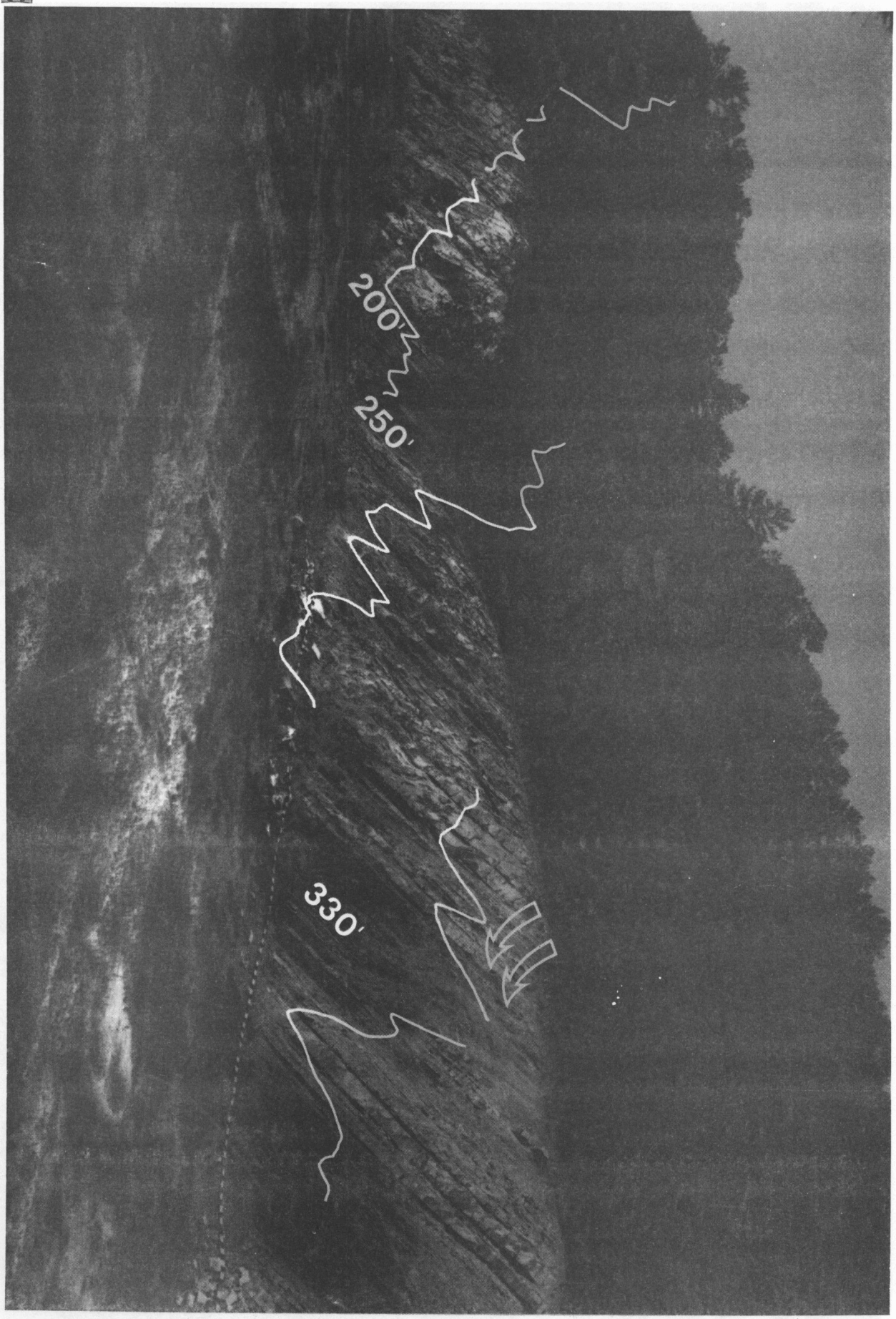
200'
250'
330'

the uses and limitations of gamma-ray logs in these types of deep-water deposits.

Lateral Continuity of Individual Beds

An issue that we addressed was the lateral continuity of individual sandstone and shale beds and how this continuity might affect rock and well log correlations over distances greater than 300 feet. To address this issue, we measured 110 individual sandstone and shale beds that could be correlated on both sides of the spillway on the basis of distinctive sedimentary features and their position within the entire vertical sequence. Since the distance between the spillway walls was known, the rate of change of bed thickness and thus, lateral continuity, could be estimated.

The sandstone and shale beds that were measured occur within two stratigraphic intervals along both sides of the spillway: (1) on the eastern wall and western wall of the

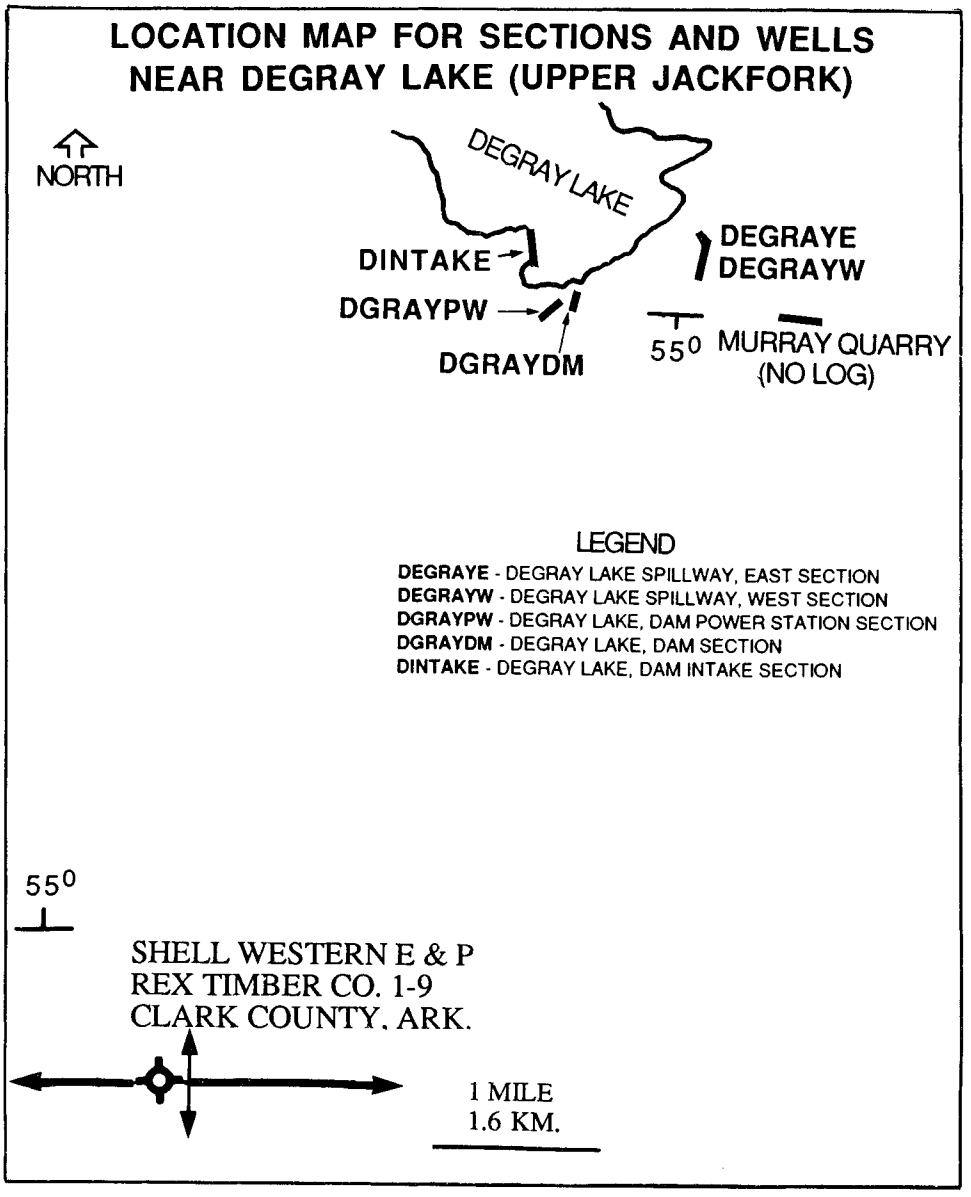

Figure 62. Location map for outcrop sections and the subsurface well near DeGray Lake. Several strikes and dips that were taken from Jackfork outcrops (B. Haley, pers. comm, 1991) are shown. The Shell well was drilled on an apparent anticlinal feature. It is not known if stratigraphic section was repeated in the borehole due to faulting.

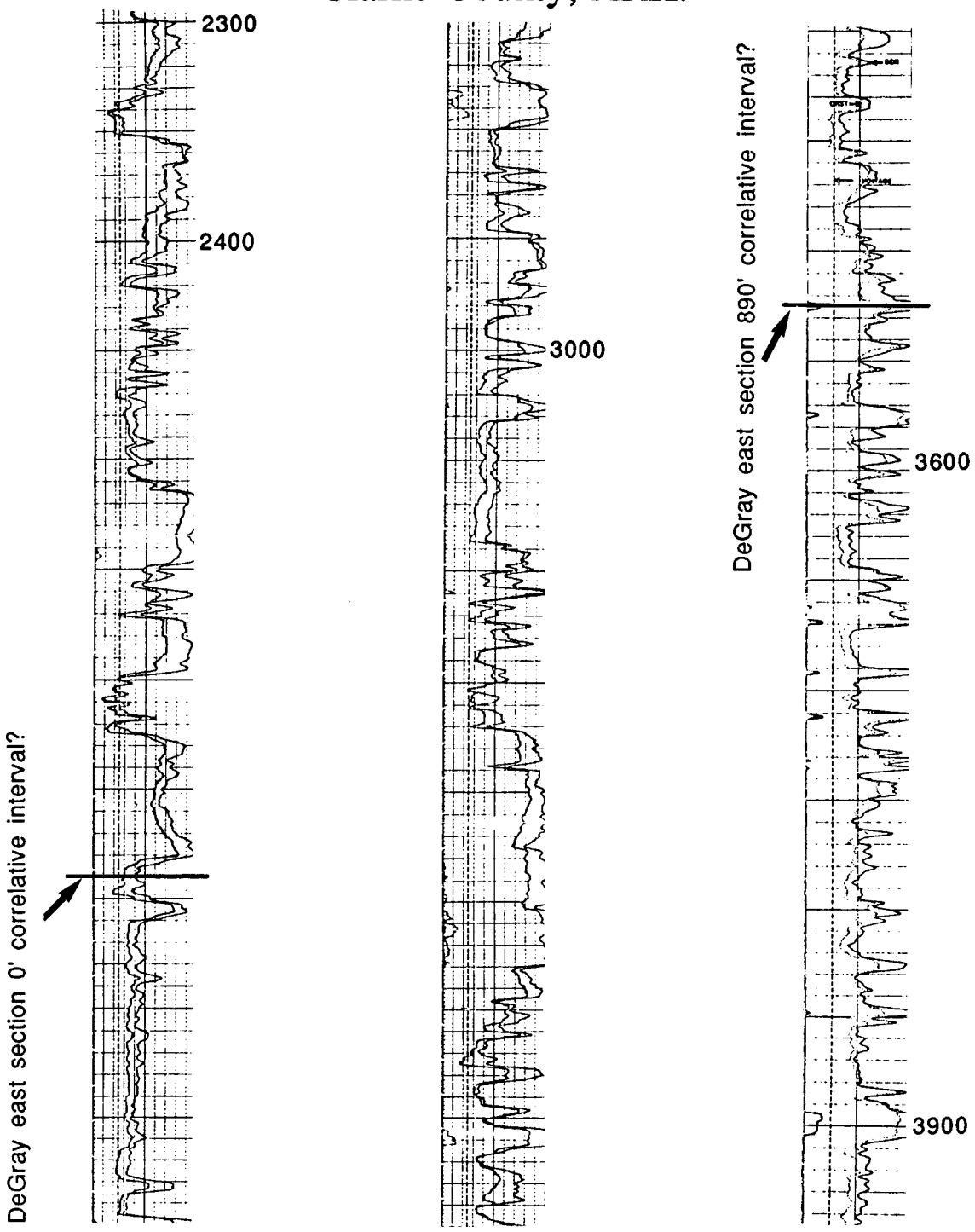

Figure 63. Subsurface gamma-ray log from the Shell Rex Timber Co. 1-9 well located southwest of the DeGray sections. The interval on the outcrop gamma-ray log from 0'-890' on the DeGray east section is similar to the interval shown on the subsurface log, and suggests that some beds may be laterally continuous over several miles (e. g., shaley sequences and beds at 894' and 444-520' on the DeGray Spillway east section are correlated with shale beds at 3525' and 3190-3280' on the subsurface log; sandstone beds at 75-200' on the DeGray Spillway east section are correlated with the sandstone at 2710-2830' on the subsurface log).

spillway at 320-350 and 330-360 feet (log depth; 650-680 feet on the east side description of Morris, 1977), respectively (Fig. 64A-C), and (2) on the eastern wall and western wall of the spillway at 365-460 feet (540-635 feet on description of Morris, 1977) and 375-470 feet (log depth), respectively (Fig. 65).

Figures 66A and B show plots of the maximum (**tmax**) vs. minimum (**tmin**) thickness of the 57 individual sandstone beds and 53 individual shale beds measured. Four trends are apparent for sandstones and shales, labelled A, B, C, and D. The reason for these trends is unclear at present, however, two of several possible explanations that seem feasible (neither of which have been tested) are: (1) each trend might record beds deposited by a different process (e.g, turbidites or slurries, confined or unconfined flows, etc.) and/or (2) measurements might have been made along different parts of individual beds and/or along beds of different orientation with respect to paleocurrent direction.

If it is assumed that the rate of change in thickness of the different bed types is constant over the lateral distance of 300 feet, then the following relationship can be defined: $dt/dx=a*t$, where **t** is bed thickness (**m**), **x** is lateral distance, and **a** is a proportionality constant. Integrating and rearranging this equation gives: $tmin/tmax = e^{-ax}$. Given that x is a constant 300 feet, it was possible to calculate an average **a** for each sandstone and shale group from the **tmin** and **tmax** measurements made on individual beds so that general equations relating bed thickness to lateral distance could be derived. The equations are listed in Figures 67A and B along with sample plots of bed thickness vs. lateral distance to 4000 feet for a sandstone and shale bed of 0.5 feet thickness (**tmax** = 0.50 feet at **x** = 0). Group D sandstones and shales, not shown in Figure 67, would plot as horizontal lines (i.e., no lateral thickness change). These trends show that even relatively thin beds are laterally continuous for distances of at least several hundreds to thousands of feet, in contrast to the limited lateral continuity of beds at Big Rock Quarry (Figs. 29 and 31). In the subsurface, most of these beds would probably be laterally continuous between typically-spaced wells (40 acre spacing), and consequently, potentially correlative on gamma-ray logs.

Correlating Individual Beds

Having established the lateral continuity of beds, we evaluated the potential for correlating individual beds on gamma-ray logs over the 300 feet distance between the spillway walls by obtaining logs at the two previously discussed stratigraphic intervals with the hand-held scintillometer at only 0.5 foot sampling intervals. For the upper sequence (see Fig. 64A), the log obtained at a 2-foot sample spacing only resolves two sandstone intervals (labelled A and B) which can be identified and correlated, but at 0.5-foot spacing, the beds can be further subdivided into individual correlative packages (A1, A2, B1, B2, and B3) and beds (a, b, c, and d) even though there is considerable change in thickness of some beds (e.g., A2, B2, B3) over 300 feet (see Figs. 64A-C). On gamma-ray logs sampled at 0.5-foot spacing, responses of most individual beds or groups of thin beds comprising the lower sequence are also correlative across both sides of the spillway (see Fig. 65).

Another interval in which the correlation of individual beds and gamma-ray log responses across the spillway has been made is at 800-850 feet (log depth) on the DeGray Spillway east and west sections. This interval (at approximately 160-190 feet on the lithologic log of Morris, 1977) has been previously discussed and comprises Sections 2 (DeGray east) and 3 (DeGray west) shown on Figures 53 and 54, respectively. Problems with correlating portions of the gamma-ray curves that were sampled at 2-foot spacing were discussed above (recall, for example, that the shale between sandstone units on the east side, Section 2, produces a major shale deflection on the log but only a minor deflection on the log of Section 3 on the west side). On gamma-ray logs sampled at the 0.5-foot spacing, however, responses of most individual beds or groups of thin beds comprising the sequence are correlative across both sides of the spillway (Fig. 68).

An example where thin beds are not continuous (or change facies) across the

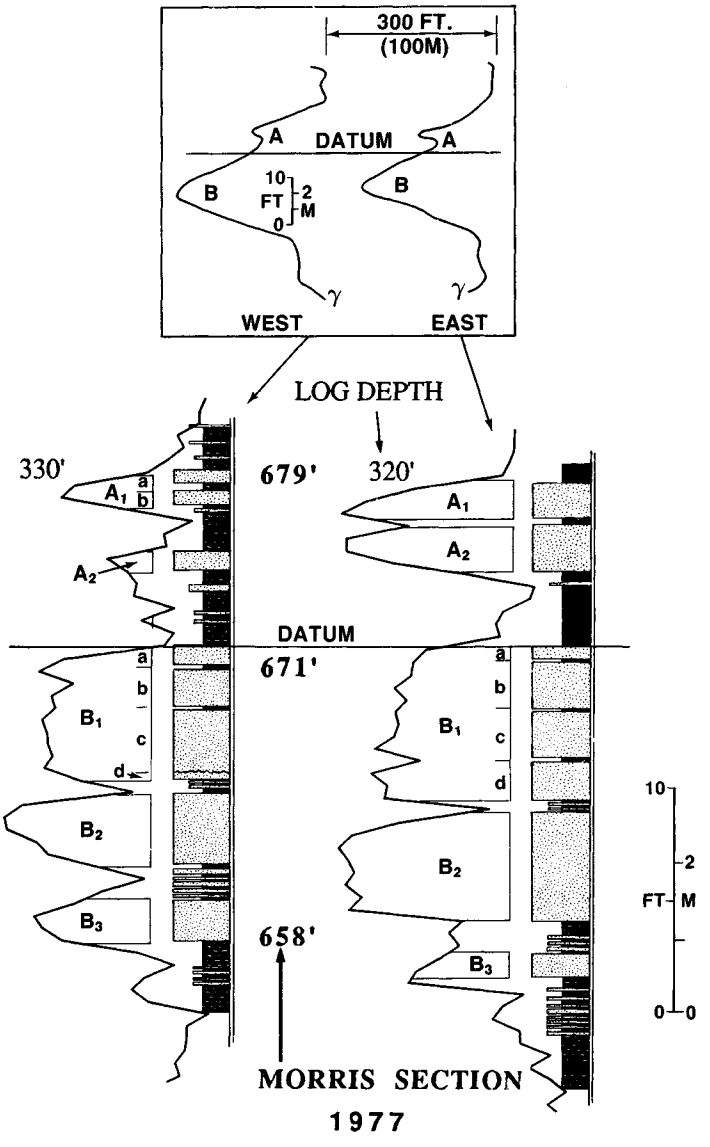

Figure 64. (A) Detailed stratigraphy and gamma-ray logs (half-foot sample spacing) for the interval 320-350 and 330-360 feet on the eastern and western walls, respectively, of DeGray Lake Spillway. See Figures 51 and 60-61 for the position of the interval within the entire spillway section. The inset shows the log interval obtained at two foot sample spacings. Detailed stratigraphy of the two major intervals, subdivided into smaller packages (A1, A2, B1, B2, and B3) and beds (a,b,c, and d) are shown: (B) Interval at the DeGray west section. (C) Interval at the DeGray east section. Note distinctive changes in bed thickness between these same stratigraphic intervals separated by 300 feet.

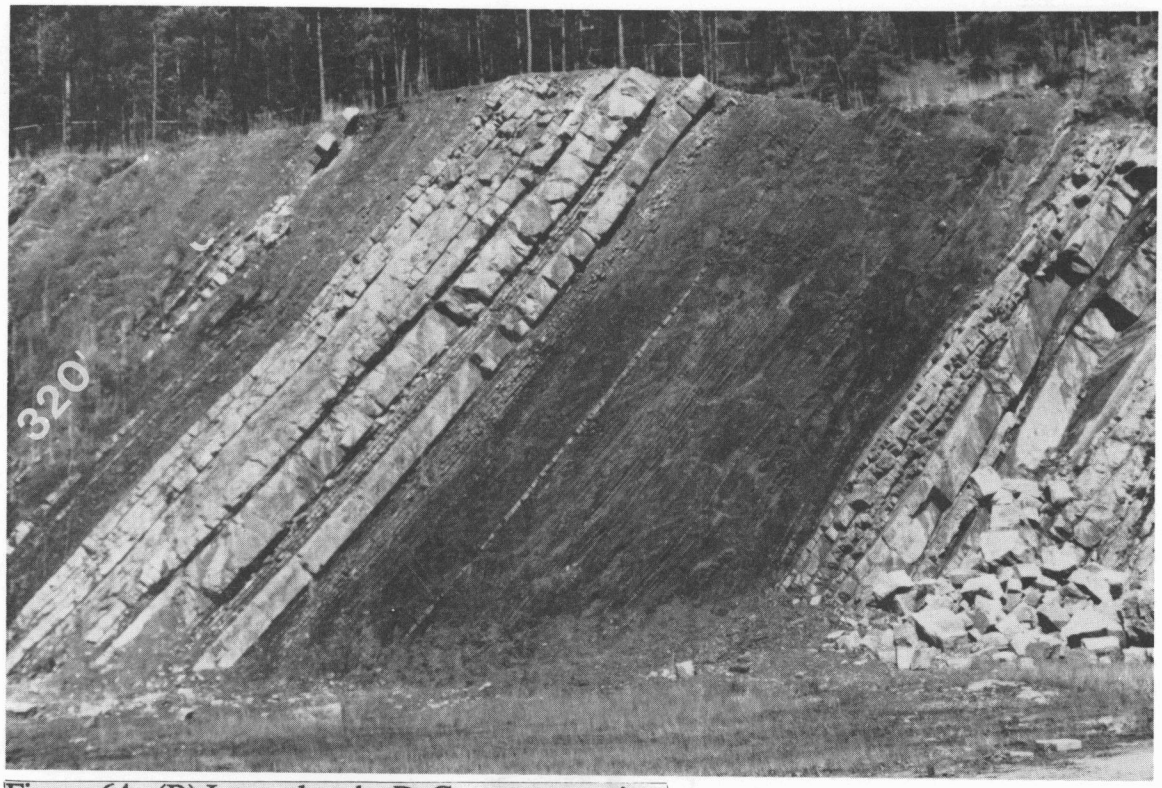

Figure 64. (B) Interval at the DeGray west section.

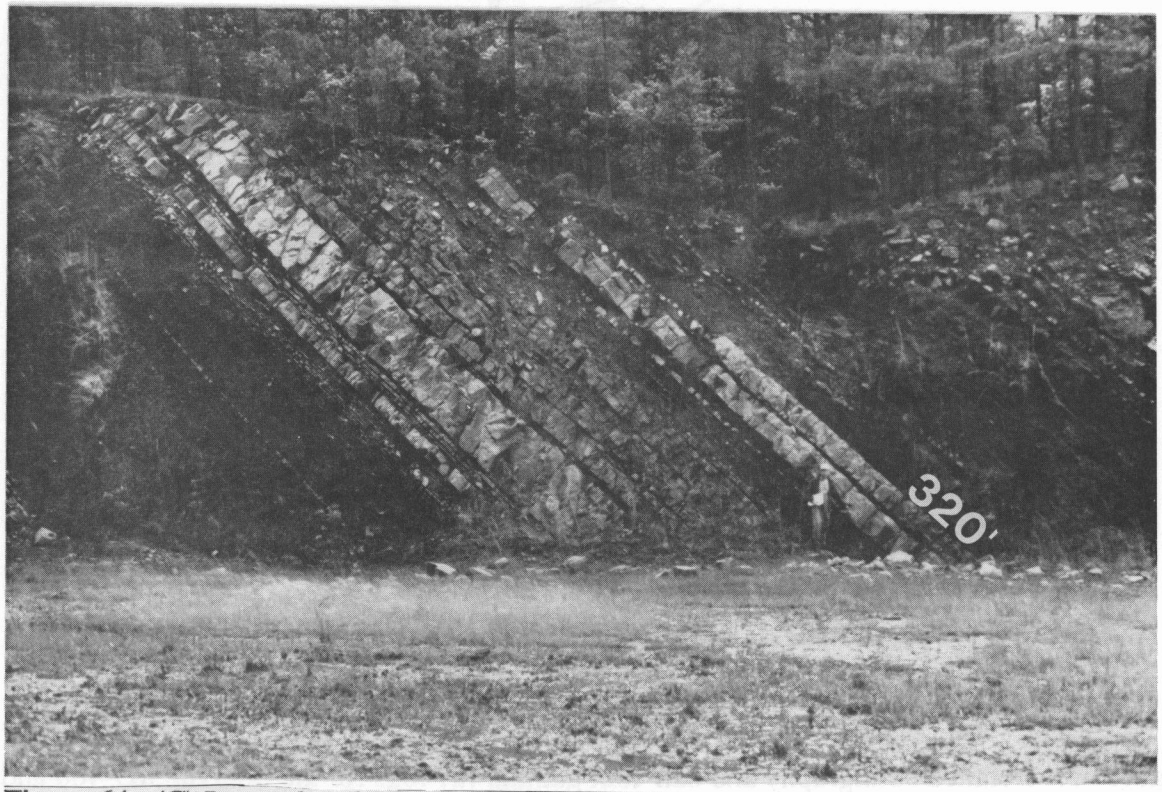

Figure 64. (C) Interval at the DeGray east section.

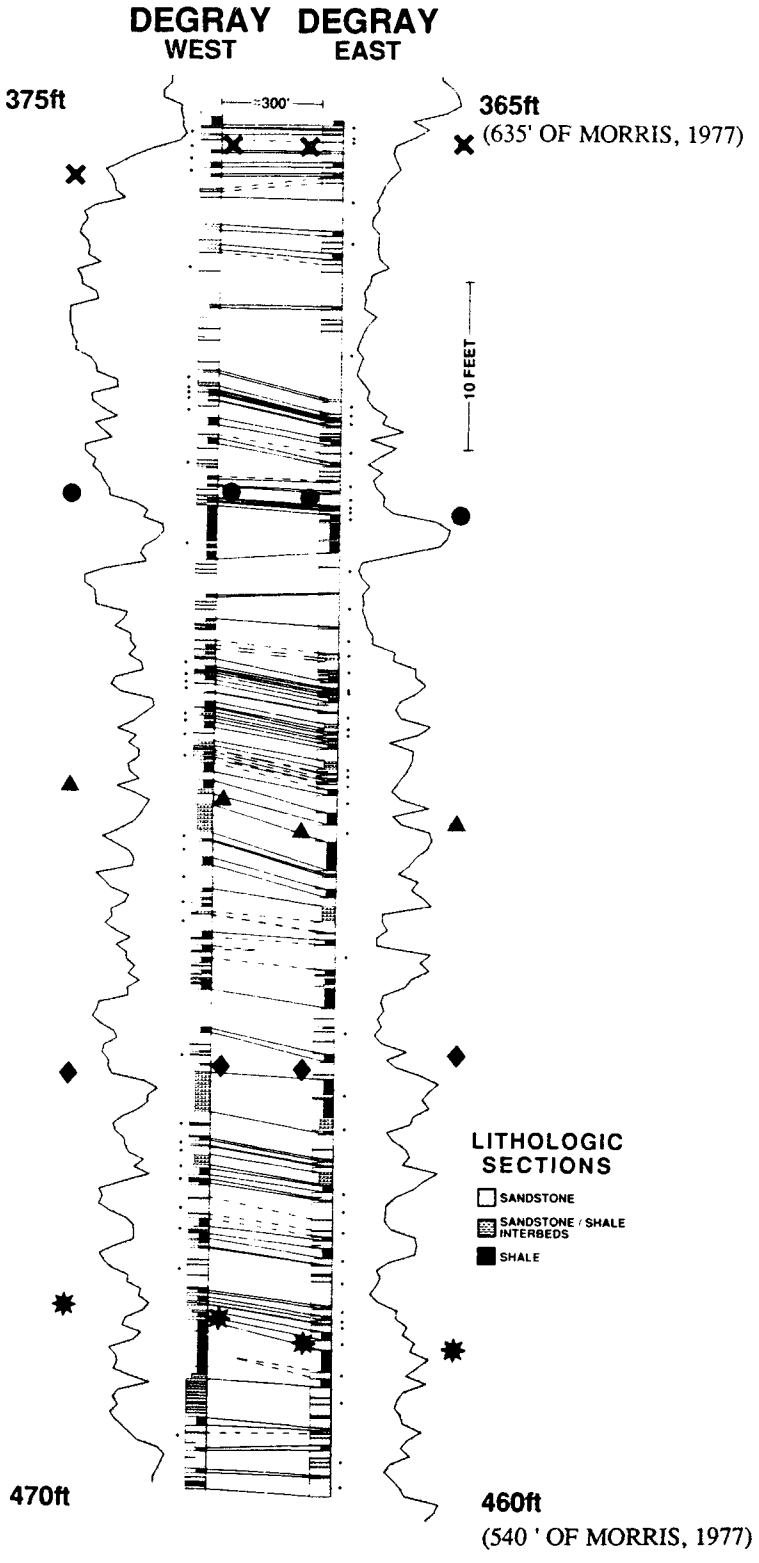

Figure 65. Detailed stratigraphy and half-foot gamma-ray logs for the interval 365-460 and 375-470 feet (log depth) along the eastern and western walls, respectively, of DeGray Lake Spillway. See Figures 51 and 60-61 for the position of the interval within the entire spillway section. The large symbols refer to some individual beds correlated between the outcrops and logs. Small dots are located adjacent to the bed that is thickest (relative to the other wall of the spillway).

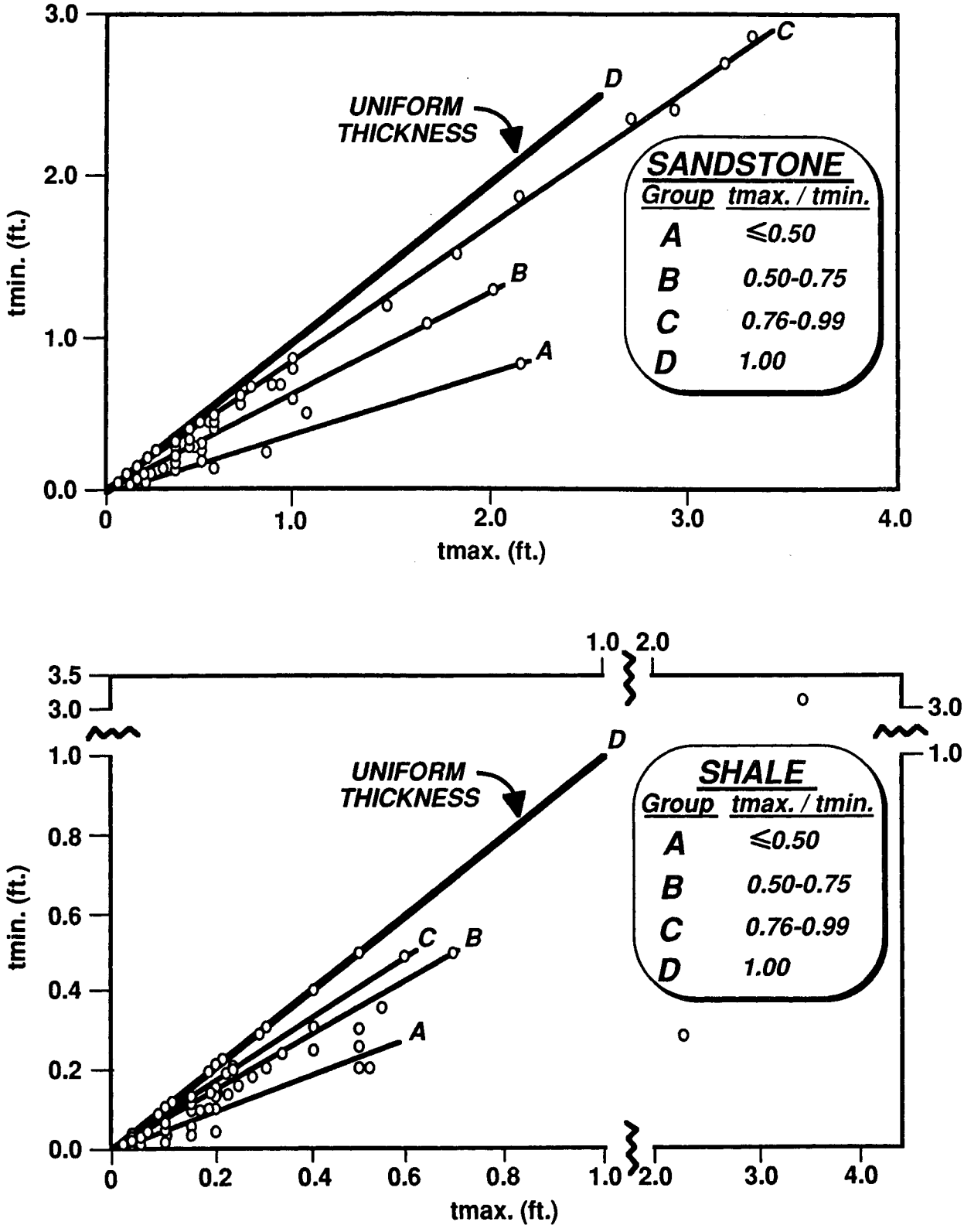

Figure 66. Measurement of 110 individual sandstone and shale beds within two stratigraphic intervals along both sides of the DeGray Lake Spillway: (A) Plot of the maximum (tmax) vs. minimum (tmin) thickness of 57 individual sandstone beds. (B) Plot of the maximum (tmax) vs. minimum (tmin) thickness of 53 individual shale beds.

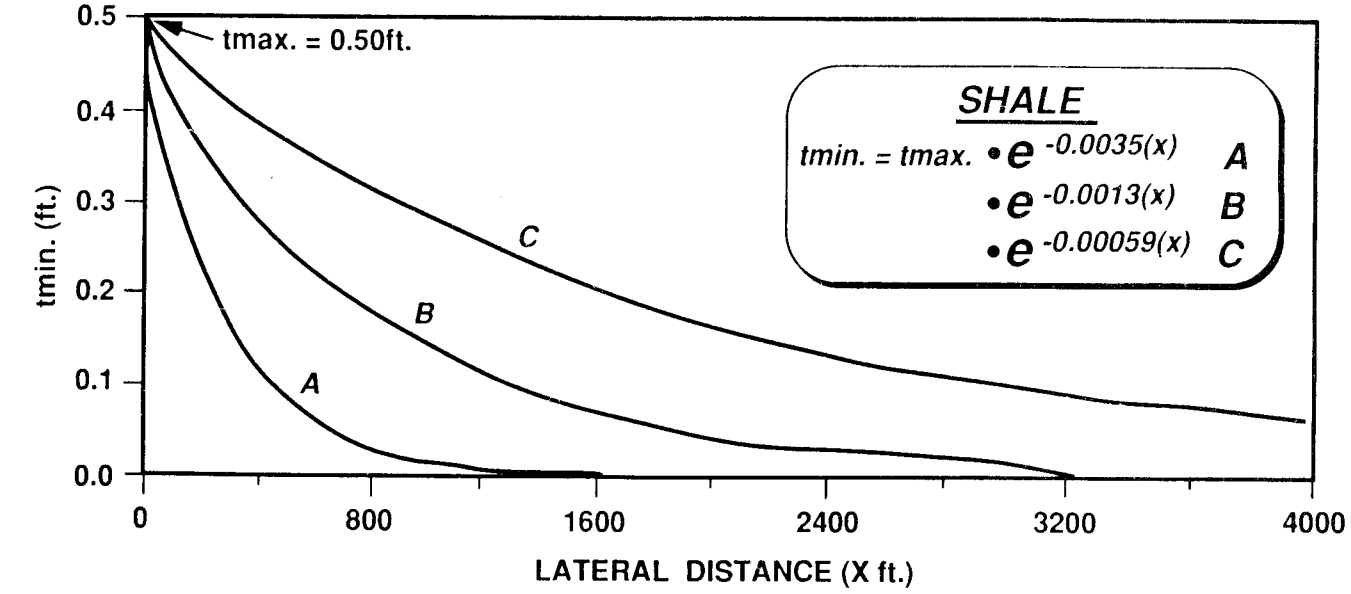

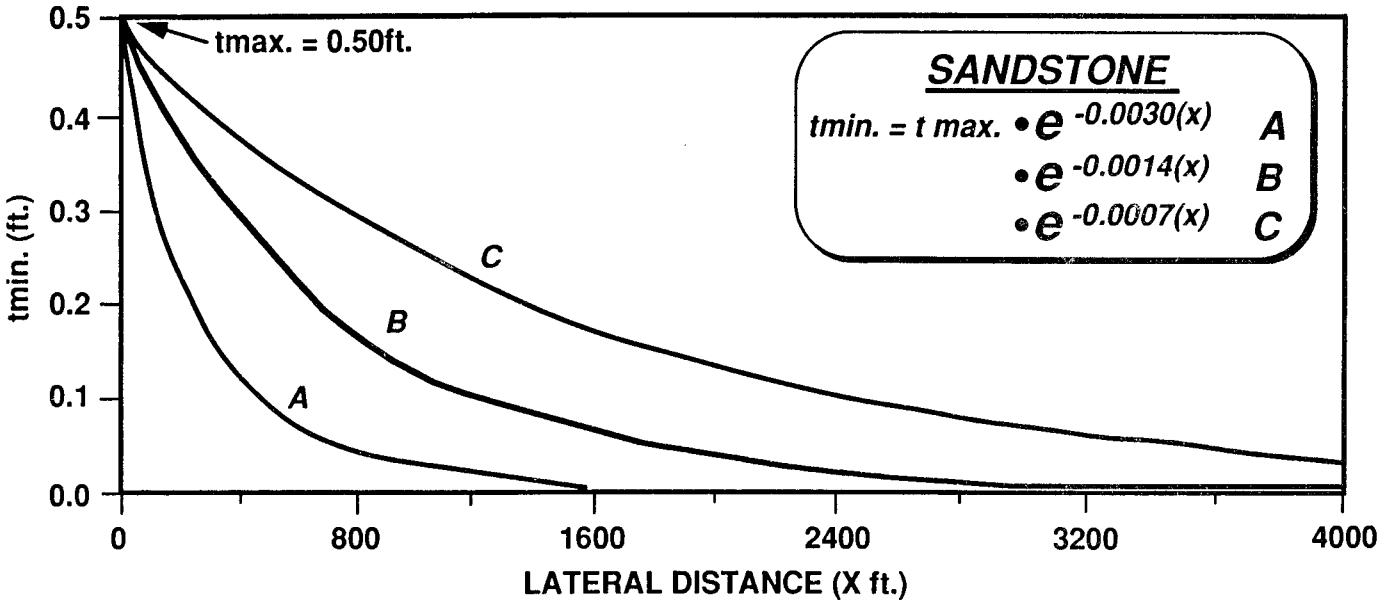

Figure 67. (A) Three empirical equations (A, B, and C) for sandstones at DeGray Lake Spillway relating bed thickness on both sides of the spillway (t max and t min) to lateral distance or continuity of the bed (x). Curves A, B, and C show the relationship for a bed that has a maximum thickness (t max) of 0.5 feet. For example, using curve A, a bed 0.5 feet thick at one point will be 0.03 feet thick over a lateral distance along the bed of 800 feet. (B) Three empirical equations (A, B, and C) for shales at DeGray Lake Spillway relating bed thickness on both sides of the spillway (t max and t min) to lateral distance or continuity of the bed (x). Curves A, B, and C show the relationship for a bed that has a maximum thickness (t max) of 0.5 feet. For example, using curve A, a bed 0.5 feet thick at one point will be 0.02 feet thick over a lateral distance along the bed of 800 feet.

spillway within this interval is also shown in Figure 68. The '175-foot' sandstone (Unit D in Figure 53) is correlative across the Spillway and sits above a bed on the east side containing climbing ripples (+ symbols in Figure 68). The gamma-ray log resolves this thin bed. However, this bed is not present on the west side of the Spillway, having possibly changed facies westward to a laminated shale and siltstone interval. Another sandstone bed directly beneath the rippled interval on the east side is a purple slurry bed with sideritic clasts at the top, and this thin bed is correlative across the Spillway with a contorted zone with folded and contorted siltstones and shales, which further changes facies westward along the outcrop into laminated shale and siltstone. The '175-foot' sandstone appears to thin slightly to the right (northwest) over a distance of several hundred feet on the photograph.

Depositional Lobes, Channels, and Compensation Cycles

Turbidite depositional sequences that appear on well logs (and in core and outcrop) to become thicker-bedded, coarser-grained, and cleaner (lower API counts) stratigraphically upward are often interpreted as 'lobes' formed by continual progradation of sediments during a depositional cycle (Selley, 1979; Shanmugam and Moiola, 1988, 1991). By contrast, those that appear to become thinner-bedded, finer-grained, and dirtier stratigraphically upward are often interpreted as 'channel-fill' deposits formed by successive upbuilding of progressively finer-grained channel-fill as a channel goes through a cycle of formation, sedimentation and channel filling/abandonment (Selley, 1979; Shanmugam and Moiola, 1988, 1991). Rider (1990) lists a number of factors other than grain-size and clay content that affect gamma-ray log response, and suggests that interpreting depositional facies from gamma-ray log shapes is tenable only under certain circumstances.

Based upon our study of the DeGray Lake Spillway sections, we suggest a factor that can be added to Rider's (1990) list is the inconclusive, but common, practice of interpreting or inferring three-dimensional facies architectures (lobes and channel-fills) from two-dimensional log data. The interval at 365-460 and 375-470 feet on the east and west walls of the spillway appears on the 2-foot log (see Fig. 51) to become thicker-bedded and cleaner (lower gamma-ray counts) stratigraphically upward, as would be typical of a 'lobe' deposit. However, the greater detail of the 0.5-foot logs (as well as the stratigraphy) shows that the sequence is really a composite of several thinner cyclical sequences (see Figs. 60, 61, and 65) that could be interpreted individually as either thickening/cleaning-upward or thinning/dirtying-upward.

Tmax of individual sandstone beds alternates vertically in a persistent fashion between the east and west walls of the spillway (see Fig. 65), which suggests that cyclicity of sedimentation occurs in a lateral as well as vertical fashion owing to back-and-forth switching of depositional axes with time. This switching would occur when one turbidite bed is deposited on the sea floor and the next younger bed is laid down in the adjacent topographic depression created by the first bed. Switching back-and-forth of individual bed axes in this manner produces 'compensation cycles' (Mutti and Normark, 1987) which appear on gamma-ray logs (and outcrops) as a complex succession of both thickening/cleaning-upward and thinning/dirtying-upward sequences.

Correlation of Compensation Cycles

Figure 69 shows a hypothetical sequence of turbidite compensation cycles (after Mutti, 1985) and gamma-ray logs through different parts of the sequence. This hypothetical example demonstrates the difficulty that one might encounter in attempting to correlate depositionally-related strata unless a well-defined stratigraphic log marker was present which could be used as a datum. In this instance, a knowledge of the expected depositional geometries would be very beneficial, if not essential, for a realistic correlation.

Figure 70 shows the concept of compensation cycles applied to the 365-460/375-470 foot DeGray Lake Spillway section and another measured section, called the DeGray Lake Intake (STOP 6), located about 5000 feet west of the spillway (see Fig. 74). Our gross

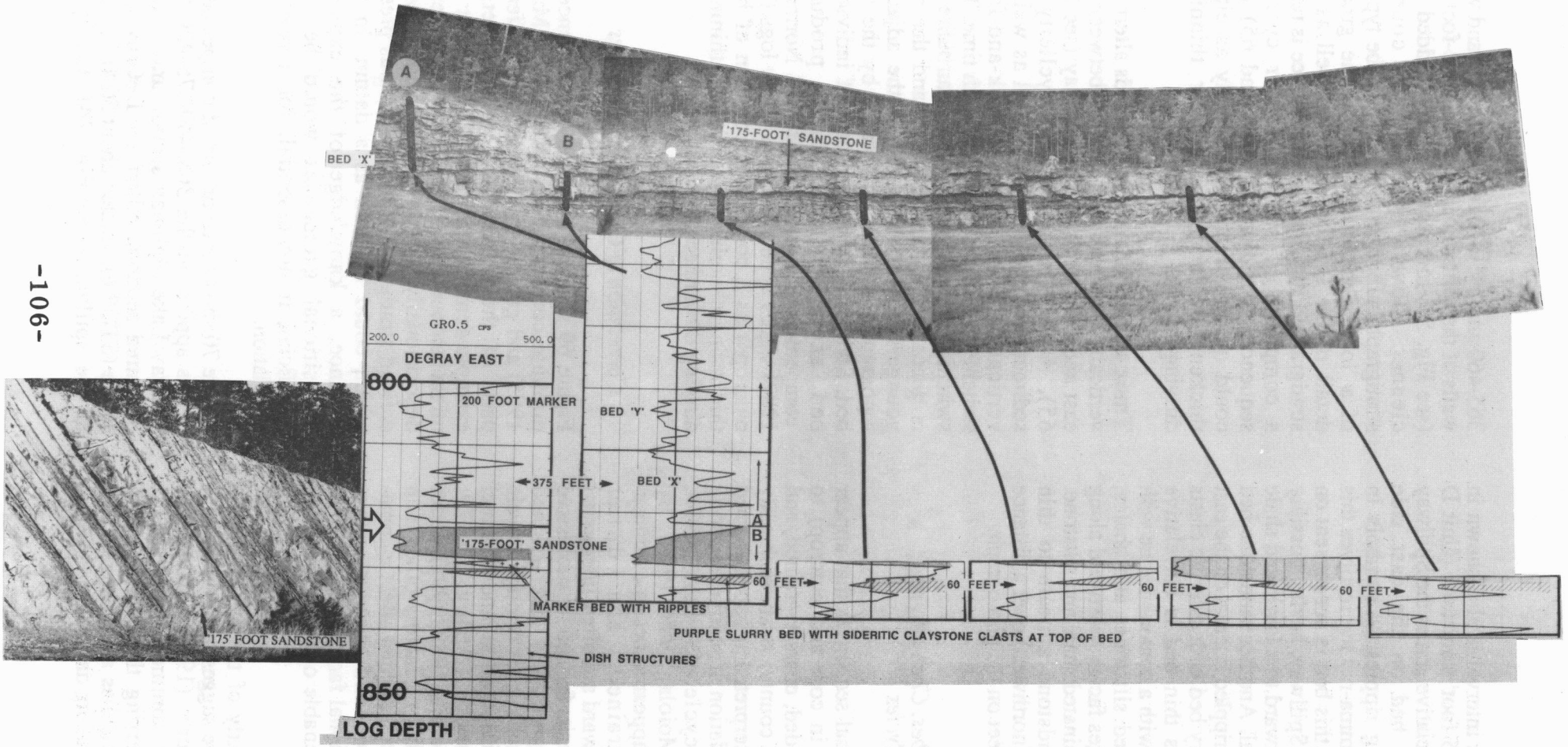

Figure 68. Correlation of individual beds and gamma-ray curve shapes in the lower part of the DeGray Spillway section, at 800-850' (on the log measured with the 2-foot sample spacing interval; see Figure 51). Gamma-ray logs were sampled at a 0.5-foot spacing. The '175-foot' sandstone appears to thin to the right (northwest) over a distance of several hundred feet on the photograph. Note gamma-ray log of thin 'maker bed' on the east side containing climbing ripples. The gamma-ray log shows that the interval is missing on the west side, having possibly changed facies to a laminated shale and siltstone interval. The underlying slurried zone is continuous across the Spillway.

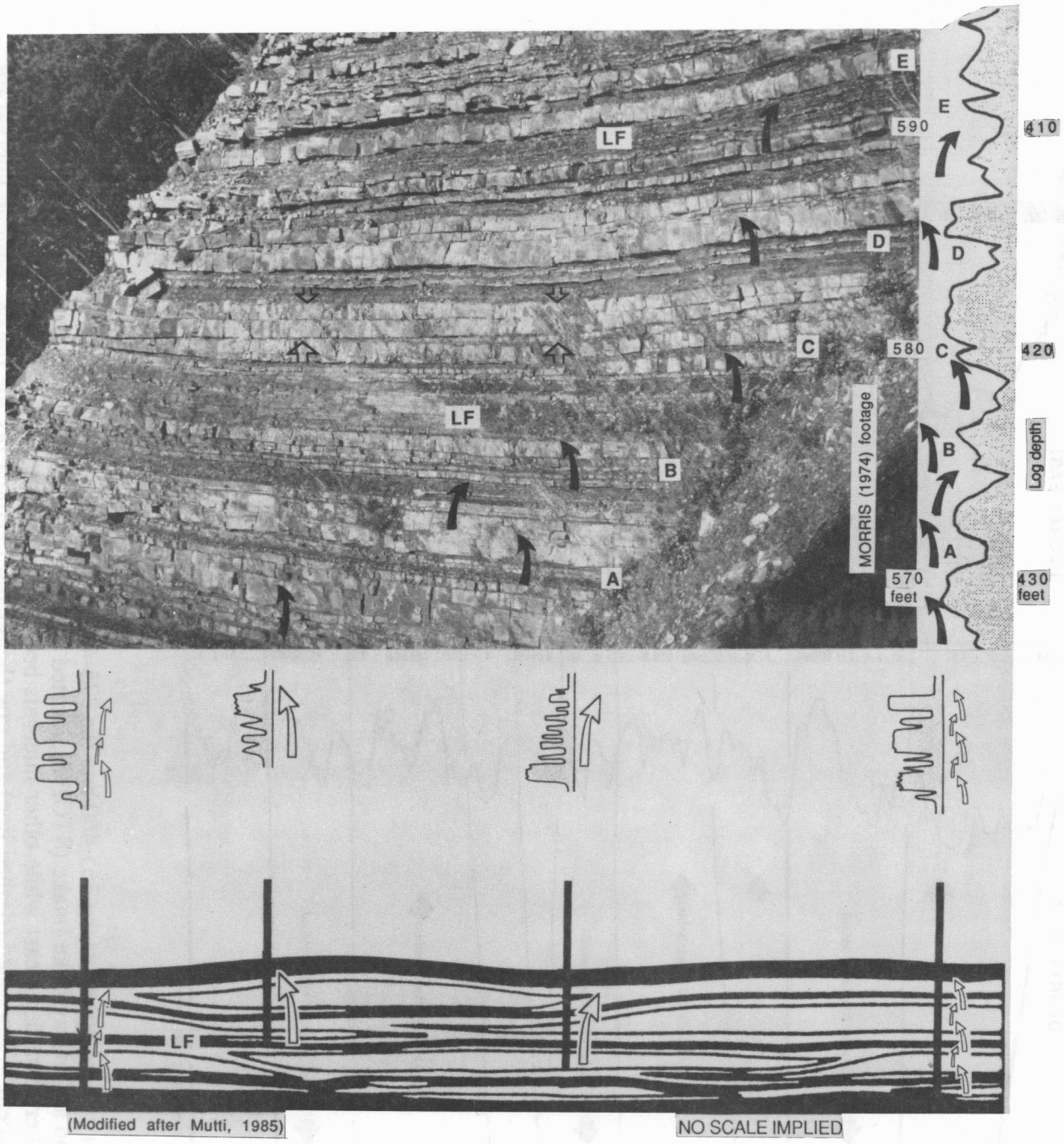

Figure 69. Example of compensation cycles (as defined by Mutti, 1985) for the DeGray Lake Spillway east section from about 570 to 590 feet on the measured section of Morris (1974) or 430 to 410 feet on the measured gamma-ray log section. Photograph of outcrop is turned so that beds appear to be flat-lying. Compensation cycles develop as an individual bed is deposited in the adjacent topographic depression created by relief of the immediately preceding bed. Bottom diagram, modified from Mutti (1985), depicts a two dimensional view of sheet-like or lobate turbidite geometries. Some sample pseudo gamma-ray logs in lower diagram are shown to illustrate how thinning/dirtying- (small arrows) and thickening/cleaning- (large arrows) upward vertical sequences can be formed by these compensation cycles. Similar arrows and interpretations are shown on the upper photograph, and correlation points are referred to in A-E. Open arrows enclose at least two beds that thicken from 1.1 to1.8 feet from far right to far left over a distance of about 26 feet.

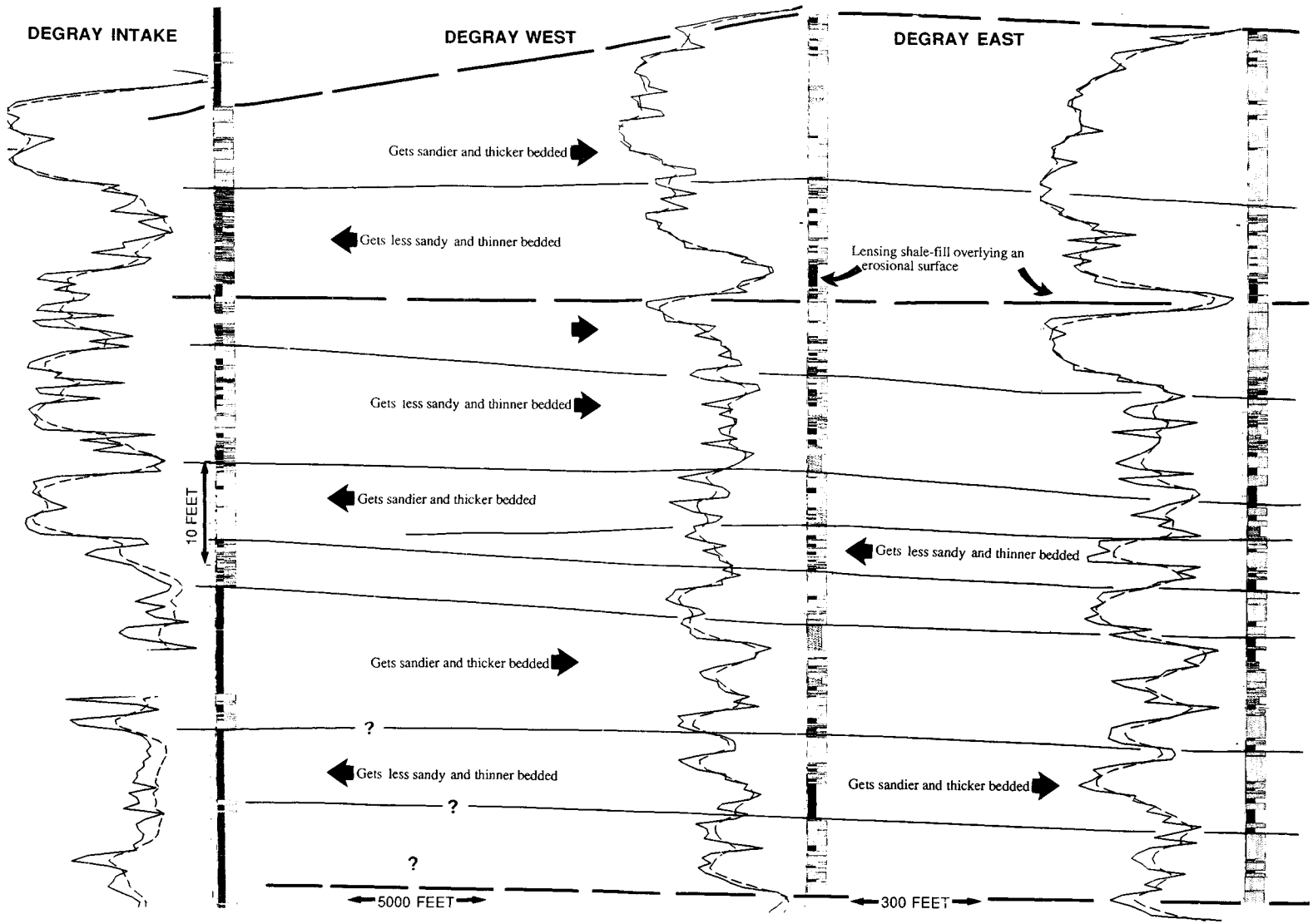

Figure 70. Concept of compensation cycles applied to the 365-460 and the 375-470 foot interval at the DeGray Lake Spillway section and the correlative section at DeGray Lake Intake (STOP 6), located about 5000 feet west of the spillway. Some intervals become sandier and thicker toward the east while other intervals become sandier and thicker toward the west. Detailed lithologic log shown adjacent to smoothed (dashed line) and raw (heavy line) gamma-ray log traces. Sample interval for gamma-ray measurements is 0.5 foot.

correlation scheme shows that some intervals become sandier and thicker toward the east while other intervals become sandier and thicker toward the west. Overall, the section becomes thinner bedded and less sandy towards the DeGray Intake section to the west of the Spillway section (Table 8). As was the case with the hypothetical example, it is evident that a knowledge of depositional geometries is essential for a realistic correlation of stratigraphic intervals or depositional cycles at this scale of well spacings. In fact if this hypothetical sequence were to be misinterpreted as laterally continuous lobes and laterally discontinuous channel-fills rather than as compensation cycles, a completely different correlation scheme would result.

	DeGray Spillway East (STOP 5)	DeGray Spillway West (STOP 5)	DeGray Intake (STOP 6)
Net Sandstone	56 (ft.)	55 (ft.)	35 (ft.)
Gross Interval Thickness	81 (ft.)	81 (ft.)	75 (ft.)
Net/Gross	.69	.68	.47
No. Sandstone beds	91	110	185
Mean Sandstone Thickness	0.36 (ft.)	0.28 (ft.)	0.09 (ft.)

Table 8. Sandstone-to-shale ratios and other data for the interval from 365-460 feet (east) and 375-470 feet (west) log depth (540-635 feet on east side description of Morris, 1977).

Sandstone/shale Ratios

Sandstone/shale ratios were determined for the DeGray Lake Spillway section. Data were collected from both the section measured by Morris (1977) as well as from the gamma-ray log. Thicknesses based upon shale cut-off values of 33%, 50%, and 65% (see method in section at STOP 1) were measured from the gamma-ray log to determine which cut-off value produced results that most closely matched the thickness of sandstone that crops out. Table 9 summarizes the results.

Overall, log-derived ratios based upon a 33% shale cut-off best match ratios calculated from the measured lithologic section; however, thin beds, as discussed above, could not be resolved by the gamma-ray logging method (2-foot sample spacing) that was used.

Bed Thickness Distributions of Sandstones and Shales

Distributions of sandstone and shale bed thickness obtained from detailed measurements of the shale-bounded, eighty foot sequence (365-460 and 375-470 foot DeGray Lake Spillway section on the east and west sides of the DeGray Lake Spillway are log normal (Fig. 71). The most frequent size class for both sandstone and shale beds is 0.25 ft., and the mean ranges from 0.28 ft. (west) to 0.36 ft. (east) (see Table 8). Many of the thicker sandstone beds are the products of amalgamation of individual sediment gravity flows in which the shale cap has been removed by scouring by subsequent flows. This gives rise to a thicker sandstone bed in which the shale barriers are intermittent or absent, and vertical flow of potential

Units = Feet		Log Data													Measured Lithologic Section Data					
			33 % SHALE CUT-OFF				50% SHALE CUT-OFF				65% SHALE CUT-OFF				Turbidite Packages Only					
Unit #	Turbidite Package Lith. Log	Total Unit Thickness *	Sand Thickness	Shale Thickness	% Sand	Snd/Sh	Sand Thickness	Shale Thickness	% Sand	Snd/Sh	Sand Thickness	Shale Thickness	% Sand	Snd/Sh	Unit #	Total Unit Thickness **	Sand Thickness	Shale Thickness	% Sand	Snd/Sh
1	0 - 80	80	44	30	(55%)	1.46	24.4	47.6	(34%)	0.51	2.4	69.6	(3%)	0.03	1	80	51	29	(64%)	1.76
2	119 - 133	14	3	11	(21%)	0.27	1.8	12.2	(13%)	0.15	-	14	(0%)	-	2	14	10	4	(71%)	2.50
3	143 - 327	182	137	55	(75%)	2.47	103.6	78.4	(57%)	1.32	55.6	126.4	(31%)	0.44	3	184	154	30	(84%)	5.13
4	330 - 344	12	9	3	(75%)	3.00	4.4	7.6	(37%)	0.58	-	12	(0%)	-	4	14	12	2	(86%)	6.00
5	351 - 451	93	64	29	(69%)	2.20	44	49	(47%)	0.90	24	69	(38%)	0.35	5	100	68	32	(68%)	2.13
6	470 - 520	16	6	10	(38%)	0.60	1	15	(6%)	0.06	-	16	(0%)	-	6	50	28	22	(56%)	1.33
7	557 - 635	96	56.4	38.4	(59%)	1.47	43	53	(45%)	0.80	25.6	70.4	(27%)	0.36	7	78	48	30	(62%)	1.60
8	658 - 680	26	15.6	10.4	(60%)	1.50	13	9	(59%)	1.44	8	14	(36%)	0.57	8	22	14	8	(64%)	1.75
9	698 - 772	73	50.4	22.6	(69%)	2.23	43	28	(61%)	1.54	36.2	34.8	(51%)	1.04	9	74	56	18	(75%)	3.11
10	800 - 930	134	126	8	(94%)	15.8	122.4	11.6	(91%)	10.6	117.6	16.4	(88%)	7.10	10	130	121	9	(93%)	13.4
11	962 - 1000	40	33.6	6.4	(84%)	5.25	32	8	(80%)	4.0	30	10	(75%)	3.00	11	38	28	10	(74%)	2.8
Totals		766	545	223.8	(71%)	2.44	432.6	319.4	(56%)	1.35	299.4	452.6	(39%)	0.66		784	590	194	(75%)	3.04

Total Shale Between Units = 216

Total Section Based on Measured Lith. Log				
Total Thickness All Turbidite Packages	Total Sand Thickness	Total Shale Thickness	% Sand	Snd/Sh
1,000	590	410	(59%)	1.43

* Total unit thickness = thickness of turbidite package as determined from Gamma-Ray Log.
** Total uint thickness = thickness of turbidite package as determined from measured lithologic section.

Table 9. DeGray Lake Spillway Sandstone/shale ratios.

hydrocarbon or other fluids within the amalgamated bed would not be impeded. In the Spillway, these beds are identified by partings between individual beds making up the amalgamated bed. This mechanism creates several laterally continuous, relatively thick sandstone beds in the DeGray Lake Spillway section.

Net Pay Thickness Distribution and Recognition on Wireline Logs

A plot of the cumulative percentage of total net pay as a function of bed thickness demonstrates that 50% of the potential 'pay' (if this were a hydrocarbon reservoir) is concentrated in beds that are less than about one foot thick (Fig. 72). Thus, a substantial portion of net pay is concentrated in individual beds that are below the resolution limits of most wireline logs. The use of gamma ray, density, or resistivity cutoffs established in relatively thick-bedded and clean portions of a reservoir are likely to grossly underestimate net pay in these thin-bedded parts. Use of a gamma-ray log cutoff (for the 2-foot sample spacing method) at the DeGray Lake Spillway section produces a wireline log estimate of net sandstone of variable accuracy depending upon the sandstone-to-shale ratio in different parts of the section (Table 9). The alternation of thin shales with thick sandstones produces overestimates of net sandstone (Units 3, 4 and 9 in Table 9). The alternation of thin sandstones with thin shales produces gross underestimates of net sandstone. For example, in Unit 2 the gamma-ray log estimate of net sandstone is 21% whereas that determined from the measured section is 71%.

In reservoirs containing thin-bedded turbidite deposits such as that exposed in the DeGray Lake Spillway section, net pay is most accurately determined through the use of borehole imaging tools such as Schlumberger's Formation Micro-Scanner (FMS) or dipmeter and microresistivity tools. These tools should be calibrated with continuous core through the reservoir interval of interest. In wells in which there are only conventional lithology, porosity and resistivity logs available, it may be necessary to apply a net sandstone factor derived from conventional core to an average log response through a given interval composed of thinly bedded alternations of turbiditic sandstone and shale.

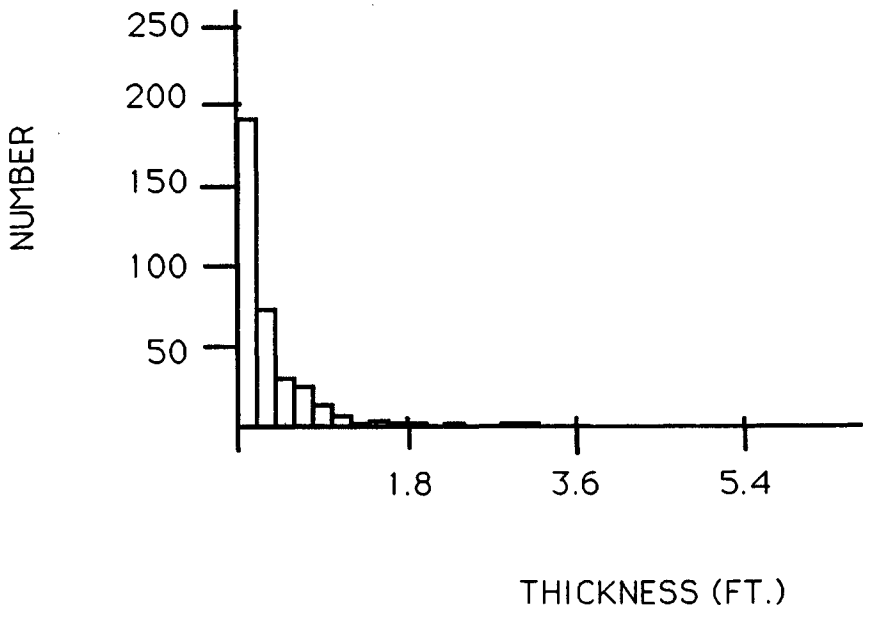

Figure 71. Log normal distribution of sandstone bed thickness obtained from detailed measurements of the eighty-foot sequence (365-460 and 375-470 foot, log depth on the east and west sides of the DeGray Lake Spillway, and the correlative interval at DeGray Intake section). The most frequent size class for the sandstone beds is 0.25 ft.

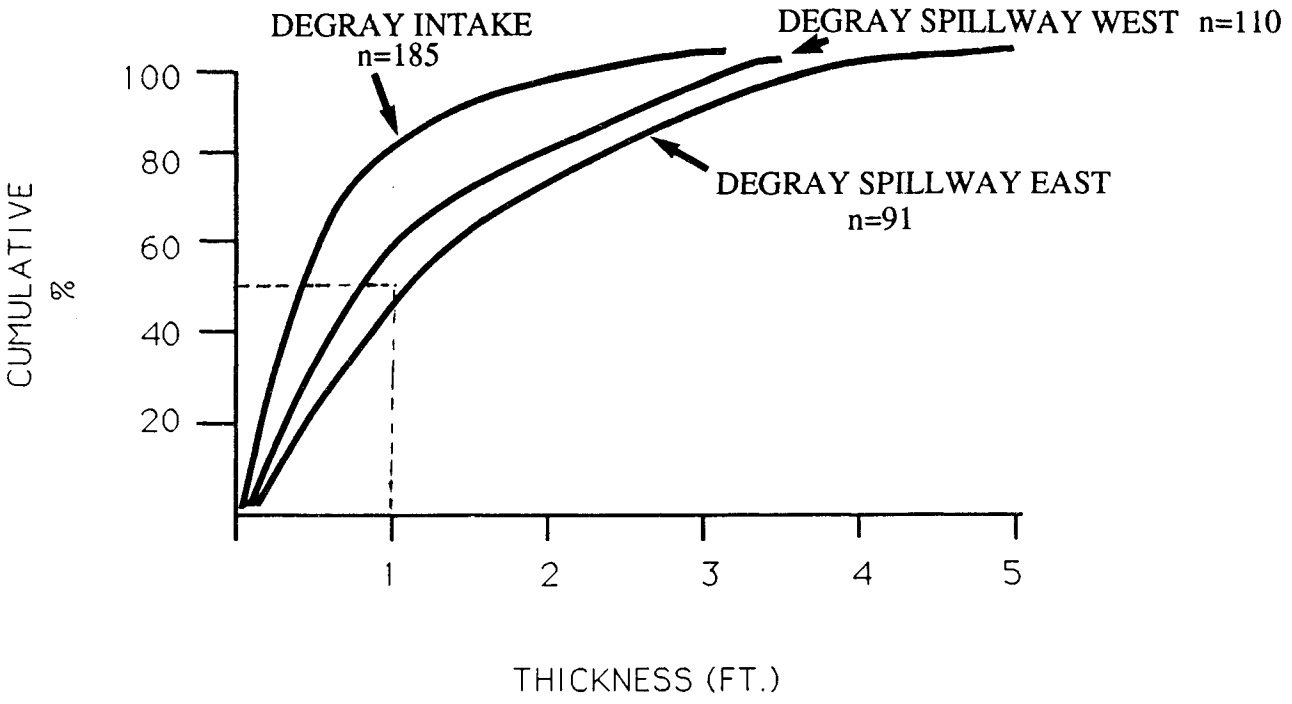

Figure 72. Plot of cumulative percentage of total net 'pay' as a function of bed thickness. Fifty percent of the pay is concentrated in beds that are less than about one foot thick.

Flow Unit Delineation

For the purposes of zoning a reservoir in order to approximate fluid flow pathways, the flow unit approach is appropriate. A flow unit is defined as a mappable portion of the total reservoir within which geological and petrophysical properties that effect the flow of fluids are consistent and predictably different from the properties of other reservoir rock volumes, i.e., flow units (Ebanks, 1987). In the most literal sense, each turbidite bed that is laterally continuous at interwell spacing is a flow unit since these beds are isolated from over- and underlying beds by laterally continuous shales. However, from a practical standpoint, such a fine subdivision is impossible to do and unnecessary.

Appropriate flow unit subdivisions useful for reservoir simulation and operations purposes are done on the scale of *packages* of beds separated by major shale breaks. Average properties of sandstones may be calculated from core plugs taken within the sandstone beds. In the DeGray Dam spillway section, even beds on the order of fractions of a foot appear to be laterally continuous over long distances (see Fig. 67). However, in flow units within which the lateral continuity of certain size class intervals of beds of the sequence is in doubt, some factor for percentage of continuous beds within the flow unit can be applied to the total net pay thickness of the flow unit.

A characteristic of these kinds of vertically stratified reservoirs is the presence of zones of substantially higher permeability. In a displacement process, these beds dominate flow. In flow unit subdivisions, these should be treated as separate flow units. Production and injection profiles through such units can identify such zones. Thicker, amalgamated packages having substantially higher permeability as determined from core plugs is another means of identifying these zones.

Seismic Modelling

One dimensional synthetic seismograms of the DeGray and Dierks (STOP 8) sections were constructed in order to give a better appreciation of the seismic resolution of these types of geologic sequences (on a quite different scale than data presented in the preceding discussions!). The vertical stratification characteristics of the sandstones and shales were interpreted from the gamma-

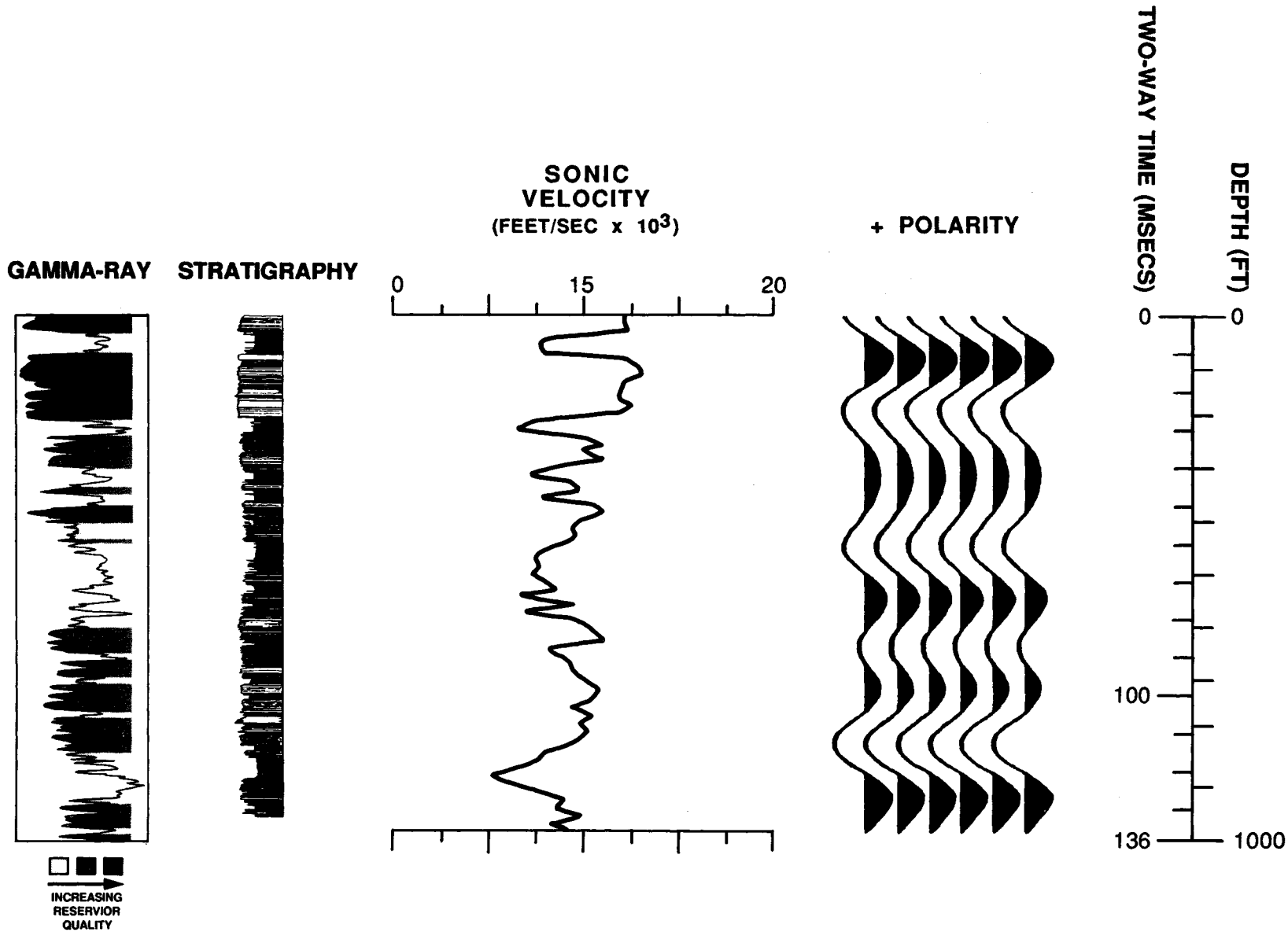

Figure 73. Outcrop gamma-ray log, measured stratigraphic section, pseudo-sonic velocity log, and one-dimensional synthetic seismogram for the DeGray Lake Spillway east section.

ray logs. Sonic logs from exploration wells in the area provided average sandstone and shale velocities of 16,500 and 12,500 feet/sec, respectively. By combining these data, vertical velocity profiles were derived from which pseudo-sonic logs were generated.

For convenience, a constant rock density of 2.5 gm/cc was used for both lithologies. The logs were convolved with a zero phase wavelet using a four-point bandpass filter (4, 12, 35, and 55 Hz) to approximate the frequency bandwidth expected on land at 10,000 feet depth.

An example of a one-dimensional synthetic seismogram for the DeGray Lake Spillway section is shown in Figure 73. Positive reflections are associated with major sand-shale interfaces, and lower amplitude events are associated with more thinly-bedded intervals.

Through this modelling approach, the vertical resolution issue is addressed and not the lateral or spatial resolution of the seismic data. Although the seismic modelling is confined to one-dimensional synthetic seismograms, the data are amenable to generating two-dimensional seismic models where more than one gamma-ray log of an outcrop is available (e. g., Big Rock Quarry, Hollywood Quarry, etc.). Two dimensional changes observed in the seismic data would certainly assist in understanding lateral changes in seismic character as they relate to lithologic changes as long as it is understood that most of the stratal units encountered in these outcrops are too thin to be uniquely resolved on conventional seismic data.

Notes

Stop 6

Lake DeGray Intake, Bismarck, Arkansas

Purpose:

This stratigraphic section, within view of the DeGray Lake Spillway, provides a good example of changes in long distance (about one mile) lateral continuity of beds as well as laterally continuous conglomeratic beds described by Breckon (1988). The conglomerate beds at the Intake are correlative with those at the south end (uppermost part of the section) of the Spillway, and the beds can be traced for several miles along strike (see Fig. 59).

Description of Locality

A portion of the stratigraphic section at this locale was measured for bed thickness and gamma-ray log character (at 0.5 and 2-foot sample spacing). This measured section correlates with the detailed section that was measured at DeGray Spillway (at approximately 375-470 feet at the DeGray Lake Spillway west section, log depth, or 550-635 feet on the section by Morris, 1977; compare with Figure 65).

In addition, gamma-ray logs were measured at two additional Jackfork localities that lie near the Dam (Fig. 75) in a higher stratigraphic interval than the beds at the Intake section.

Interpretation and Reservoir Implications

Much of the interpretation of this section has been interwoven in the comparable section described at STOP 5 (DeGray Lake Spillway). Figure 70 shows the concept of compensation cycles applied to the DeGray Lake Spillway and the DeGray Lake Intake sections. Our gross correlation scheme shows that some intervals become sandier and thicker toward the east while other intervals become sandier and thicker toward the west. As was the case above, it is evident that a knowledge of depositional geometries is essential for a realistic correlation of stratigraphic intervals or depositional cycles at this scale of well spacings (see discussion in previous section, STOP 5). This correlation attempt, while not perfect, can be thought of as representative of a typical oil field in which planning of well spacing scenarios for development of hydrocarbon resources from similar deep-water sandstones is critical. By correlating lithogenetic packages instead of 'layer-cake' lithologies (or sandstone to sandstone), a better description of the reservoir would result and productivity of the hydrocarbons would be enhanced.

Notes

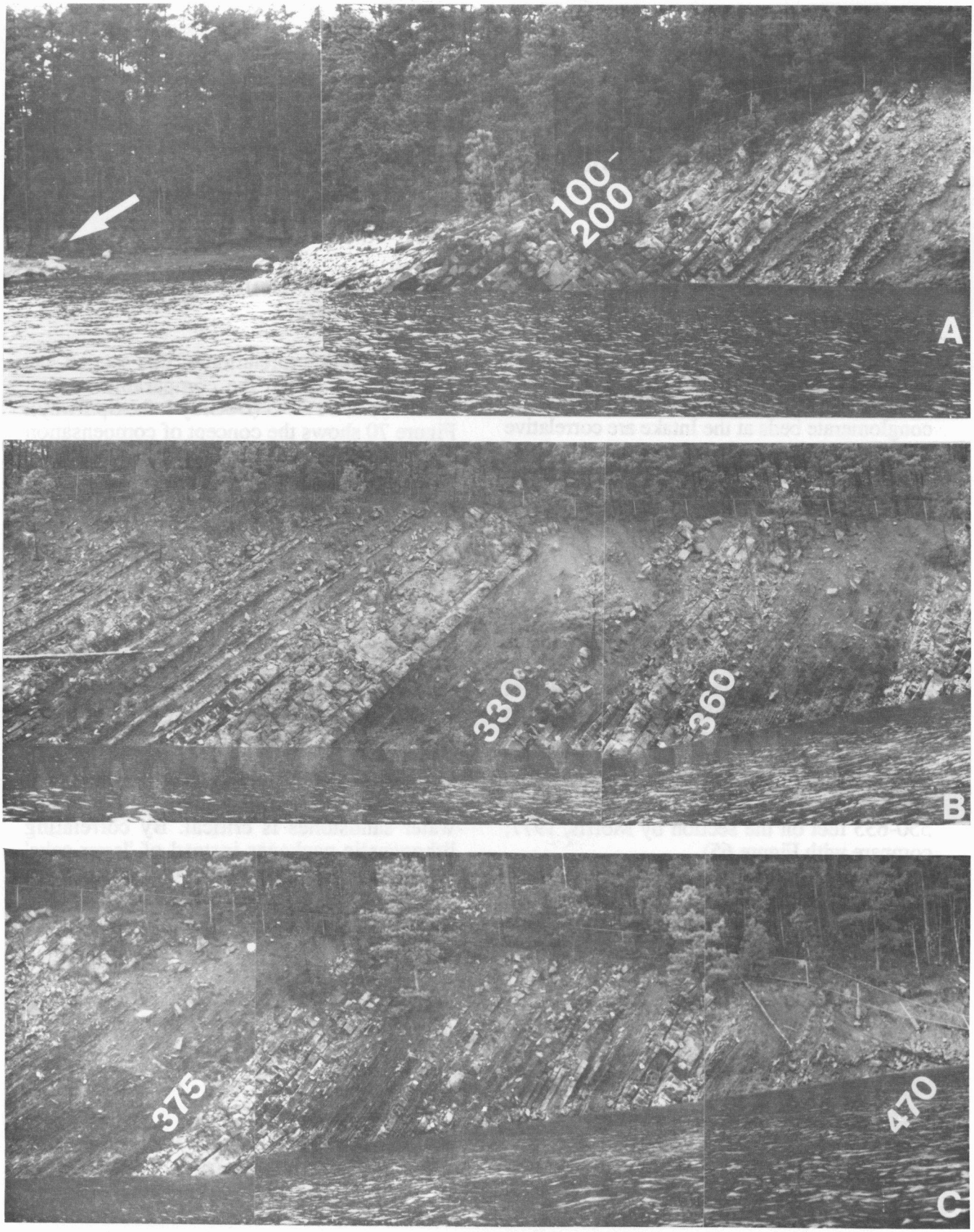

Figure 74. DeGray Intake section. Numbers on photograph refer to correlative interval at DeGray Spillway west section (log depth). See Figure 70 for detailed bed-thickness sketch. Compare with equivalent interval shown in Figure 65. (A) Upper part of section. Conglomeratic bed shown at arrow. (B) Middle part of section. Section is equivalent to interval at 330-360 feet (log depth) at Spillway west (see Figure 64 A-C). (C) Lower part of section is equivalent to 375-470 feet (log depth) on the Spillway west section.

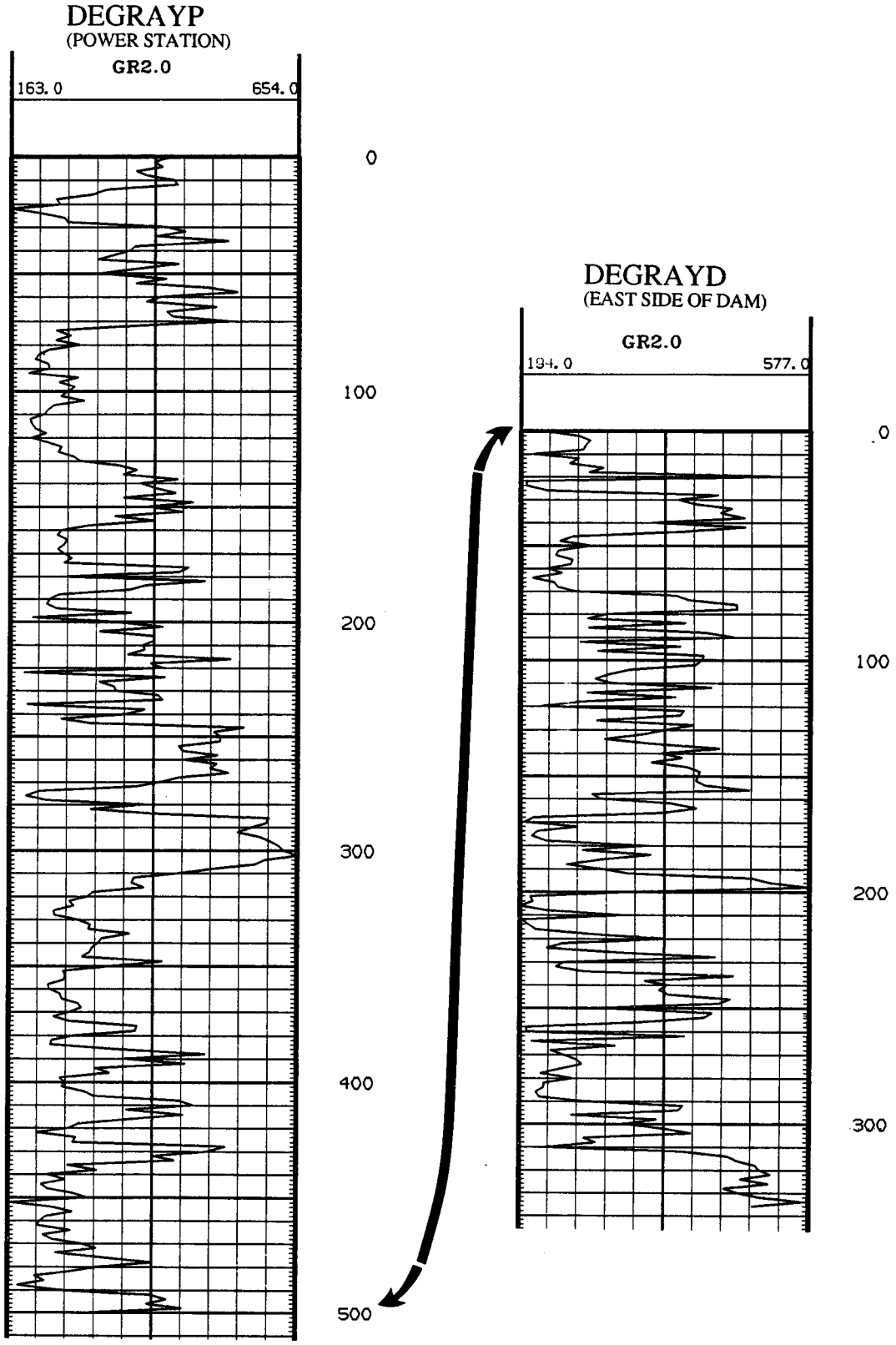

Figure 75. Gamma-ray logs (2-foot sample spacing) taken at the DeGray Power Station (DEGRAYP) cut (west side of out take) and Dam (DEGRAYD) cut (east side of out take) sites. The section at DEGRAYP is stratigraphically higher. Refer to Figure 62 (page 97) for location of logs.

Stop 7

Hollywood Quarry, north of Hollywood, Arkansas

Purpose:

The purpose of this stop is to view the sedimentology and bedding characteristics of laterally discontinuous, lenticular and laterally continuous, sheet-like facies, and provide an opportunity to observe and understand a complex three-dimensional 'guts of a reservoir' perspective in a deep-water sequence having a structurally complex overprint.

Description of Locality

Hollywood Quarry, located about 10 miles west of the DeGray Lake Spillway, offers an excellent opportunity to study a section through a sequence of massive to thickly-bedded upper Jackfork sandstones roughly equivalent in stratigraphic position to units in and between the upper part of the DeGray Lake Spillway and Murray Quarry sections further to the east. The units have been interpreted by Stone and McFarland (1981) as having been deposited in middle submarine fan channels derived from the south-southeast.

This quarry exposes both lenticular and sheet-like turbidite strata; in addition, some faults cut through the quarry. A logging exercise was designed to develop a scaled-down representation of well logs and spacing patterns as might occur in a subsurface oil or gas field. With such a representation, it is possible to demonstrate potential correlation pitfalls which might be encountered in fields with these types of geological complexities.

Bedding strikes uniformly N20-30E and dips 10-15 degrees west. The rocks are cut by a number of minor high-angle faults, most trending east-west to northeast-southwest (Fig. 76). The exposed section totals 140 feet thick (Fig. 77).

Interpretation

Stratigraphy and Sedimentation

The lower 88 feet of section is a lenticular, fining- and thinning-upward channel-fill sandstone sequence (Fig. 78) that rests on shale. The base is a 5-foot-thick layer of quartz-granule conglomerate containing abundant clasts of deformed shale and mudstone ripped up from the underlying unit. Granule conglomerate occurs throughout the lower 33 feet of the channel fill interbedded with poorly-stratified, granule-bearing medium- to coarse-grained sandstone. Large internal channels are locally defined by lenticular conglomerate layers. The sandstones are generally massive, although some show well-developed water-escape structures. Traction structures are absent, suggesting that most of the sediment was deposited by suspended-load fallout from high-density turbidity currents.

The upper 55 feet of the channel-fill sequence consists of well stratified, thick to medium-bedded, predominantly medium-grained quartzose sandstone. Sandstone beds average 2 to 4 feet thick (Fig. 79A-B) and show abundant water-escape structures and soft-sediment deformation features. Near the top, the sandstones become slightly muddy and one or two slurried units are interbedded with the cleaner sandstones. The top of the channel sequence is marked by a prominent rust-stained unit containing large, vertical water-escape channels.

The top 52 feet of the quarry section (Fig. 80A) consists of interbedded units of predominantly medium-grained sandstone and shale. Sandstone units include layers of relatively clean, light gray, quartzose sandstone, from less than an inch to several feet thick, deposited by turbidity currents. Thicker turbidites are dominated by water-escape structures, especially dish structures, and many show ripped-up shale clasts. Only a few of the thinnest turbidites show well-

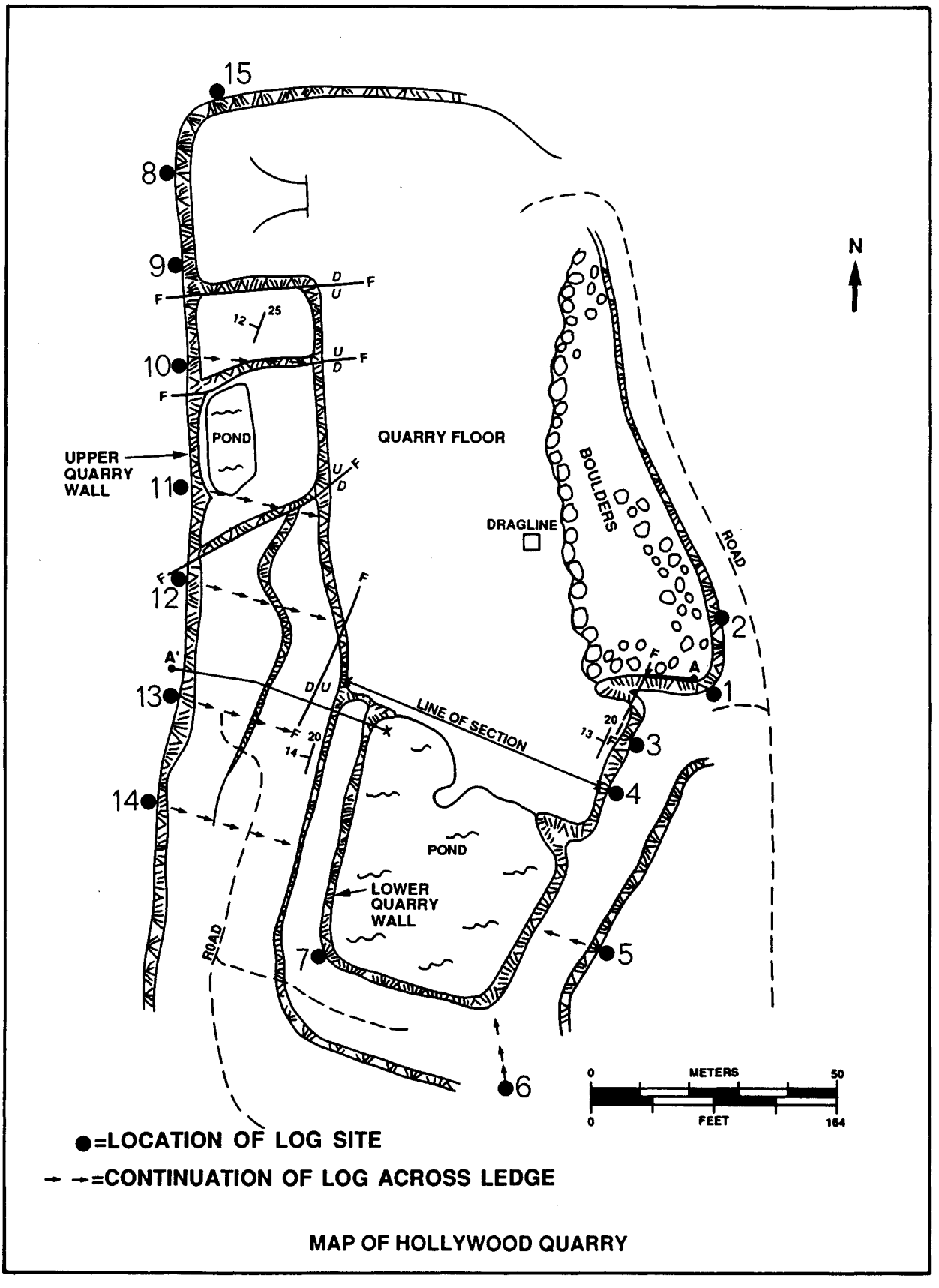

Figure 76. General sketch map of Hollywood Quarry showing line of section (Fig. 77) and principal faults cutting the Jackfork sequence. Location of logging sites shown.

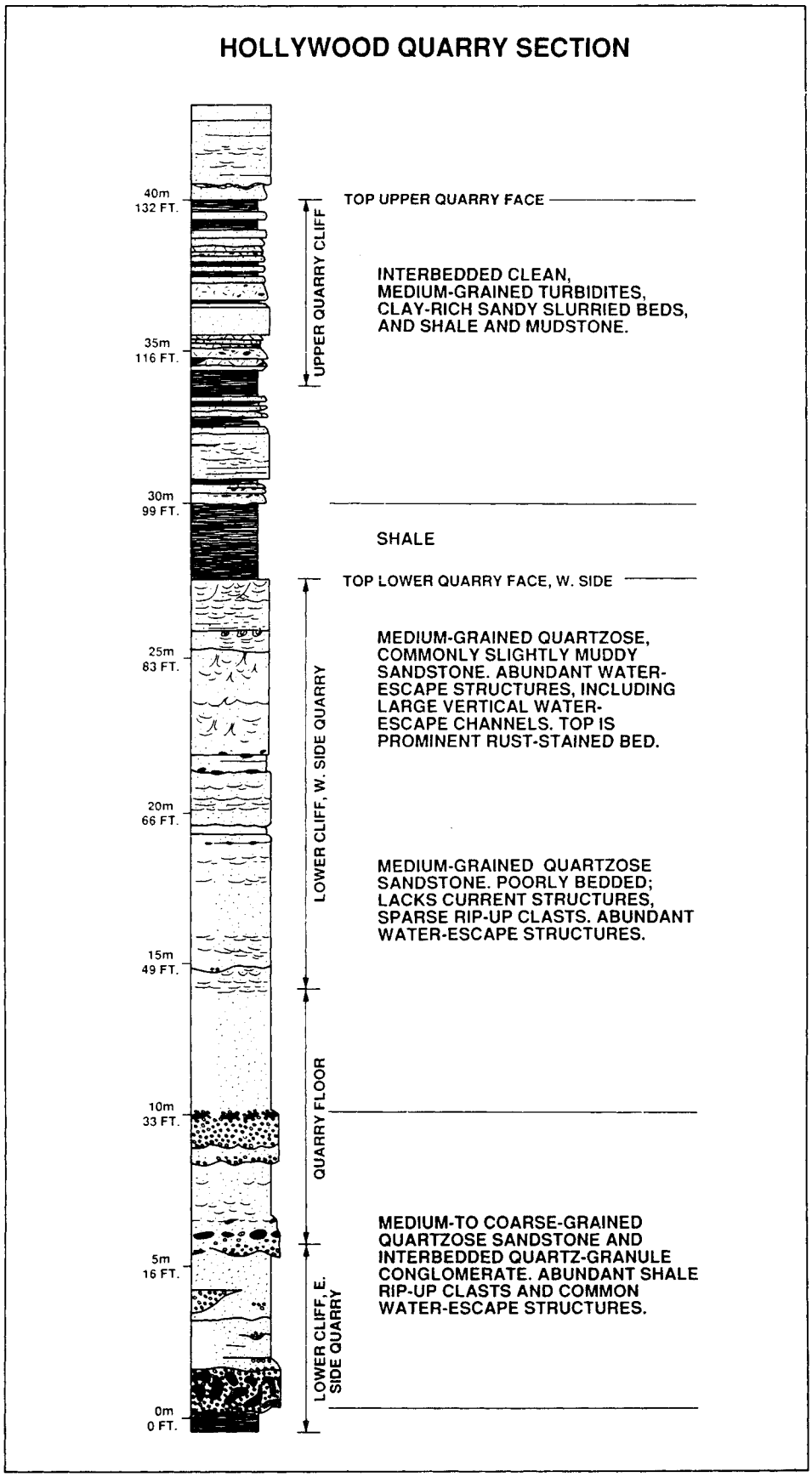

Figure 77. Stratigraphic column of the Jackfork sequence exposed in the Hollywood Quarry, Arkansas. Line of section is located on Figure 76.

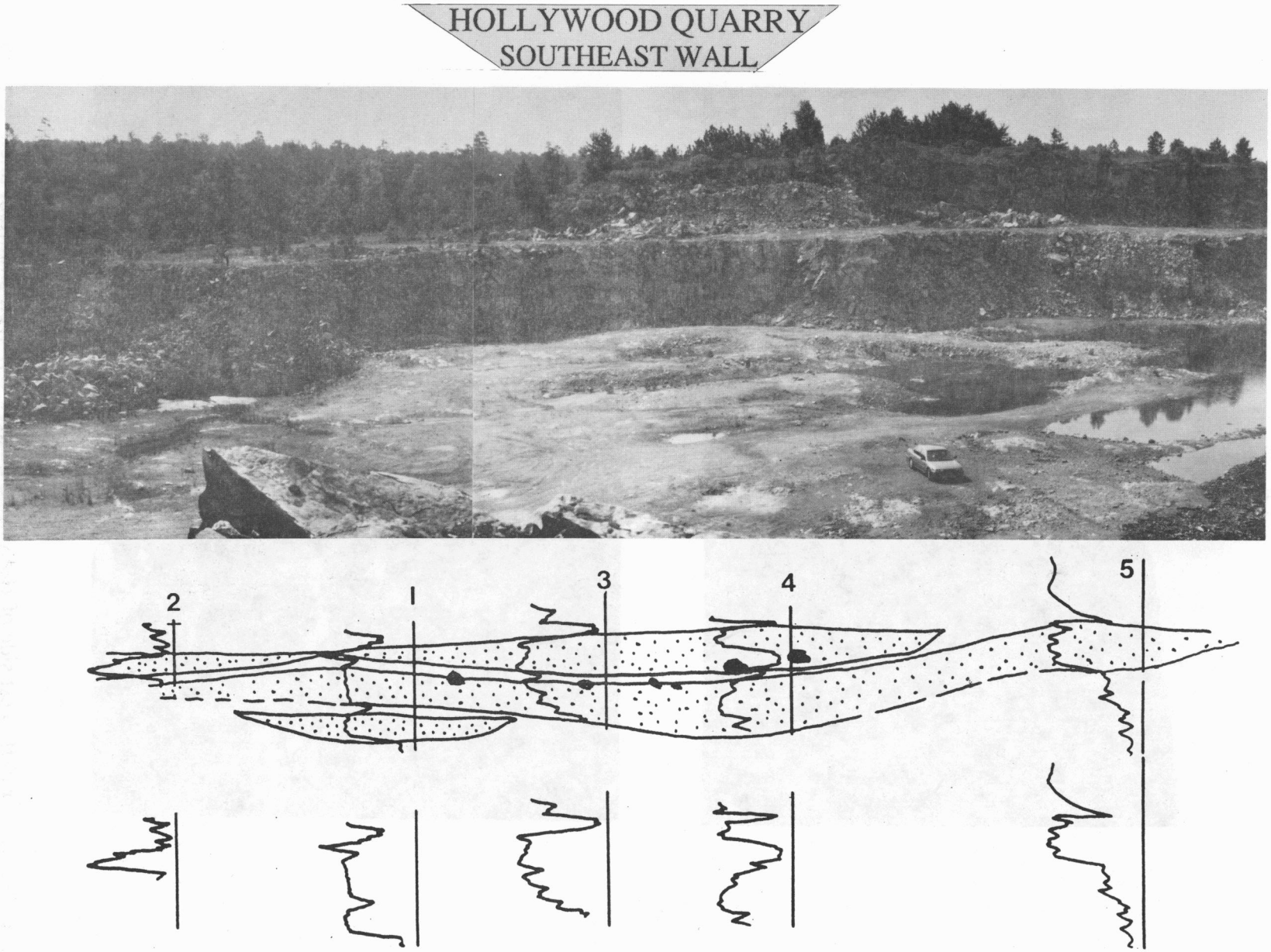

Figure 78. Lower 88 feet of section at Hollywood Quarry consisting of several channels, the lowest one resting on shale. Clasts of deformed shale and mudstone ripped up from the underlying unit are locally present.

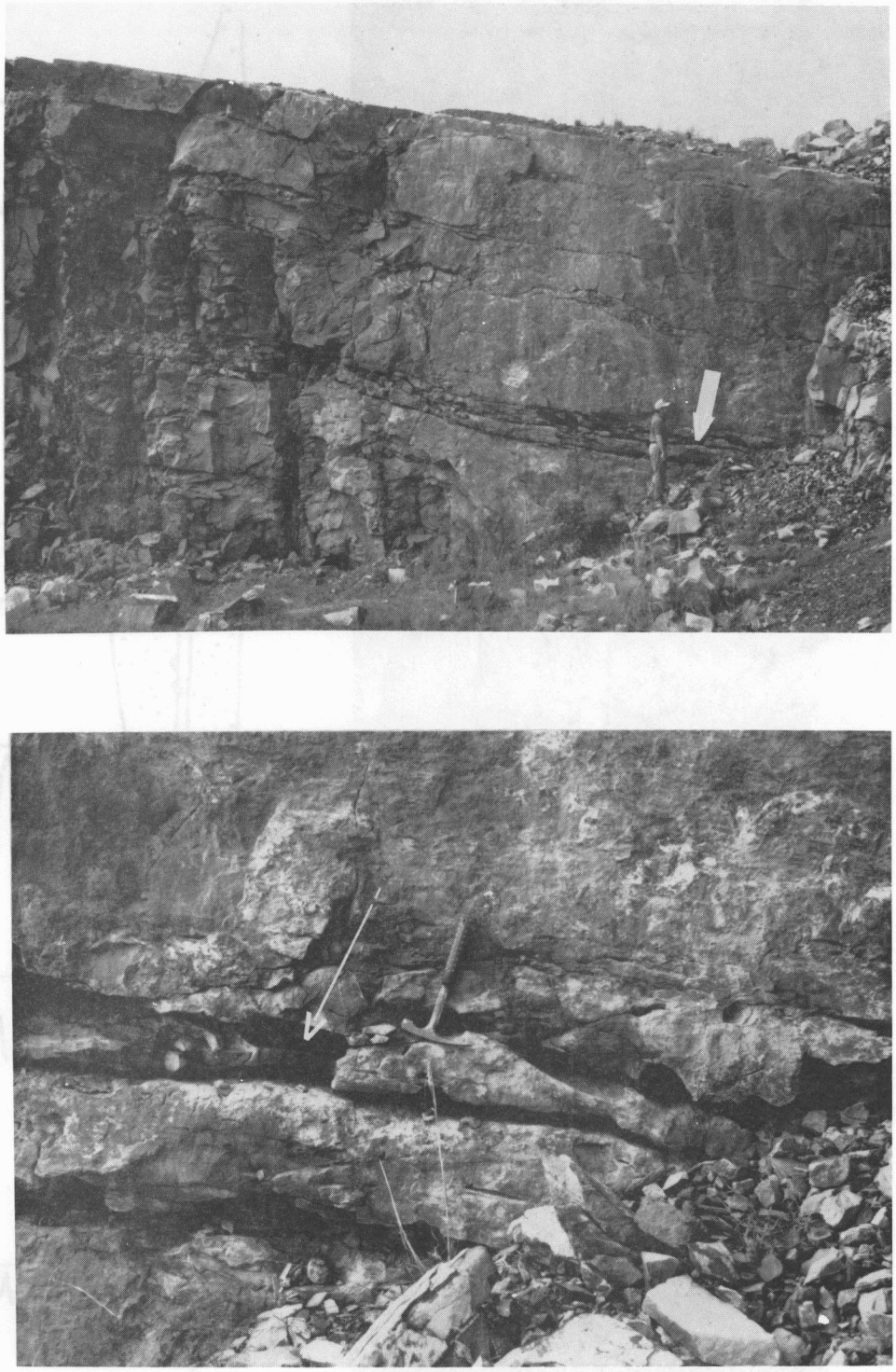

Figure 79. Lower cliff, west side of Hollywood quarry. (A) Well-stratified, thick- to medium-bedded, medium-grained quartzose sandstone with sharp basal contact. (B) Close-up of area shown at arrow in A, with large mudstone clasts (arrow).

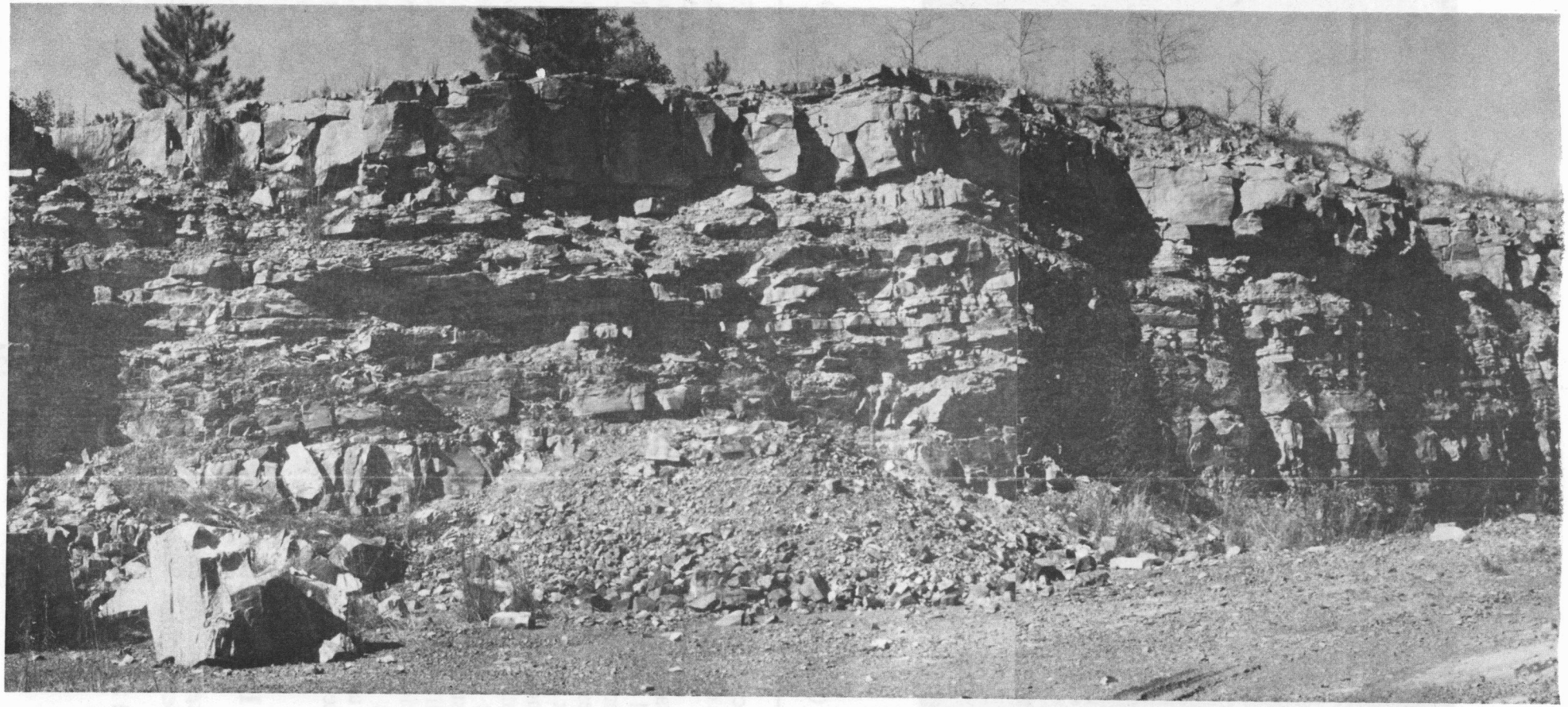

Figure 80. Upper part of section on the west cliff of the quarry. (A) The top 52 feet of the quarry section consists of interbedded units of predominantly medium-grained sandstone and shale. Sandstone units include relatively clean quartzose sandstone, from less than an inch to several feet thick, deposited by turbidity currents. (B) Well-developed traction structure (cross-lamination) within thin turbidite. Underlying bed is a clay-rich, sandy slurry bed.

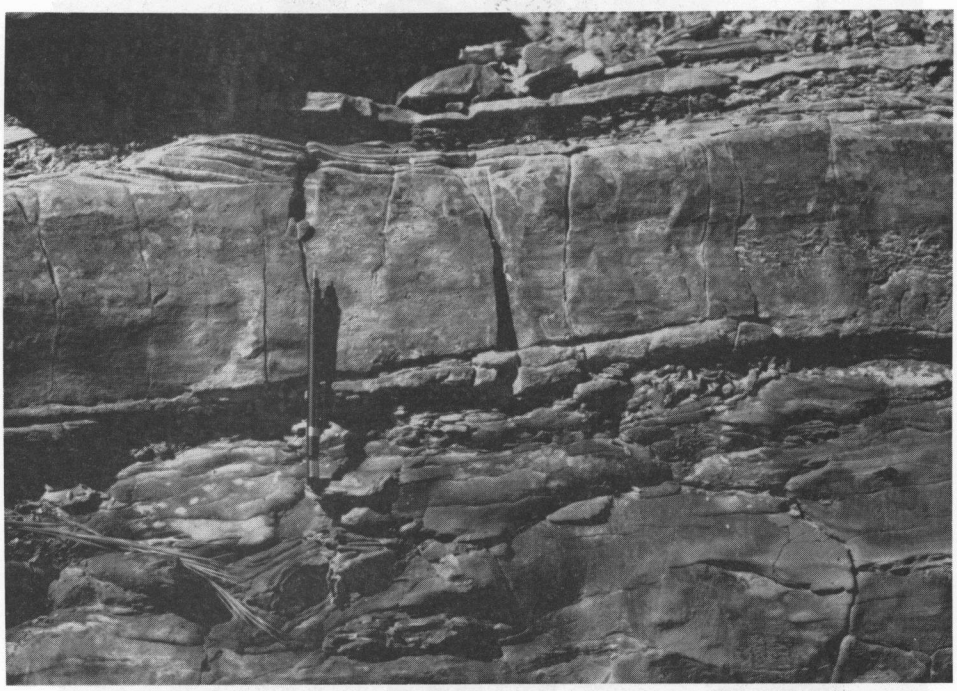

Figure 80B. (caption on previous page).

developed traction structures, such as flat lamination and cross-lamination (Fig. 80B).

A number of sandy units in the upper part of the Hollywood Quarry section are composed of very dirty, brown to gray, poorly indurated sandstone. These beds range from 4 to about 24 inches thick and contain a high proportion of mud, commonly 15% to 35%. They lack current and water escape structures but show soft-sediment deformation features and abundant mudstone clasts. These units appear to represent dilute debris flows or slightly cohesive slurries that may have formed as small failures on mud-covered submarine slopes. They are clearly distinct from the cleaner turbidite sands.

Reservoir Implications

Logging Exercise: Correlation of Logs in a Complex Geologic Setting

Figures 81 and 82 shows the gamma-ray logs obtained by the logging truck and scintillometer methods (see Figure 76 for locations of logging sites in the quarry). The beds strike about north 25 degrees east and dip 10 degrees to the northwest so that the beds on the east wall of the quarry dip beneath those on the west wall. The upper part of the southern half of the west wall comprises laterally discontinuous strata. The northern half of the west wall contains more laterally continuous, but highly faulted beds. The east wall contains thick, lenticular sandstones and pebbly sandstones which are probably correlative with the pebbly sandstones at the top of DeGray Lake Spillway. In this example, if only logs were available, the correlations shown in Figure 83 most likely would not have been made. Considering that these logs are relatively closely-spaced, this exercise demonstrates some of the uncertainty in well log correlations that might be anticipated in oil and gas fields of complex facies architecture and structure. Coring of development wells for detailed sedimentologic and stratigraphic analysis, utilizing Formation microscanner (FMS) or dipmeter logs for recognizing thin beds, and utilizing 3D seismic

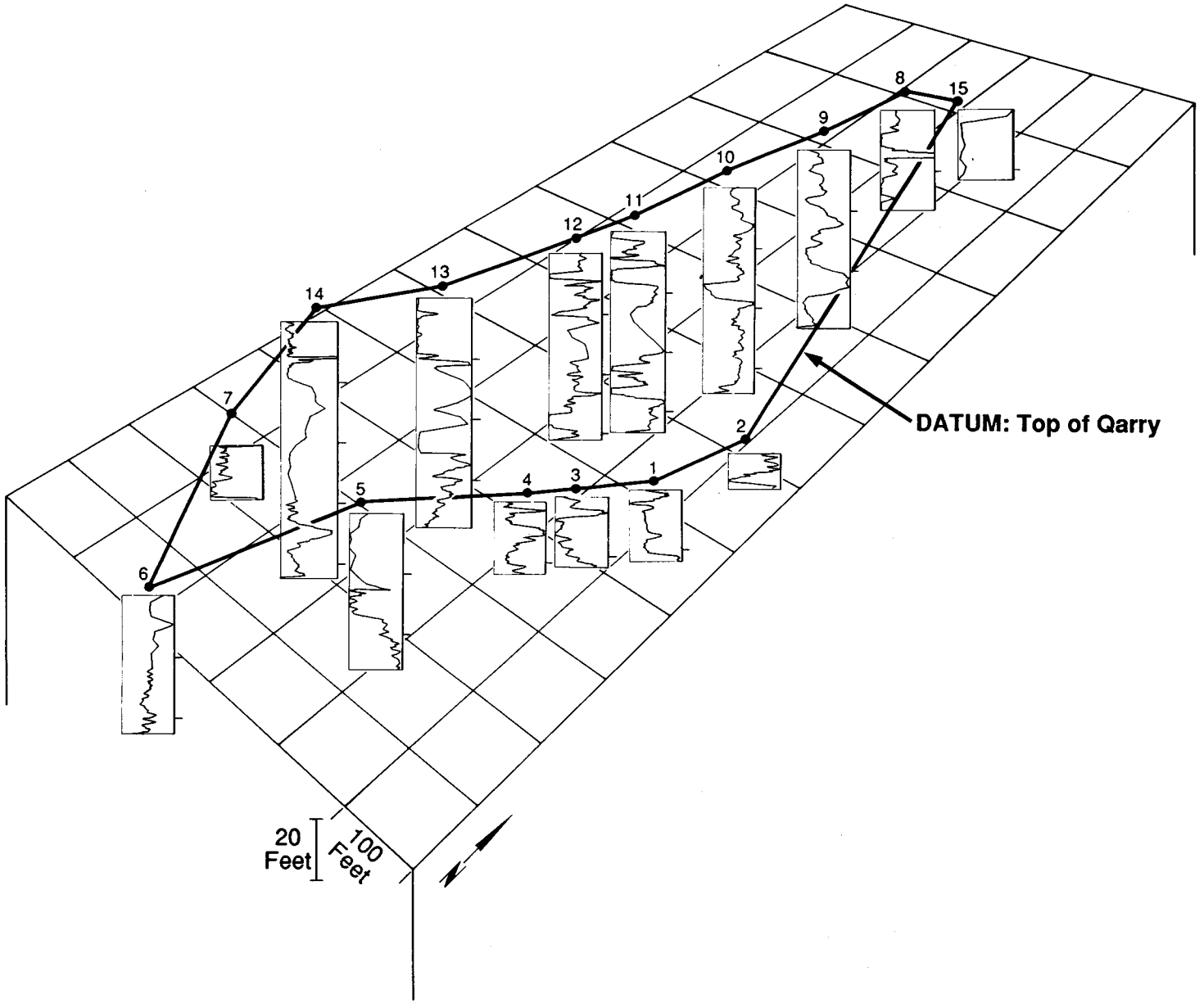

Figure 81. Location of the fifteen gamma-ray logs obtained with the logging truck at Hollywood Quarry. Heavy line connects the top of the cliff wall.

surveys for structural and stratigraphic interpretation, in addition to well testing, would reduce this uncertainty in such situations and aid in the understanding of interval heterogeneity.

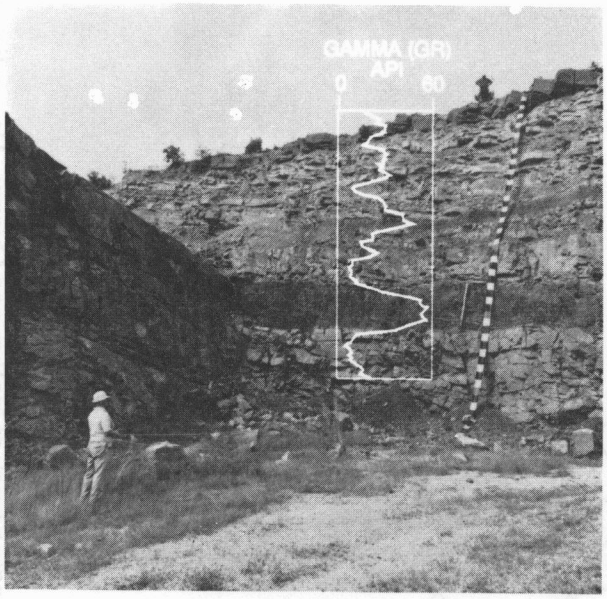

Figure 82. Typical gamma-ray log (log site #9; see Figs. 76 and 81). Gamma-ray sonde (large arrow) being raised from the base of the west wall of Hollywood Quarry by a cable (small arrow) attached to the logging truck (not in view). This logging run produced the gamma-ray log that is superimposed upon the quarry wall in the photograph. Note the scale marked in one foot increments.

Notes

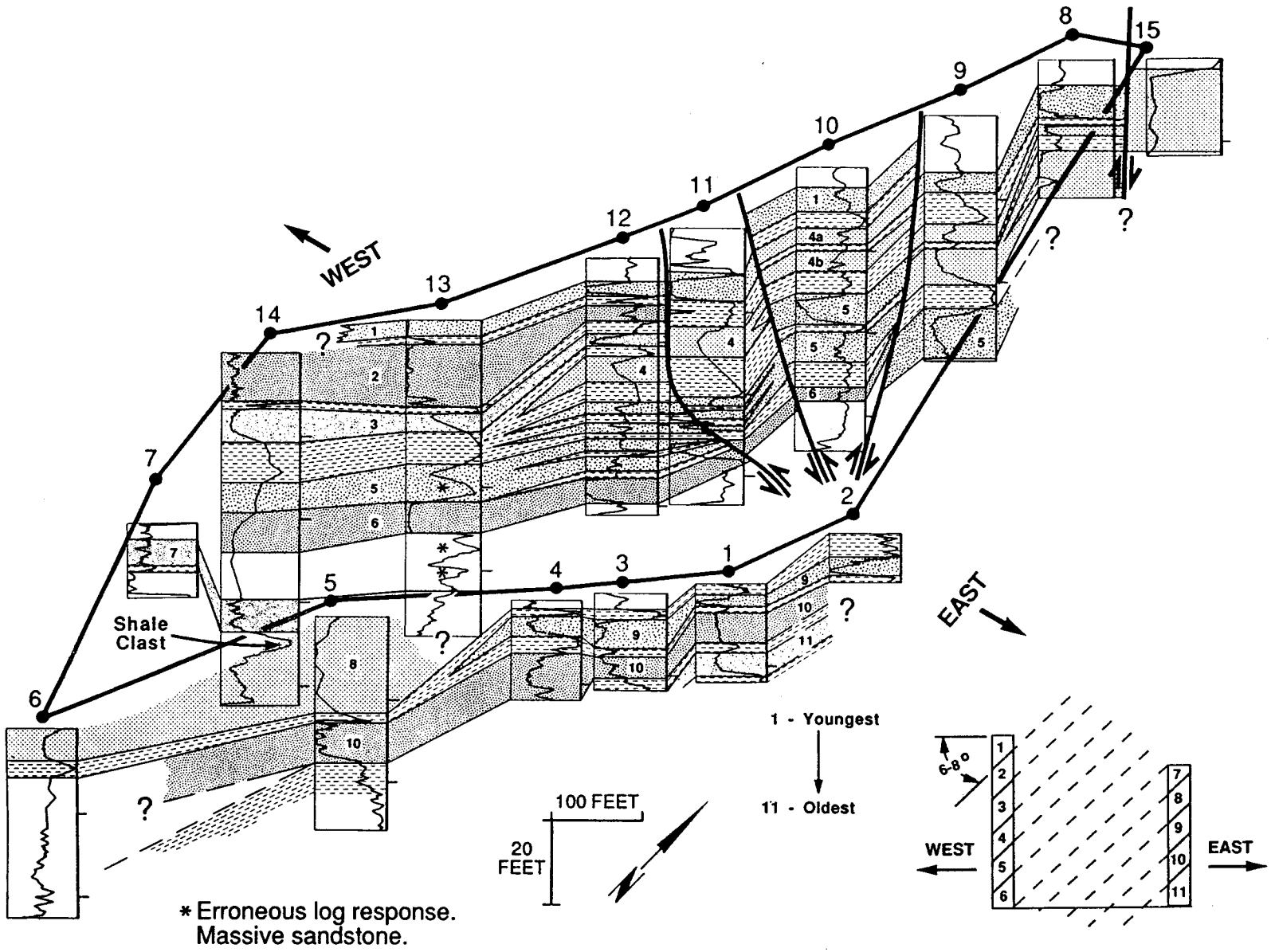

Figure 83. Gamma-ray log correlations at Hollywood Quarry.

Field Trip Itinerary and Description (Day 3)

Laterally Continuous, Sheet-like Facies/Laterally Discontinuous, Lenticular Facies

Stop 8

Dierks Lake Spillway, near Dierks, Arkansas

Purpose:

The purpose of this final stop of the field trip is to observe lower Jackfork sandstones and shales, discuss lateral heterogeneity of the units and relationships of gamma ray logs to predicting reservoir quality, and interpret the processes of deposition related to the occurrence of slurried fine-grained turbidites versus hemipelagic sedimentation.

Description of Locality

The Dierks Lake Spillway section is located about 60 miles west of the DeGray Lake Spillway. It consists of over 600 feet of lower Jackfork strata. The lower part of the section was interpreted by LeBlanc (1984) as deep-fan lobe deposits, the middle portion as deep-sea fan channel and fan lobe sediments, and the upper part as deep-sea fan channel sequences. Link and Roberts (1986) suggest that these units comprise middle to outer fan depositional lobes.In general, sandstones are more numerous and thicker upsection. The Dierks spillway can be subdivided into several thick sandstone cycles separated by thinner mudstone units, much like the section at DeGray Lake Spillway.

Interpretation

Stratigraphy and Sedimentation

The Dierks Lake Spillway section (Fig. 84) displays the same general types of sedimentation units that we have seen at DeGray Lake Spillway. However, careful examination of the mudstone intervals between sandstone beds, especially in the lower portion of the outcrop on the west side, shows that they are not primarily laminated hemipelagic mudstone or discrete muddy turbidites, but instead, debris flow deposits related to the waning stages of deposition of the underlying turbiditic sandstone beds. They thus represent more muddy turbidity currents than those at DeGray. The lower Jackfork interval that is present in more distal portions of the basin (Fig. 85) to the west contains a greater amount of interbedded debris flow deposits and hemipelagic shales. The upper part of the Dierks section contains discontinuous sandstones having erosional bases (channels?) and amalgamated contacts.

Gamma-ray logs (Figs. 86 and 87A-C) were obtained along both sides of the spillway (about 600 feet apart) using the hand-held scintillometer. The east side of the spillway is composed principally of thick, amalgamated, lenticular sandstones. The base of this section is a highly contorted and folded shaley interval (Fig. 88): the relative influence of tectonics and soft sediment deformation of this interval has been debated at the outcrop for many years! We correlate this interval with a shale at about 260 feet on the gamma-ray log taken on the west side of the spillway. Sandstones on both sides of the spillway above this horizon are difficult to correlate on logs owing to their lenticularity, and are cleanest, as indicated by best relative reservoir quality (see Fig. 58).

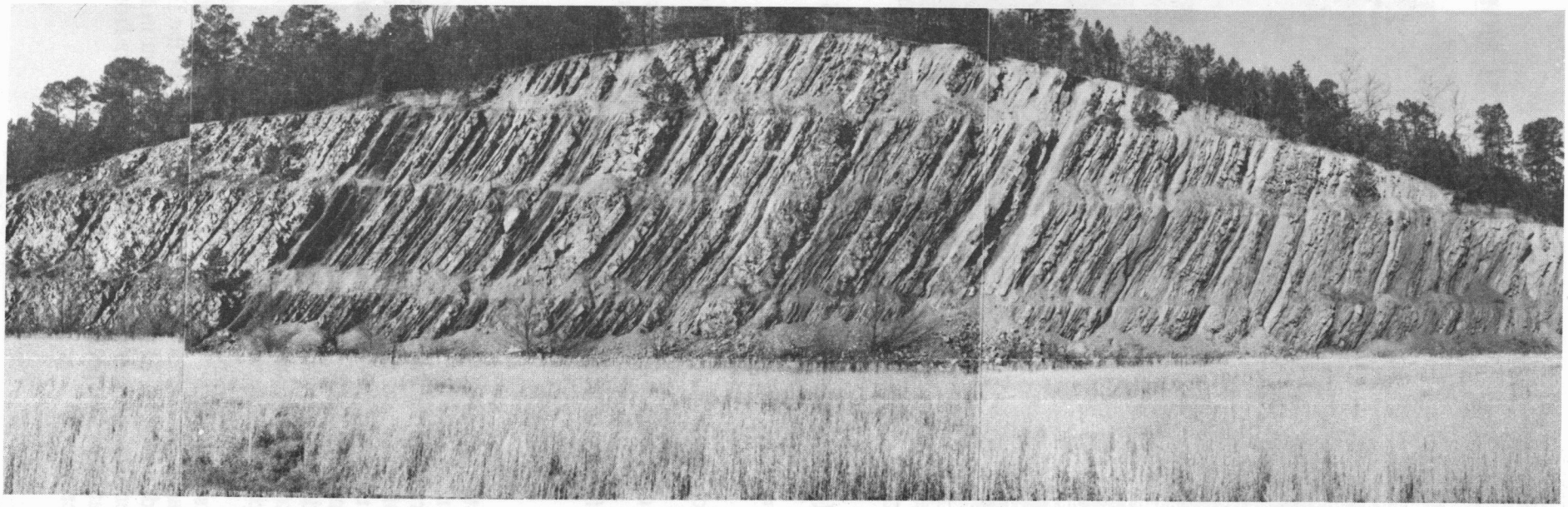

Figure 84. Lower Jackfork section at Dierks Lake Spillway (west section).

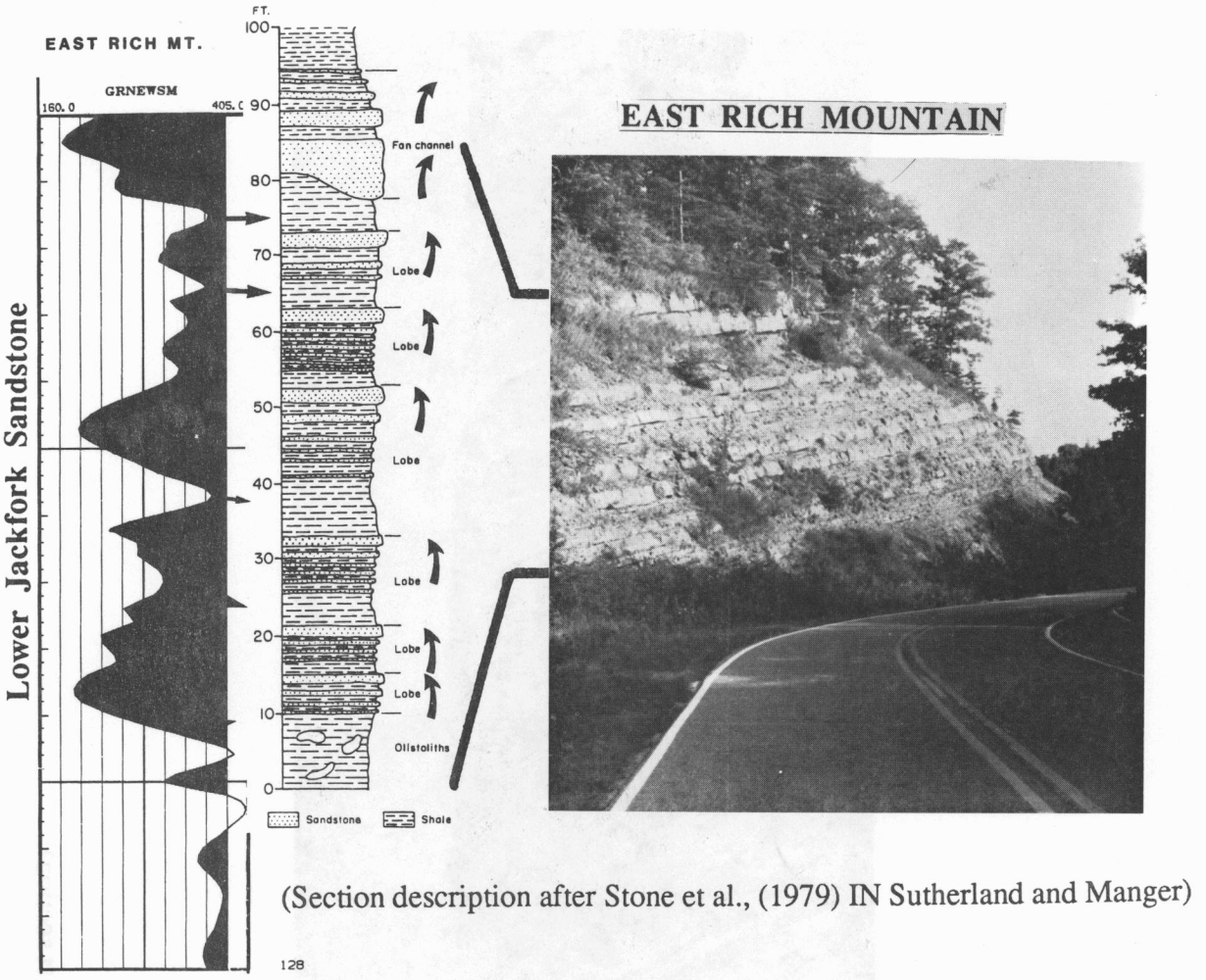

Figure 85. Section at Rich Mountain, eastern Oklahoma (measured section modified after Stone et al., 1979, IN Sutherland and Manger). The lower Jackfork interval at this locality in Oklahoma consists of numerous compensation cycles and abundant interbedded hemipelagic and debris flow mudstones, and represents a depositional site that was distal to that found at Dierks Lake Spillway.

The individual sandstone bed thickness appears to be greater at Dierks (lower Jackfork) than at DeGray (upper Jackfork), although the amount of shale, as a whole, increases. There is 10% more net sandstone in the DeGray outcrop (Jim Doyle, pers. comm., 1988) than in the Dierks section, based on counting sandstone thickness on the respective logs. Log-to-outcrop correlations appear to be better because of the thicker, individual sandstone beds at Dierks, and hence the two-foot sampling interval was able to better define the individual beds and contacts. Laterally discontinuous facies were more apparent (or more easily recognized) at Dierks (especially in the upper part of the outcrop).

Below the 260 foot shale on the west side of the spillway, evenly-bedded sandstones form thickening- or thinning-upward stratigraphic intervals. These are interpreted as having been deposited as compensation cycles, in a manner analogous to that at DeGray Lake Spillway; the vertical sequences are not considered to be submarine fan lobes and channels.

An outcrop gamma-ray log, pseudo-sonic velocity log, and one-dimensional synthetic seismogram for the Dierks Lake Spillway west section is shown in Figure 89 for comparison with similar data from DeGray Lake Spillway (see Fig. 73).

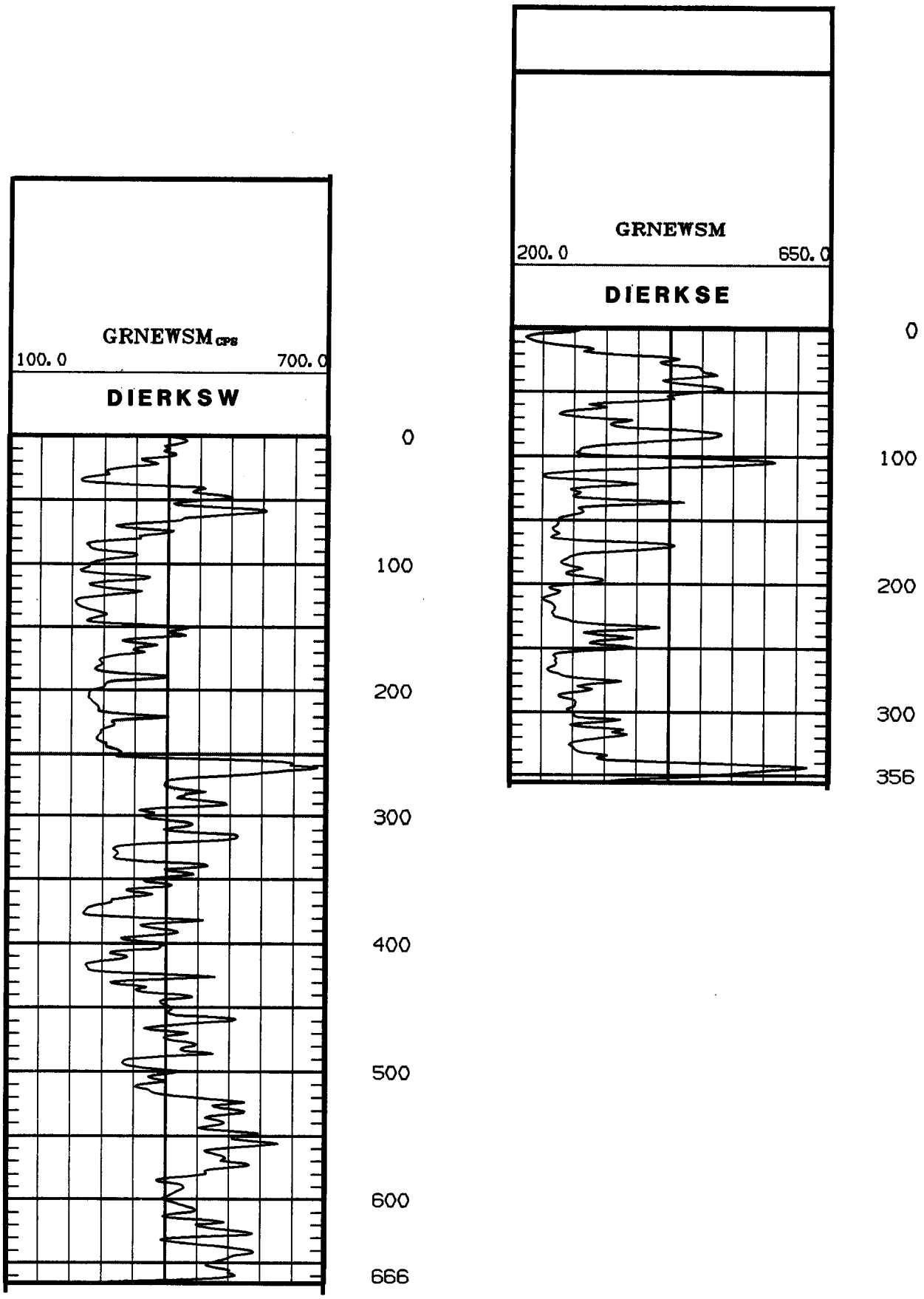

Figure 86. Gamma-ray logs obtained with a hand-held scintillometer (two foot sample spacing) along the east and west walls of Dierks Lake Spillway. The two walls are spaced about 800 feet apart.

Figure 87. Gamma-ray logs superimposed on Dierks Lake Spillway west (A, B) and east (C) section. Point of overlap for the two photographs for the Dierks west section is shown at arrows. Pertinent log footages are shown. The logs were sampled at the 2.0-foot spacing.

190'
250'
335'
B

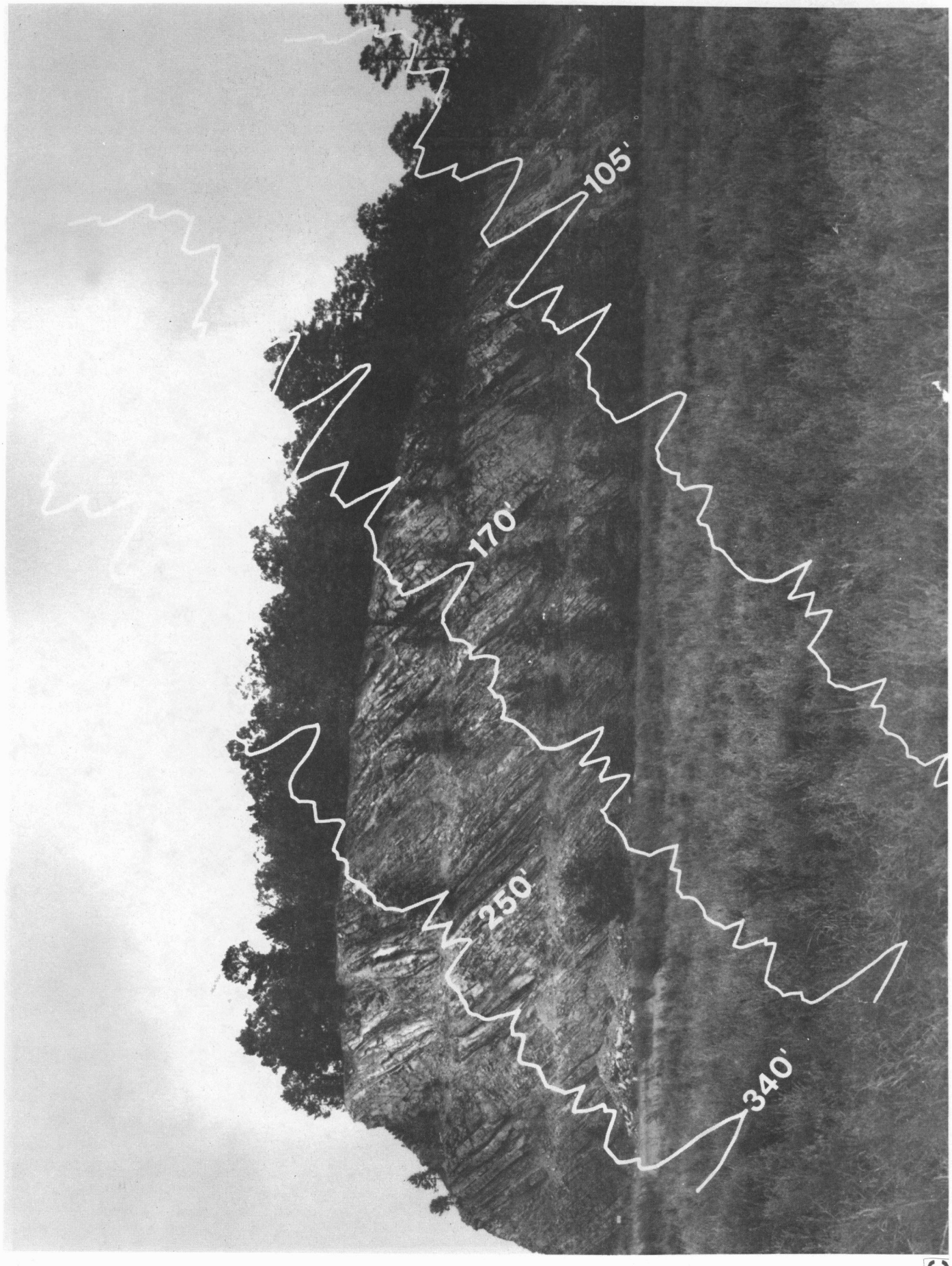

C

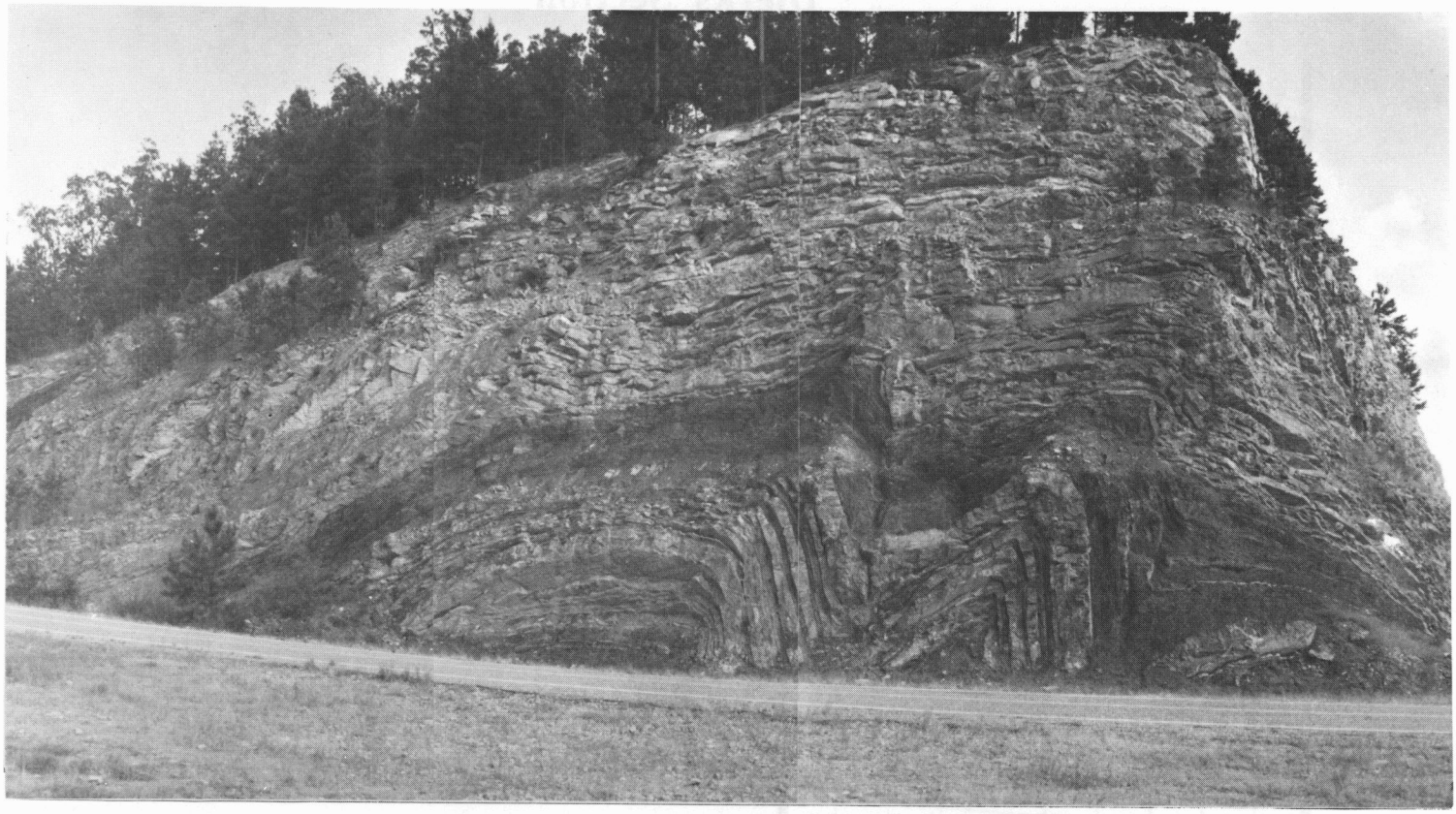

Figure 88. Lower part of the Dierks Spillway east section (350 feet log depth). Tectonic or soft-sediment-deformation?

Reservoir Implications

Petrography of Jackfork Sandstones and Relationship to Gamma-ray Logs

A total of seven rock samples were taken from the DeGray (East) and Dierks (West) localities in order to interpret possible reservoir quality (see discussion on Reservoir Quality Characterization in an earlier portion of this guidebook). Examples that illustrate relative reservoir quality are shown in Figures 49, 50, and 58 and Table 6). For example, samples A, B, and C from Dierks (Fig. 49) were obtained in order to relate matrix content to gamma-ray counts. Sample DIERKSW1 is characterized as a "dirty" sandstone in the field, has a matrix content of 16%, and has a gamma-ray count of 440. Sample DIERKSW2 is a "moderately dirty", sandstone having a matrix content of 7% and a count value of 370. Sample DIERKSW3 is characterized as a "clean" sandstone in the field, has matrix content of 2%, and has a gamma-ray count of 292. The clay and/or organic matrix is interpreted to be responsible for the bulk of the variation in gamma-ray count (see discussion from STOP 5).

Five intervals of the Dierks Spillway west section (Fig. 90) were sampled (see Appendix II) because of their distinct log curve shapes. The interval between 490' and 520' would commonly be interpreted as a "coarsening-up", prograding lobe sequence. This sequence is characterized by samples DK1-3. the grain size plot shows a distinct fining-up trend while the matrix plot displays an upward decrease. This trend is responsible for the log response. Samples DK4 and DK5 characterize the lower portion of an apparent fining-up cycle from 385'-423'. Those two samples indicate a coarsening-up trend and a decrease in matrix between 406' and 420'. The shale at 400'-404' probably is responsible for the major gamma-ray count deflection in the middle of the cycle, even though the sands seem to be "cleaning" upwards. Samples DK6-8, at 378',

Dierks Section

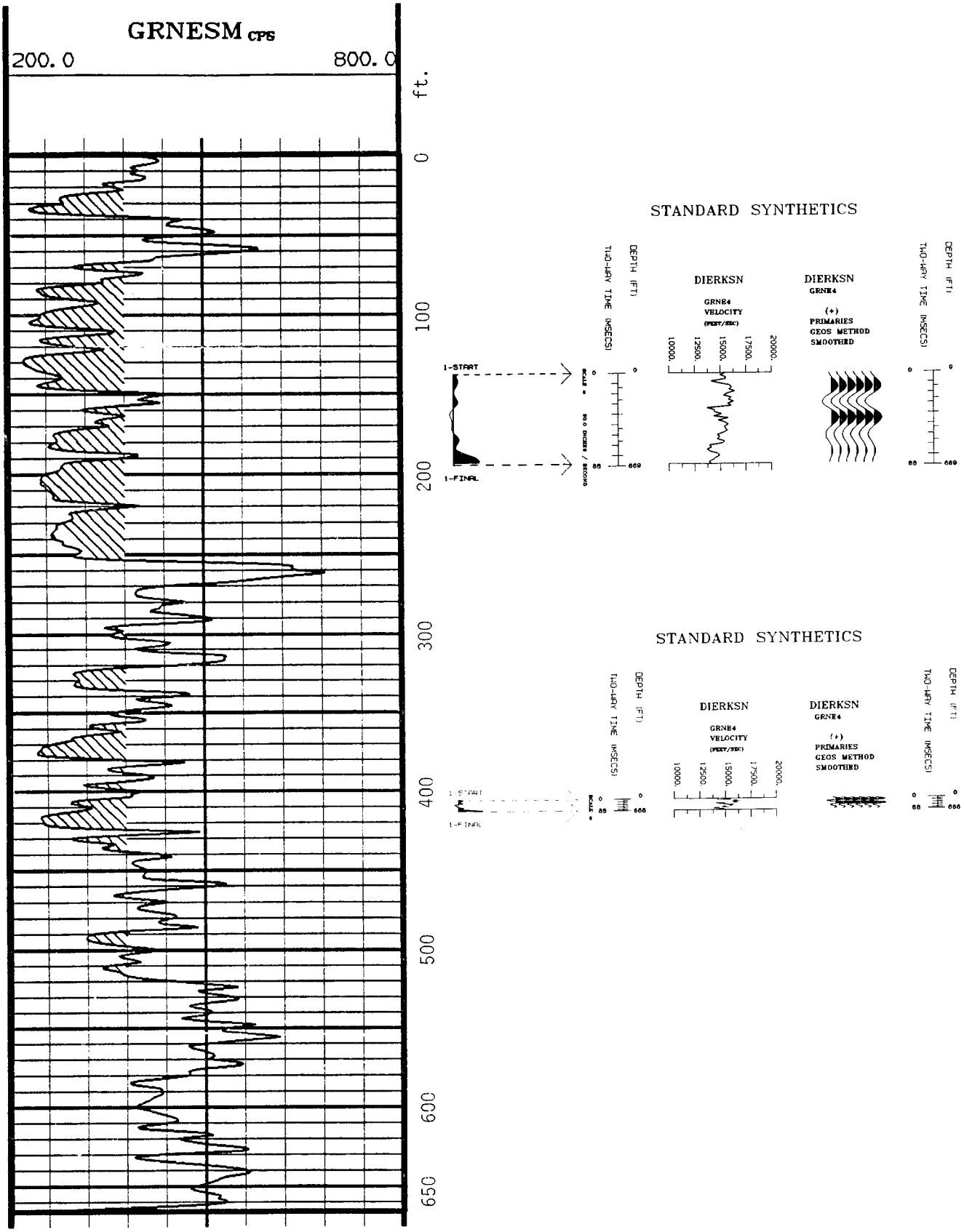

Figure 89. Outcrop gamma-ray log, pseudo-sonic velocity log, and one-dimensional synthetic seismogram for the Dierks Lake Spillway west section.

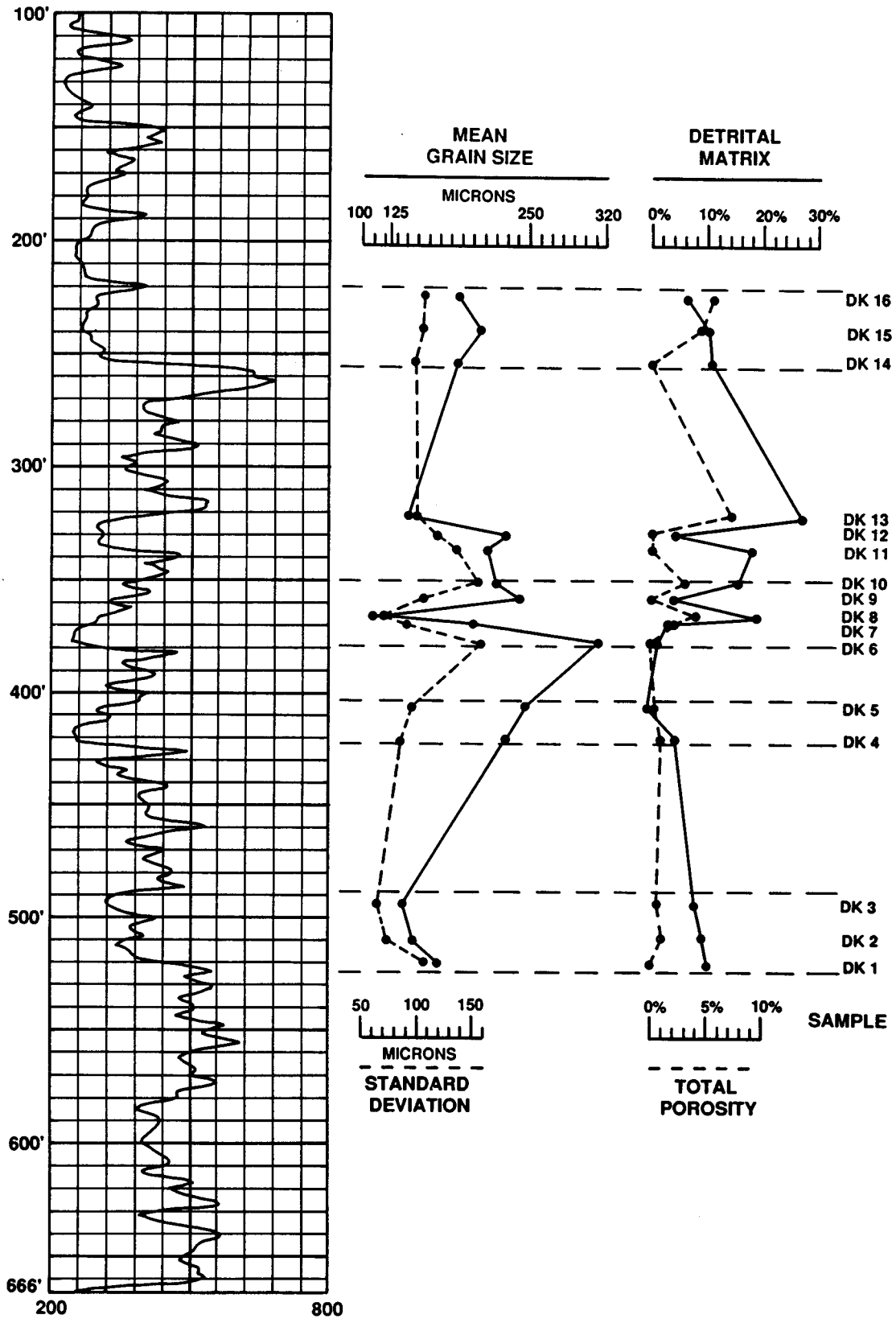

Figure 90. Detailed log and data plot for the Dierks Lake Spillway west section, 222'-520'. See text for discussion.

370', and 366' respectively, represent the lower part of an apparent "fining-up" channel cycle. The grain size plot for these three samples does show a fining-up trend along with an upward increase in matrix (and porosity) in keeping with the expected interpretation of the log. Samples DK9 and DK10, at 358' and 352' respectively, although apparently part of the same log cycle, show a marked coarsening and matrix increase. The sand at 320'-337', with a blocky curve shape, is characterized by samples DK11, DK12, and DK13, at 336', 330', and 322' respectively. The samples show an erratic grain size trend and a "dirty" base and top for the sand, partially responsible for the high gamma-ray count. The overlying and underlying shales also probably account for some of the deflection in the curve. The blocky sand from 222'-255' is characterized by samples DK14, DK15, and DK16, 254', 238', and 224' respectively. They show an erratic grain size trend, somewhat coarser in the center of the sand and a gradual decrease in matrix, which is very subtly expressed in the gamma-ray curve.

Acknowledgments

We wish to express our appreciation to James Ebanks, Jr., and Andrew Slatt for field assistance in obtaining some of the logs, Douglas Lawson for his advice on the mathematics of estimating laterally continuity of strata, Galen Treadgold for his assistance in generating synthetic seismograms, and Joe Senftle for analyzing the geochemistry. Fred Behnken and Pat Whalen searched admirably, but in vain, for various microfossils. Jake Gerhard ably identified rare palynomorphs. Bob Siegfried arranged for the use of the ARCO logging truck, which was manned by Joe Smith and Larry Patterson. Paul Weimer and Marty Link contributed the data in Appendix I.

This manuscript benefitted from earlier reviews by Jim Lorsong, Eric Pasternack, and Phil Lowry; however, the content of this paper is the sole responsibility of the authors. ARCO Oil and Gas Company and ARCO International Oil and Gas Company allowed us to present this information, and the drafting departments performed their usual high-quality work. Ray Slay provided his photographic expertise. Smokehouse Barbecue (Route 7 near Bismarck, Arkansas) aptly provided ribs and strawberry pie to lucky field trip participants.

Jordan would especially like to thank E. Mutti for showing him novel ways of looking at turbidites in the Pyrenees on an ARCO-sponsored field seminar.

References

Bookman, J. W., 1953, Lithology and petrology of the Stanley and Jackfork Formations: Journal of Geology, v. 61, no. 2, p. 152-170.

Bouma, A. H., 1962, Sedimentology of Some Flysch Deposits: Elsevier, Amsterdam, 168 p.

Breckon, C. E., 1988, Sedimentology and facies of the Pennsylvanian Jackfork Group in the Caddo Valley and DeGray Quadrangles, Clark County, Arkansas: Ph. D. dissertation, The University of Tulsa, 134 p.

Chamberlain, C. K., 1978, A Guidebook to the Trace Fossils and Paleoecology of the Ouachita Geosyncline, SEPM Guidebook, Tulsa Oklahoma, 68 p.

Cline, L. M., 1960, Stratigraphy of the Late Paleozoic rocks of the Ouachita Mountains, Oklahoma: Oklahoma Geological Survey Bulletin No. 85, 113 p.

Danielson, S. E., Hankinson, P. K., Kitchings, K. D., and A. Thompson, 1988, Provenance of the Jackfork Sandstone, Ouachita Mountains, Arkansas and eastern Oklahoma, *in* J. D. McFarland, ed., Arkansas Geological Commission, Contributions to the Geology of Arkansas Miscellaneous Publications, v. 3, No. 18-C, p. 95-112.

Dickerson, W. D., 1986, Sedimentology and petrology of the Hot Springs Sandstone (Lower Mississippian) of the Ouachita Mountains, Arkansas: Louisiana State University, Unpublished M. S. thesis, 151 p.

Ebanks, W. J., 1987, Flow unit concept - Integrated approach to reservoir description for engineering projects (abs.): Amer. Assoc. Petrol. Geol. Bull., v. 71, p. 551-552.

Goldstein, A.R., 1959, Petrography of the Paleozoic sandstones form the Ouachita Mountains of Oklahoma and Arkansas, *in* Cline, L. M., Hilseweck, W. J., and D. E. Feray, eds., The Geology of the Ouachita Mountains: A Symposium, Dallas Geological Society, p. 97-116.

Gordon, M., 1973, Correlation of the Carboniferous rocks of the Ouachita Geosyncline with those of the adjacent shelf: Geological Society of America Abstracts with Programs, v. 5, no. 3, p.259.

_____, and C. G. Stone, 1969, New evidence for dating Carboniferous flysch deposits of the Ouachita Geosyncline, Arkansas and Oklahoma: Amer. Assoc. Petrol. Geol. Bull., v. 53, p.719.

Houseknecht, D. W., and S. M. Matthews, 1985, Thermal maturity of Carboniferous strata, Ouachita Mountains: Amer. Assoc. Petrol. Geol. Bull., v. 69, p. 335-345.

Howe, D., 1989, Surface gamma-ray profiling technique applied to Cretaceous Ferron Sandstone, east-central Utah (abs.): Amer. Assoc. Petrol. Geol. Bull., v. 73, p. 365.

Klein, G., 1966, Dispersal and petrology of sandstones of the Stanley-Jackfork boundary, Ouachita fold belt, Arkansas and Oklahoma: Amer. Assoc. Petrol. Geol. Bull., v. 50, no. 2, p. 308-326.

Le Blanc, R. J., 1984, Lower Jackfork Sandstone at Dierks Lake Spillway, *in* Stone, C. G. and B. R. Haley, eds., A Guidebook to the Geology of the Central and Southern Ouachita Mountains, Arkansas: Arkansas Geological Commission Guidebook 84-2, p. 8-12.

Link, M. H., and M. T. Roberts, 1986, Pennsylvanian paleogeography for the Ozarks, Arkoma, and Ouachita basins in east-central Arkansas, *in* Stone, C.

G., and B. R. Haley, eds., Sedimentary and Igneous Rocks of the Ouachita Mountains of Arkansas: Arkansas Geological Commission, Guidebook, pt. 2, p. 37-60.

Link, M.H., and C. G. Stone, 1986a, Jackfork Sandstone at the abandoned Big Rock Quarry, North Little Rock, Arkansas, *in* Stone, C. G. and B. R. Haley, 1986, Sedimentary and Igneous Rocks of the Ouachita Mountains of Arkansas: Guidebook Geol. Soc. Amer. Ann. Mtg., San Antonio, p. 1-8.

Link, M. H. and C. G. Stone, 1986b, Jackfork Sandstone at I-430 roadcut in northwest Little Rock, *in* Stone, C. G., and B. R. Haley, eds., Sedimentary and Igneous Rocks of the Ouachita Mountains of Arkansas: Guidebook Geol. Soc. Amer. Ann. Mtg., San Antonio, p. 8-10.

Lock, B. E. and J. R. Fisco, 1979, Outer deep-sea fan depositional lobe sequence from the Jackfork Group of southern Arkansas (abs): Gulf Coast Assoc. Geol. Society Trans., v. 29, p. 281.

Loeblich, A., and H. Tappan, 1988, Foraminiferal Genera and Their Classification, Van Nostrand Reinhold Co., New York, 969 pp.

Lowe, D. R., 1976, Subaqueous liquified and fluidized sediment flows and their deposits: Sedimentology, v. 23, p. 285-308.

_____, 1982, Sediment gravity flows: II. Depositional models with special reference to the deposits of high-density turbidity currents: Journ. Sedimentary Petrology, v.52, p. 279-297.

_____, 1989, Submarine depositional processes and facies: Paleozoic sediments of the Ouachita Mountains, Arkansas and Oklahoma, *in* Lowe, D., Jordan, D., McGowen, J., D'Agostino, A., Handford C. R., Suchecki, R., and Slatt, R., eds., ARCO Deep-water Sandstone Field Trip Guidebook, Ouachita Mountains, Arkansas, April 1-2, 1989, 80 p.

McFarland, J. D., III, 1988, Turbidite exposures near DeGray Lake, southwestern Arkansas, Geol. Soc. Amer. Cent. Field Guide--South-Central Section, p. 173-275.

McKerrow, W. S., 1978, The Ecology of Fossils: The MIT Press, Cambridge Massachusetts, 384 p.

Middleton, G. V., 1966, Experiments on density and turbidity currents. I. Motion of the head: Canadian Jour. Earth Sci., v. 3, p. 523-546.

Middleton, G. V., 1967, Experiments on density and turbidity currents. III. Deposition of sediment: Canadian Jour. Earth Sci., v. 4, p. 475-505.

Middleton, G. W., and W. J. Neal, 1989, Experiments on the thickness of beds deposited by turbidity currents: Jour. Sed. Petrol., v. 59, p. 297-307.

Miller, M.E., 1985, The use of cathodoluminescence colors for interpreting the provenance of the Jackfork Sandstones, Arkansas: University of Cincinnati, Unpublished M.S. Thesis, 145 p.

Moiola, R. J., and G. Shanmugan, 1984, Submarine fan sedimentation, Ouachita Mountains, Arkansas and Oklahoma: Gulf Coast Assoc. Geol. Soc. Trans., v. 34, p. 175-182.

Morris, R. C., 1971, Stratigraphy and sedimentology of the Jackfork Group, Arkansas: Amer. Assoc. Petrol. Geol. Bull., v. 55, p. 387-402.

_____, 1973, Flysch facies of the Ouachita Trough--with examples from the spillway at DeGray Dam, Arkansas, *in* Stone, C.G., Haley, B.R., and G. W. Viele, eds., A guidebook to the geology of the Ouachita Mountains, Arkansas: Ark. Geol. Comm. Guidebook, p. 158-168.

_____, 1974, Sedimentary and tectonic history of the Ouachita Mountains, IN W. R. Dickinson, ed., Tectonics and Sedimentation: Soc. Econ. Paleontologists and Mineralogists, Spec. Pub., no. 22, p. 120-142.

_____, 1977, Flysch facies of the Ouachita Trough - with examples from the spillway at DeGray Dam, Arkansas, *in* C. G. Sloan, ed., Symposium on the Geology of the Ouachita Mountains: Arkansas Geol. Commission, v. 1, p. 158-169.

_____, Proctor, K. E., M. R. Kock, 1979, Petrology and diagenesis of deep-water sandstones, Ouachita Mountains, Arkansas and Oklahoma: Soc. Econ. Paleontologists and Mineralogists, Spec. Pub., no. 26, p. 263-279.

Mutti, E., 1985, Turbidite systems and their relations to depositional sequences, *in* G. G. Zuffa, ed., Provenance of Arenites: D. Reidel Publ. Co., Dordrecht, p. 65-93.

_____, and W. R. Normark, 1987, Comparing examples of modern and ancient turbidite systems: Problems and concepts, *in* Leggett, J. K. and G. G. Zuffa, eds., Marine Clastic Sedimentology: Concepts and Case Studies, p. 1-38.

Niem, A. R., 1976, Patterns of flysch deposition and deep-sea fans in the lower Stanley Group (Mississippian), Ouachita Mountains, Oklahoma and Arkansas: Sedimentary Petrology, v. 46, p. 633-646.

Owen, M. R., 1984, Sedimentary petrology and provenance of the Upper Jackfork Sandstone (Morrowan), Ouachita Mountains, Arkansas, USA: University of Illinois, Ph. D. Dissertation, 167 p.

_____, and A. V. Carozzi, 1986, Southern provenance of Upper Jackfork Sandstone, southern Ouachita Mountains: Cathodoluminescence petrology: Geol. Soc. Amer. Ann. Bulletin, v. 97, p. 110-115.

Potter, P. E., and A. E. Scheidegger, 1966, Bed thickness and grain size: graded beds: Sedimentology, v. 7, p. 233-240.

Provo, L. J., Kepferle, R. C., and P. E. Potter, 1977, Three Lick Bed: Useful stratigraphic marker in the Upper Devonian Shale in Eastern Kentucky: Energy Research and Development Administration, Morgantown Energy Research Center, CR-77-2, 56 p.

Rider, M. H., 1990, Gamma-ray log shape used as a facies indicator: critical analysis of an oversimplified methodology, *in* Hurst, A., Lovell, M. A., and A. C. Morton, eds., Geological Applications of Wireline Logs: Geol. Soc. Spec. Publ. 48, p. 27-37.

Sadler, P. M., 1982, Bed-thickness and grain size of turbidites: Sedimentology, v. 29, p. 37-51.

Selley, R. C., 1979, Dipmeter and log motifs in North Sea submarine-fan sands: Amer. Assoc. Petrol. Geol. Bull., v. 63, p. 905-917.

Shanmugam, G. and R. J. Moiola, 1988, Submarine fans: Characteristics, models, classification, and reservoir potential: Earth-Sci. Rev., v. 24, p. 383-428.

_____, and R. J. Moiola, 1991, Types of submarine fan lobes: Models and implications: Amer. Assoc. Petrol. Geol. Bull., v. 75, p. 156-179.

_____, Moiola, R. J., and J. K. Sales,1988, Duplex-like structures in submarine fan channels, Ouachita Mountains, Arkansas: Geology, v. 16, p. 229-232.

Slatt, R. M., Phillips, S., Boak, J. M., and M. B. Lagoe, in press, Scales of geological heterogeneity of a deep-water sand giant oil field, Long Beach Unit, Wilmington Field, California:

Appendix I

Worldwide sedimentary basins with hydrocarbon production from turbidite systems. Tables 3-8 and accompanying Figures 2, 4, and 6 from Weimer and Link (1991). Used with permission of the authors.

Table 3

North American Sedimentary Basins with Petroleum Production from Submarine Fans and Turbidite Systems

Basin	Age	Formation	Tectonic Setting	Field Name	References
CANADA					
Alberta	Devonian	_____	Craton (CDF)	_____(O)	Cook, 1983
Beaufort	Oligocene	Kugmallit Kopanoar	Passive	+Kopanoar (OG) Koakoak (OG) Tarsiut (OG)	Willumsen & Cote, 1982 Dixon et al., 1985
MEXICO					
Campeche	Paleocene	_____	Passive (CDF)	+Ixtoc (O)	Cook, 1983
Gulf Coast	Upper Cretaceous	Tamabra	Passive (CDF)	+Poza Rica (O)	Enos, 1985
Salinas	Lower Cretaceous	_____	Passive (CDF)	+Reforma (O)	Aguayo et al., 1985
Tampico-Misantlia	Eocene/ Paleocene	Chihontepec	Passive (SCF)	_____(O)	Busch & Govela, 1978
Vera Cruz	Miocene	_____	Foreland	Petronoverro (O)	Helu et al., 1977
TRINIDAD					
Paria	Miocene	Herrerva Nariva	Wrench	Barrackpore (O)	A. Salvador, pers. comm., 1988 Abelwhite & Higgins, 1968
UNITED STATES					
Anadarko	*Pennsylvanian	Tonkawa	Wrench/Rift	_____ (G)	Kumar & Slatt, 1984
		Medrano	Wrench/Rift	_____ (G)	Galloway et al., 1977

Appalachian	*Devonian	Bradford	Foreland	+Bradford (O) Sage Brush (O)	Dixon, 1972
Arkoma	*Pennsylvanian	Red Oak (Atoka)	Foreland	Red Oak (G)	Vedros & Fisher, 1978
				Wilburton (G)	Houseknecht, 1986
Eel River	Pliocene	Rio Dell	Forearc	Tompkins Hill (G) Table Bluff (G)(ABD)	Parker, 1988 COGF, 1982
Gulf Coast	*Pleistocene	_____	Passive	Garden Banks 72 (OG)	Kolb et al., 1989
	*Pliocene	_____	Passive	East Breaks 160 (OG) High Island A-537 (OG) Jolliet (O)	Braithwaite et al., 1988 Braithwaite et al., 1988 Prescott et al., 1988
	Miocene	_____	Passive	_____(OG)	Morton et al., 1988 Ventress & Smith, 1984
	Oligocene	Frio (Hackberry)	Passive (SCF)	_____(G)	Paine, 1971 Curtis & Echols, 1984 Ewing & Reed, 1984
	Eocene	Wilcox (Yoakum)	Passive (SCF) (SCT)	_____(G)	Berg, 1984; Galloway et al., this volume
				Yoakum (G)	Chuber, 1986
	Paleocene	Wilcox (La Vaca)	Passive (SCF)	_____(G)	Galloway et al., this volume
	Upper Cretaceous	Olmos	Passive	_____	Tyler & Ambrose, 1986
		Woodbine-Eagle Ford	Passive	_____(G)	Siemers, 1981
Los Angeles	*Pliocene	Pico Repetto	Wrench	Inglewood (O) +Wilmington (O) +Long Beach (O)	COGF, 1974 Yerkes et al., 1965 Conrey, 1967
	*Miocene	Puente	Wrench	+Wilmington (O) +Huntington Beach (O) Newport (O) +Santa Fe Springs (O)	Slatt et al., 1988 Gourley, 1975 Taylor, 1976 Redin, 1984

		Topanga(?)	Wrench	Inglewood (O) Wilmington (O)	COGF, 1974
	Jurassic	Catalina Schist	Subduction Zone	Playa Del Rey (O) El Segundo (O) Hyperion (O) Wilmington (O)	COGF, 1974
Marathon	Pennsylvanian	Tesnus	Foreland	Pinon (O)	Reed & Strickler, 1990
	Devonian (?) to Lower Miss.	Caballos	Foreland	McKay Creek (O) Thistle (O)	T. Reid, pers. comm., 1990
Ouachita	Pennsylvanian	Jackfork	Foreland	Hogeye Hollow (O)	R. Fay, pers. comm., 1990
	Mississippian	Stanley	Foreland	Reddin (O) Moyers (O) Gumbo (ASPH)	Suneson et al., 1990
	Ordovician	Big Fork Arkansas Novaculite	Passive (CH)	Potato Hill (G) Isom Springs (O)	Suneson et al., 1990
Palo Duro	Pennsylvanian	_____	Wrench (CDF)	Mayfield (O)	Crevello et al., 1985
Permian	Permian	Spraberry-Dean	Intracratonic	Ackerly (O) Jo-Mill (O)	Handford, 1981 Galloway et al., 1983 Guevara, 1988
		Bell Canyon	Intracratonic	Geraldine-Ford (O) Wheat (O)	Williamson, 1979 Galloway et al., 1983
		Bone Springs	Intracratonic (CDF)	Mescalero Escarpe (O)	Saller et al., 1989
	Pennsylvanian	Cisco	Intracratonic	Jameson (O) Flowers (O)	Galloway et al., 1983
Piceance	Upper Cretaceous	Mancos	Foreland	Rock Canyon (G)	Witherbee et al., 1983
Ridge	Miocene	Castaic	Wrench	Elizabeth Canyon (O) (ABD)	Stitt, 1987

Sacramento	*Eocene	Markley	Forearc (SCF, SCT)	+Rio Vista (G)	COGF, 1982
	*Paleocene	Meganos	Forearc (SCT)	East Island (G)	COGF, 1982
				South Orkney (G)	COGF, 1982
		Martinez	Forearc(SCF)	Marine Prairie (G)	Hacker, 1984
		Princeton	Forearc (SCT)	Corning, Greenwood (G) Perkins Lake (G)	
	*Upper Cretaceous	Winters	Forearc	Cache Creek (G) Winters (G) Union Island (G)	Williamson & Hill, 1981 Tillman et al., 1981
		Forbes	Forearc	Grimes, Arbuckle Willows-Beehive Bend (G)	Imperto & Nilsen, 1990
		Dobbins	Forearc	Willows-Beehive Bend (G)	COGF, 1982
		Guinda	Forearc	Willows-Beehive Bend (G)	COGF, 1982
Salinas-Santa Cruz	Miocene	Monterey "Sand"	Wrench	King City (O)	COGF, 1974
	Oligocene	San Lorenzo	Wrench	Moody Gulch (O) (ABD)	COGF, 1982
	Eocene	Butano	Wrench	La Honda (OG)	COGF, 1982
				Oil Creek (O)	COGF, 1982
San Joaquin	*Miocene	Stevens	Wrench	+Elk Hills (OG)	
		Republic		+Midway-Sunset (O)	COGF, 1985
		Webster	Wrench	+Buena Vista (O)	
		Moco T			
		Santa Magarita/ Potter			
	Oligocene	Temblor	Forearc	Asphalto, N. Belridge N. Antelope Hills (OG)	COGF, 1985
	Eocene	Tejon, Pt. Rocks,	Forearc	Cantua Creek, Pyramid Hills(OG)	COGF, 1985
		Gatchell (Cantua)		San Emigdio Creek (OG)	COGF, 1985
	Upper Cretaceous	Panoche, Moreno Blewett, Tracy	Forearc	Pyramid Hills (G)	COGF, 1985
Santa Maria	Pliocene	Pismo	Wrench	Arroyo Grande (O)	COGF, 1974
		Sisquoc		Cat Canyon (O)	
		Santa Margarita		Edna (O)	
	Miocene	Pt. Sal	Wrench	Lopez Canyon (O)	COGF, 1974
	Cretaceous-Jurassic	Knoxville	Subduction	_____(O)	COGF, 1974

Uinta	Paleocene	Green River	Intermontane	Altamont (O)	Fouch et al., 1990
Ventura	*Pleistocene	Pico	Wrench	+Ventura (O) Rincon (O)	COGF, 1974
	*Pliocene	Repetto Modelo	Wrench	Carpinteria (O) Dos Cuadras (O) San Miguelito (O) Pitas Point(G) Castaic Junction (O)	Hsu, 1977, Younse, 1988 Sylvester & Brown, 1988 Nelson et al., 1988 COGF, 1974
	*Miocene	Monterey Rincon Topanga	Wrench	Hondo (OG) S. Elwood (O) Sockeye (OG)	COGF, 1974 Rarey, 1988
	Eocene	Cozy Dell Matilija	Forearc Forearc	Cuarta (OG) Sacate, Pescado (G) Molino (G)	COGF, 1974 Taylor, 1976
	Upper Cretaceous	Chatsworth	Forearc	Horse Meadows (O) Mission (O)	Hall, 1981 Link et al., 1984
Washakie	Upper Cretaceous	Lewis	Foreland	_____(O)	McMillen & Winn, this volume
Western Overthrust, Nevada	Mississi-ppian - Devonian	Diamond Peak	Foreland	Pine Valley (O)	T. Nilsen, pers. comm., 1990

ABBREVIATIONS:

* Ages of Large Turbidite Reservoirs in Basin
(O) Mainly Oil Production
(OG) Both Oil and Gas Production
(G) Mainly Gas Production
(CDF) Carbonate Debris Flows
+ Large Reserves - Estimated to be 500 MMBO Recoverable or Equivalent Gas Reserves
(ABD) Abandoned Oil or Gas Field
(SCF) Submarine Canyon Fill Reservoir
(SCT) Submarine Canyon Truncation Trap
(RCD) Resedimented Chalk Deposits
(ASPH) Asphalite deposits
(CH) Resedimented chert
(COGF) California Oil and Gas Fields (reference)
_____ Not Known

ACKNOWLEDGMENTS: J. Armentrout, B. Berman, R. Fay, T. Fouch, W. Galloway, R. Haupt, B. Macurda, A. Morrissey, T. Nilsen, T. Reed, T. Reid, A. Salvador, C. Stone, R. Walker, R. Weimer, B. Welton, and J. Welton

Table 4
South American Sedimentary Basins with Petroleum Production from Submarine Fans and Turbidite Systems

Basin	Age	Formation	Tectonic Setting	Field Name	References
BRAZIL					
Barreirinhas	Cretaceous	Bom Gosto	Wrench	Sao Joao (OG)	Bruhn et al., 1988
Campos	Miocene	Campos	Passive	Albacora (O)	Souza et al., 1989
	*Oligocene	Campos	Passive	+Albacora (O) +Marlim (O)	Carminatti & Scarton, this volume
			(SCF)	Moreia (O)	Bruhn & Moraes, 1988b
	*Eocene	Campos	Passive (SCT) (SCT)	Albacora (O) Bicudo (O) Bonito (O) Enchova (O Vermelho (O)	Souza et al., 1989 Peres & Arso, 1986 Peres & Arso, 1986 Bruhn & Moraes, 1988b
	*Upper Cretaceous	Campos	Passive	Albacora (O) Carapeba (O) Namarodo (O)	Souza et al., 1989 Bruhn & Moraes, 1988b Bacoccolli et al., 1980
Ceara	Upper Cretaceous	Urbarana	Passive	Espada (O)	Ojeda, 1982
Espirito Santo	Eocene	Urucutuca	Passive	Lagoa Parda (O)	Bruhn & Moraes, 1989
	Upper Cretaceous	Urucutuca	Passive	Fazenda Queimadas (O)	Bruhn & Moraes, 1988b
		Urucutura	Passive	Fazenda Cedro (O)	Rangel, 1984 Lindseth & Beraldo, 1985

Table 5

African Sedimentary Basins with Petroleum Production from Submarine Fans and Turbidite Systems

Basin	Age	Formation	Tectonic Setting	Field Name	References
ANGOLA					
Cuanza	Lower Cretaceous	_____	Rift (lacustrine)	_____(O)	T. McHargue, pers., comm., 1988
CAMEROON					
Cameroon	Lower Tertiary - Upper Cretaceous	Passive	Passive (SCT)	Sanaga Sud (O)	Pauken, 1990
EGYPT					
Gulf of Suez	Miocene	Rudeis	Rift	Ramadan (O)	Brown, 1980
GABON					
Gabon	Upper Cretaceous	Batanga	Passive	Barbier (O) Grondin(O) Mandaros (O)	D. Boote, pers. comm., 1988 Vidal, 1980 Dailly, 1982
		NTchengue	Passive	Anguille (O) Topile (O)	D. Boote, pers. comm., 1988
	Lower Cretaceous	_____	Rift (lacustrine)	_____(O)	Brice, 1982
ISRAEL					
Sinai	Lower Cretaceous	_____	Passive (SCF)	Helez (O)	Cohen, 1976

IVORY COAST					
Ivory Coast	Upper Cretaceous	_____	Passive	Belier (O)	Clifford, 1986
MOROCCO					
Rharb	Miocene	Rharb-Prerif Guadalquivir	Foreland	Haricha (G)	W. Ziegler, pers. comm., 1990
NIGERIA					
Niger Delta	*Pliocene	Agbada	Passive (intra-slope basins)	_____(OG)	Damuth & Link, 1987
	*Miocene	Agbada	Passive (intra-slope basins)	_____(OG)	Damuth & Link, 1987

ABBREVIATIONS:
* Ages of Large Turbidite Reservoirs in Basin
(O) Mainly Oil Production
(OG) Both Oil and Gas Production
(G) Mainly Gas Production
+Large Reserves - estimated to be 500 MMBO Recoverable or Equivalent Gas Reserves
(SCT) Submarine Canyon Truncation Trap
_____ Not Known

ACKNOWLEDGMENTS: D. R. D. Boote, L. F. Brown, T. McHargue, R. M. Mitchum, Jr., M. O. Withjack, and W. Ziegler

Potiguar	Upper Cretaceous	Ubarana	Passive	Agulha (O)	Ojeda, 1982
	Lower Cretaceous	Pendencia	Syn-rift (lacustrine)	Upanema (O)	Bruhn & Moraes, 1988a
Reconcavo	Lower Cretaceous	Candeias	Syn-rift (lacustrine)	Riacho de Barra (O)	Bruhn et al., 1985
		Marfim	Syn-rift (lacustrine)	Jacupe (G)	Bruhn et al., 1988
		Salvador	Syn-rift (lacustrine)	Aratu (G)	Bruhn & Moraes, 1988b
		Taquipe	Syn-rift (lacustrine)	Cassarongongo (O)	Bruhn & Moraes, 1988b
Santos	Upper Cretaceous	Itajai	Passive	Merluza (G)	Szatmari et al., 1985
Sergipe-Alagoas	Oligocene	Piacabucu	Passive	Dourado (O)	Morelli, 1989
	Eocene	Piaçubucu	Passive	Guaricema (O)	Morelli, 1989
		Dolwado			Szatmari et al., 1985
	Lower Cretaceous	Coqueiro Seco	Syn-rift (lacustrine)	_____ (O)	Figueiredo, 1981
ECUADOR					
Guayaquil	Miocene	_____	Forearc	_____(G)	M. Quinones, pers. comm., 1990
	Paleocene-Eocene	Estancia/ Chanduy	Forearc	Ancon (O)	Morales, 1983
PERU					
Talara	Paleocene-Eocene	Lutitas Talara	Forearc	Talara (O)	Munoz, 1980
VENEZUELA					
Paria	Miocene	_____	Wrench	_____ (O)	A. Shultz, pers. comm., 1990

ABBREVIATIONS

* Ages of Large Turbidite Reservoirs in Basin
(O) Mainly Oil Production
(OG) Both Oil and Gas Production
(G) Mainly Gas Production
+ Large Reserves - Estimated to be 500 MMBO Recoverable or Equivalent Gas Reserves
(SCF) Submarine Canyon Fill Reservoir
(SCT) Submarine Canyon Erosion Trap
_____ Not Known

ACKNOWLEDGMENTS: C. Bruhn, M. George, P. Guimaraes, W. Peres, M. Quinones, A. Schultz, and W. Ziegler

---

Table 6

European Sedimentary Basins with Petroleum Production from Submarine Fans and Turbidite Systems

Basin	Age	Formation	Tectonic Setting	Field Name	References
AUSTRIA - CZECHOSLOVAKIA - SWITZERLAND					
Molasse	Miocene	_____	Foreland	_____(G)	Moiola & Malzer, 1982
	Oligocene	Puchkirchen	Foreland	_____(G)	Robinson & Zimmer, 1989
Vienna	Miocene	_____	Wrench	_____	Harding & Tuminas, 1989
	Eocene	_____	Foreland	_____	Harding & Tuminas, 1989
FRANCE					
Aquitaine	Lower Cretaceous	Cazaux	Passive	Cazaux (O)	Institut Francais du Petrol, 1986
HUNGARY					
Pannonian	Pliocene	_____	Foreland-wrench (lacustrine)	Kunmadaras (G)	W. Abbott, pers. comm., 1989
	upper Miocene	_____	Foreland-wrench	Hajouszoboszlo (G) Nadudvar (G)	W. Abbott, pers. comm., 1989
ITALY					
Ionian	middle-upper Miocene	Santa Nicola Hera-Lacinia	Foreland	Luna (O)	F. Fonnesu, pers. comm., 1988
North Adriatic	Pleistocene	Sabbie di Asti	Foreland	Barbara (G)	F. Fonnesu, pers. comm., 1988
	upper Pliocene	Porto Garibaldi	Foreland	Porto (G) Garibaldi (G)	F. Fonnesu, pers. comm., 1988
	lower	Porto Corsini	Foreland	Porto (G)	F. Fonnesu, pers.

	Pliocene			Corsini (G)	comm., 1988
	Miocene	_____	Foreland	_____(G)	Pierri, 1983
South Adriatic	upper Pliocene	_____	Foreland	Torrente (G) Tona (G)	F. Fonnesu, pers. comm., 1988
	lower upper Pliocene	Ascoli Satriano	Foreland	Paliono (G)	F. Fonnesu, pers. comm., 1988
		Candela	Foreland	Candela (G)	Casnedi, 1988
	lower Pliocene	Cellino	Foreland	Cellino (O)	Casnedi, 1983
	Upper Cretaceous	Scaglia	Foreland	Emilio (O) David (O)	F. Fonnesu, pers. comm., 1988
Po	upper Miocene	Marnoso-Arenacea	Foreland	Corte-Maggiore (OG)	F. Fonnesu, pers. comm., 1988
	Miocene	_____	Foreland	_____	Rizzini & Angelari, 1987
SOVIET UNION - POLAND					
Carpathian	Miocene	Menelit	Foreland	Dolina (O)	J. Clarke & G. Ulmishek, pers. comm., 1990
UNITED KINGDOM - NORWAY					
Central Graben	*Eocene	_____	Post-rift sag	+Montrose (O) Maureen (O) Cod (G) Josephine (O) +Alba (O)	Fowler, 1975 Carmen & Young, 1981 Winter et al., 1989
	*Paleocene	Andrew	Post-rift sag	+Forties (O) Andrew (O) Gamma (G) Gryphon (G)	Kulpecz & van Guens, 1990 Walmsley, 1975 Bowman et al., in press Pegrum & Jones, 1984 _____
		Ekofisk	Post-rift sag (RCD)	+Ekofisk (G)	Schatzinger et al., 1985
	Upper Cretaceous	Tor	Post-rift sag	+West Ekofisk (G)	D'Heur, 1984

Viking Graben	Oligocene	_____	Post-rift sag	_____	K. Glennie, 1989, pers. comm.
	*Eocene	_____	Post-rift sag	+Frigg (G) NE Frigg (G) Odin (G)	Heritier et al., 1979 McGovney & Radovich, 1985
	*Paleocene	_____	Post-rift sag	Balder (O) +Beryl (O) Heimdal (G)	Sarg & Skjold, 1982
	*Lower Cretaceous/ Upper Jurassic	Brae	Syn-rift	N. & S. Brae (O) Thelma (O) Toni (O) Tiffany (O)	Stow, 1985
		Miller	Syn-rift	Miller (O)	Bowman et al., in press
		Magnus	Syn-rift	+ Magnus (O)	De'Ath & Schuyleman, 1981
Witch Ground Graben (Moray Firth)	Lower Cretaceous	Scapa	Syn-rift	Scapa (O)	Boote & Gustav, 1987
				N. Claymore (O)	Harker, 1988
	*Upper Jurassic	Claymore	Syn-rift	+Claymore (O)	Maher & Harker, 1987
			Syn-rift	Tartan (O) Highlander (O) Galley (O) Chanter (O)	Harker et al., 1987 R. Schmitt, pers. comm., 1990

ABBREVIATIONS:

* Ages of Large Turbidite Reservoirs in Basin
(O) Mainly Oil Production
(OG) Both Oil and Gas Production
(G) Mainly Gas Production
+Large Reserves - Estimated to be 500 MMBO Recoverable or Equivalent Gas Reserves
(SCF) Submarine Canyon Fill Reservoir
(SCT) Submarine Canyon Truncation Trap
(RCD) Resedimented Chalk Deposits
_____ Not Known

ACKNOWLEDGMENTS: W. A. Abbott, D. R. D. Boote, J. Clarke, M. Cope, F. Fonnesu, T. Fouch, K. Glennie, P. Homewood, H. G. Oesterle, M. Richards, R. Schmitt, G. Ulmishek, and W. Zieglar

Table 7

Asian Sedimentary Basins with Petroleum Production from Submarine Fans and Turbidite Systems

Basin	Age	Formation	Tectonic Setting	Field Name	References
CHINA					
Bohai (Gulf)	*Oligocene	Shahejie	Syn-rift (lacustrine)	Yihez huang (O) Miyana	J. Zeng, pers. comm., 1990
East China Sea	Oligocene-Eocene	_____	Syn-rift (lacustrine)	_____(O)	Li, 1990 G. Ulmishek, pers. comm., 1990
Huabei	*Oligocene	Shahejie	Syn-rift (lacustrine)	Yihez huang (O) Miyana	X. Zhang, pers. comm., 1988
Subei (South China Sea)	*Oligocene	_____	Syn-rift (lacustrine)	_____ (O)	X. Zhang, pers. comm., 1988
	Jurassic-Cretaceous	_____	Syn-rift (lacustrine)	_____(O)	X. Zhang, pers. comm., 1988
Tsaidam (Daidam) (Chaidamu)	Pliocene-Oligocene	_____	Foreland (lacustrine)	Fhizigou (O)	G. Ulmishek, pers. comm., 1990
INDONESIA					
North Sumatra	Miocene	Bessitang	Wrench	Palu Tabuhan Barat (O)	H. Oesterle, pers. comm., 1988
IRAN-OMAN-TURKEY					
Zagros	Tertiary-Cretaceous	_____	Foreland	_____ (O)	T. Nilsen, pers. comm., 1990

KOREA					
Gyeongsang Tertiary		_____	Post-rift (lacustrine)	_____	T. Fouch, pers. comm., 1990
	Cretaceous	_____	Syn-rift (lacustrine)	_____	Choi, 1986
JAPAN					
Akita	Pliocene	Tentokuji	Backarc	Sarakawa (O)	K. Aoyagi, pers. comm., 1988
	Miocene	Onnagawa	Backarc	Toyokawa (O) Yabase (O) Michikawa (O)	Aoyagi & Iijima, 1983 Aoyagi, 1985
MALAYSIA-SABAH					
Malay	Pliocene-Miocene	_____	Wrench	_____	Whittle & Short, 1978
Brunei-Sabah	Miocene	_____	Wrench	Tembungo (O)	Level & Kasumajaya, 1985
PHILLIPINES					
Palawan North	Miocene	Galoc	Post-rift	Galoc (O)	Saldivar-Sali et al., 1981 Link & Helmold, 1988
		St. Paul	Post-rift (CDF)	Nido A & B (O)	Lighty et al., 1983 Longman, 1985
SOVIET UNION					
Caspian North	Permian	_____	Foreland?	Kenkiyak (O)	G. Ulmishek, pers. comm., 1990
Caucasus North	Miocene-Oligocene	Maykop	Foreland	Khadyzh-inskaya(O)	Levorsen, 1967
Kura	Pliocene	Productive	Foreland	+Neftyanye kamni (O)	J. Clarke & G. Ulmishek, pers. comm., 1990

Volga-Ural	Missis-sippian - Devonian	Malinov	Intracratonic	+Mukhan-ouskoye(O)	G. Ulmishek, pers. comm., 1990
West Siberia	Cretaceous	Neocomian	Intracratonic	+Samatlor (O)	J. Clarke, G. Ulmishek, pers. comm., 1990
		Achimov		_____	G. Ulmishek, pers. comm., 1990
SYRIA					
Gazientap	Lower Cretaceous	Rutbach	Wrench	_____	Lovelock, 1984
TAIWAN					
Taiwan	Oligocene	_____	Wrench	_____ (O)	T. Lee, pers. comm., 1990
YEMEN					
Yemen	Jurassic	_____	Syn-rift	_____	Maycock, 1988

ABBREVIATIONS:
* Ages of Large Turbidite Reservoirs in Basin
(O) Mainly Oil Production
(OG) Both Oil and Gas Production
(G) Mainly Gas Production
(CDF) Carbonate Debris Flows
+ Large Reserves - estimated to be 500 MMBO recoverable or equivalent gas reserves
_____ Not Known

ACKNOWLEDGMENTS: K. Aoyagi, D. R. D. Boote, M. Bourque, J. Clarke, T. Fouch, T. Lee, T. Nilsen, H. G. Oesterle, G. Ulmishek, J. Zeng, & X. Zhang

Table 8

Australian and New Zealand Sedimentary Basins with Petroleum Production from Submarine Fans and Turbidite Systems

Basin	Age	Formation	Tectonic Setting	Field Name	References
AUSTRALIA					
Dampier	Lower Cretaceous	Mardie	Passive	Rosily	Hocking et al., 1988
		Flag	Passive	Harriett (O)	Kopsen & McGann, 1985; Osbourne & Howell, 1987; Boote & Kirk, 1989
		Malouet	Passive		Eriyagama et al., 1988
	Upper Jurassic	Dupuy	Rift	Barrow (O)	Woodside Offshore Petroleum, 1988
		Biggada	Rift		Woodside Offshore Petroleum, 1988
Gippsland	*Eocene	_____	Passive (SCT)	Halibut (O)	Esso Australia, 1988
	*Paleocene	_____	Passive (SCT)	Mackerel (O)	Brown, 1986
	Lower Cretaceous	_____	Passive (SCT)	Hapuku (O)	Esso Australia, 1988
NEW ZEALAND					
Taranaki	Miocene	Mokau	Passive	Mokau	W. Loomis, pers. comm., 1990
	Oligocene	Tangaroa	Passive	_____	Gresko et al., 1990

ABBREVIATIONS:
* Ages of Large Turbidite Reservoirs in Basin
(O) Mainly Oil Production
(OG) Both Oil and Gas Production
(G) Mainly Gas Production
(CDF) Carbonate Debris Flows
+ Large Reserves - Estimated to be 500 MMBO
Recoverable or Equivalent Gas Reserves
(SCT) Submarine Canyon Truncation Trap
_____ Not Known

ACKNOWLEDGMENTS: D. R. D. Boote, D. G. Jordan, W. Loomis, and B. Macurda

---

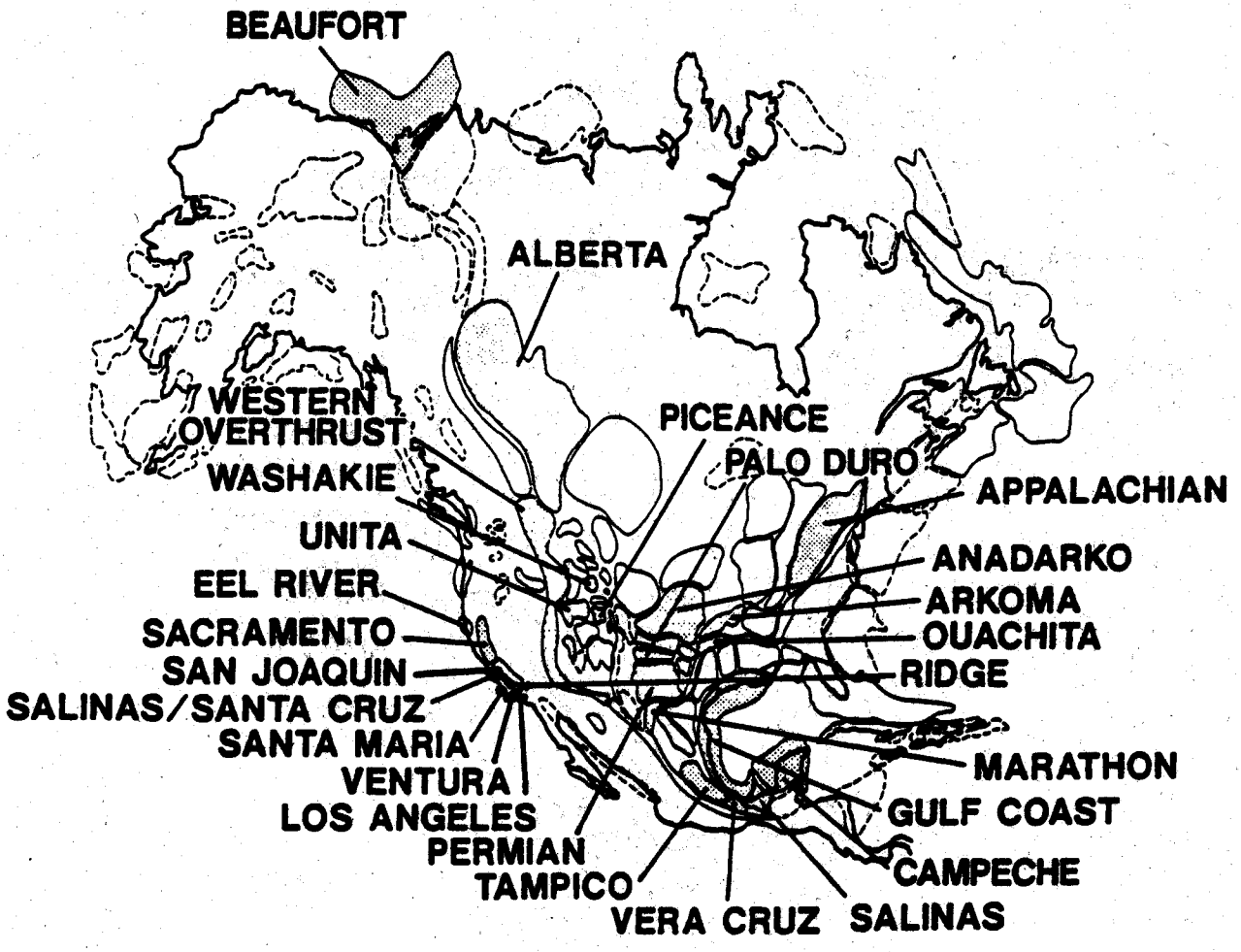

Figure 2. North American sedimentary basins showing: (a) petroleum productive basins with turbidite fields (dotted infill pattern), (b) petroleum productive basins (solid line), and (c) non-petroleum productive basins (dashed line). Base map after St. John (1984).

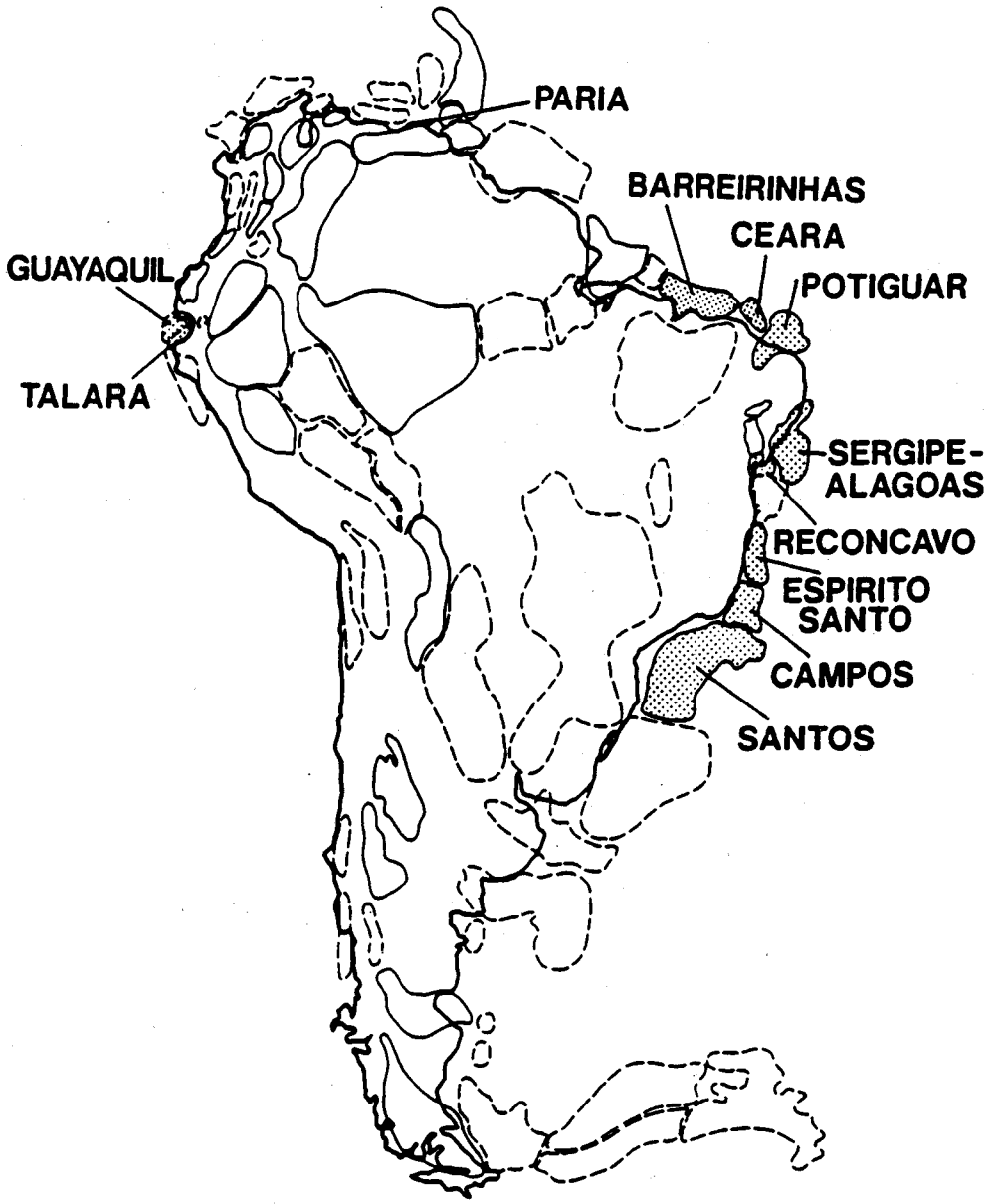

Figure 3. South American sedimentary basins showing: (a) petroleum productive basins with turbidite fields (dotted infill pattern), (b) petroleum productive basins (solid line), and (c) non-petroleum productive basins (dashed line). Base map after St. John (1984).

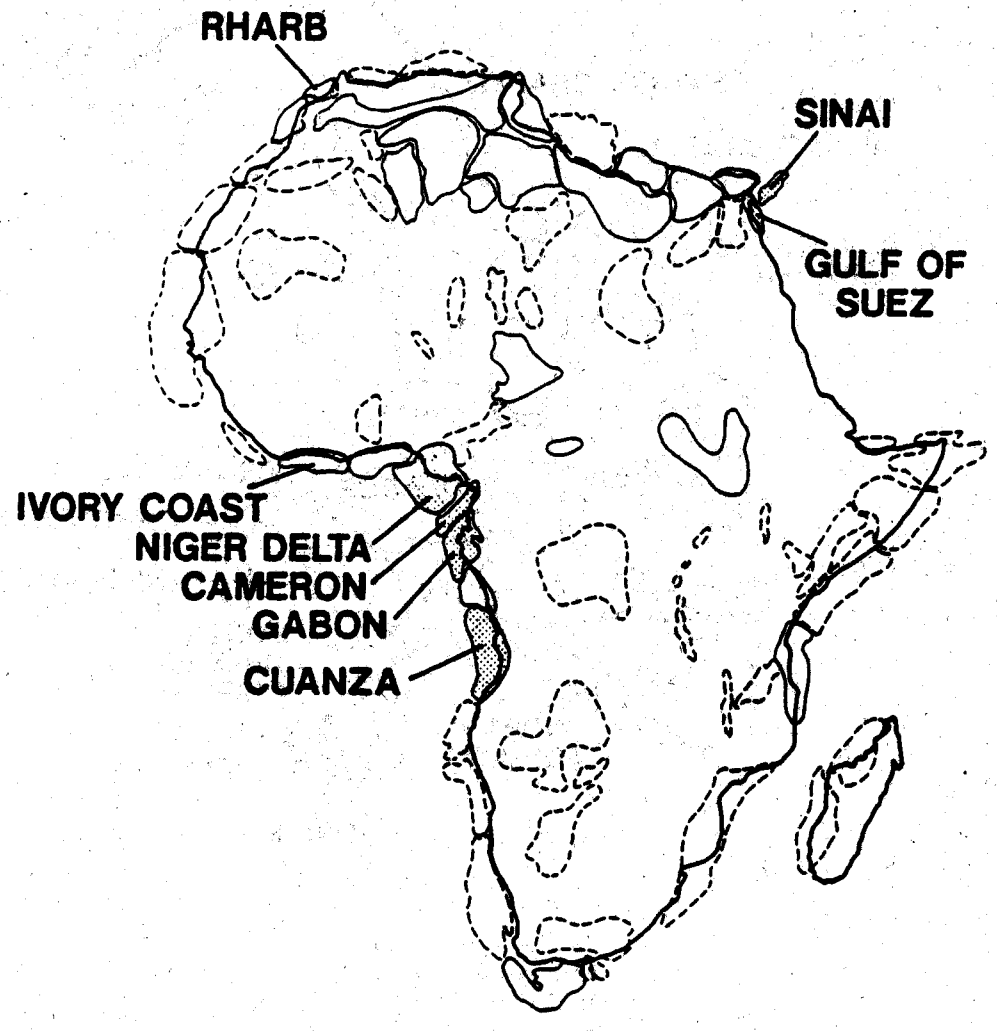

Figure 4. African sedimentary basins showing: (a) petroleum productive basins with turbidite fields (dotted infill pattern), (b) petroleum productive basins (solid line), and (c) non- petroleum productive basins (dashed line). Base map after St. John (1984).

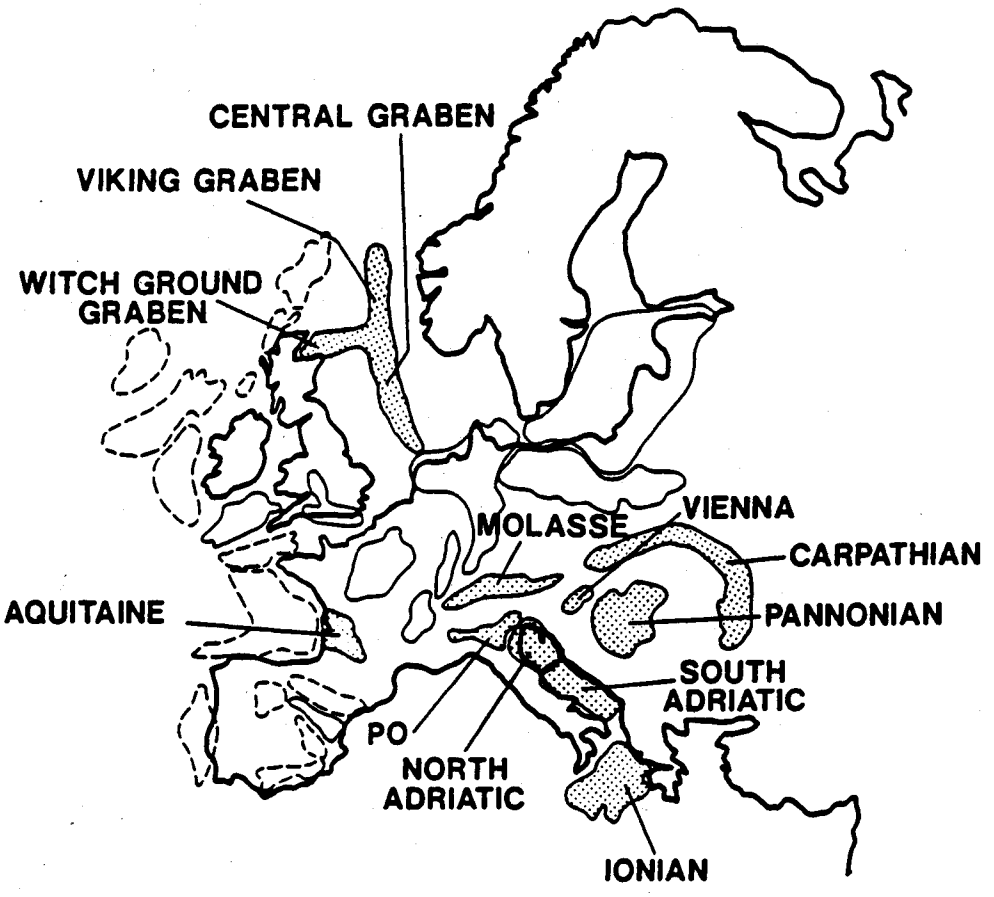

Figure 5. European sedimentary basins showing: (a) petroleum productive basins with turbidite fields (dotted infill pattern), (b) petroleum productive basins (solid line), and (c) non- petroleum productive basins (dashed line). Base map after St. John (1984).

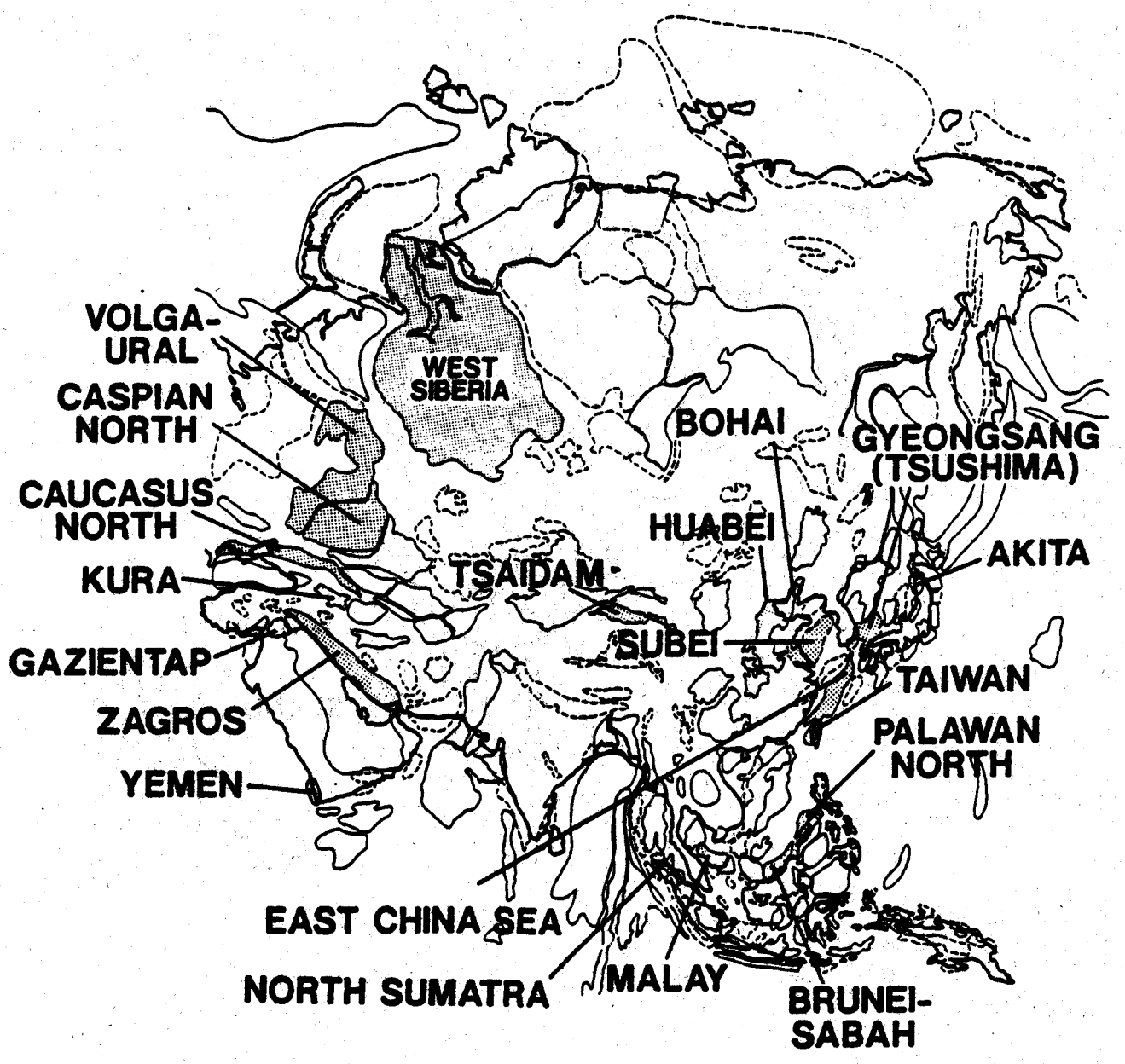

Figure 6. Asian sedimentary basins showing: (a) petroleum productive basins with turbidite fields (dotted infill pattern), (b) petroleum productive basins (solid line), and (c) non-petroleum productive basins (dashed line). Base map after St. John (1984).

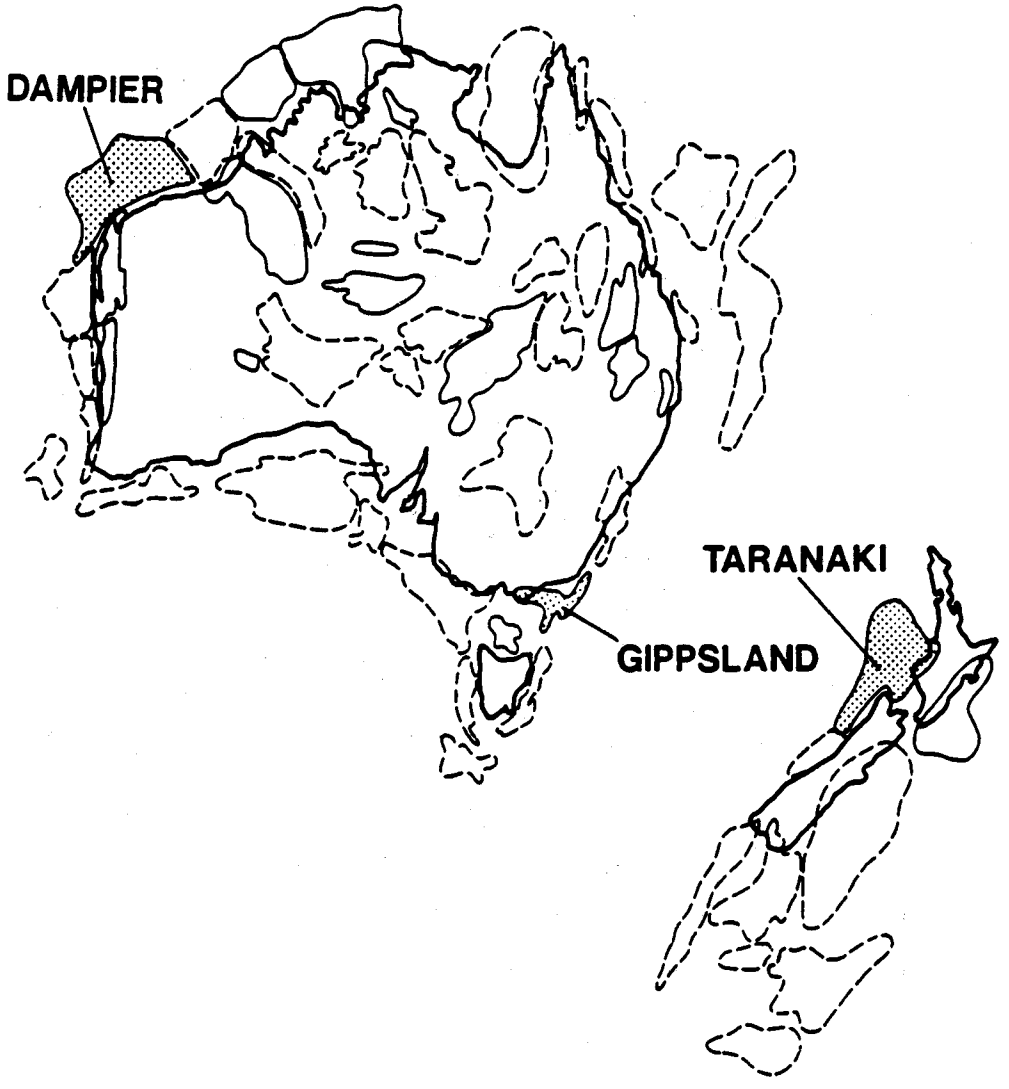

Figure 7. Australian and New Zealand sedimentary basins showing: (a) petroleum productive basins with turbidite fields (dotted infill pattern), (b) petroleum productive basins (solid line), and (c) non-petroleum productive basins (dashed line). Base map after St. John (1984).

Appendix II

Spreadsheets of petrographic data from 59 samples from DeGray Lake and Dierks Lake spillway exposures.

Captions for Appendix Figures:

II-A. Cross-plot of Mean Grain Size versus Quartz Cement Percent. There is a general trend, with some scatter, indicating coarser-grained sandstones have a higher content of quartz cement.

II-B. Cross-plot of Mean Grain Size versus Total Porosity Percent. There is a clear trend, with some scatter, that very fine and lower fine grained sandstones possess the highest porosity in the population of samples.

II-C. Cross-plot of Mean Grain Size versus Normalized Lithic Percent. There is a clear trend that shows that finer grained samples are richer in lithic fragments.

II-D. Cross-plot of Normalized Lithic Fragment Percent versus Total Porosity Percent. Although there are two populations of samples, there is a clear trend that the most porous rocks are limited to a lithic content of 6%-16%.

II-E. Cross-plot of Normalized Matrix Percent versus Total Porosity Percent. Although there are two populations of samples, there is a clear trend that the most porous rocks are for the most part limited to a matrix content of 5%-15%.

II-F. Cross-plot of Mean Grain Size versus Standard Deviation. There is a general trend, with some scatter, indicating an increase in grain size leads to an increase in the standard deviation.

II-G. Cross-plot of Total Porosity versus Standard Deviation.

II-H. Ternary plot of Quartz-Feldspar-Lithic Fragments (Q-F-L) normalized percentages for all samples from DeGray East, West, and Dierks West. All samples cluster above the 82% quartz line and to the right of the 8% feldspar line. Lithic content shows the greatest variability, with possibly a slight trend to enrichment in lithics at DeGray relative to Dierks. Chert is counted with other lithic fragments, not added to quartz.

II-I. Ternary plot of Plutonic-Metamorphic-Volcanic (P-M-V) rock fragment normalized percentages for all samples from DeGray East, West, and Dierks West. There is variation along the P-M axis and an clear trend towards the V pole at DeGray with a near-total absence of volcanic rock fragments at Dierks West.

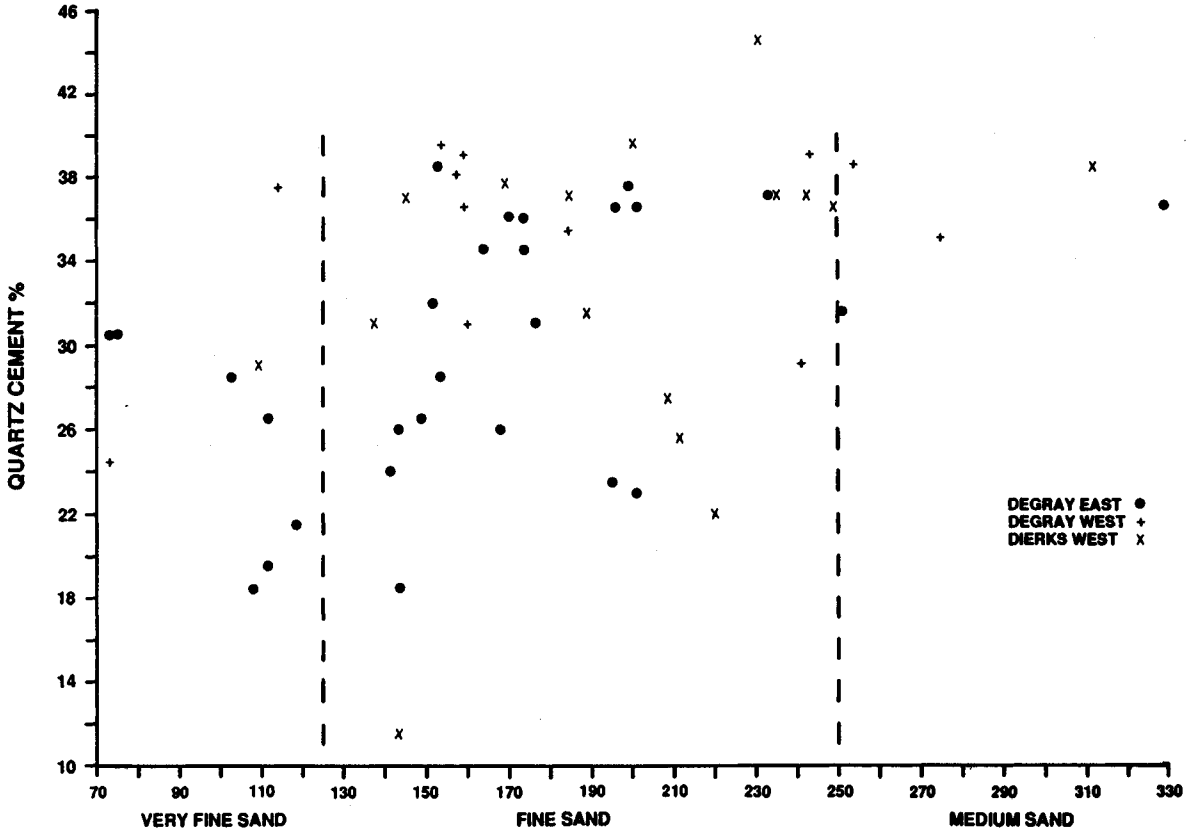

APPENDIX FIGURE II-A

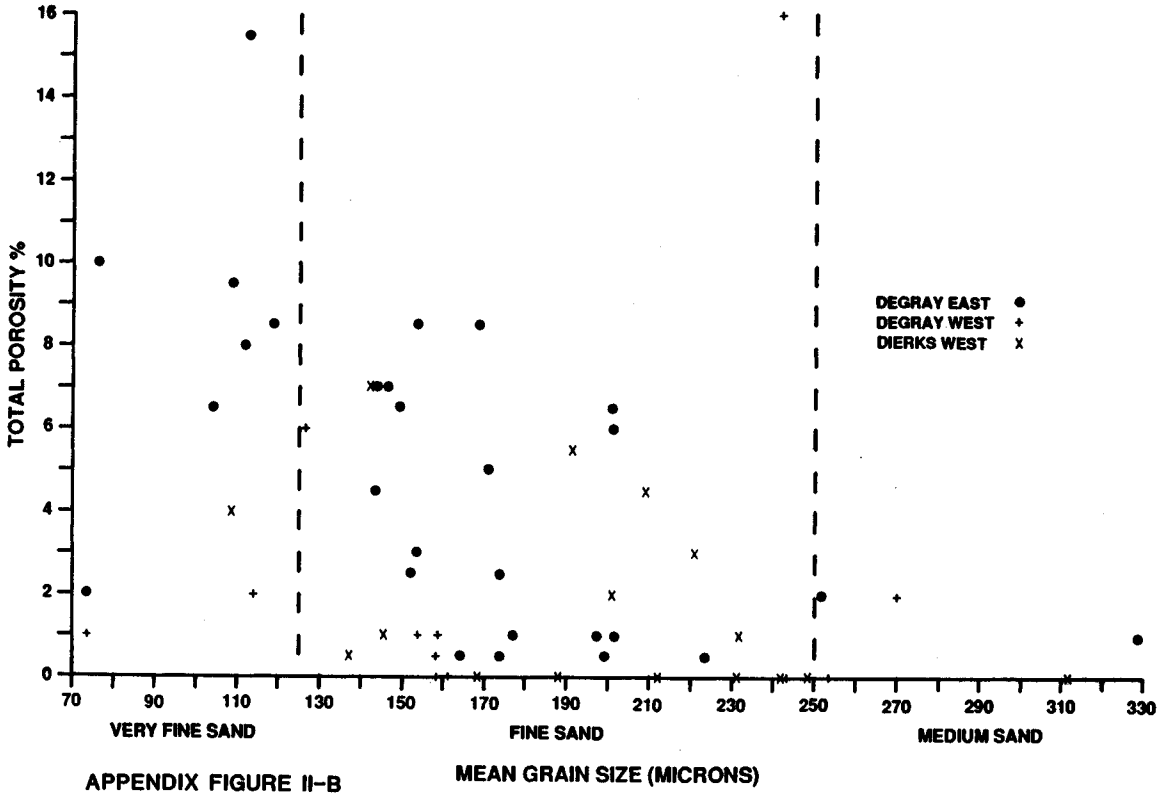

APPENDIX FIGURE II-B

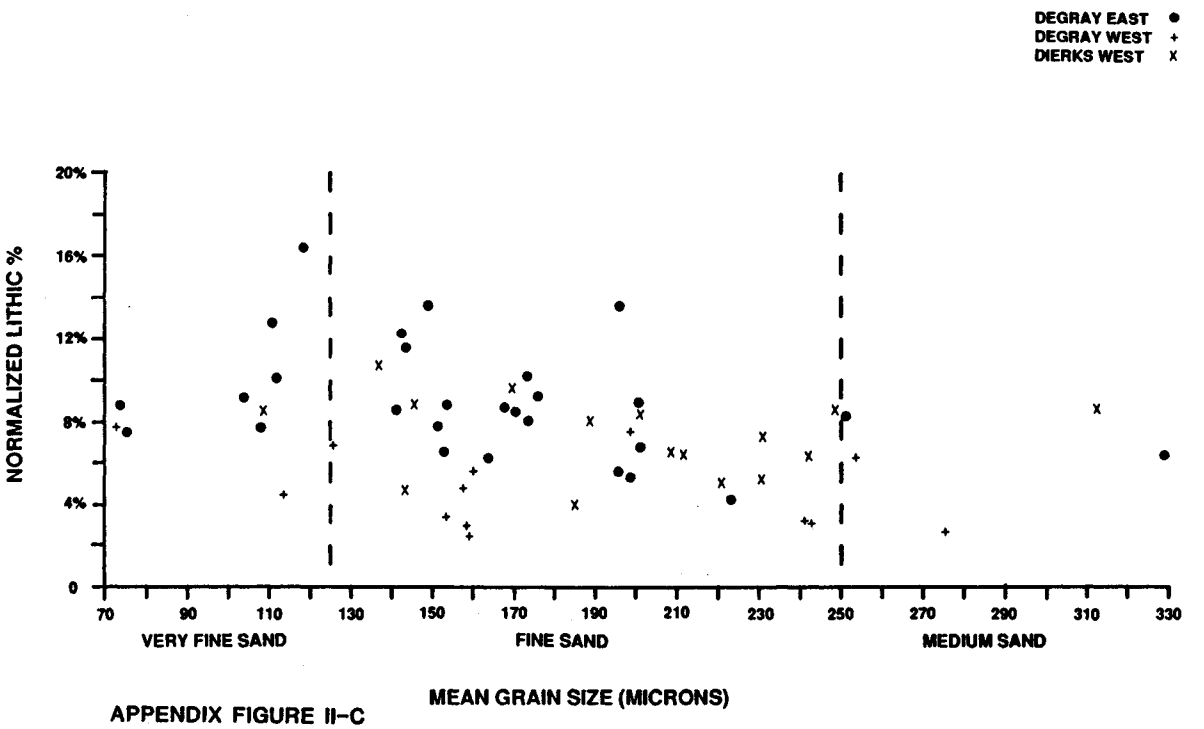

APPENDIX FIGURE II-C

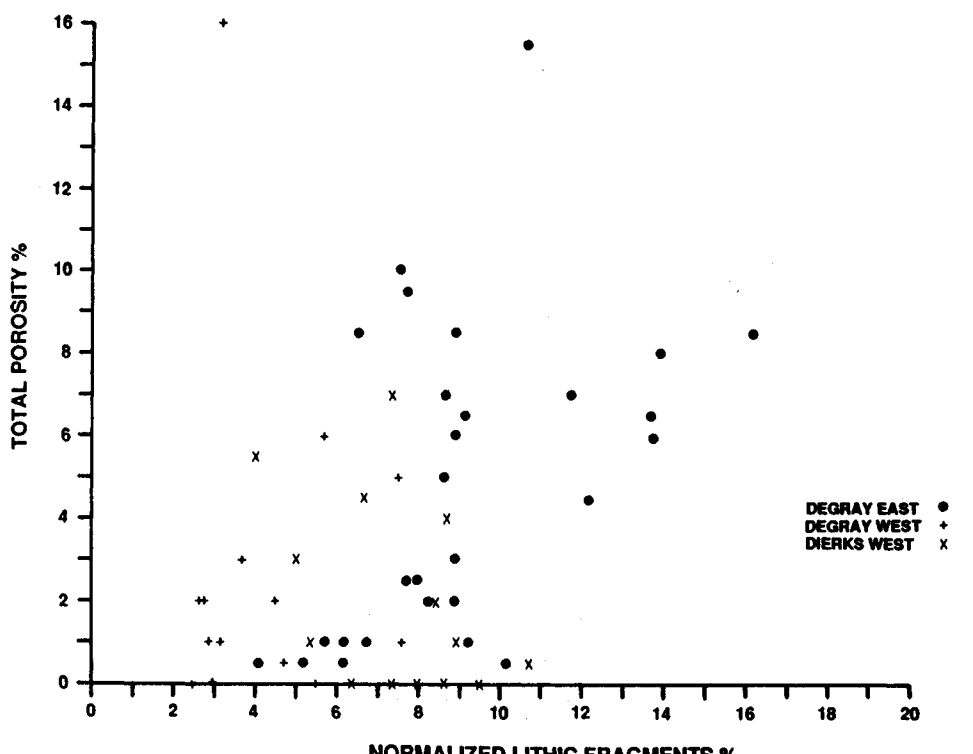

APPENDIX FIGURE II-D

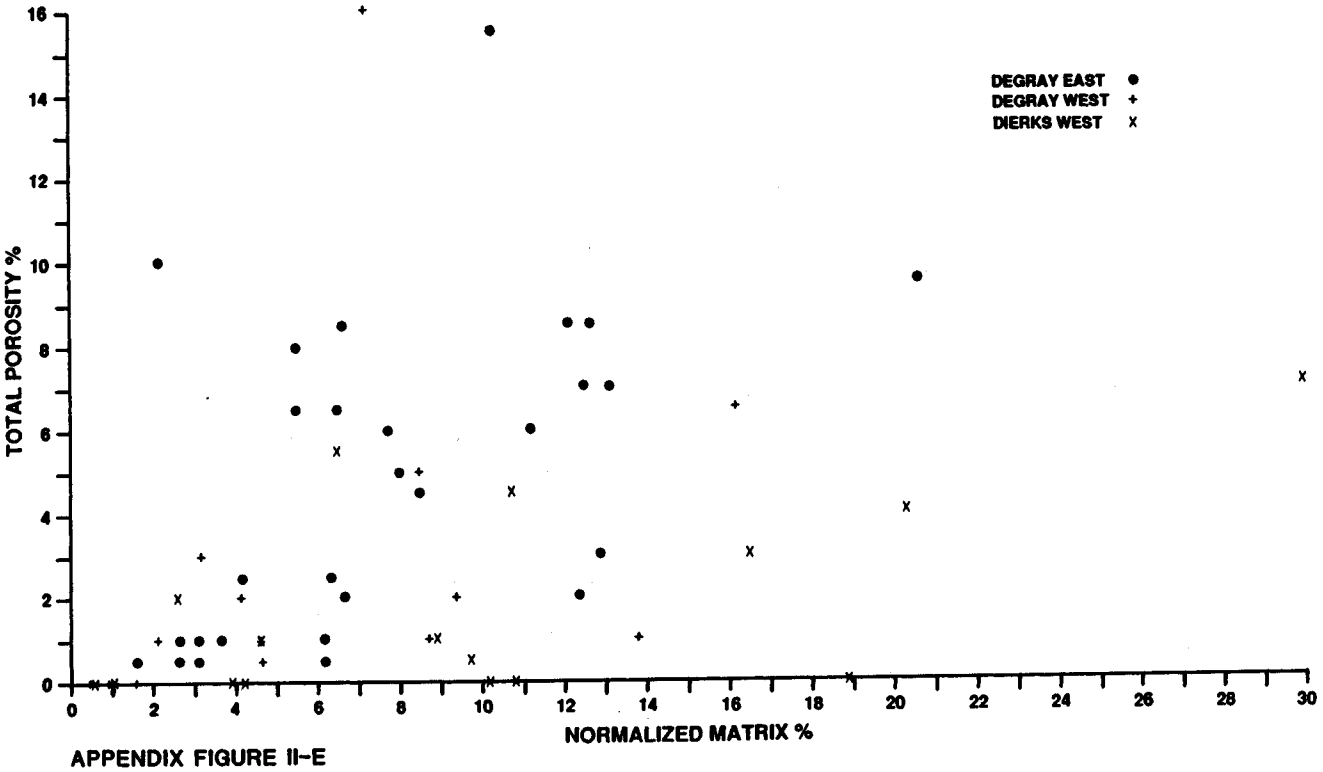

APPENDIX FIGURE II-E

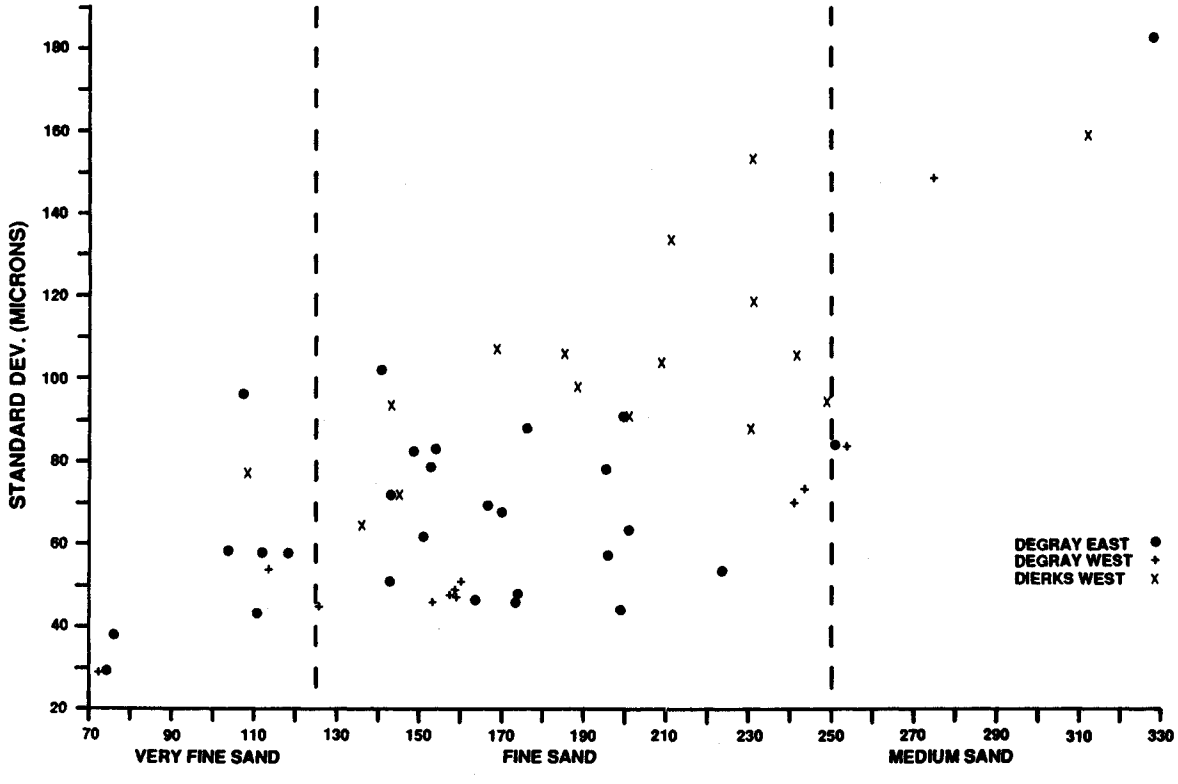

APPENDIX FIGURE II-F

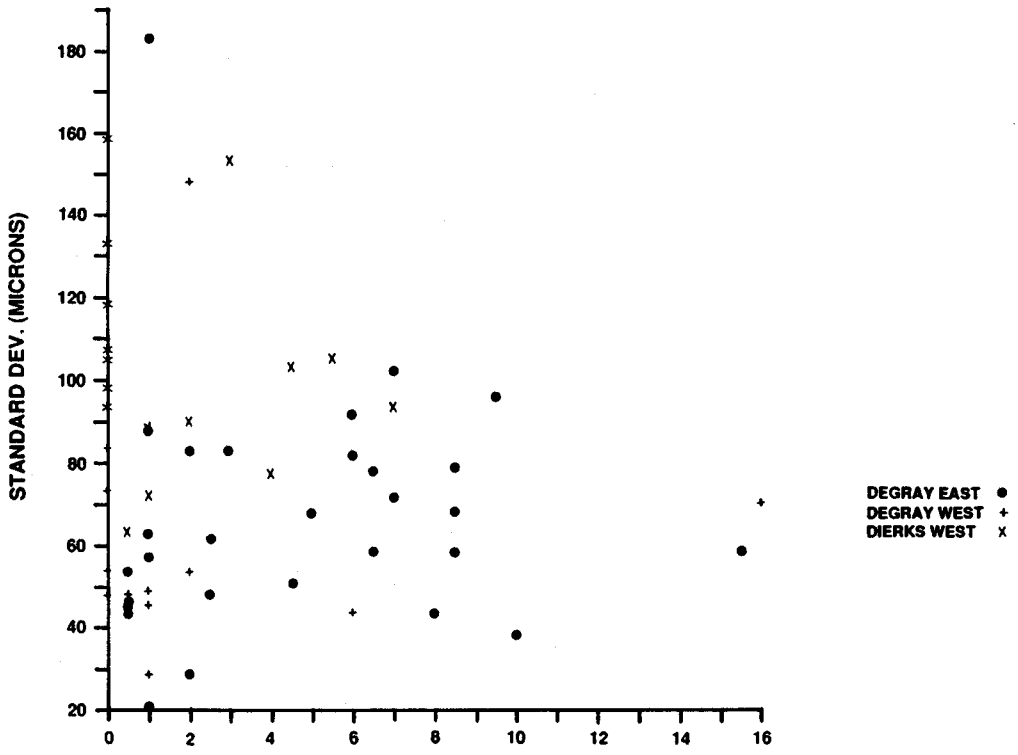

APPENDIX FIGURE II-G

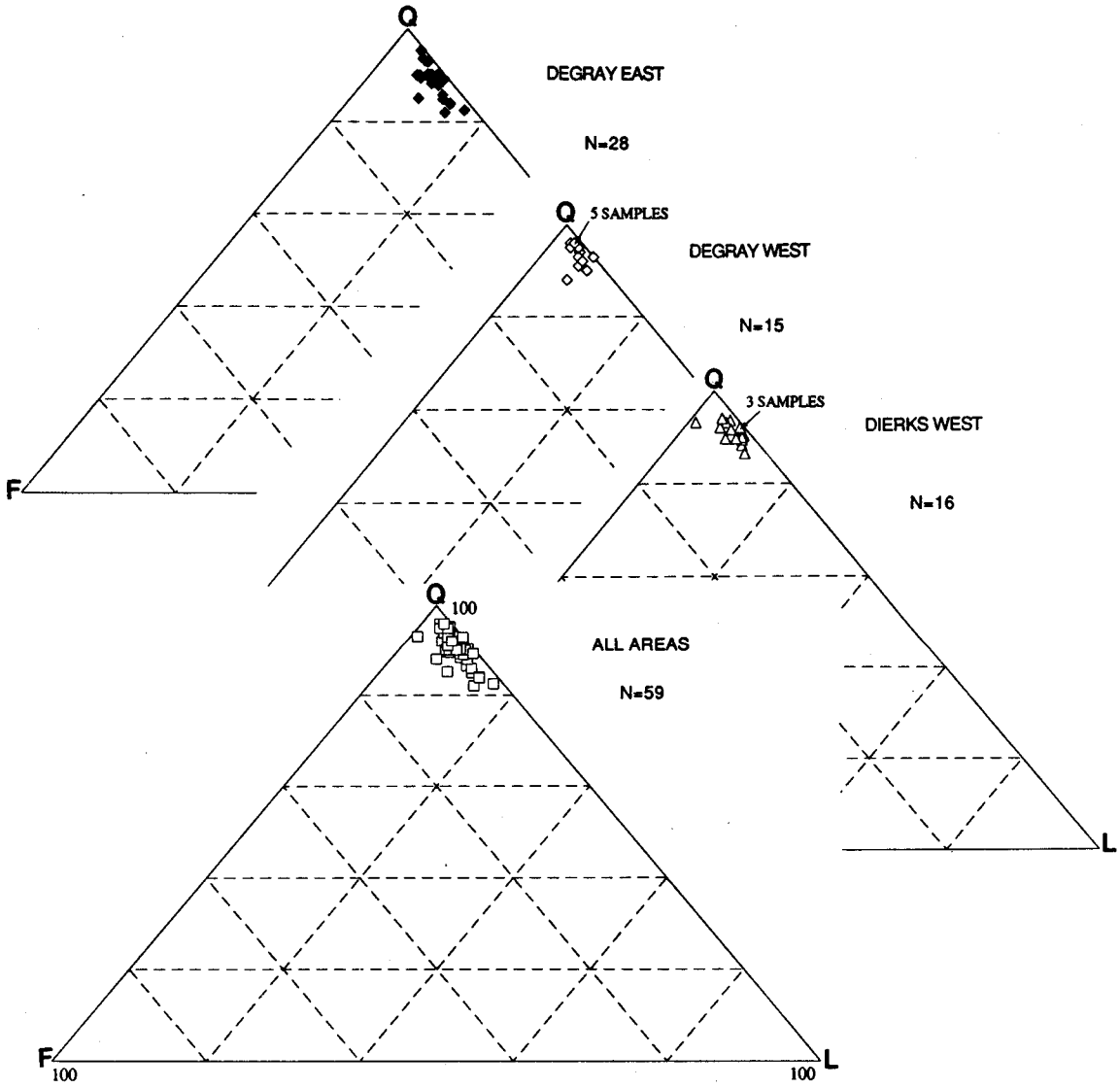

APPENDIX FIGURE II-H

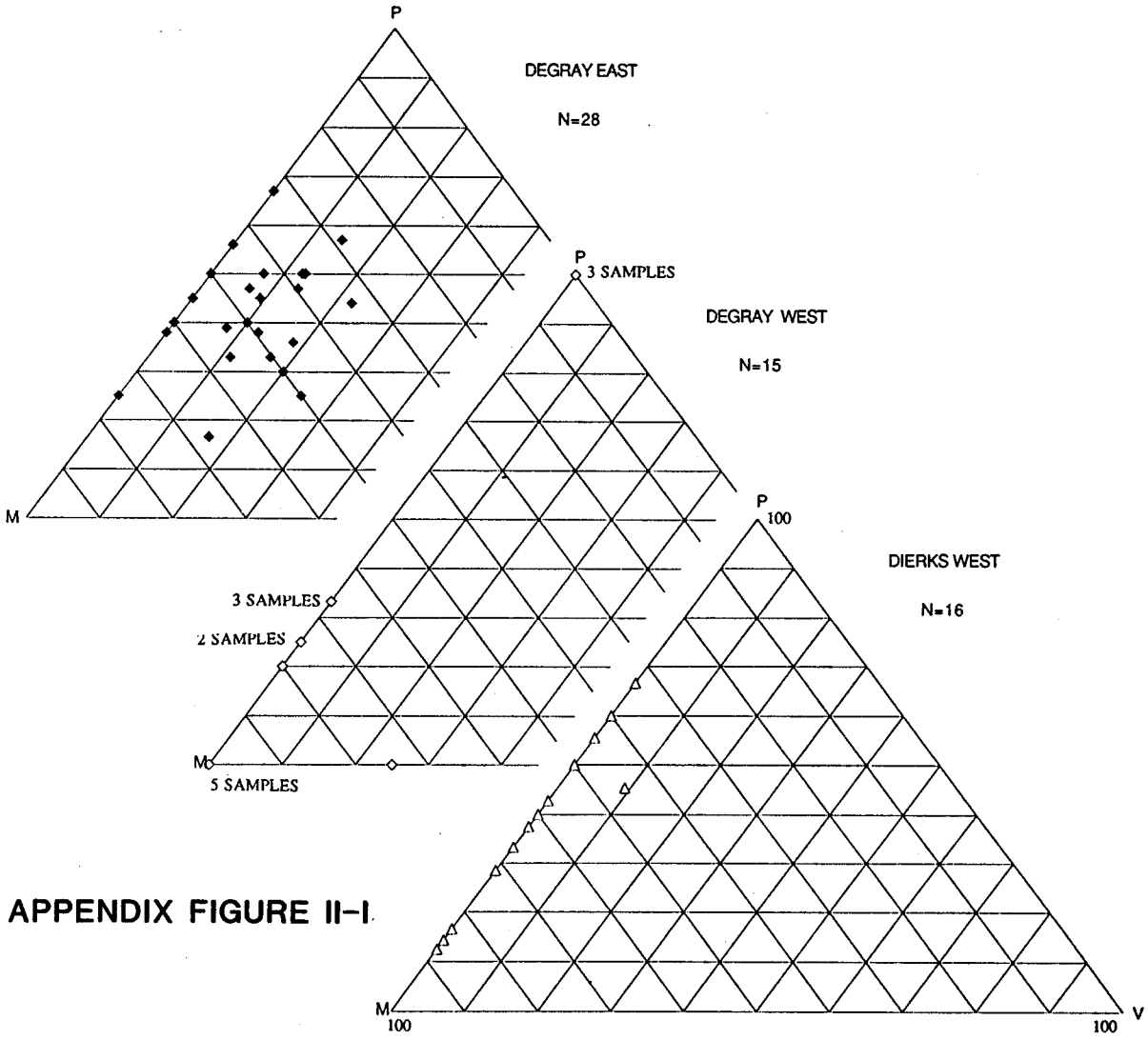

APPENDIX FIGURE II-I

DEGRAY EAST DATA

SAMPLE	LOG'	MONO	POLQ	QTZ O	PLAG	K-SP	CHRT	PFR	MRF	VRF	SRF	A MTX	D MTX	HV M	MICA	BITU	1° I Ø	2° IG Ø	TOT Ø	Ø+BITU
DGE 1	954'	37.5	0.5	38.5	2	1	2	0.5	2	0.5	0.5	2	4		0.5		2.5	6	8.5	
DGE 2	936'	46.5	3.5	23	2.5		2	3.5	3	0.5	1.5	2	6		1.5		0.5	4	4.5	
DGE 3	924'	42.5	2	26.5	2	1	4	3.5	3.5	0.5	0.5	2	3		1		0.5	7.5	8	
DGE 4	852'	51.5	1.5	23	0.5		3	2	1.5	1		3	7				3.5	2.5	6	
DGE 5	850'	48.5	2.5	18.5	1.5	0.5	4	1	2	1	1.5	1.5	9.5		1	3.5		3.5	3.5	7
DGE 4	849'	44	1.5	26	0.5	0.5	1.5	1.5	2.5	0.5	1	1.5	10					8.5	8.5	
DGE 6	846'	45	2.5	24	1.5	1	2.5	2	1.5	0.5	0.5	2	9.5		0.5	1.5		5.5	5.5	7
DGE 7	844'	47.5	3.5	23.5	1.5		4	3.5	3	1	0.5	2	3		0.5	0.5		6	6	6.5
DGE 8	842'	42.5	2	21.5	1		3	3	4.5	1.5	1	1	10	0.5	0.5			8.5	8.5	
DGE 9	841'	44.5	1.5	19.5	1.5		2.5	1.5	2.5	1		1	7.5		1.5	9.5	1	5	6	15.5
DGE 10	838'	41.5	2	26.5	2		4	2.5	3.5	0.5	1	1.5	9		1	1		5	5	6
DGE 11	833'	46	5	31	0.5	1	2.5	2	2.5	1	0.5	0.5	6		1			1	1	
DGE 12	830'	44	2	18.5	1.5		1.5	1.5	2.5			1	17.5		0.5	6		3.5	3.5	9.5
DGE 13	826'	44.5	4.5	32	1	1.5	1.5	2	2.5		1	0.5	5.5		1			2.5	2.5	
DGE 14	821'	43	7	36.5	1	2.5	4	1	1		0.5	4.3	2.5		0.5		0.5	0.5	1	
DGE 15	819'	45.5	4.5	31.5	1.5	0.5	2.5	1.5	2.5	1		1.5	5		0.5	0.5		1.5	1.5	2
DGE 16	818'	49	2	36.5	1.5	1	2.5	4	1.5	0.5			2.5					1	1	
DGE 17	816'	40	1.5	36	2		3	1.5	2	0.5	0.5	0.5	7		0.5	0.5		4.5	4.5	5
DGE 18	809'	47	2	28.5	1.5		2.5	2.5	2.5		0.5	0.5	5.5		0.5	4		2.5	2.5	6.5
DGE 19	806'	41	2	28.5	3	2	2	2.5	2.5	0.5		1	11.5		0.5	0.5		2.5	2.5	3
DGE 20	344'	44.5	1.5	30.5	1		2.5	2	2.5	0.5		1.5	10.5		1	0.5		1.5	1.5	2
DGE 21	342'	52	2.5	34.5	1		1	2	2.5			0.5	2.5		0.5		0.5		0.5	
DGE 22	338'	49	3	37.5	1		0.5	2.5	2				1.5		0.5	2	0.5		0.5	
DGE 24	333'	50	3	36.5	1		1.5	2	1	0.5	0.5	0.5	2.5					1	1	
DGE 25	332'	48	2	34.5	1	0.5	1.5	2	2.5	0.5	1	0.5	3.5				0.5	2	2.5	
DGE 26	331'	34	2	30.5	1.5		3	0.5	1.5		0.5		15.5		1	4		6	6	10
DGE 27	325.5'	49.5	5.5	37	0.5		1.5	1	1.5				2.5					0.5	0.5	
DGE 28	324'	45	2	36	0.5		5	3	1.5			1	5					0.5	0.5	

DEGRAY EAST DATA

SAMPLE	LOG'	MTRX	SLT	C SLT	VFG	FG	MG	CG	MGS	STD D	Q	F	L	F	M	C	P	M	V	
DGE 1	954'	7.4	0.9	5.5	38.8	35.2	12		153.5	79	90	3.5	6.5	51.1	6.6	42.3	16.6	66.8	16.6	
DGE 2	936'	10.7		5.3	28.6	53.5	1.8		143.6	50.8	84.9	2.9	12.2	67	8.5	24.5	50	42.8	7.2	
DGE 3	924'	5.6	1.8	9.4	49	33.9	6.4		111.8	43.3	82.6	3.5	13.9	65.4	5.5	29.1	46.6	46.6	6.8	
DGE 4	852'	12.3		0.9	21	43.8	21	1.7	200.9	91.5	90.4	0.7	8.9	67	7.7	25.3	44.4	33.3	22.3	
DGE 5	850'	15.9	3.3	8.4	21	42	9.2		144.4	71.7	85.8	2.5	11.7	66.8	13.1	20.1	25	50	25	
DGE 4	849'	16.6		6.9	26.6	43.3	13.3		167.8	69.7	89.9	1.3	8.8	58.8	12.6	28.6	33.3	55.5	11.2	
DGE 6	846'	16	5.9	11.7	28.6	26	11.7		141.5	102.6	88.3	3.1	8.3	61.6	12.5	25.9	50	37.5	12.5	
DGE 7	844'	5.6		1.9	16	54.7	21.7		195.3	78.5	84.6	1.8	13.6	69.3	5.54	25.2	46.6	40	13.4	
DGE 8	842'	16.6	5	5.8	43.3	27.5	1.6		118.9	57.9	82.5	1.3	16.2	64.3	12.1	23.6	33.3	50	16.7	
DGE 9	841'	13	4.3	13.9	40.8	24.3	3.5		112.5	58.9	87.9	2	10.1	66.2	10.3	23.5	30	50	20	
DGE 10	838'	15.2	0.8	8.5	31.3	33	11		149.3	82.2	83.8	2.5	13.7	60.6	11.2	28.2	38.5	53.8	7.7	
DGE 11	833'	10.7	3.6	1.8	29.5	33.9	20.5		176.7	87.7	89.1	1.7	9.2	62.2	6.2	31.6	36.3	45.4	18.3	
DGE 12	830'	25.9	14	18.5	22.9	12.6	5.9		107.8	96	90.2	2.1	7.7	58.8	20.6	20.6	37.5	62.5	0	
DGE 13	826'	9.9	1.8	1.8	27.9	51.3	7.2		151.8	61.7	89.5	2.8	7.7	60.6	6.3	33.1	44.5	55.5	0	
DGE 14	821'	4.7			12.9	40.9	41.9	12.4	329.7	183.7	90.1	3.7	6.2	60.4	3.6	37	50	50	0	
DGE 15	819'	9.1			3.6	45.4	41.8		251.4	84.1	89.5	2.3	8.2	61	6.6	32.3	30	50	20	
DGE 16	818'	4.7			10.4	68.6	16.1		201.7	63.5	90.6	2.7	6.7	60.6	2.6	36.8	50	37.5	12.5	
DGE 17	816'	12.3	0.9	9.6	12.2	52.6	12.2		170.2	67.9	89.1	2.3	8.6	53.9	8	38.1	37.5	50	12.5	
DGE 18	809'	9.9	6.3	18.9	38.7	26.1			104.2	58.5	89	1.9	9.1	62.9	6.5	30.6	50	50	0	
DGE 19	806'	18.7	0.8	8.1	30	27.6	14.6		154.1	83.9	85.1	6	8.9	57.5	12.9	29.5	45.4	45.4	9.2	
DGE 20	344'	17.3	9	24.8	42	6.6			74	29.8	90	1.2	8.8	56.2	12.4	31.4	40	50	10	
DGE 21	342'	4.7			16.1	75.2	38.8		164.8	45.5	982.7	1.1	6.2	61.9	3.1	35	44.5	55.5	0	
DGE 22	338'	2.9			3.9	81.5	11.6		199.4	44.5	93.7	1.1	5.2	59.8	1.6	38.6	55.5	44.5	0	
DGE 24	333'	4.7			7.6	72.4	15.2		196.7	57	93.2	1.1	5.7	60.1	3.1	36.8	57.1	28.5	14.4	
DGE 25	332'	6.5			18.7	68.2	6.5		174.8	48.6	90.3	1.7	8	60.5	4.1	35.4	40	50	10	
DGE 26	331'	23.6	9.1	20.6	31.2	8.4			75.7	37.7	90.4	2.1	7.5	57.3	2.1	40.6	25	75	0	
DGE 27	325.5'	4.7			3.8	61.9	29.5		223.5	54.2	95.3	0.6	4.1	60.1	2.6	37.3	40	60	0	
DGE 28	324'	9.1		0.9	15.4	70.9	3.6		173.8	45.1	89.2	0.6	10.2	57.5	6.2	36.3	66.6	33.3	0	

DEGRAY WEST DATA

SAMPLE	LOG'	MONQ	POL Q	QTZ O.	PLAG	KSP	CHRT	PRF	VFR	MRF	SRF	A MTX	D MTX	PMTRX	CARB	HV M	MIC	ACC	FOS	1° I Ø	2° IG Ø	FRAC Ø	TOTØ
DGW1	360'	49.5	2.5	24.5	1.5		3.5			3		0.5	12	1			1			1			1
DGW2	359'	47	3.5	36.5	0.5		2	0.5					8	0.5		0.5						1	1
DGW3	357'	47	4	38	1.5		2.5	0.5		1.5			4	0.5							0.5		0.5
DGW4	354'	51	5	39	1.5		1.5			1			1										0
DGW5	351.5'	47	3.5	39.5	0.5		2	1					4	0.5			1				1		1
DGW6	350.5'	41.5	2.5	27	2	0.5	2.5		0.5	1.5		3.5	6	2.5			1			4.5		1.5	6
DGW7	349'	42	3	37.5	2		2.5			1.5		2.5	6.5			0.5				2			2
DGW8	341'	47	3.5	31	5.5		3	0.5		1.5		1	6		1								0
DGW9	340'	39.5	5	29	1.5		1	0.5		1		2	4					0.5		15	1		16
DGW10	336'	48.5	8.5	39	0.5		1.5			1.5			0.5										0
DGW11	34'	47	19.5	22	1		3	0.5				2	3				1				3		3
DGW12(C)	30.5'	25	46.5	20	1		1	0.5		1		0.5	1.5				1		1		1		1
DGW12(S)	30.5'	43.5	8	38.5	1.5		3.5	0.5		2			1.5			0.5	0.5						0
DGW14	9'	52	3	35	1		1	0.5		1		1	3				0.5			2			2
DGW15	7'	44	1.5	34.5	0		3			3	0.5	4.3	3.5				0.5			2	3		5
SAMPLE	LOG'	MTRX	SLT	CSLT	VFG	FG	MG	CG	VC	GRAN	PEB	MGS	STD D	Q	F	L	F	M	C	P	V	M	
DGW1	360'	21.2	5.5	26.7	44.9	1.5						73.7	29.2	90.5	1.9	7.6	61.2	13.8	25	0	0	100	
DGW2	359'	14.5		0.8	19.6	62	3.4					159.5	49.3	96.6	0.5	2.9	54.3	8.7	37	100	0	0	
DGW3	357'	8.2		0.9	20.1	64	6.4					157.7	47.6	93.6	1.7	4.7	57.3	4.6	38	25	0	75	
DGW4	354'	1.9		0.9	21.5	73	2.9					159.8	47.7	95.9	1.6	2.5	60	1	39	0	0	100	
DGW5	351.5'	8.2		0.9	24.7	62	3.6					153.4	45.7	96.2	0.6	3.2	55.1	4.6	40	100	0	0	
DGW6	350.5'	23	0.7	6.9	34.6	35						125.7	44.7	91	3.3	5.7	54.8	16.2	29	0	25	75	
DGW7	349'	15.2	3.3	12.7	40.6	27	0.8					114.4	54	93.2	2.3	4.5	52.3	9.3	38	0	0	100	
DGW8	341'	12.3			21	64	2.6					160.3	46.4	88.6	5.9	5.5	61	7	32	25	0	75	
DGW9	340'	10.7			3.5	52	33.9					241.5	70	94.8	2	3.2	58.1	77.2	35	33.3	0	66.7	
DGW10	336'	0.9			5.9	49	44.5					243.6	73.4	96.5	0.5	3	60.5	0.5	39	0	0	100	
DGW11	34'	5.6			5.6	40	41.5	2.8			4.7	595.4	1447.7	95.1	1.2	3.7	73.9	3.2	23	100	0	0	
DGW12(C)	30.5'	1.8		0.9	8.7	48	27.1	0.9	1.8	0.9	8.7	728.4	1547.1	96.3	1.1	2.6	77.3	2.1	21	33.3	0	66.7	
DGW12(S)	30.5'	2.9			3.9	43	48.5	1.9				254.3	83.7	92.3	1.6	6.1	59.6	1.6	39	20	0	80	
DGW14	9'	7.4			11.1	37	37	7.4				275	148.6	96.2	1.1	2.7	60	4.1	36	33.3	0	66.7	
DGW15	7'	13.8			12.9	53	20.7							92.5	0	7.5	55	8.5	37	0	0	100	

DIERKS WEST DATA

SAMPLE	LOG'	MON Q	POL Q	QTZ O.	PLAG	K-SP	CHRT	PRF	MRF	VRF	SRF	A MTX	D MTX	HV M	MICA	1° I Ø	2° I6 Ø	TOT Ø	
DKW1	520'	40	1	37.5	2		2.5	2.5	2.5	0.5	0.5		10		1			0	
DKW2	510'	41	2	37	1.5		3.5	0.5	3.5		0.5		8.5		1		1	1	
DKW3	494'	43.5	2.5	31	1	1.5	4.5	2	3			1.5	8		1		0.5	0.5	
DKW4	420'	47	4	36.5	1		1.5	0.5	3				4.5		1		1	1	
DKW5	406'	49	3.5	37	1		4	1.5	3				1.5		0.5			0	
DKW6	378'	45.5	4.5	38.5	0.5	0.5	3.5	2	3				1		1			0	
DKW7	370'	43	3.5	39.5	1.5		4	1.5	2		0.5		2.5		2		2	2	
DKW8	366'	37.5	0.5	29	1		2.5	1.5	2.5				19		2.5	1	3	4	
DKW9	358'	48	3	37	0.5		3	1	2				4		1.5			0	
DKW10	352'	48	4.5	22	1.5		1.5	1.5	1				15.5		1.5		3	3	
DKW11	336'	42.5	3	25.5	1.5		2	2	1			2	18	0.5	2		0	0	
DKW12	330'	41.5	1	45.5	0.5		2	2.5	2.5				4		0.5			0	
DKW13	322'	46	1	11.5	2			0.5	2.5				27		2.5		7	7	
DKW14	254'	45	2	31.5	2		1.5	2.5	2		1		10.5	0.5	1.5			0	
DKW15	238'	44	3	27.5	2.5		2	1	2.5			2	10		0.5		4.5	4.5	
DKW16	224'	42.5	2.5	37	1.5		1	1	1.5			0.5	6		1	1.5	4	5.5	
SAMPLE	LOG'	MTRX	SLT	C SLT	VFG	FG	MG	CG	MGS	STD D	Q	F	L	F	M	C	P	M	V
DKW1	520'	16.6	0.8	6.6	25.8	38.3	10.8	1.6	169.7	107.1	88.2	2.3	9.5	52	10.2	37.8	45.4	45.4	9.2
DKW2	510'	14.5	4.3	5.9	24.8	43.6	6.8		145.2	72.6	89.4	1.7	8.9	53.6	8.7	37.7	12.5	87.5	0
DKW3	494'	13.8	0.8	9.5	29.3	43.1	3.5		137	64.3	86.5	2.8	10.7	58.9	9.7	31.4	40	60	0
DKW4	420'	8.2			10.1	45.9	35.8		230.9	87.6	93.6	1.1	5.3	58.2	4.6	37.2	14.3	85.7	0
DKW5	406'	0.9			8.9	45.5	43.6	0.9	249.1	94.5	90.4	1	8.6	62.1	0.5	37.4	33.3	66.6	0
DKW6	378'	1.9			1.9	36.3	50.9	8.8	312.1	158.2	90.3	1	8.7	60.1	1	38.9	40	60	0
DKW7	370'	4.7	1.9	3.8	20	38.1	31.4		200.8	90.3	90	1.6	8.4	57.1	2.6	40.3	42.8	57.2	0
DKW8	366'	27.5	9.4	16.6	22.5	21	2.9		109.1	77.3	89.9	1.4	8.7	48.7	20.3	31	37.5	62.5	0
DKW9	358'	7.4			12	39.8	36.1	4.6	242	105.5	93.1	0.6	6.3	58.4	4	37.6	33.3	66.6	0
DKW10	352'	23.6	1.5	6.1	20.6	22.9	20.6	4.6	220.7	153.7	93.1	1.9	5	60.1	16.5	23.4	60	40	0
DKW11	336'	26.4	29.4	6.6	13.9	25.7	22	22	212.4	133.3	91.6	2	6.4	54.4	18.9	26.7	66.6	33.3	0
DKW12	330'	7.4		1.8	17.6	39.8	31.5	1.8	230.2	118.9	92.1	0.6	7.3	50.2	4.1	45.7	50	50	0
DKW13	322'	35	1.9	14.9	16.9	22.7	8.4		143.6	94.1	92.1	3.2	4.7	57.5	29.8	12.7	16.6	83.4	0
DKW14	254'	17.3		4.1	22.3	36.3	19.8		188.7	98.2	89.7	2.3	8	57.1	10.8	32.1	55.5	44.5	0
DKW15	238'	16.6		2.5	14.1	40.8	25	0.8	208.3	104.1	89.7	3.7	6.6	59.7	10.7	29.6	28.5	71.5	0
DKW16	224'	10.7	2.7	3.6	23.2	38.4	21.4		185.7	105.2	94.2	1.8	4	53.7	6.5	39.8	40	60	0

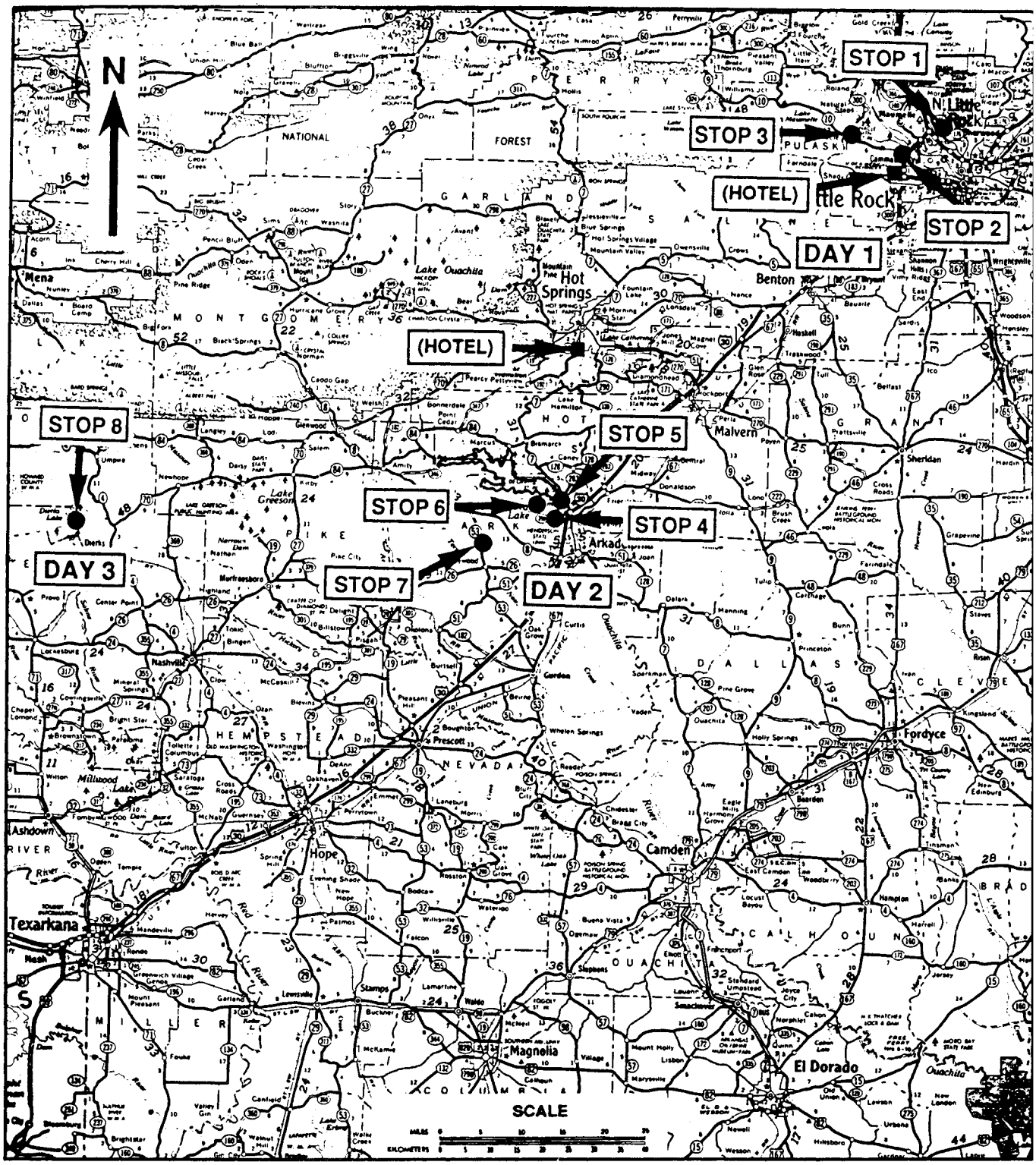

ISBN 1-879325-15-2